MULTI-OBJECTIVE EVOLUTIONARY OPTIMIZATION IN GREENHOUSE CONTROL FOR IMPROVED CROP YIELD AND ENERGY TRADEOFFS

By

José R. Llera Ortiz

A DISSERTATION

Submitted to
Michigan State University
in partial fulfillment of the requirements
for the degree of

Electrical Engineering—Doctor of Philosophy

2020

ABSTRACT

MULTI-OBJECTIVE EVOLUTIONARY OPTIMIZATION IN GREENHOUSE CONTROL FOR IMPROVED CROP YIELD AND ENERGY TRADEOFFS

By

José R. Llera Ortiz

The worldwide increase in demand for fresh fruits and vegetables has led to a search for strategies to manage greenhouses in ways that not only meet this demand, but that are also economically viable and environmentally sustainable. A well-established approach for managing greenhouse microclimate is through the automatic control of its mechanical systems such as heaters, ventilators, and shade screens. Such a system is a form of closed-loop control, but only with respect to the greenhouse microclimate, rather than the crop being grown. In practice, conventional greenhouse control is criticized for this focus on climate control instead of crop production, as well as the complexity of managing these systems due to an excessive number of user settings [1]. A more comprehensive form of closed-loop optimal control in greenhouses has been proposed to provide a better degree of control by adjusting the greenhouse climate in response to the growth of the crop being cultivated, but it is still dependent on the external climate around the greenhouse and can lack acceptable alternatives due to the nonlinear nature of the interactions between environmental conditions and plant growth. Unfortunately, monitoring of the real-time response of the crop is not viable for this type of closed-loop control – what can be used instead is a rather sophisticated *state model* of crop production so that the microclimate conditions can be controlled in order to optimize their effects on the *predicted* seasonal crop production. Further, this model and the greenhouse microclimate model into which it is integrated must be executable in a short enough timeframe to allow running it thousands of times to optimize the performance of the controller for a given greenhouse structure and location. Having developed such a model, we propose using a form of evolutionary multi-objective optimization to discover a suite of user-selectable control strategies that balance crop productivity with the financial costs of greenhouse climate control. Each of the Pareto-optimal controllers discovered by this approach defines a *range* of conditions to be maintained via

specified control actions, depending upon the crop state and external environmental conditions. Due to the large number of candidates present as the output, the decision-making process will be aided by considering common user preferences as well as algorithmically examining the robustness of solutions in the final Pareto-optimal frontier.

ACKNOWLEDGMENTS

I would like to thank Prof. Percy Pierre for his financial support and guidance through the Sloan Engineering Program, as well as his heartfelt efforts to see my degree to its completion even after retirement. The international collaboration between Prof. Lihong Xu, his graduate students, and the BEACON Center at MSU was invaluable for the completion of this dissertation. Dr. Chenwen Zhu and Dr. Prakarn Unachak helped build the foundations for the simulation software used in this dissertation, and this research would not have been as fruitful without their efforts. Prof. Erik S. Runkle's extensive knowledge on growing plants in controlled environments was invaluable in steering our research in the right direction. Prof. Kalyanmoy Deb's passion for using evolutionary computation as a tool for producing useful and innovative design principles inspired the methodology for interpreting the results in this dissertation. Prof. Nelson Sepúlveda's financial support, guidance, and contagious optimism was invaluable during the last stages of my Ph.D. program. Finally, Prof. Erik D. Goodman's mentorship, financial support, and above all confidence in my abilities throughout these years was indispensable, especially in times where I would doubt my own abilities. I will always be grateful for being provided a unique opportunity to take on this complex, multidisciplinary engineering problem by using some of the fascinating techniques developed in the field of evolutionary computation.

TABLE OF CONTENTS

LIST OF TABLES

LIST OF FIGURES

KEY TO SYMBOLS AND ABBREVIATIONS

State variables

CO_2	Carbon dioxide concentration (mg/m^3)
T	Temperature (°C)
VP	Vapor Pressure (Pa)

Subscripts

24	24-hour mean
48	48-hour mean
_fr	Subscript denoting a post-fruit-set variable or setpoint
Air	Greenhouse air compartment
Blow	Indirect air heating system
Boil	Boiler heating system
Boiler	Alternate subscript denoting the boiler heating system
D	Denotes that variable applies to midday period
Dst	Destination
E	Denotes that variable applies to evening period
Electricity	Denoting the use of electricity as a resource
ExtCO2	External CO_2 source
Fog	Fogging system
Glob	Global radiation (W/m^2)

M	Denotes that variable applies to morning period
N	Denotes that variable applies to nighttime period
Off	Threshold for a greenhouse actuator to be turned off
On	Threshold for a greenhouse actuator to be turned on
Out	Outside air temperature
Pad	Pad and fan cooling system
Roof	Greenhouse roof ventilation opening
Shading_i	Greenhouse internal shading screen
Shading_e	Greenhouse external shading screen
Side	Greenhouse side ventilation opening
Src	Source
ThScr	Thermal screen
Thermal	Alternate subscript for thermal screen
Vent	Greenhouse roof and side ventilation openings
Water	Denoting the use of water as a resource

Other abbreviations

Cap	Capacity of the associated state variable and/or greenhouse design element
CNY	Chinese Yuan
CRS	Controlled Random Search
cv	Cultivar
Eq	Equation

Eqs	Equations
FIR	Far Infrared Radiation
MIMO	Multi-Input-Multi-Output
MOCC	Multi-Objective Compatible Control
MOEA	Multi-Objective Evolutionary Algorithm
MPC	Model Predictive Control
NFR	Net Financial Result
NIR	Near Infrared Radiation
NSGA-II	Non-Dominated Sorting Genetic Algorithm II
p	Cost associated with consumption of a limited resource (CNY)
ppm	Parts Per Million
P	Cost associated with operation of a greenhouse element (CNY)
PAR	Photosynthetically Active Radiation
PE	Polyethylene
PID	Proportional-Integral-Derivative controller
R	Flux density (W/m^2)
RH	Relative Humidity
u	Climate control variable
U	Alternate abbreviation for a climate control variable
VPD	Vapor Pressure Deficit

Other variables

$CO_{2AirExtMax}$	Upper bound for the dynamic CO_2 setpoint (ppm)
$CO_{2AirExtMin}$	Lower bound for the dynamic CO_2 setpoint (ppm)
$CO_{2AirExtOn}$	Current value of the dynamic CO_2 setpoint (ppm)
h_{Tcan24}	Growth inhibition function based on 24-hour mean canopy temperature
h_{Tcan}	Growth inhibition function based on instantaneous canopy temperature
I_{Glob}	Outside global radiation (W/m^2)
$I_{GlobMax}$	Threshold for the outside global radiation above which the CO_2 setpoint will be at its maximum (W/m^2)
MC_{Fruit}	Rate of carbohydrate flow into fruit ($mg/m^2 \times s$)
n_Dev	Total number of fruit development stages, of which the last stage may be harvested
sr_offset	Offset used to subtract from calculated sunrise time (minutes)
ss_offset	Offset used to subtract from calculated sunset time (minutes)
t_0	Greenhouse simulation starting time
t_f	Greenhouse simulation ending time
v_{wind}	Outdoor wind speed (m/s)

Symbols

Φ	Capacity of the associated system
€	Euro currency sign
ρ	Reflection coefficient
τ	Transmission coefficient

1 Introduction

1.1 Objectives and Scope

The objective of this thesis is to build upon existing greenhouse models that allow the simulation of greenhouse and tomato plant growth dynamics, and to use evolutionary algorithms with this model in order to find and analyze practical control strategies that can improve upon existing strategies. Validation of these strategies will consist of reproducing the original results utilizing a classical control strategy and then comparing them to these optimized control strategies. Optimized control strategies that are found will be examined for economic viability as well as robustness against varying weather conditions and sensitivity to variations in control parameters. Resulting control strategies are designed and expected to be viable for validation in real greenhouses but doing so is beyond the scope of this thesis, as it would involve considerable time and expense. Since greenhouse parameters as well as user requirements have a staggering amount of variation, we are limited to only parameters currently available to us. However, the methodology proposed here can be applied by others by introducing their own greenhouse parameters, costs, and other design constraints.

1.2 Introduction

Worldwide, the greenhouse industry is the fastest growing sector of agricultural production, with global demand for fruits and vegetables having doubled in the last ten years [2]. A key factor in meeting this demand is employing automatic greenhouse control that adjusts the microclimate of a greenhouse based on sensor feedback. This demand is particularly acute in China, which has funded a team at Tongji University, under the leadership of Prof. Lihong Xu, to study ways in which greenhouse productivity can be optimized. Through a long-established research relationship with Prof. Erik Goodman of MSU, they have assembled a team including Prof. Erik Runkle of the Department of Horticulture, MSU; Prakarn Unachak, a former Ph.D. student at MSU; Chenwen Zhu, a former Ph.D. student at Tongji University and visiting scholar at MSU; and Dr. Yuanping Su, a graduate of Prof. Xu's doctoral program and visiting scholar at MSU. The author and Prof. Goodman have made several visits to Tongji University and the

experimental greenhouses they have constructed, helping their understanding of the real-world facets of greenhouse control. The activities of this team laid the groundwork under which this work was begun by the author. Collaboration continues with Prof. Xu, Dr. Su, and Prof. Runkle; the others have graduated and moved on to other activities.

Due to the reliance on open-loop control or on closed-loop control aimed only at maintaining preselected setpoints for various greenhouse microclimate variables, most commercially available conventional greenhouse controllers have problems providing optimal control due to the lack of an on-line feedback mechanism that allows the controller to make adjustments based on the current growth dynamics of the entire crop production system [1]. A related method, closed-loop greenhouse control, promises higher crop yield at lower cost by adjusting the indoor climate in accordance with the response of the crop being cultivated. Even so, an obstacle to acceptance of these controllers is the lack of decision freedom of the user, which is necessary for adapting to unexpected environmental conditions [1]. An approach that is more energy efficient than conventional control and provides users with the freedom to adjust controller behavior is needed to help meet the increasing demand for fruits and vegetables considering yield, quality, and production inputs. Our proposed approach incorporates a tomato crop yield model as part of the closed-loop control by using the model-predicted seasonal crop yield as an overall measure of fitness for a control strategy. Thus, this control approach requires a detailed crop growth model allowing prediction of the effect of microclimatic conditions at any time on the ultimate seasonal yield, by tracking their effects on a state model of the crop growth. This approach will yield multiple solutions that show the tradeoffs between crop yield and energy costs using evolutionary algorithms.

Using multi-objective evolutionary algorithms, or MOEAs, we can obtain a set of greenhouse control strategies that can balance multiple conflicting objectives. For our purposes, energy consumption and crop production are considered as the objectives to optimize. One particular property we are interested in while using MOEAs is that of elitism during search, which involves preserving the fittest Pareto non-dominated individuals from a previous generation and keeping them unchanged into the next generation.

This guarantees that the overall quality of solutions does not decrease from one generation to the next. In order to obtain the parent population for the next generation, the current generation's parent population and the offspring are combined and then sorted according to the concept of non-domination. Since all the parent members are included, this ensures elitism is employed in the algorithm. The next generation is then created by adding members from the current sorted, combined population starting from the lowest ranked members. If all solutions from a particular rank cannot be added to the next parent population, the crowding operator is used to rank in order of descending crowding distance, and then the necessary number of members is chosen to fill the population. One example of such an algorithm is described in Figure 1.1.

Energy savings are achieved by taking advantage of the crop's ability to tolerate environmental fluctuations. This is known due to the effects of sub-optimal and supra-optimal instantaneous and mean temperatures being studied extensively for tomatoes, which has led to the development of temperature-based growth inhibition functions for the tomato crop model [3]. This behavior allows us to relax controller setpoints to allow a wider range of temperatures than would normally be deemed acceptable in practice, as long as the control strategy itself does not trigger the negative effects of these growth inhibition factors. For example, it may be unnecessary to maintain a high nighttime temperature if there was little photosynthetic activity during the day and the outdoor temperature is low. User decision freedom is achieved by enabling users to choose among a set of evolved control strategies, with different control parameters for the lower and upper limits to allow variation, depending on the crop state and typical external weather conditions of the site. The behavior of the crop model's growth inhibition factor is illustrated in Figure 1.2. These define an optimal range of temperatures for both instantaneous and 24-hour mean temperatures in order to grow the crop, and subsequently play a major role in maximizing crop yield. Of course, these curves are only one of the components in the instantaneous photosynthesis model, which also depends heavily on leaf area index, level of photosynthetically active radiation (PAR), and of CO_2 concentration in the greenhouse canopy.

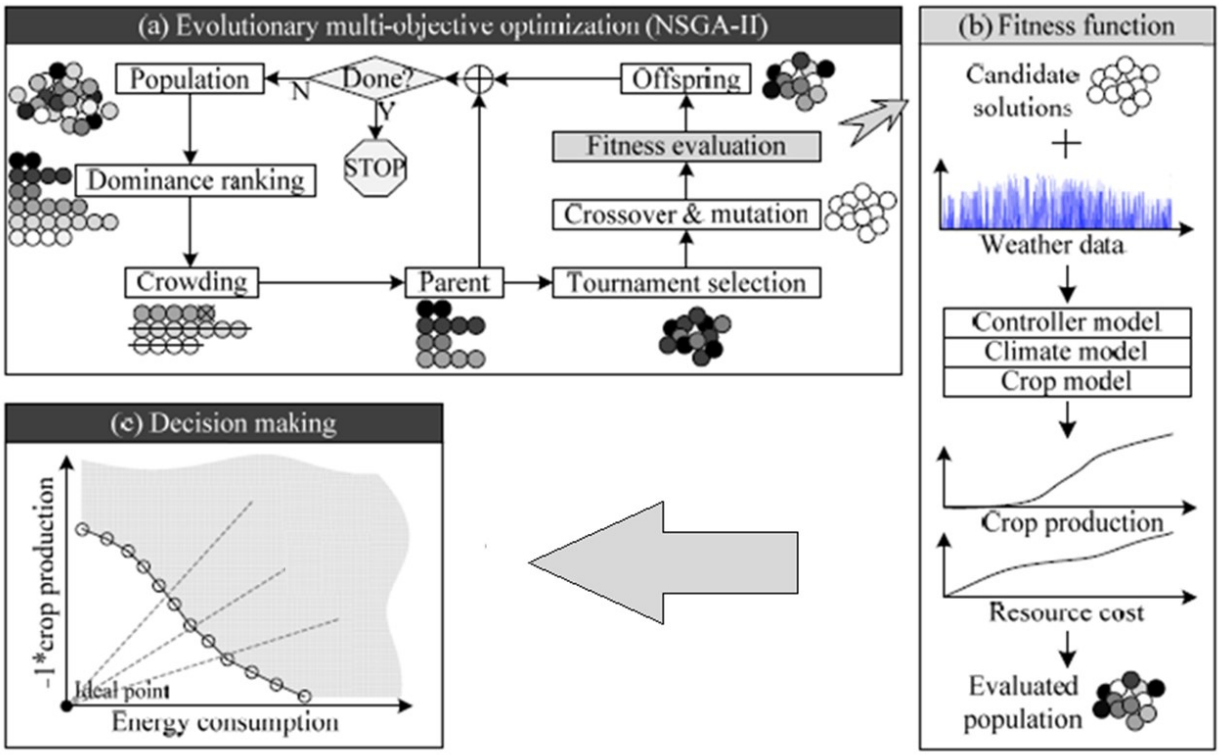

Figure 1.1. Detailed illustration of the proposed method for optimizing greenhouse control strategies: NSGA-II, a multi-objective problem solver (a), components of the fitness function (b), and a resulting Pareto set of control strategies (c).

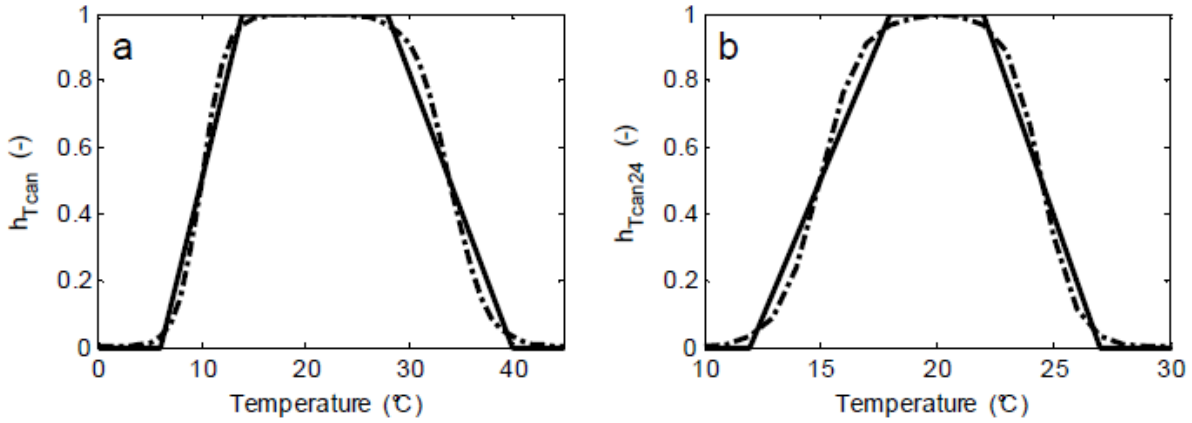

Figure 1.2. The growth inhibition functions used as part of Vanthoor's crop model [4]. The horizontal axes on the left and right represent instantaneous canopy temperature and 24-hour mean temperature, respectively. The solid lines represent a non-differentiable implementation of the functions, while the dotted lines represent a differentiable version of the functions. The values h_{Tcan} and h_{TCan24} are used as scaling factors that limit the flow of carbohydrates into the tomato crop.

1.3 Control Strategy Optimization Methodology

Vanthoor's proposed approach for the greenhouse design optimization step utilizes CRS (population-based controlled random search [5]), which is appropriate for the scope of the optimization problem framed originally: limited search space and single objective. Due to the introduction of crop yield as an objective and dramatically expanding the search space, we changed the approach by using a type of heuristic multi-objective search algorithm called the "Non-dominated Sorting Genetic Algorithm-II (NSGA-II)" [6]. Another major difference is that the end-goal of our optimization step is the acquisition of novel control strategies by optimizing over a wide range of possible control parameters while using a fixed set of greenhouse elements; Vanthoor utilized a fixed control strategy. Environmental effects on attributes of the tomato crop that are associated with its quality (e.g., flavor, nutrition, etc.) are not considered in the economic model (described in Section 4.1.2), and it was assumed that the greenhouse environmental conditions produced by the evolved control strategies discussed in this thesis do not affect tomato quality. Instead, the output of the tomato crop yield model while using evolved control strategies will only differ from a classical strategy (described in Section 6.2) with regards to the amount that was harvested.

The use of NSGA-II allows us to find multiple solutions consisting of the Pareto-optimal set of control strategies. We treat greenhouse climate control as a multi-objective problem comprising two conflicting objectives: resource cost (water, electricity, etc.) and crop yield. Evolutionary algorithms maintain a population of candidate solutions in which individuals compete with one another based on a fitness function. In this case, candidate solutions are greenhouse control strategies, and the fitness function is based on a simulation of an integrated cultivation system including a greenhouse climate state model combined with a tomato growth state model. As in biological evolution, new candidate solutions are generated via recombination and mutation of highly fit "parent" solutions. These offspring are then incorporated into the population, and, if highly fit themselves, compete for space in the next generation [7].

Figure 1.1 is a detailed illustration of our approach. In Figure 1.1a, NSGA-II is used to obtain sets of Pareto-optimal greenhouse controllers. Each individual in the NSGA-II population is a control strategy that is evaluated by a fitness function to determine its survivability, as depicted in Figure 1.1b. This fitness function comprises three components: the objective functions being optimized, the greenhouse/crop yield model that is used to evaluate the control strategy, and the meteorological data used as input to the greenhouse model. A sample Pareto-optimal set of control strategies is shown in Figure 1.1c. Details regarding the individual control strategies and each component of the fitness function are described in more detail below.

2 Literature Review

Modeling of greenhouse production of crops has been a longstanding research topic, because of the importance of optimizing the behavior of the greenhouse control system to maximize crop production while minimizing operating costs. These sometimes-conflicting objectives give the decision maker a great deal of freedom to choose, but also the responsibility of choosing wisely. Historically, even the earliest efforts [8] at automated greenhouse control recognized the importance of making the control system responsive to changes in external environmental conditions (including temperature, relative humidity, wind speed and direction, etc.).

The majority of greenhouse optimization studies focus on control performance and climate control with regards to maximizing net financial gain [1], that is, combining the value of the crop produced and the cost of producing it. Due to the scope of these studies, components such as a crop yield model are typically not considered, with the focus instead being on maintaining the greenhouse microclimate in a state thought to be optimal for plant productivity. Part of this is due to there being a limited number of plants that are well enough understood to form a complete state model, as well as the lack of well-studied and economically viable methods to obtain real-time feedback on plant biomass increase. The later approaches, such as that implemented by Vanthoor [4], introduce simplified models of plant growth, increasing the robustness of the approach by calculating the effects on the ultimate objective, crop yield, rather than on an arbitrarily determined physical parameter(s) of the greenhouse. However, introduction of crop modeling dramatically increases the complexity of the simulation required to determine the benefits of a particular control algorithm, so progress on this front has partially relied on the advance in computational speeds before researchers have used such models.

In order to determine the economic and crop yield effects of a specific greenhouse controller, it is necessary to combine several models together: a greenhouse climate (or microclimate) model, a crop yield model and an economic model. Of these three, finding an adequate crop yield model proves to be particularly challenging; even with the use of parallel computing and a relatively small number of

greenhouse designs to evaluate, the computational time required for applying optimization algorithms can be prohibitive [4]. That said, tomato currently makes for an ideal crop, as knowledge on modelling tomato yield is widely available [9].

Most of the early publications approached the topic of optimal greenhouse control from the point of view of classical control methods, which define greenhouse environmental control as an optimal control problem. For example, N. Sigrimis and N. Rerras applied a linear model for greenhouse control which views the greenhouse environment as a multi-input-multi-output (MIMO) system [10]. It uses as inputs such variables as external temperature, relative humidity, wind velocity and direction, and insolation. It also uses internally measured evapotranspiration rates, and state variables such as internal air temperature, internal air relative humidity and soil temperature to determine how various control actions should be modulated (heaters, window openings, exhaust fans, etc.).

H. J. Tantau discussed the benefits of optimal control of temperature, humidity, and supplemental lighting, resulting in reduced overall costs, reduced growing periods and increased crop yields [11]. However, he also noted the importance of plant growth models, as they can provide valuable feedback to online control systems, and knowledge in this area was still lacking at the time.

E. J. van Henten and J. Bontsema defined greenhouse cultivation of a lettuce crop as an optimal control problem to determine the ideal temperature and CO_2 strategies for its cultivation, using the mean values of historical weather data as a method of forecasting [12]. This resulted in lower energy costs and CO_2 consumption compared to using control strategies that do not take the weather into account. While it had its benefits, they also noted that this method needs improvement to better cope with differences between predicted and actual weather.

K. G. Arvanitis, P. N. Paraskevopoulos and A. A. Vernardos proposed an adaptive control strategy for greenhouse air temperature [13]. Multiple samples of the greenhouse air temperature were taken over the course of a predefined sampling period, which were then used to compute a constant-gain controller that modulates the heating system.

I. Seginer and R. W. McClendon compared various dynamic optimization techniques and talked about their drawbacks in the context of greenhouse cultivation: depending on the technique used, a grower may have difficulty making multiple sequential decisions during a growing season, or it may be unacceptably inefficient when solving problems with many state variables [14]. To address this problem, they proposed reducing the number of state variables in one of their approaches to reduce the computational complexity of the problem. Depending on which state variables were removed, the results ranged from sub-optimal but acceptable to more inferior results. They also used historical data from previous optimal control solutions to train a neural network that could produce control decisions that are appropriate for current environmental conditions, with good results.

A related effort, aimed at reducing the number of state variables in the greenhouse model, was undertaken by the team at Tongji University, as reported in [15]. It proposed a simplified model with significantly reduced state variables while still describing a combined greenhouse climate and crop yield model. In addition, some of the state variables were simplified through curve fitting techniques. The results show that the reduced model was effective at producing similar results to its counterpart. Moreover, this research shows one method for validating these results by using already available data from a previously validated greenhouse microclimate-crop yield model [4].

Several researchers have approached the multi-objective optimization problem using the techniques of stochastic optimization, including particle swarm optimization and evolutionary methods.

A. Hasni et al. test the use of genetic algorithms versus particle swarm optimization to obtain the optimal set of parameters for the greenhouse itself by simulating a reduced greenhouse model iteratively with the parameters optimized through said methods [16]. They found that their particle swarm implementation outperformed their genetic algorithm approach.

Q. Zou et al. proposed a control strategy developed using model predictive control (MPC), combined with particle swarm optimization [17]. The proposed control strategy was able to reduce energy consumption

due to heating and ventilation while maintaining the same temperature ranges as their conventional controller.

A. Ramírez-Arias et al. addressed the existence of multiple conflicting objectives when it comes to optimal greenhouse control [18]. They define three main objectives: maximizing profit, fruit quality and water-use efficiency. In order to find setpoints that balance these three objectives, they proposed a hierarchical control architecture that takes advantage of the different time scales in which greenhouse-related processes operate. This way, optimal setpoints may be calculated for slower processes (such as crop growth), and then sent to the next "layer" to be adjusted when necessary for faster processes (such as greenhouse air temperature). The use of multiple timescales for both state and environmental variables is found in [19].

H. Hu et al. used evolutionary algorithms to address the issue of determining proportional integral and derivative (PID) control parameters for greenhouse climate control [20]. By defining multiple performance measures as objectives and using NSGA-II, an evolutionary algorithm, they were able to develop a tuning method for PID controllers used in greenhouses that can account for multiple conflicting objectives. In this sense, it is an important precursor of the work reported in this dissertation, which uses a genetic algorithm to optimize PID parameters of various controllers.

M. Mahdavian, S. Sudeng, and N. Wattanapongsakorn similarly used NSGA-II, with the focus lying on optimizing PID controller performance with regards to temperature and light supplementation [21]. In this case, a crop yield model was not considered.

Y. Su, L. Xu, and E. D. Goodman proposed an approach based on adaptive dynamic programming [22], which uses neural networks to estimate the value function and resulting control strategy for the greenhouse. While this approach yielded good results, it relied on calculating "virtual" control inputs for the greenhouse actuators that were not always attainable in a real setting, resulting in cases where a "nearly optimal" set of control inputs were used as a compromise instead.

A notable example utilizing multi-objective optimization methods on greenhouse problems is the use of multi-objective compatible control, or MOCC [23]. The method behind MOCC relies on dividing the optimization process into two layers: the compatible optimization level and the compatible control level. The former works by obtaining Pareto-optimal fronts for control variables while also obtaining additional sub-optimal solutions. The process of obtaining sub-optimal solutions involves relaxing the control variables associated with a point in the Pareto-optimal front, which makes for a useful backbone for creating practical solutions by providing a set of alternatives.

The multi-objective work above, and the work reported in this dissertation all make use of evolutionary computation techniques. These approaches, including especially the genetic algorithm metaheuristic used here, date from the late 1960's and the seminal work of John Holland [24], who first put forth the genetic algorithm, although it was not yet called that. Another milestone was the book of David Goldberg [25], and there have been thousands of papers published since using the genetic algorithm and other derivative forms of evolutionary computation. In the context of multi-objective evolutionary optimization, the article by K. Deb et al. [6] in which NSGA-II was first presented has been cited more than 35,000 times. An excellent overview of the field was presented in [26].

The most important prior work, providing much of the modeling framework for the algorithms developed here, is that of Vanthoor [4]. It provides a complete mechanistic model by incorporating a tomato crop yield model and also addresses potential issues and design considerations when attempting to optimize various aspects of a greenhouse system; he also points out that multi-factorial optimization for greenhouse design is promising due to prior research on complex problems in other application domains.

Part of the design process in Vanthoor's model-based greenhouse design method involves determining the economic analysis and viability of a greenhouse design, along with an optimization step to improve the net financial gain of operating the greenhouse. As mentioned in Section 1.3, his proposed approach utilizes population-based controlled random search, or CRS [5]. Due to the scope of the optimization problem being limited to a small set of greenhouse design elements (to form different combinations with)

and a single objective, this was a satisfactory approach to determining an optimal solution. However, it was imperative that this approach be modified in order to account for our approach being a multi-objective optimization problem with many more parameters to be determined, requiring evaluation of thousands of seasons of simulated greenhouse operation under a variety of climatic conditions in order to allow evolution of optimal and robust controller behaviors. Such simulation would have been impractical with Vanthoor's greenhouse model, as that model used numerical integration methods that often reduced timesteps to millisecond levels to achieve numerical convergence, because of the stiffness of the equations used in his state model. An overview of a model-based greenhouse design method can be seen in Figure 2.1, along with the modification of the optimization process.

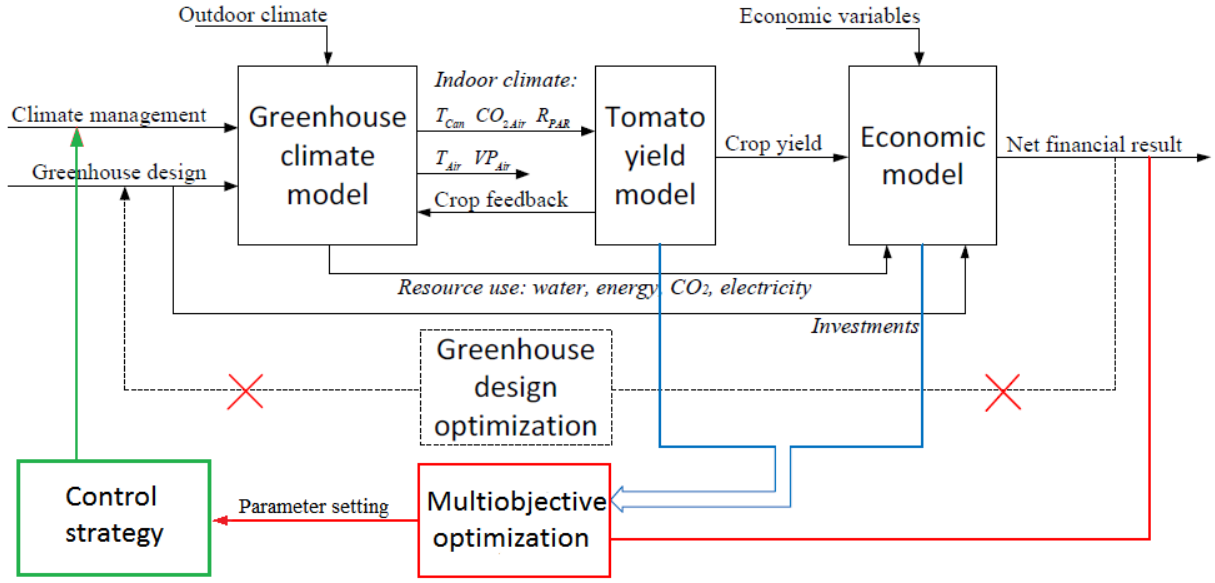

Figure 2.1. In our implementation of Vanthoor's model-based greenhouse design method [4], the optimization step, which was previously aimed towards greenhouse design optimization with a single objective (net financial result), is replaced with a multi-objective optimization step that considers crop yield value and variable costs. Inputs such as the canopy temperature (T_{Can}), greenhouse air CO_2 concentration (CO_{2Air}), photosynthetically active radiation flux density (R_{PAR}), greenhouse air temperature (T_{Air}), and the vapor pressure of the greenhouse air (VP_{Air}) are used in the tomato yield model to obtain the final yield.

Historically, one of the challenges with crop yield modeling is the complexity of their description. Mechanistic models, such as TOMGRO [27], define the processes that drive the tomato crop growth as a set of state variables whose behavior is described by differential equations. Even in its earliest, simplest form, TOMGRO defined 69 state variables, expanding to 574 state variables for the latest version at the

time [9]. This can be daunting not only from the perspective of reproducibility of results when implementing such a model, but also because it makes using these crop yield models to optimize greenhouse control impractical, if not outright impossible. These challenges have led to multiple efforts to simplify the models while maintaining acceptable levels of accuracy [18, 28-30].

Although Vanthoor's primary goal in his work was to describe a methodology for obtaining a greenhouse design suitable for a given climate and locale [4], one of the advantages of his combined model description is that the total number of state variables is relatively small despite including the three models pictured in Figure 2.1 (i.e., greenhouse climate model, tomato yield model, and economic model). To achieve this, some assumptions and simplifications were made by Vanthoor among the three models, but subsequent validation studies confirmed their efficacy. In addition, having an economic model provided the framework for evaluating the viability of a greenhouse design by incorporating the fixed and variable costs of operating a greenhouse (as well as the resulting profit of the tomato crop), allowing for well-informed decision making without relying on the crop yield's dry weight or other physical parameters (such as leaf area index, or LAI) which may be obtuse for non-growers.

Despite these advantages, some challenges remained with Vanthoor's methodology. First, not all the greenhouse design elements included in the greenhouse climate model description contained the necessary information for reliable reproducibility of its intended behavior. Second, the inclusion of certain greenhouse design elements caused an excessive increase in the stiffness of the differential equations describing the greenhouse model, resulting in computational times that made it impractical to use evolutionary algorithms like NSGA-II. Finally, since detailed descriptions on greenhouse controllers and their behavior are not available, it presents difficulties in determining whether an improved greenhouse control strategy would help improve the economic viability of a design.

Since the objective of this thesis is to find more optimal greenhouse control strategies by using evolutionary algorithms, these challenges were addressed by doing the following: 1) greenhouse design elements with insufficient information for reliable reproducibility of their behavior are omitted, 2)

greenhouse design elements that were found to contribute excessive stiffness to the differential equations describing the greenhouse model are omitted, and 3) as a baseline, a greenhouse controller based on Vanthoor's description is implemented as one of the control strategies studied in this thesis, while stating the assumptions necessary for the controller to be functional. Due to the modularity of the greenhouse climate model described by Vanthoor, the omissions made of certain climate control elements (like pad and fan cooling, for example) do not adversely affect the efficacy of the model. Moreover, this approach coincides with the greenhouse design and climate model used in one of his studies. More details on these changes are available in Chapter 4.

3 Modification of a Classical Greenhouse Control Model for Evolutionary Optimization

The contents of this chapter are partially based on our prior published work, and can be found in [31].

The validation step performed by Vanthoor [4] used ordinary differential equation (ODE) solvers with variable time steps in order to solve all model equations. Due to the stiffness of the differential equations in these models and the high number of greenhouse season evaluations that are needed when doing evolutionary multi-objective optimization on a more flexible control architecture, the optimization process and model used by Vanthoor are impractical due to their excessive computational time. In order to address this, the model has been refined such that a fixed integration timestep of 60 seconds can be used, and a fourth-order Runge-Kutta solver is used instead of a variable-step-size solver, which dramatically reduces the runtime of the optimization process.

Vanthoor's climate model is defined by a set of energy and mass fluxes in the form of temperature, CO_2 concentration and vapor pressure. An example of these fluxes and how they relate to state variables can be seen in Figure 3.1. This model assumes that the air inside each compartment in the greenhouse is completely mixed. However, even with this assumption these fluxes (or transfers) of mass and energy between well-mixed compartments often result in high levels of stiffness of the differential equations, and therefore unacceptably high computational costs that make it impractical to use such a model for optimization purposes. Most notably, the fluctuations in temperature induced by using these equations with a fixed and longer timestep are not what physical laws would predict, and the large gradient induced would actually result in mixing between compartments that would dramatically exceed the limits of the climate model. In order to ensure proper mixing, after each step of the ODE solver, we implemented a mixing equation, T_{Mix_SrcDst}, for more even distribution of heat fluxes from a source state variable T_{Src} and a destination state variable T_{Dst}:

$$T_{Mix_{SrcDst}} = \frac{cap_{Src} \cdot T_{Src} + cap_{Dst} \cdot T_{Dst}}{cap_{Src} + cap_{Dst}} \ [°C] \tag{3.1}$$

where cap_{Src} ($J \times K^{-1} \times m^{-2}$) is the heat capacity of the source air compartment of the flux, T_{Src} (°C) is the current temperature from the source air compartment of the flux. These mixing equations conserve heat between the compartments they are mixing and have a strong stabilizing effect on the behavior of the greenhouse climate model. The terms cap_{Dst} and T_{Dst} are similarly defined, but for a destination air compartment *Dst*.

Once T_{Mix_SrcDst} is calculated, the new heat flux, H_{Mix_SrcDst} is defined as:

$$H_{Mix_{SrcDst}} = cap_{Src} \times (T_{Src} - T_{Mix_{SrcDst}}) \; [W \times m^{-2}] \tag{3.2}$$

where cap_{Src} ($J \times K^{-1} \times m^{-2}$) is the heat capacity of the source air compartment of the flux, T_{Src} (°C) is the current temperature from the source air compartment of the flux, and T_{Mix_SrcDst} is the mixed temperature between the source and destination air compartments.

Lastly, the state variables are updated with the heat flux contributed by H_{Mix_SrcDst}:

$$T_{Src} = T_{Src} + \frac{H_{Mix_{SrcDst}}}{cap_{Src}} \; [°C] \tag{3.3}$$

$$T_{Dst} = T_{Dst} + \frac{H_{Mix_{SrcDst}}}{cap_{Dst}} \; [°C] \tag{3.4}$$

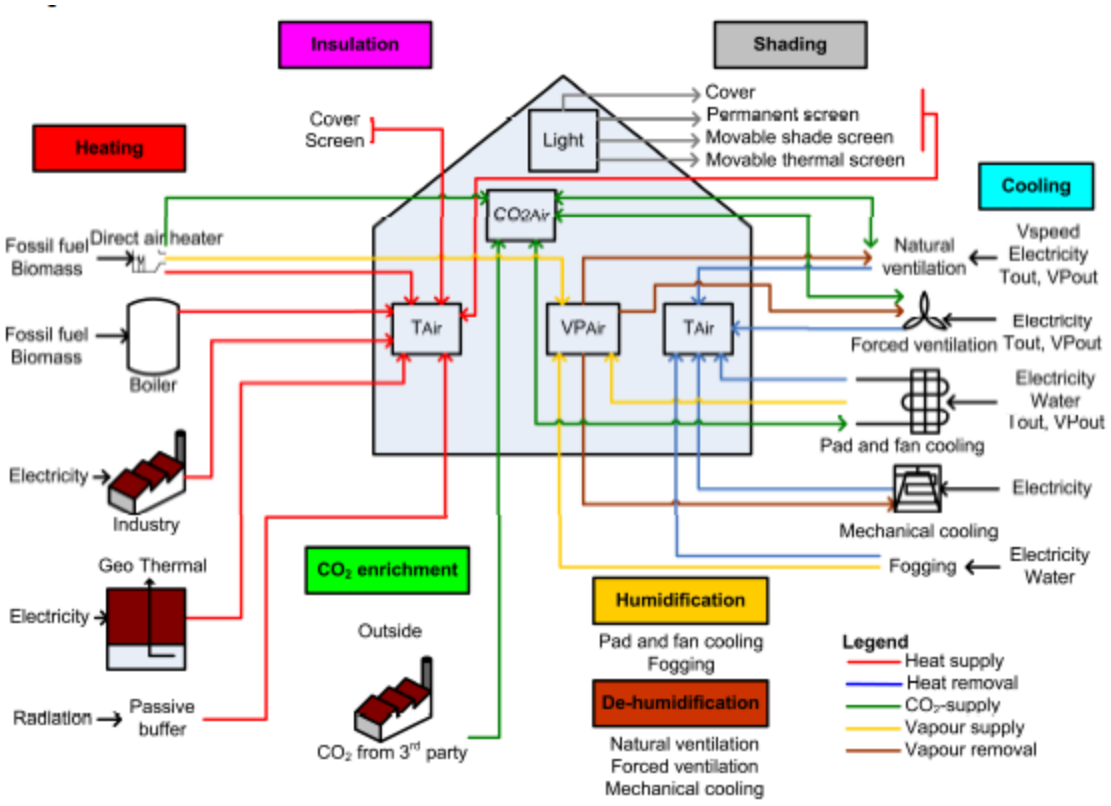

Figure 3.1. Potential design elements used to manage the greenhouse climate. The colored arrows represent the various mass and energy fluxes which dictate the model's behavior [4].

3.1 Individual Control Strategies

One of the major factors in tomato crop cultivation is, under varying environmental conditions, to properly balance temperature with the available light, so as not to waste energy maintaining optimal temperatures while the photosynthetic light is in short supply, unless artificial lighting is available to boost photosynthesis. This will help maximize accumulation of carbohydrates in the plant as well as carbohydrate outflow to its various organs, which ultimately results in maximizing harvestable fruit. Higher temperatures under lower light conditions simply raise the loss of carbohydrates to respiration, which is higher at higher temperatures, so to expend energy to raise canopy temperature under low light conditions is counterproductive. Based on concepts from compatible control [23], we developed an interval controller that is designed to maintain the internal greenhouse temperature within crop-favorable ranges, depending on environmental conditions, which can dramatically affect the energy cost/crop production tradeoff. This controller includes switching rules for decisions about heating,

dehumidification, ventilation, shading, and carbon dioxide injection and is supplemented with conflict-resolving rules and provides for limited user intervention. Figure 3.2 contains an example of such an interval controller.

We have divided the overall control strategy into two main segments: daytime and nighttime control strategies. This allows the greenhouse to have differing temperature ranges during these times when the presence of sunlight affects the usefulness of maintaining a specific range of temperatures. This is further divided during daytime into morning, midday, and evening temperature intervals. In addition, switching times between daytime and nighttime strategies are defined in order to allow the controller to pre-emptively change strategies before sunrise or sunset so that it may accommodate the anticipated changes in temperature and light levels and in desirable temperature and light levels. Greenhouse heating and cooling is accomplished using PID controllers; this includes boilers, cooling pads and ventilation. Each of these has its respective gain parameters which will also be optimized, making part of the optimization process a parameter tuning problem. CO_2 injection is also assumed to be available and used by the control strategy, and a range of CO_2 values is maintained by the controller. Finally, a threshold for global radiation is defined which the controller uses to determine whether deployment of a shading screen is necessary.

To evolve these interval controllers, individuals (i.e., sets of the optimizable parameters of the controller) within the evolutionary algorithm comprise a set of discretized floating point numbers: daytime and nighttime temperature intervals, PID gain parameters (for controlling boiler, cooling pad and ventilation greenhouse elements), carbon dioxide intervals, daytime and nighttime strategy switching times, and maximum global radiation values. During fitness evaluation, these parameters define the behavior of the controller and how it responds to the meteorological data used as input to the greenhouse model.

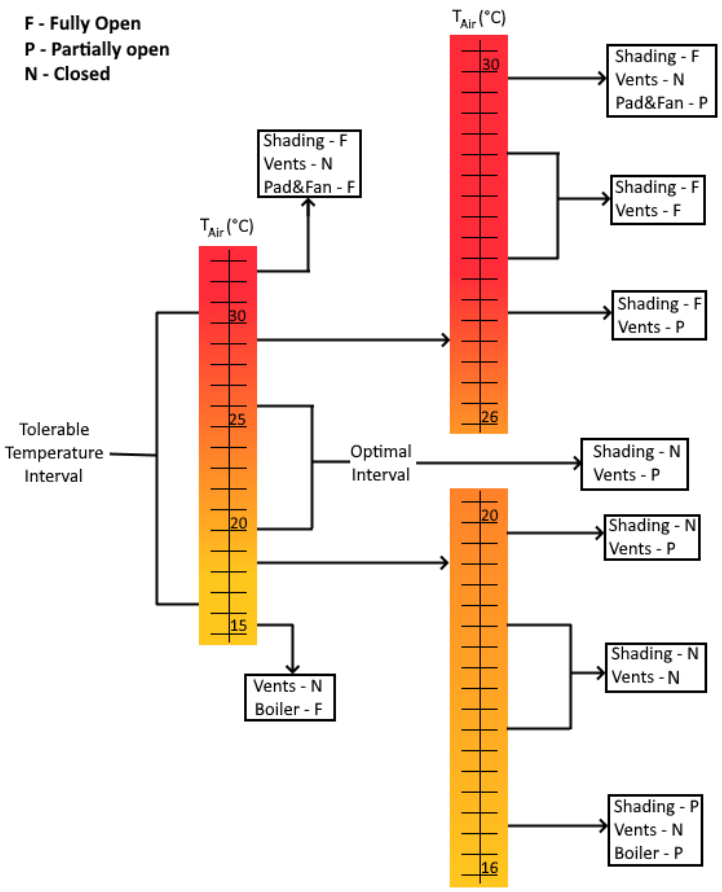

Figure 3.2. Example of an implementation of the proposed interval controller, for some arbitrary time of day. Instead of strictly following temperature setpoints, it allows for a range of temperatures in which some control actions (or none) may be taken as long as the temperature stays within a certain range.

3.2 Objective Functions

The two objectives being optimized are crop production (f_{Yield}) and resource cost (f_{Cost}). These objectives are calculated following the simulation of the greenhouse/crop yield model with an individual control strategy over a predefined time horizon ($[t_0, t_f]$). Specifically, crop production is the finite integration of the carbohydrates flowing into fruit (MC_{Fruit}) during the final development stage (n_Dev). The integral that defines f_{Yield} is described in Eq. (3.5).

$$f_{Yield} = \int_{t_0}^{t_f} MC_{Fruit(n\_Dev-1)Fruit(n\_Dev)} dt \tag{3.5}$$

The resource costs consist of the sum of costs related to resource consumption, including water (p_{Water}), electricity ($p_{Electricity}$), and supplemental CO_2 (p_{CO2}) in Chinese Yuan (CNY, based on locale of the weather data that were available for this study). The cost for each unit of these resources was constant and supplemental lighting was not considered. The capacities associated with each actuator are based on data provided by Vanthoor [4], and a summary of the most important values for actuators associated with climate management can be seen in Table 3.1. Resource costs are driven by the operation of the following actuators: boiler (u_{Boiler}, P_{Boiler}), pad and fan (u_{Pad}, Cap_{Pad}, P_{Pad}), roof vents (u_{Roof}, P_{Roof}), side vents (u_{Side}, P_{Side}), thermal screen ($u_{Thermal}$, $P_{Thermal}$), external shading screen ($u_{Shading\_e}$, $P_{Shading\_e}$), internal shading screen ($u_{Shading\_i}$, $P_{Shading\_i}$), and CO_2 enrichment (u_{CO2}, Cap_{CO2}). The integral that defines f_{Cost} is defined in Eq. (3.6).

$$f_{Cost} = \int_{t_0}^{t_f} \left[\begin{array}{l} p_{Water} * (u_{Pad} * Cap_{Pad}) + p_{Electricity(peak/off\text{-}peak)} * (u_{Boiler} * P_{Boiler} + u_{Pad} * P_{Pad} \\ + \Delta u_{Roof} * P_{Roof} + \Delta u_{Side} * P_{Side} + \Delta u_{Thermal} * P_{Thermal} + \Delta u_{Shading\_e} * P_{Shading\_e} \\ + \Delta u_{Shading\_i} * P_{Shading\_i}) + p_{CO_2} * (u_{CO_2} * Cap_{CO_2}) \end{array} \right] dt \tag{3.6}$$

Assuming both objectives are modeled as minimization problems, one would determine the lower bound for each objective, or ideal point, and try to reach it. However, the tradeoff between these two objectives determines how closely the evolved Pareto set can approach the ideal point.

Table 3.1. Capacities and coefficients for the major greenhouse design elements associated with active climate management. Transmission and reflection coefficients for near infrared (NIR), far infrared (FIR), and photosynthetically active radiation (PAR) of the internal shading screen, external shading screen, and thermal screen are included.

Parameter Description	Parameter Name/Symbol	Unit	Value
Capacity of the CO_2 enrichment system	Cap_{CO2}	mg/s	4.3×10^5
Capacity of the air flux through the pad and fan cooling system	Cap_{Pad}	m^3/s	50
Capacity of the boiler heating system	Cap_{Boil}	Megawatts (MW)	1
NIR reflection coefficient of the internal shading screen	$\rho_{Shading\_iNIR}$	-	0.3
PAR reflection coefficient of the internal shading screen	$\rho_{Shading\_iPAR}$	-	0.3
FIR reflection coefficient of the internal shading screen	$\rho_{Shading\_iFIR}$	-	0
NIR transmission coefficient of the internal shading screen	$\tau_{Shading\_iNIR}$	-	0.6
PAR transmission coefficient of the internal shading screen	$\tau_{Shading\_iPAR}$	-	0.6
FIR transmission coefficient of the internal shading screen	$\tau_{Shading\_iFIR}$	-	0.1
NIR reflection coefficient of the external shading screen	$\rho_{Shading\_eNIR}$	-	0.2
PAR reflection coefficient of the external shading screen	$\rho_{Shading\_ePAR}$	-	0.2
FIR reflection coefficient of the external shading screen	$\rho_{Shading\_eFIR}$	-	0
NIR transmission coefficient of the external shading screen	$\tau_{Shading\_eNIR}$	-	0.7
PAR transmission coefficient of the external shading screen	$\tau_{Shading\_ePAR}$	-	0.7
FIR transmission coefficient of the external shading screen	$\tau_{Shading\_eFIR}$	-	0.1
NIR reflection coefficient of the thermal screen	$\rho_{ThermalNIR}$	-	0.7
PAR reflection coefficient of the thermal screen	$\rho_{ThermalPAR}$	-	0.7
FIR reflection coefficient of the thermal screen	$\rho_{ThermalFIR}$	-	0.45
NIR transmission coefficient of the thermal screen	$\tau_{ThermalNIR}$	-	0.25
PAR transmission coefficient of the thermal screen	$\tau_{ThermalPAR}$	-	0.25
FIR transmission coefficient of the thermal screen	$\tau_{ThermalFIR}$	-	0.11

3.3 Greenhouse Model

To estimate fruit production and resource cost for an individual control strategy, we have implemented and adapted a comprehensive greenhouse and tomato crop model [4]. The greenhouse climate is based on an energy and mass balance model, while the tomato growth (based on *Lycopersicon esculentum* L. *cv.* Pitenza [32]) is described by a buffer of carbohydrates that accumulates with photosynthesis, and must

balance the distribution of these carbohydrates among all plant organs: the stems, leaves, and fruit (if fruit set has occurred). The tomato cultivar was chosen based on the coefficients that were available to convert from dry matter to fresh weight [32]. Although flexible enough to fit a variety of realistic greenhouses, the model implementation is very detailed and computationally expensive, especially considering that a new simulation is required for every unique individual encountered during evolutionary search. We therefore performed several model simplifications, including the reduction of time resolution by forcing a fixed time step of 60 seconds, merging of state variables (e.g., reducing overall depth considered for the soil temperature from 5 layers to 1), and model revisions on flux calculations such as those described in Eqs. (3.1 – 3.4). Based upon sensitivity analyses in the simulation domain, these modifications appear to have negligible impact on the overall behavior of the model and decrease computation time dramatically.

3.4 Meteorological Data Acquisition and Configuration

We used a meteorological database consisting of hourly weather data collected over six years in the Shanghai area [33] as weather input to the greenhouse/crop yield model. A summary of the mean values for the weather data used in this chapter is shown in Figure 3.3. The data required by the model includes external temperature, humidity, wind speed, carbon dioxide concentration, and solar radiation. These were extracted and linearly interpolated to a finer resolution as needed.

Considering the typical time scales of greenhouse systems, we selected 5 minutes as the constant control interval. This provides a small enough interval for finer greenhouse control while allowing a fixed time step of the same size. Unless otherwise specified, simulations were performed over a 300-day production period for each individual in the population. For reproducibility of results, other simulation lengths may be used. In addition, multiple runs with different weather inputs were used to ensure the robustness of the final Pareto-optimal set. To avoid over-fitting of resulting control strategies, leave-one-out cross-validation [34] was used to structure the data for training and independent validation.

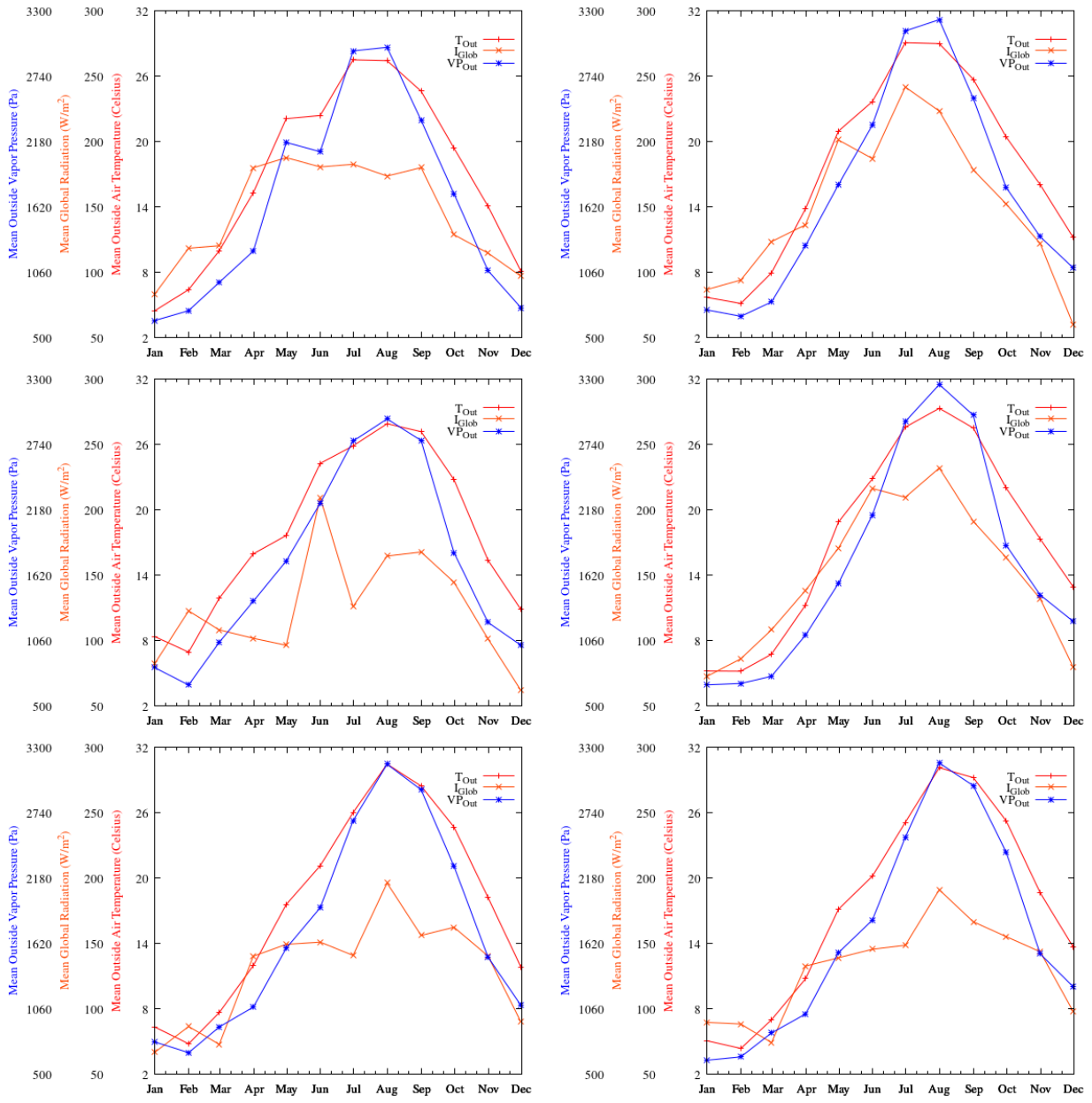

Figure 3.3. Summary of the monthly mean values for the outside air temperature (T_{Out}), global radiation (I_{Glob}), and outside vapor pressure (VP_{Out}) for the 2007 – 2012 years in the Shanghai region. An ambient CO_2 concentration of 340 ppm was assumed.

3.5 Description of Early Evolved Results

Figure 3.4 plots the Pareto-optimal sets from three independent simulations of our evolutionary algorithm (hollow marks, lower left). Shown here are the values of the two different objectives, resource cost and crop production. To improve interpretation, we report the negative harvestable fresh fruit (i.e., -1×kg/m^2) such that the goal for both objectives is to minimize their respective values as much as possible. Each of

the three replicates was trained on different weather data; Figure 3.4 shows the objective values for weather data that were not used during training (the "left out" data) but used for this simulated season. As shown here, productivity ranged from 5.5 to 10.5 kg/m^2 per year, while resource cost ranged from 62,100 to 113,000 CNY per year. Examining the parameters of the resulting individual control strategies showed that a relatively high nighttime temperature was always preferred if high productivity was desired, around 18 degrees Celsius. This would guarantee the tomato crop would remain inside an optimal range of temperatures that would prevent crop growth inhibition. On the other hand, low-yield points in the Pareto set had lower resource costs due to having lower nighttime temperatures overall, around 12 – 14 degrees Celsius. Intuitively, lower nighttime temperatures are preferred for the crop since it reduces plant respiration and maintaining higher nighttime temperatures will result in increased heating costs without immediate benefit to crop growth. However, the increased crop production resulting from these higher nighttime temperatures suggests that it is beneficial to maintain these temperatures in anticipation of daytime, allowing for the greenhouse to reach an optimal temperature for crop growth once sunlight is available.

3.6 Result Comparison

To compare the effectiveness of the optimization process, we evaluated a classical setpoint-based controller [4] on the same greenhouse/crop yield model and weather data. The isolated solid points in Figure 3.4 are the objective values corresponding to this controller on the three sets of weather data. Compared to the setpoint controller, the average evolved strategy reduced resource cost by 10.2% and increased yield by 12.9%. Moreover, we found a 19.9% increase in yield given the same resource cost, and a 32.5% decrease in resource cost given the same yield.

Some understanding of the differences between the evolved control strategies and the set-point controller can be gained by examining the accumulated actuator usage for the boiler and the external shading screen. As shown in Figure 3.4a, a randomly selected evolved controller (dotted line) used both the boiler and

shading screen less frequently than the set-point controller (solid line), which lowered the resource cost and increased photosynthetic activity, respectively.

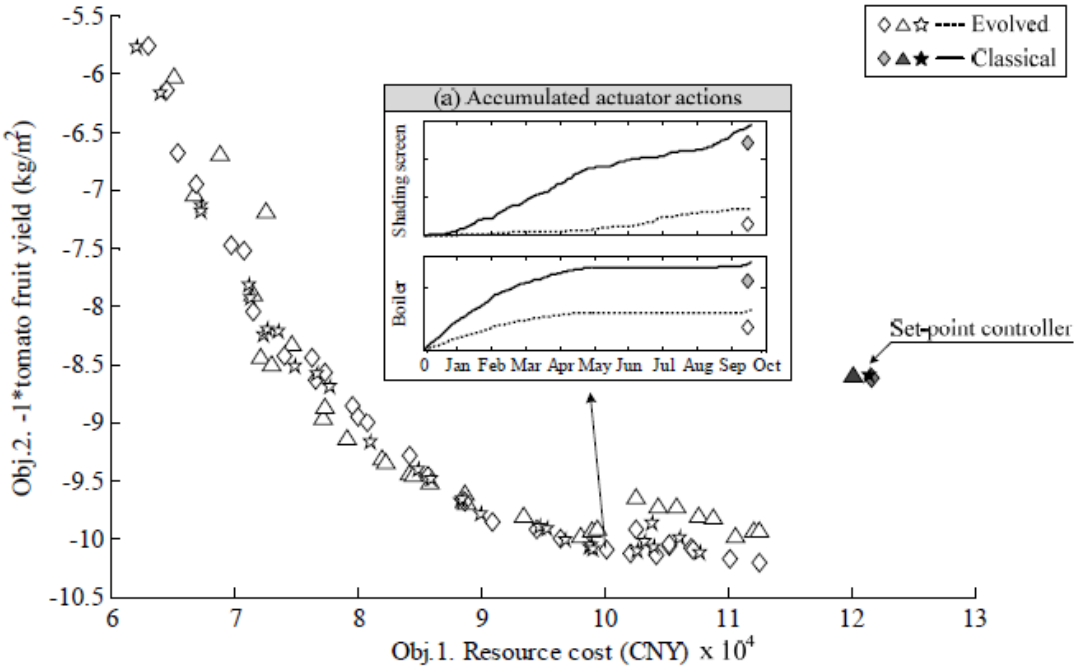

Figure 3.4. Yearly resource cost and crop yield for three independent Pareto-optimal sets on validation weather data (hollow points). Objective values for a classical setpoint controller on the same weather data (solid points). Accumulated boiler and shade screen usage for an evolved strategy compared to the setpoint controller (a).

3.7 Control Strategy Selection

The three Pareto sets in Figure 3.4 all share the same trend. Picking the diamond set (◊) as an example, all the solutions in this set are relatively evenly distributed throughout objective space. This leads to an interesting question: How should a user select a strategy to control a greenhouse? While expert knowledge plays an important role in this decision-making process, there are several approaches that can be identified: (1) maximum fruit yield, (2) maximum affordable resource cost, (3) maximum average fruit yield per unit of resource, (4) minimum resource input per unit fruit yield, and (5) expected economic return. While approaches (1) and (2) do not explicitly take both objectives into account, approaches (3) and (4), which specifically acknowledge both objectives, are likely to select a control strategy near the

middle of the Pareto set. Approach (5) would require a more sophisticated economic analysis that goes beyond determining energy costs of the greenhouse during a crop cycle.

3.8 Discussion

Although these results are encouraging, additional refinement of the microclimate and plant models is necessary. Once compared with results reported by Vanthoor, it is clear that there are some drawbacks with the model implementation in these early results: the crop yield is inadequate for the weather and the greenhouse configuration used (which included roof and side ventilation, cooling pads and boiler heating). Since this type of greenhouse configuration provides excellent climate control that ensures the tomato crop can grow in near-optimal conditions, very high crop yields were expected, but not attained in this case. Additionally, such a greenhouse configuration would be very costly to implement and would require a proportionally large return on investment to be worthwhile. In contrast, according to Vanthoor's results, a simple "Parral"-type greenhouse, which only includes manual ventilation and whitewash, could provide more than double the yield of a "high resource cost" type solution depicted in Figure 3.4 [4]. To address this, the greenhouse crop yield model was revisited, and improvements in the model resulted in increased crop yield thanks to increased canopy PAR absorption which allowed us to better validate the results. In addition, various performance measures were proposed and used in this thesis to narrow down solutions from a large pool of candidates, as the process of control strategy selection described earlier is still relatively vague.

First, while it is possible to find a very good solution that contains desirable trade-offs between operational costs and yield, it is important to consider the effect of any perturbations in the decision space of the solution. For example, it is possible that during the deployment of a candidate control strategy, the greenhouse system is unable to strictly enforce each of the parameters inside the chromosome. This can lead to a variety of undesirable effects; these range from a considerable reduction in fitness to a solution becoming financially unviable (by having a negative net financial result, or NFR, covered in Section 7.2). One of the earlier proposals to measure robustness in evolutionary algorithms can be seen in [35], which

involves obtaining the effective fitness of an individual by calculating the mean with respect to its neighboring individuals. Figure 3.5 shows the effect of determining mean fitness around the neighborhood of a Pareto-optimal set of solutions.

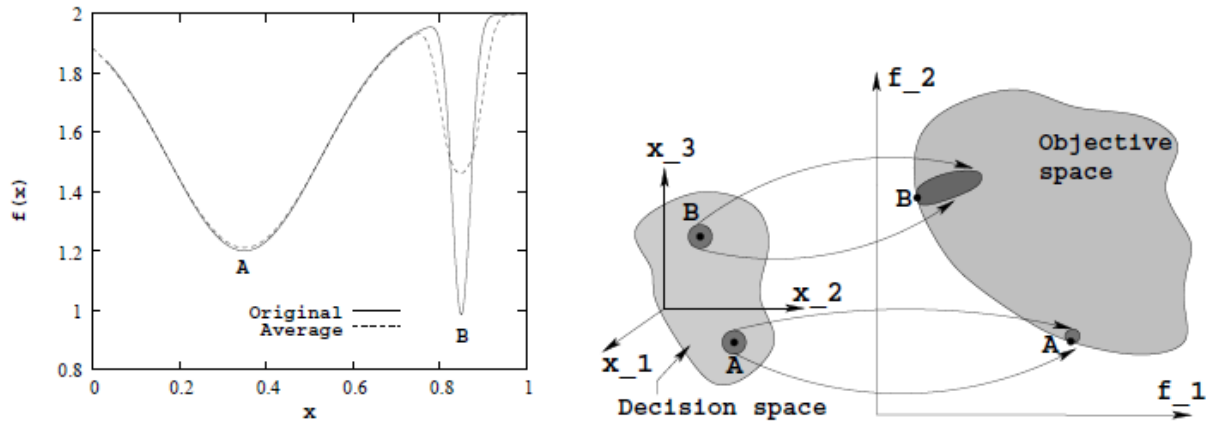

Figure 3.5. The image on the left portrays the effect of changing x in a single-objective problem. The image on the right shows the effect of changing x1, x2 and x3 in a two-objective problem. [35]

The robustness of the evolutionary process is examined next. Multiple independent NSGA-II runs were performed and the trends of the Pareto-optimal set over time were examined for consistency. If these runs converge on a similar Pareto-optimal set over many generations, it will help confirm that NSGA-II is appropriately exhausting the search space and approaching a global optimum set of solutions. To this end, we used the normalized hypervolume of the Pareto-optimal set as a performance measure for multiple independent runs. This performance metric can also be used as part of a procedure to compare different types of evolved controllers to assess their feasibility (with respect to each other). These results are reported in Section 7.3.

Finally, robustness against variations in weather conditions as well as control setpoints was examined. For the former, in order for a solution to be of practical use to a decision maker, it must be able to perform reasonably well with a variety of weather patterns. To achieve this, each individual in the population is examined against multiple sets of weather data. The choice of which weather data sets are used depends largely on the location and user preference. Results of this study are reported in Section 7.4. For the latter,

we introduce perturbations on the evolved control setpoints and measure its negative impact on each objective. We then summarize this impact by calculating the area of the enclosing polygon created from the perturbations, which provides a straightforward method for sorting solutions based on their robustness to these perturbations. Details on this approach, as well as the results are reported in Section 7.5.

4 Evolution of a Classical Controller Using Improved Model

The contents of this chapter are partially based on our prior published work, and can be found in [36].

In the previous section, we detailed some of the major changes and their rationale in a modified version we produced of the microclimate-crop yield model described in [4]. Despite the considerable performance improvements, the difference between the results obtained and validated by Vanthoor and the simulated crop yields from the modified model was unacceptably high, even though the dynamics of the two models appeared quite similar. Thus, we proposed implementing the microclimate-crop-yield model largely as Vanthoor presented it but making major modifications to the control strategies themselves after consideration of Vanthoor's published results. Due to the modular nature of Vanthoor's combined model, we were able to leave out extraneous elements that need not be included in the configurations of a greenhouse we chose to simulate. While this approach is still significantly more computationally expensive than our model reported in Chapter 3, these configurations are much more amenable to optimization through evolutionary computation, as the stiffness of their underlying differential equations does not have a large effect on the runtime of the ODE solver.

In this section we show first our attempt at replicating the behavior of a classical controller designed for tomato crops to validate the agreement of our revised model with earlier published work. Second, we use NSGA-II to evolve microclimate control setpoints based on an earlier model-based greenhouse design method, which includes an economic model driven by the microclimate-crop yield model.

4.1 Combined Model Overview

All the parameters required to describe the characteristics of the greenhouse design and climate control, including the economic parameters associated with them, were obtained from Vanthoor's greenhouse case study in Almería, Spain [4].

4.1.1 Microclimate-Crop Yield Model

The microclimate-crop yield model consists of a mechanistic model that describes mass and energy flows among the crop, greenhouse compartments, surrounding greenhouse construction elements and the

outside weather, inducing changes over time in temperature, CO_2 concentration, plant weight and vapor pressure. These flows are defined as a set of differential equations, which allows the use of ordinary differential equation solvers. The combined model state variables and their respective differential equations were implemented as described by Vanthoor, with minor model simplifications.

The state variables of the tomato crop yield model represent the accumulation of carbohydrates in the plant from photosynthesis and how they are distributed to fruits, leaves, stems, and roots. Other essential plant processes, such as maintenance and growth respiration, plant transpiration and fruit set, are modeled as well. Irrigation and fertigation are assumed to be non-limiting and their cost is included in the economic model. The final tomato crop yield is obtained by accumulating the amount of dry matter that is harvested in real time after fruit set begins, and then converting it to fresh weight.

4.1.2 Economic Model

The economic model's primary goal is to calculate the annual net financial result. Vanthoor defines the net financial result as:

$$Q_{NFR}(t_f) = -Q_{Fixed} + \int_{t=t_0}^{t=t_f} \dot{Q}_{CropYield} - \dot{Q}_{Var}\, dt \tag{4.1}$$

where $Q_{CropYield}$ (€×m^{-2}×year^{-1}) is the value of the tomato crop, Q_{Var} (€×m^{-2}×year^{-1}) consists of the variable costs (costs associated with the crop, resources used and labor), and Q_{Fixed} (€×m^{-2}×year^{-1}) represents the cost of all tangible assets that do not depend on crop growth. For consistency and ease of comparison, euros (€) will be used as the currency for this (and subsequent) chapters.

Since Q_{Var} and $Q_{CropYield}$ both depend on state variables that change over time, they are also treated as state variables themselves in the combined model. Market price fluctuations and tomato crop quality were not considered, and a mean tomato price is assigned to each greenhouse design instead based on the climate control techniques available and market prices observed by Vanthoor during the entire growing season.

4.1.3 Greenhouse Design and Control

Ten greenhouse designs were evaluated in the economic model study by Vanthoor in [4]. A classical control strategy was used, which supports a combination of static temperature and relative humidity setpoints and a dynamic CO_2 setpoint. The CO_2 setpoint increases linearly with outside global radiation and decreases linearly with respect to the current roof and side ventilation opening.

The available climate management techniques included roof and side ventilation, a retractable thermal screen, whitewash, indirect air heating, boiler heating, a fogging system, and a CO_2 enrichment system. Based on the layout of the greenhouse designs described by Vanthoor, the thermal screen is assumed to be positioned between the greenhouse air compartment and top compartment. The setpoint is disabled if its associated greenhouse construction element is not included in the design. For example, the dynamic CO_2 setpoint requires a CO_2 enrichment system, otherwise it will remain unused. All the greenhouse designs that were simulated in this chapter assume that the greenhouse structure is covered in a single polyethylene (PE) layer which provides a global transmission of 57% (54% with a thermal screen deployed), with a rectangular shape of 200 x 50 meters, resulting in a floor area of 10000 m^2. Whitewash applications vary depending on the time of year and can be either result in a 25% or 50% decrease of the global transmission (these values were decreased further by 50% if a fogging system was present). A summary of the important values associated with the greenhouse design elements is in Table 4.1, and further details can be found in [4].

Table 4.1. Capacities for the major greenhouse design elements associated with active climate management.

Parameter Description	Parameter Name/Symbol	Unit	Value
Capacity of the CO_2 enrichment system	Φ_{ExtCO2}	mg/s	1.39×10^4
Capacity of the fogging system	Φ_{Fog}	kg/s	1.39
Capacity of the indirect air heating system	Cap_{Blow}	Megawatts (MW)	0.50
Capacity of the boiler heating system	Cap_{Boil}	Megawatts (MW)	1.16

4.2 Model Validation Results

Vanthoor conducted a study in which ten different types of greenhouse designs were simulated, with the goal of finding the design with the best net financial result. These results were provided for one growing season (2006-2007) and show a variety of useful outputs, such as the crop yield, crop economic return, fixed costs, and variable costs. To help validate our model implementation, these results were used to compare against ours.

Due to the limited availability of the weather data used by Vanthoor in his studies, we used software to estimate weather data based on a given location and time of year (with additional details available on Section 4.3.2). The average outdoor climate values in Table 4.2 show that there are some discrepancies between the original and estimated climatic input values. Most notably, the estimated temperature mean is significantly lower, while having greater extremes. However, the average global radiation, relative humidity and wind velocity values are more similar, of which global radiation is particularly important because it strongly affects both microclimate and photosynthetic rate.

Table 4.2. Average outdoor climate values provided by a) Vanthoor [4], compared with b) the estimated weather for the same site used in this thesis.

	Period	T_{out} *(°C)*	T_{out} *<5% (°C)*	T_{out} *>95% (°C)*	*Global radiation* $(MJ \times m^{-2} \times day^{-1})$	*RH (%)*	v_{wind} *(m/s)*
a)	2006-2007	17.7	9.1	27.4	16.9	69.7	2.9
	2007-2008	17.8	10.2	27.7	17.1	67.7	3.3
	2008-2009	17.2	8.3	28.1	17.2	67.9	3.3
b)	2006-2007	14.4	3.7	29.4	16.4	58.4	2.6
	2007-2008	15.5	5.3	29.4	16.9	58.9	2.7
	2008-2009	15.8	4.9	31.5	17.7	56.7	2.8

Table 4.3 contains a summary of our economic model output compared with the original simulated output. The outputs consist of tomato crop yield ($kg \times m^{-2}$), crop value ($€ \times m^{-2} \times year^{-1}$), variable costs (VC, $€ \times m^{-2} \times year^{-1}$) and net financial result (NFR, $€ \times m^{-2} \times year^{-1}$) of ten greenhouse designs. Parral (P) is a type of "low-tech" greenhouse with only roof and side ventilation. The greenhouse construction elements used

for the different designs are as follows: a whitewash application (W), a CO_2 enrichment system (C), a fogging system (F), an indirect air heating system (H_), and a boiler heating system (H). Fixed costs are not shown, as they are identical for both cases. The main sources of discrepancy in the variable costs come from CO_2 utilization being overestimated and water costs being underestimated. The CO_2 enrichment system was treated as an on–off controller, which, combined with the controller update interval of five minutes, resulted in excessive CO_2 utilization. This can be remedied by using a smaller update interval for controlling the CO_2 enrichment system. Insufficient plant transpiration is the cause of low water costs, as this plant process determines the amount of water that is used for irrigation. We used a mean tomato price for the entire growing season while Vanthoor used a mean weekly tomato price, thus conversions from crop yield to crop value will differ. Despite these discrepancies and the differences in the estimated weather, Figure 4.1 shows the crop yield's response to increasing technology is similar. Ideally, matching historical weather data should be used for more accurate comparison, but such data were not available.

Table 4.3. Simulation comparison results between a) Vanthoor [25], compared with b) our simulated results for the 2006 - 2007 season.

a)	*P*	*W*	*WC*	*WF*	*WFC*	*WH*	*WH*	*WHC*	*WHF*	*WHFC*
Yield	21.88	23.99	25.78	26.45	28.15	27.71	28.35	31.89	31.34	35.03
Value	9.77	11.01	11.86	12.33	13.15	13.65	14.89	17.22	16.42	18.47
VC	6.59	6.82	7.82	7.17	8.25	9.31	8.88	10.18	9.28	10.65
NFR	-0.25	-0.31	-0.84	0.15	-0.49	-0.92	-0.94	-0.29	-0.32	-0.03
b)										
Yield	22.42	24.24	25.25	25.23	26.44	29.86	33.57	36.09	35.27	37.79
Value	9.28	10.82	11.75	11.03	12.06	15.03	17.85	18.85	17.76	19.03
VC	6.38	6.62	7.89	6.76	8.9	10.46	9.32	10.68	9.52	10.98
NFR	-0.53	-0.29	-1.02	-0.74	-2.24	-0.69	1.58	0.84	0.78	0.19

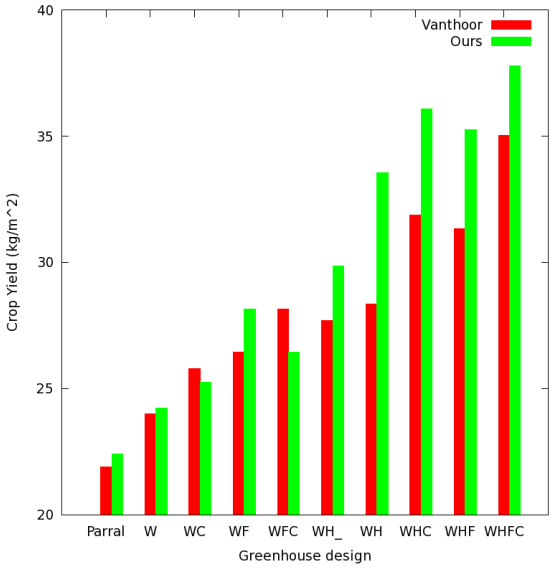

Figure 4.1. Vanthoor predicted tomato yield vs our predicted yield as a function of greenhouse technology level.

4.3 Greenhouse Simulation and Evolution Setup

4.3.1 Greenhouse Design

Out of the ten available designs, we chose the greenhouse design with the most climate management techniques possible (i.e., "highest tech"). This provides us with the highest number of setpoints to evolve, and therefore maximizes the search space for optimizing the originally published control strategy.

The microclimate-crop model is implemented in C++, combined with the Open BEAGLE framework for evolutionary computation [37] that supports NSGA-II, modified to allow parallelization using the OpenMP API [38]. To solve the differential equations that govern the microclimate-crop model, we used a library that supports an adaptive step-size, fourth-order Runge-Kutta method [39].

4.3.2 Outdoor Climate Data

Because Vanthoor did not make available the weather data used in his research, we used a meteorological service [40] that uses weather prediction models to approximate the climate data for a specified date and locale—namely, Almería, Spain, the location Vanthoor used in his thesis to evaluate his economic model. The latitude and longitude coordinates and height above sea level were used as inputs to obtain hourly climate data for the same time periods in 2006 – 2009. Outdoor CO_2 levels were obtained by interpolating

monthly global CO_2 measurements provided by the National Oceanic & Atmospheric Administration [41]. The average values of the output provided by the estimated weather is summarized in Table 4.2.

4.3.3 Control Strategy Implementation

Some assumptions were necessary for the controller implementation. Unless otherwise specified, all actuators operate on an on-off basis, including roof and side ventilation. First, the controller has an update interval of five minutes. Second, the boiler valve output is determined by a PID controller, with gain parameters (not shown) evolved ahead of time using NSGA-II, to match the fuel consumption costs reported by Vanthoor. Third, the thermal screen is retractable in two stages. Fourth, the fogging system operates for a maximum of 120 seconds in any five-minute interval. This is based on practice [42] to avoid wetting the leaves and potentially damaging the plants due to the salt content in the fogging system's water reservoir[1].

4.3.4 NSGA-II Initialization

Evolution parameters can be seen in Table 4.4. The parameters were pragmatically chosen based on the computing resources available and the size of the chromosome. Each simulation was run on a computer with two 2.4Ghz 14-core Intel Xeon E5-2680v4 processors, for a maximum of 28 cores. Since the simulation is parallelized by assigning one individual to each core, the population size is set to multiples of 28 to minimize downtime from unused cores. The number of generations was determined based on the approximate amount that can be completed in 96 hours.

Table 4.4. NSGA-II parameters used for this study.

Parameter	Value
Population size	28 - 84
Generations	360 - 1000
Two-point crossover probability	0.3
Uniform mutation probability	0.04

[1] In some cases, we may show examples of evolved control strategies that assume that the fogging system can operate without any limitations (i.e., up to 5 minutes at a time). Such cases are only used for easier interpretation of results and will be labeled accordingly.

4.3.5 Chromosome Representation

The chromosome consists of values stored in an integer vector that are converted to floating point values when used in the model. Before using a value from the chromosome, the integer value is converted to a floating-point number using the specified range and step size. This makes the search process more efficient by eliminating differences that are not significant in practice. Since the goal is to optimize greenhouse control setpoints, the chromosome simply consists of a combination of static setpoint values and the thresholds on climatic variables used to calculate the dynamic CO_2 setpoint. $T_{AirVentOn}$ defines the greenhouse air temperature above which roof and side ventilation is always open. Similarly, $T_{AirVentOff}$ defines the greenhouse air temperature below which roof and side ventilation is always closed. $RH_{AirVentOn}$ is the greenhouse air relative humidity threshold above which ventilation is turned on. $CO_{2AirVentOn}$ is the greenhouse air CO_2 concentration below which ventilation is turned on (to replenish the greenhouse air CO_2 concentration back to ambient levels). $T_{AirBoilOn}$ is the greenhouse air temperature below which the boiler heating system is turned on. $T_{OutThScrOn}$ is the outside air temperature below which the thermal screen is deployed. The dynamic CO_2 setpoint is a function of: $CO_{2AirExtMax}$, which determines the upper bound for the CO_2 setpoint, $CO_{2AirExtMin}$, which determines the lower bound of the CO_2 setpoint and $I_{GlobMax}$, which determines the global radiation threshold above which the CO_2 setpoint reaches its upper bound. Below that, the setpoint decreases linearly towards its lower bound with global radiation. The chromosome with its range of values and desired resolution can be seen in Table 4.5.

Table 4.5. Chromosome representation. Values in this range are stored as integers after multiplication with an appropriate factor.

Parameter	**Range**	**Step Size**
$T_{AirVentOn}$ (°C)	[10, 30]	0.1
$T_{AirVentOff}$ (°C)	[10, 30]	0.1
$RH_{AirVentOn}$	[0.1, 1]	0.01
$CO_{2AirVentOn}$ (ppm)	[100, 500]	0.1
$T_{AirBoilOn}$ (°C)	[10, 30]	0.1
$T_{OutThScrOn}$ (°C)	[10, 30]	0.1
$CO_{2AirExtMax}$ (ppm)	[500, 1000]	0.1
$CO_{2AirExtMin}$ (ppm)	[100, 500]	0.1
$I_{GlobMax}$ ($W \times m^{-2}$)	[200, 1000]	0.1

4.3.6 Fitness Function

The fitness function consists of the economic model's output as described in Eq. (5.1), divided into two objectives: the economic value of the crop yield and the variable costs. We use the negative of the crop value so that both objectives are treated as minimization problems. We use three consecutive growing seasons based on the estimated weather data in the growing periods summarized in Table 4.6, with a pair of objective values generated for each season. To determine the final values for each objective, we choose the worst-case objective pair of all three (i.e., the year that yields the worst net financial result).

Table 4.6. Greenhouse simulation parameters used for evolving setpoints in Almería, Spain case study. "WHFC" denotes the use of whitewash (W), a boiler heating system (H), a fogging system (F) and a CO_2 enrichment system (C).

Parameter	Value
Growing periods	August 1st, 2006 – July 1st, 2007
	August 1st, 2007 – July 1st, 2008
	August 1st, 2008 – July 1st, 2009
Simulation Length	334 days
Coordinates	36°48'N, 2°43'W
Height above sea level	151 meters
Greenhouse design	WHFC

4.3.7 Post-Pareto Front Processing

Once a satisfactory Pareto front is obtained, the fitness of each individual in the population is recalculated using climate data from a new weather season to test the efficacy of evolved solutions against "unknown" weather (sometimes called a validation step). The population is also sorted based on the net financial result, which allows us to easily prune solutions that either perform worse than the original setpoints or otherwise fall below an acceptable threshold for net financial result.

4.4 Pareto Front, Validation Step and Sorting

4.4.1 Pareto Front

The Pareto front is shown in Figure 4.2, and it is compared with the original setpoints based on a classical control strategy by Vanthoor [4]. Although not many solutions dominate the original setpoints, the original is clearly not Pareto-optimal. Optimizing with a larger population size of 84 was beneficial

despite the added computational cost per generation, as it contained a better distribution of non-dominated solutions with the same simulation time (96 hours).

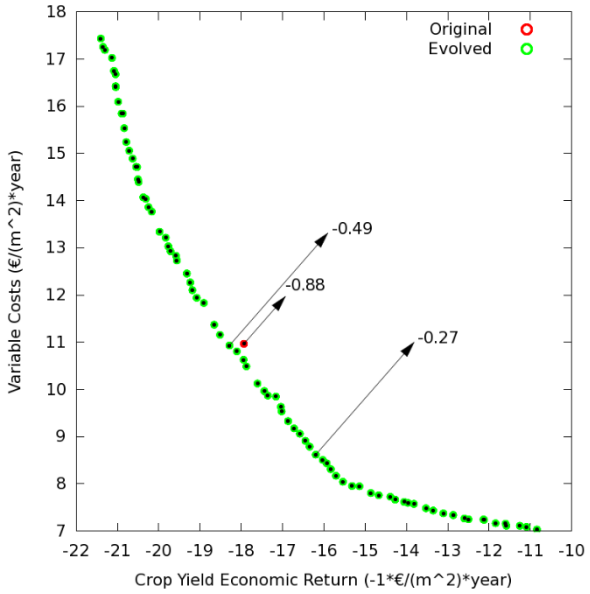

Figure 4.2. Pareto front consisting of the evolved control setpoints compared against the original control setpoints. The worst-case net financial result of the original setpoint and two evolved setpoints is shown.

4.4.2 Validation Step

To verify the efficacy of the evolved solutions, we test the output of the economic model when using a new season of estimated weather data from the same locale (2009-2010). The results for all four growing seasons are summarized in Table 4.7 and show that the evolved setpoints performed reasonably well with "unknown" weather from the same locale.

Table 4.7. Economic model output (€×m^{-2}×year^{-1}), comparing the original setpoints vs a "low-cost" solution and a "high-value" solution obtained from the Pareto front in Fig. 4. Net financial results (NFR) for all four years are added up.

	Original			**Low Cost**			**High Value**		
Period	**Crop Value**	**Var. Costs**	**NFR**	**Crop Value**	**Var. Costs**	**NFR**	**Crop Value**	**Var. Costs**	**NFR**
2006-2007	19.03	10.98	0.19	17.29	8.65	0.79	19.39	10.88	0.66
2007-2008	20.69	11.41	1.44	18.72	9.11	1.76	21.10	11.42	1.83
2008-2009	17.95	10.97	-0.88	16.20	8.62	-0.27	18.29	10.93	-0.49
2009-2010	18.90	10.96	0.09	17.23	8.76	0.62	19.29	10.95	0.49
Total			**0.85**			**2.91**			**2.49**

4.4.3 Sorting Results

Table 4.8 shows a partial list of the population after it is sorted by the net financial result. The larger population size was beneficial, as it was able to find solutions with a superior net financial result with greater frequency. The original setpoints yielded a worst-year NFR of -0.88, so most of these results are superior–all are superior for population size 84, which is clearly preferable.

Table 4.8. Worst-year net financial result (€×m^{-2}×year^{-1}) of the nine best evolved solutions (in terms of NFR) in optimization runs with different population sizes.

NFR	
Pop. Size = 84	Pop. Size = 28
-0.28	-0.36
-0.30	-0.37
-0.31	-0.42
-0.32	-0.62
-0.32	-0.67
-0.32	-0.75
-0.32	-0.78
-0.34	-1.00
-0.34	-1.18

Table 4.9. Original setpoints compared with setpoints of two evolved solutions: a "low-cost" solution and a "high-yield" solution.

Parameter	Original	Low-Cost	High Yield
$T_{AirVentOn}$ (°C)	23	22.5	22.5
$T_{AirVentOff}$ (°C)	20	26	24.6
$RH_{air\_vent\_off}$	0.90	0.70	0.82
$CO_{2air\_vent\_off}$ (ppm)	200	171.6	164.3
$T_{air\_boil\_on}$ (°C)	16	10	15.7
$T_{out\_ThScr\_on}$ (°C)	18	16.3	16.7
CO_{2Air_ExtMax} (ppm)	850	508.7	585.8
CO_{2Air_ExtMin} (ppm)	365	266.4	112.6
$I_{GlobMax}$ ($W \times m^{-2}$)	500	875.8	206.2

4.4.4 Decision Making

Since the worst-case measurements for the net financial result were all negative, these could all be considered "unviable" solutions. However, these evolved setpoints still outperform the original setpoints, and depending on the planning horizon, the grower can consider other seasons that have a positive net financial result and assess whether the risk is worthwhile by considering the net financial result over multiple seasons.

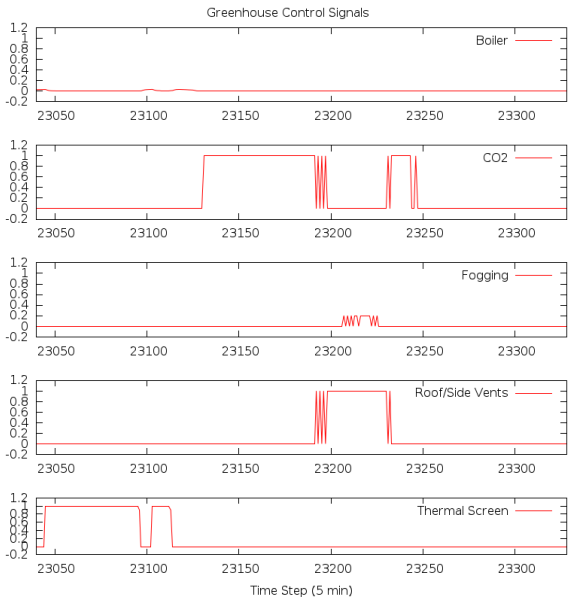

Figure 4.3. High-yield solution control signals over a 24-hour period.

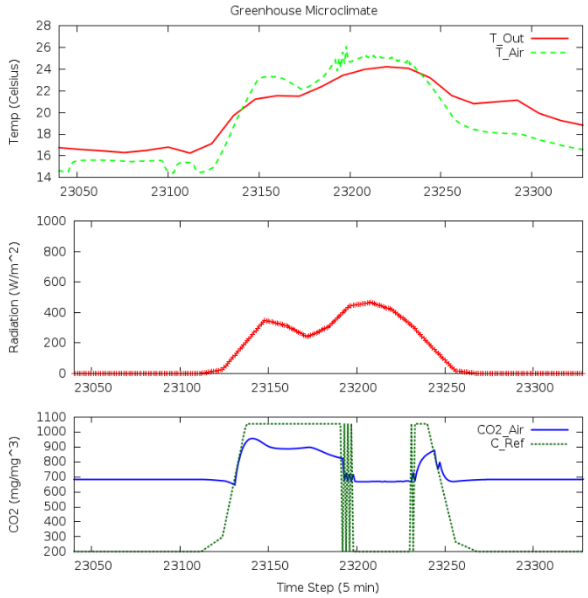

Figure 4.4. High-yield solution microclimate over a 24-hour period. T_Out denotes the outside air temperature, T_Air denotes the greenhouse air temperature, CO_2_Air denotes the CO_2 concentration of the greenhouse air and C_Ref denotes the current value of the dynamic CO_2 setpoint.

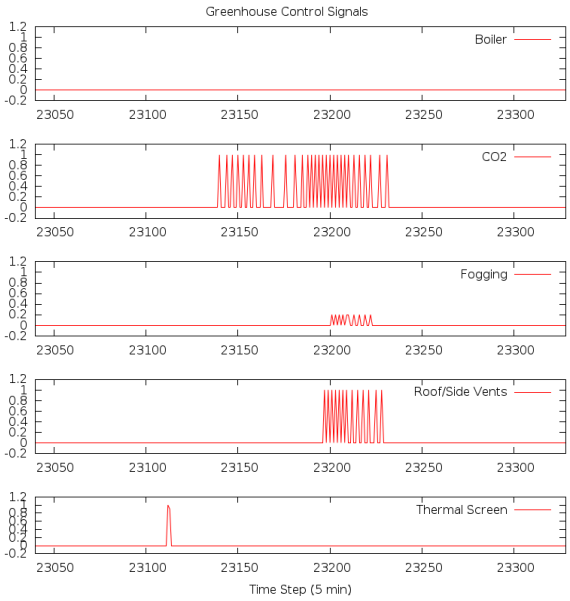

Figure 4.5. Low-cost solution control signals over a 24-hour period.

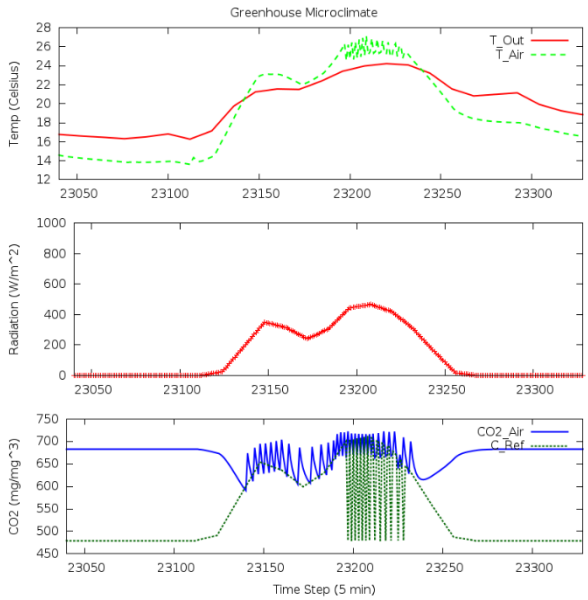

Figure 4.6. Low-cost solution microclimate over a 24-hour period. T_Out denotes the outside air temperature, T_Air denotes the greenhouse air temperature, CO_2_Air denotes the CO_2 concentration of the greenhouse air and C_Ref denotes the current value of the dynamic CO_2 setpoint.

4.5 Discussion

In this chapter we showed that multi-objective evolutionary algorithms like NSGA-II can be used to aid in the design stages of greenhouse construction by allowing optimization of the control setpoints to enter into the evaluation of the various optional technologies to be deployed. In addition, these setpoints can be evolved between growing seasons as new data become available and as input costs change. We found evolved control setpoints that outperform the original setpoints in two objectives: maximizing the economic value of the crop yield and minimizing the variable costs, even when using a new set of weather data that was not used during the evolutionary optimization process. Using estimated weather data as input to the microclimate-crop yield model produced outputs that were mostly similar to those published in Vanthoor's study, with some exceptions. Historical weather data should ideally be used for more accurate estimates of the net financial result, but the estimated weather data were sufficient for validating the crop yield trends with respect to increasing technology levels, thus the evolved setpoints still provided useful information on how to improve the net financial result when considering the tradeoffs between the two conflicting objectives. For purposes of this chapter, the search space during the

evolution process was limited to 9 integer variables that define the setpoints for a fixed control strategy, but later chapters will define more complex control strategies to evolve, as well as containing metrics to evaluate their performance vis-a-vis other control strategies.

5 Using Multi-objective Optimization to Evolve More Sophisticated Controllers

The contents of this chapter are partially based on our prior published work, and can be found in [43].

The previous chapter covered the use of evolutionary computation to optimize the setpoints of a fixed greenhouse control strategy. Although the results show that we can evolve setpoints that dominate the original values that were based on expert knowledge, it assumes a rigid control strategy where the only changes possible are in the values of the setpoints themselves. This was done to limit the search space during evolution and thus provide faster convergence towards a Pareto-optimal front, but this leaves open the possibility of testing additional incremental changes in complexity to seek improvements in performance. In this chapter we propose a simple change to improve the sophistication of an existing control strategy—allowing it to adjust setpoints based on the time of day. In addition, we explore and discuss notable features present in the evolved controllers and propose a performance metric for comparing different evolved controller designs. NSGA-II and model implementation details remain the same as used in Chapter 4 unless otherwise specified.

5.1 Problem Formulation

The economic model incorporates the fixed costs of greenhouse construction elements, the variable costs associated with growing the crop and the value of the crop itself. Based on [4], the net financial result (NFR) is defined as:

$$Q_{NFR}(t_f) = -Q_{Fixed} + \int_{t=t_0}^{t=t_f} \dot{Q}_{CropYield} - \dot{Q}_{Var}\, dt \tag{5.1}$$

where $Q_{CropYield}$ (€×m^{-2}×year^{-1}) is the value of the tomato crop, Q_{Var} (€×m^{-2}×year^{-1}) consists of the variable costs (costs associated with the crop, resources used and labor), and Q_{Fixed} (€×m^{-2}×year^{-1}) represents the cost of all tangible assets that do not depend on crop growth.

The fitness function consists of the economic model's output as described in Eq. (5.1), divided into two objectives: the economic value of the crop yield and the variable costs, $f_1(x)$ and $f_2(x)$, respectively. We use the negative of the crop value so that both objectives are treated as minimization problems, subject to a penalty function for solutions that have a net financial result (NFR) that is inferior to the NFR of the original setpoints used in the classical control strategy. In other words, solutions will not be penalized if $NFR(x) \geq NFR_{Original}$, where $NFR_{Original}$ is the worst-case net financial result of the original setpoints.

In order to be able to compare with the original Vanthoor data, we evaluate control strategies over three consecutive growing seasons, based on example estimated weather data, which results in a pair of objective values being generated for each season. To determine the final values for each objective, we choose the worst-case objective pair of all three (i.e., the year that yields the worst net financial result). The optimization problem is then defined as follows:

$$\min\big(f_1(x), f_2(x)\big) \tag{5.2}$$

$$s.t. \quad x \in X$$

where $f_1(x) = -Q_{CropYield}$ and $f_2(x) = Q_{Var}$ as defined in (5.1). Although the optimization problem is unconstrained, solutions with inferior NFR will be penalized according to the following penalty function:

$$P(x) = \frac{\left|NFR_{Original} - NFR(x)\right|}{\left|NFR_{Original}\right|} + 1 \tag{5.3}$$

Using (5.3) as a scaling factor, the new values for the objectives are $f_1(x) = f_1(x)/P(x)$ and $f_2(x) = f_2(x) \times P(x)$, respectively. Since $f_1(x)$ is minimizing the negative of the crop value, $P(x)$ must be applied as a division operation to penalize that objective.

Since the goal is to optimize greenhouse control setpoints, the chromosome simply consists of a combination of static setpoint values and the thresholds on climatic variables used to calculate the dynamic CO_2 setpoint. $T_{AirVentOn}$ defines the greenhouse air temperature above which roof and side ventilation is always open. Similarly, $T_{AirVentOff}$ defines the greenhouse air temperature below which roof

and side ventilation is always closed. $RH_{AirVentOn}$ is the greenhouse air relative humidity threshold above which the ventilation is turned on. $CO_{2AirVentOn}$ is the greenhouse air CO_2 concentration below which the ventilation is turned on. $T_{AirBoilOn}$ is the greenhouse air temperature below which the boiler heating system is turned on. $T_{OutThScrOn}$ is the outside air temperature below which the thermal screen is deployed. The dynamic CO_2 setpoint is a function of: $CO_{2AirExtMax}$, which determines the upper bound for the CO_2 setpoint, $CO_{2AirExtMin}$, which determines the lower bound of the CO_2 setpoint, and $I_{GlobMax}$, which determines the global radiation threshold above which the CO_2 setpoint reaches its upper bound. Below that, the setpoint decreases linearly with global radiation towards its lower bound. The chromosome with its range of values and desired resolution can be seen in Table 5.1.

Table 5.1. Chromosome representation. Values in this range are stored as integers after multiplying by an appropriate factor.

Parameter	**Range**	**Step Size**
$T_{AirVentOn}$ (°C)	[10, 30]	0.1
$T_{AirVentOff}$ (°C)	[10, 30]	0.1
$RH_{AirVentOn}$	[0.1, 1]	0.01
$CO_{2AirVentOn}$ (ppm)	[100, 500]	0.1
$T_{AirBoilOn}$ (°C)	[10, 30]	0.1
$T_{OutThScrOn}$ (°C)	[10, 30]	0.1
$CO_{2AirExtMax}$ (ppm)	[500, 1000]	0.1
$CO_{2AirExtMin}$ (ppm)	[100, 500]	0.1
$I_{GlobMax}$ ($W \times m^{-2}$)	[200, 1000]	0.1

Using the controller discussed in Chapter 4 as a basis, we ask the following: if we would like to improve this controller, would there be a considerable improvement in one or more objectives if we were to split the control strategy in such a way as to allow different setpoints based on the time of day? This time partitioning should, in theory, provide a greenhouse control strategy the ability to exploit weather patterns present during key parts of the day. For example, dawn is a critical moment for optimizing plant growth in greenhouses due to the transition from nighttime to daytime. Based on temperature setpoints used by classical control strategies, as well as existing knowledge of optimal temperature ranges for the tomato

crop [4], ideal nighttime temperature is significantly lower than the ideal temperature for photosynthetic activity. To exploit this, we should ideally have setpoints defined that can quickly and efficiently transition between nighttime and daytime conditions, as well as having setpoints defined for other times of day that can evolve separately. A summary of such an approach is shown below in Figure 5.1.

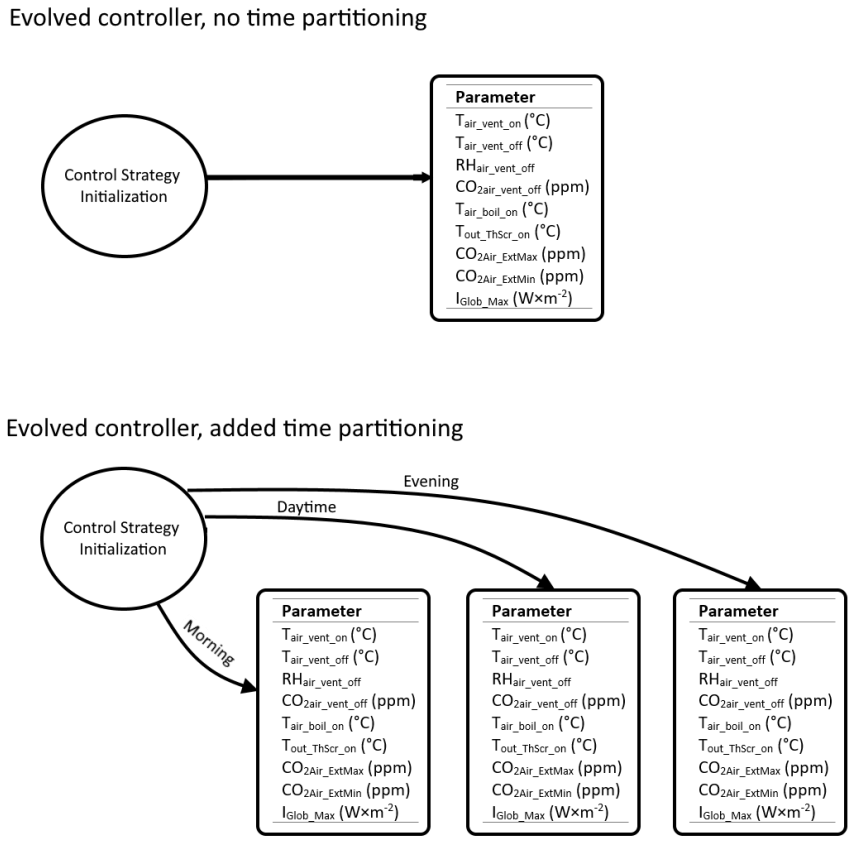

Figure 5.1. Introducing time partitioning to a greenhouse control strategy.

5.2 Methodology and Results

Despite its known shortcomings, and because it is not computationally expensive for two- or three-objective problems, we use the normalized hypervolume [44] as a performance metric for comparing different evolved controllers, choosing a nadir point of [0, 50] based on expected worst-case values. We apply a Mann-Whitney U test [45] with a sample size of n = 5 to determine if the time-partitioned controller is statistically significantly higher in the hypervolume performance metric compared to a

controller without a time-partitioning feature. Each sample consists of the resulting hypervolume of the final population after running NSGA-II for 100 generations while starting with a randomly initialized population. Evolved solutions were also tested by simulating a new season of estimated weather data from the same locale. The results for all four growing seasons are summarized in Table 5.2 and show that the evolved setpoints performed reasonably well with "unknown" weather from the same locale.

Examples of Pareto fronts from both evolved controllers are shown in Figure 5.2**,** and they are compared with the performance of classical setpoints. Both evolved controllers contain solutions that dominate these classical setpoints, and the time-partitioned controller obtained better solutions in some regions of its Pareto front relative to the evolved controller without time partitioning. This is due to the time-partitioned controller having a chromosome that is triple in size compared to the simpler counterpart, requiring more function evaluations to achieve the same performance. On the other hand, we can simply take advantage of the setpoints that the simpler controller uses to seed the time-partitioned controller, allowing us to achieve better results without relying solely on the genetic algorithm itself (as shown in Figure 5.3). More details are available in Section 5.4.

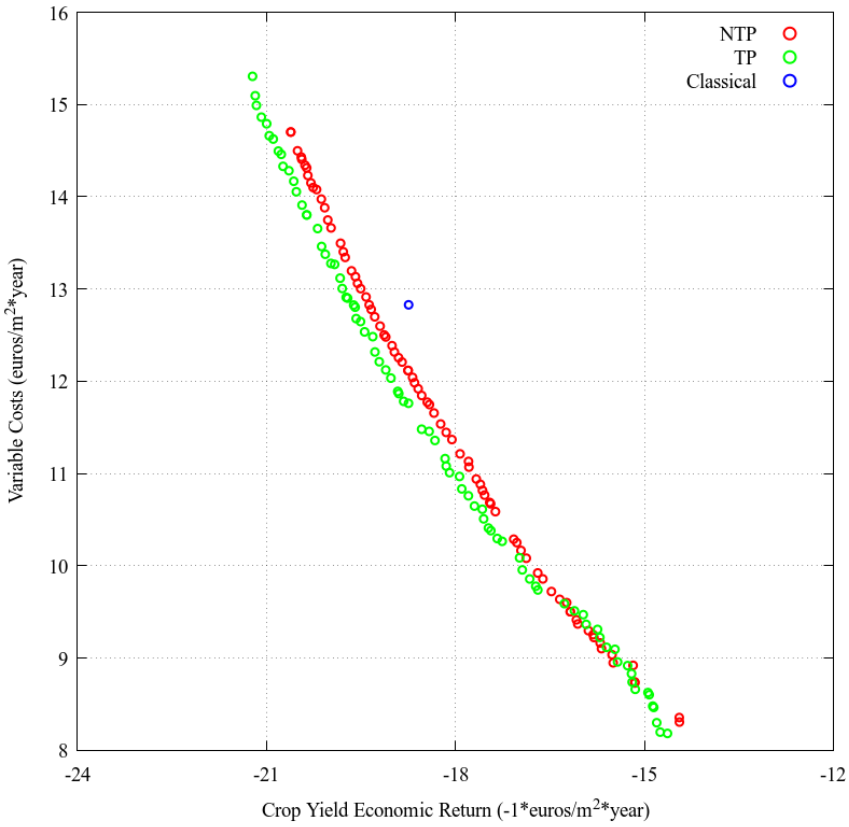

Figure 5.2. Overlapped Pareto fronts consisting of the evolved control setpoints (NTP, red) and the evolved control setpoints with time partitioning (TP, green) compared against classical control setpoints (blue).

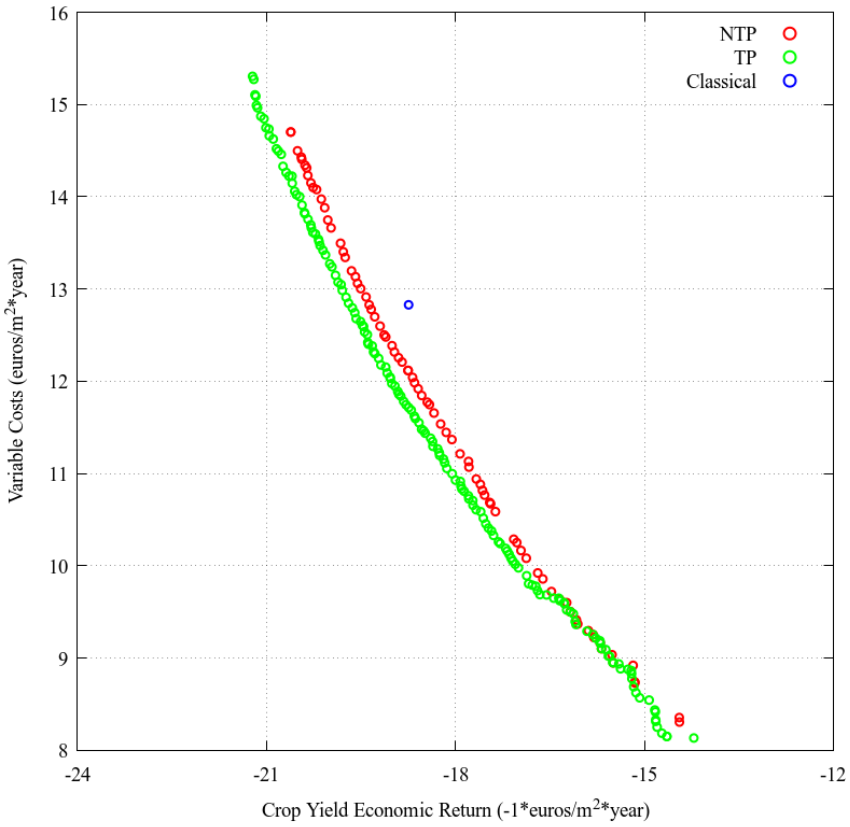

Figure 5.3. Example of control setpoints with time partitioning (TP, green) benefiting from seeding with evolved setpoints without time partitioning (NTP, red). The green lower right region is no longer dominated by the "less sophisticated" control strategy.

Table 5.3 shows a partial list of the populations of both evolved controllers after they are sorted by the net financial result. The original setpoints yielded a worst-year NFR of -0.88; therefore, these results are superior—a negative NFR would reflect that the greenhouse would operate at a loss for that year. In addition, some of these solutions dominate the original setpoint (see Figure 5.2), so they are clearly preferable.

Table 5.2. The outputs of the economic model (€×m^{-2}×year^{-1}), comparing the original setpoints vs a "low cost" solution and a "high value" solution obtained from the Pareto front in Fig. 2. Net financial results (NFR) for all four years are added up.

	Original			**Low Cost**			**High Value**		
Period	**Crop Value**	**Var. Costs**	**NFR**	**Crop Value**	**Var. Costs**	**NFR**	**Crop Value**	**Var. Costs**	**NFR**
2006-2007	19.03	10.98	0.19	17.29	8.65	0.79	19.39	10.88	0.66
2007-2008	20.69	11.41	1.44	18.72	9.11	1.76	21.10	11.42	1.83
2008-2009	17.95	10.97	-0.88	16.20	8.62	-0.27	18.29	10.93	-0.49
2009-2010	18.90	10.96	0.09	17.23	8.76	0.62	19.29	10.95	0.49
Total			**0.85**			**2.91**			**2.49**

Table 5.3. Worst-year NFR (€×m^{-2}×year^{-1}) of the top eight evolved solutions (sorted by decreasing NFR), of a) the evolved controller and b) the evolved controller with time partitioning.

Net Financial Result	
a)	b)
0.194	0.387
0.175	0.364
0.167	0.354
0.166	0.347
0.163	0.344
0.154	0.340
0.153	0.328
0.116	0.324

5.3 Decision Making

A grower could simply choose the top solution in a list sorted by net financial result (as seen in Table 5.3). However, by observing the tradeoffs in a Pareto front the grower has access to additional information to make more informed decisions. For example, a grower may want to opt for solutions that provide greater crop value (which, in this case, provide greater yield), so they can meet unusually high demand for a crop even if the current market price does not fully compensate for the increased variable costs. On the other hand, opting for non-dominated solutions with notably low variable costs provides the grower with more environmentally friendly solutions that can reduce water and fossil fuel usage. Although not shown, these variable costs may be broken down into their individual components such as

water costs, fossil fuel costs, CO_2 costs and labor costs. Examples of these solutions are shown in Table 5.4.

Table 5.4. Original setpoints compared with setpoints of two evolved solutions: a low-cost solution and a high-yield solution.

Parameter	Original	Low-Cost	High-Yield
$T_{AirVentOn}$ (°C)	23	22.5	22.5
$T_{AirVentOff}$ (°C)	20	26	24.6
$RH_{air\_vent\_off}$	90	70	82
$CO_{2air\_vent\_off}$ (ppm)	200	171.6	164.3
$T_{air\_boil\_on}$ (°C)	16	10	15.7
$T_{out\_ThScr\_on}$ (°C)	18	16.3	16.7
CO_{2Air_ExtMax} (ppm)	850	508.7	585.8
CO_{2Air_ExtMin} (ppm)	365	266.4	112.6
$I_{GlobMax}$ ($W \times m^{-2}$)	500	875.8	206.2

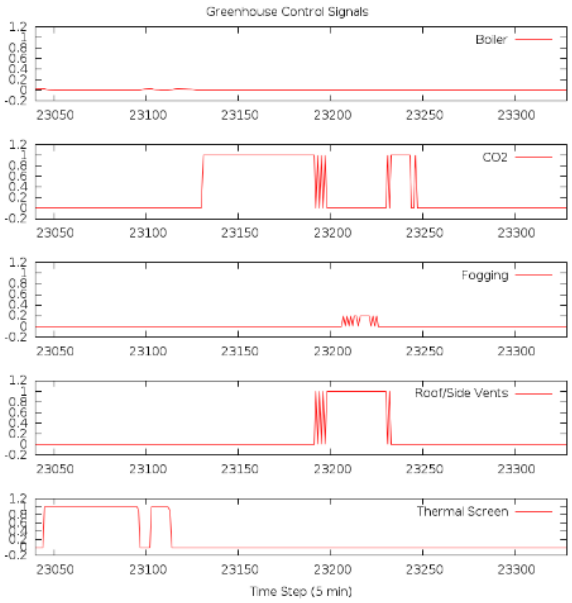

Figure 5.4. High-yield-solution control signals in a 24-hour period.

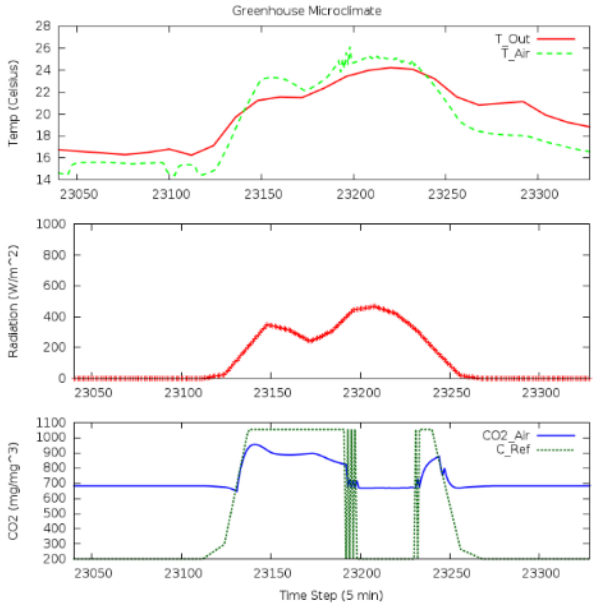

Figure 5.5. High-yield-solution microclimate over an example 24-hour period. T_Out is outside air temperature, T_Air is greenhouse air temperature, CO_2_Air is CO_2 concentration of greenhouse air and C_Ref is current value of the dynamic CO_2 setpoint.

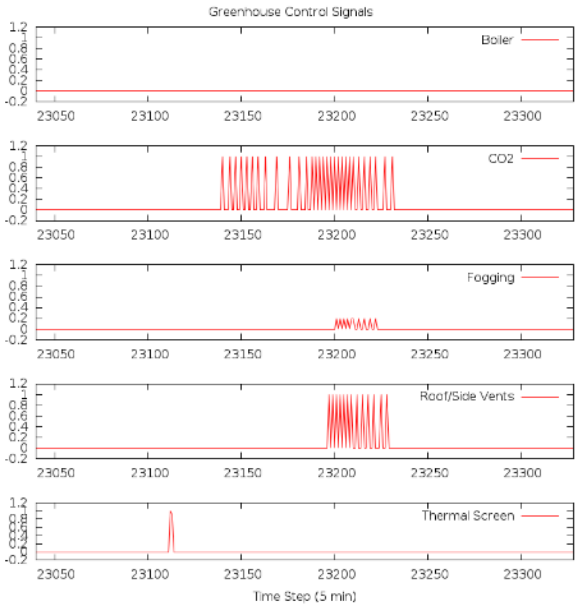

Figure 5.6. Low-cost-solution control signals in a 24-hour period.

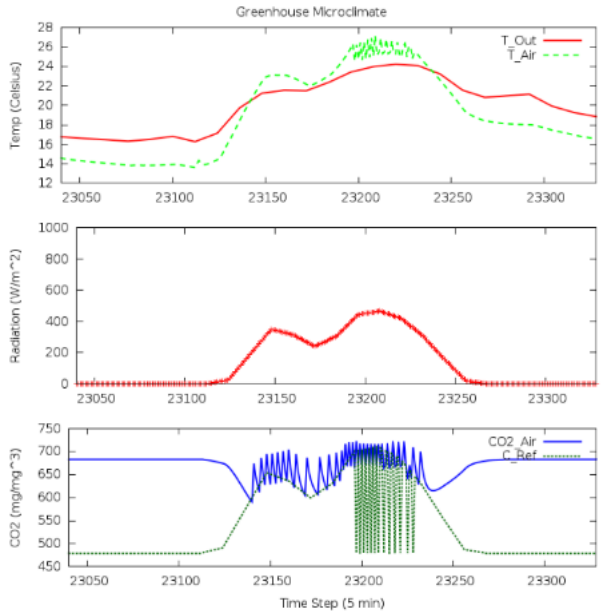

Figure 5.7. Low-cost-solution microclimate over an example 24-hour period. T_Out is outside air temperature, T_Air is greenhouse air temperature, CO_2_Air is CO_2 concentration of greenhouse air and C_Ref is current value of the dynamic CO_2 setpoint.

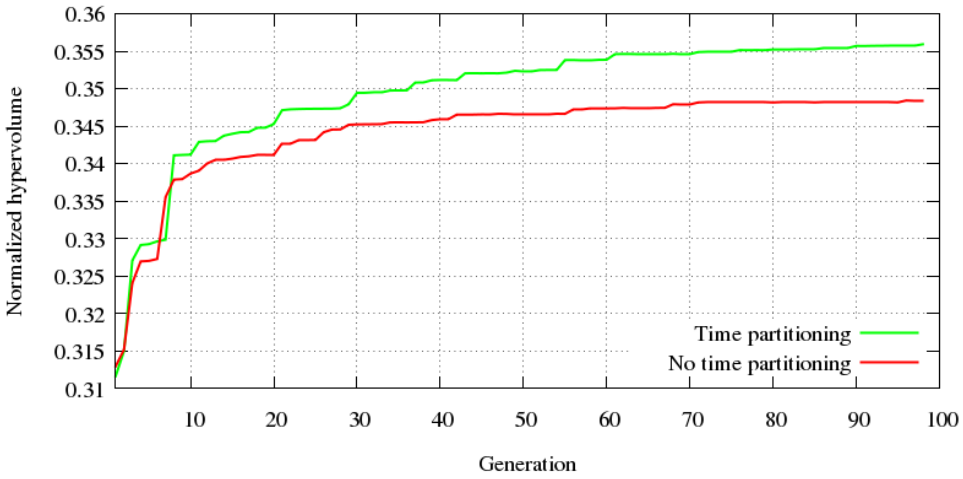

Figure 5.8. Normalized hypervolume for the evolved, non-time-partitioned controller (red), and the evolved, time-partitioned controller (green).

Figure 5.4 and Figure 5.5 show the control signals and greenhouse microclimate for a high-yield solution, while Figure 5.6 and Figure 5.7 show the control signals and greenhouse microclimate for a low-yield solution. The high-yield solution is characterized by a more aggressive CO_2 enrichment strategy in which the dynamic CO_2 setpoint reaches its upper bound as soon as the global radiation is above 206 (in this case). This increases the value of the crop but also increases the variable costs in the process. The low-

cost solution has a significantly lower setpoint for turning on the boiler, $T_{AirBoilOn}$, which naturally reduces fossil fuel costs. This is accompanied by a more conservative CO_2 enrichment setpoint caused by a much higher value for $I_{GlobMax}$, resulting in less frequent use and therefore reduced variable costs overall. Both low-cost and high-yield solutions have a much higher value for $T_{AirVentOff}$, which results in roof and side ventilation remaining closed during hotter weather. Normally this setpoint is used to help conserve heat by sealing the greenhouse during cold weather, but in this case the higher setpoint is used to keep the greenhouse sealed up for longer periods of time, increasing the efficiency of CO_2 enrichment while relying on the fogging system for cooling. This process of finding patterns that emerge by means of using an optimization technique is called "innovization" [46]. Since the non-time-partitioned controller has a much smaller feature space (9 integer values), it is relatively simple to manually "innovize" some of the patterns present in high-yield and low-cost solutions. However, this process was not considered for the time-partitioned controller. Automating some of the innovization process would be preferable in this case, though it is beyond the scope of this thesis.

Since the worst-case measurements for the net financial result were all positive in Table 5.3, these could all be considered financially viable solutions. However, even if they were negative, these evolved setpoints can still outperform the original setpoints as long as this value is greater, and depending on the planning horizon, the grower can consider other seasons that have a positive net financial result and assess whether the risk is worthwhile by considering the net financial result over multiple seasons. If the grower is obligated to pay the fixed costs for an already built greenhouse, whether or not a crop is planted, it is still clearly advantageous to select the control setpoints that provide the best tradeoff between the two objectives.

5.4 Performance of the Time-Partitioning Feature

The rationale for letting a controller choose setpoints based on the time of day is relatively straightforward: ideally the control strategy should take advantage of the characteristics that correspond to

the time of day—i.e., to evolve separate setpoints for the periods in which sunrise, midday and sunset occur.

Figure 5.2 shows that adding this time-partitioning feature to the evolved controller improves solutions in some regions of the Pareto front. It is trivially possible to eliminate all regions where the non-time-partitioned controller dominated the time-partitioned controller, simply by supplying the non-time-partitioned values to the time-partitioned controller for all the partitioned time periods. Time-partitioned solutions dominating the non-dominated solutions were not discovered in some parts of Figure 5.2 because the expensive fitness function did not allow enough function evaluations with the triple-size chromosome to discover those settings. Instead of adding superfluous function evaluations to reach the same result, we took advantage of the modular nature of the time-partitioning feature: it was designed such that, if necessary, it can behave like a controller that does not change its setpoints based on the time of day by simply using identical sets of values for all times of day: morning, midday, and evening. An example Pareto front that takes advantage of this property was shown in Figure 5.3.

Despite the significant increase in the search space, the time-partitioned evolved controller eventually outperforms its counterpart based on the hypervolume performance metric, showing solutions that the non-time-partitioned version has not produced (as seen in Figure 5.8). This improvement is also reflected in Table 5.3, due to the presence of solutions with greater NFR compared to the other evolved controller, and in Figure 5.2, where we can observe regions where the time-partitioning feature produces solutions that dominate the other evolved controller. By running a Mann-Whitney's U test, we evaluated the statistical significance of the difference in hypervolumes that results from adding this time partitioning feature. Results show that the two groups of hypervolume measurements differed significantly ($U = 0$, $n_1 = n_2 = 5$, $P < 0.01$, two-tailed), and the sample values are summarized in Table 5.5.

Table 5.5. Mann-Whitney U test results comparing groups of hypervolumes, where a) is the non-time-partitioned controller, while b) uses time-partitioning.

Normalized Hypervolumes	
a)	b)
0.347626963	0.352650132
0.347393334	0.351999245
0.346688732	0.351094193
0.346627517	0.350488993
0.346103962	0.349433818

5.5 Discussion

We restricted our study to two objectives primarily to ease visualization, but more objectives may be added. For example, tomato quality is a desirable characteristic that could conflict with both yield and energy costs. Moreover, the net financial result could be added as an objective. While sorting the Pareto front based on net financial result is a simple way to aid decision making, by not including this metric as an additional objective, we forego one of NSGA-II's inherent advantages, elitism. This results in otherwise "elite" individuals (with respect to the net financial result) not being guaranteed survival to future generations. We also limited the scope of the simulations to using estimated weather data from the same dates and locale used in [4] (followed by an additional year). Future studies should use historical weather data when available and examine the effects of including a larger number of growing seasons during the evolution process as well as the efficacy of this method for different dates and locales. In addition, other greenhouse design elements commonly used in tomato production should be included, such as pad-and-fan cooling and supplemental lighting.

Although it is beyond the scope of this thesis, a logical extension of our proposed method is to optimize greenhouse designs alongside their climate control setpoints. Since different greenhouse designs will have different numbers of setpoints associated with them, an alternative multi-objective evolutionary algorithm that supports variable length chromosomes should be used. In addition, the greenhouse setpoint optimization problem may be replaced with a more generic control strategy optimization problem. For example, a control strategy could be proposed in which setpoints are replaced by operating regions that

can be evolved, similar to the concept of multi-objective compatible control [47]. Because of the potentially staggering implications in computational time, some model reductions in the microclimate-crop model may be necessary to make these optimization problems practical. A member of the joint MSU-Tongji University Greenhouse Control team, Dr. Yuanping Su, has developed a control optimization strategy using a surrogate model and is currently preparing a manuscript for publication of this work.

We have shown in this chapter that multi-objective evolutionary algorithms like NSGA-II can be used to aid the grower in the design stages of greenhouse construction by optimizing the control setpoints. These setpoints can be evolved between growing seasons as new data become available and as input costs change. We have found evolved control setpoints that outperform the original setpoints in two objectives: (i) maximizing the economic value of the crop yield and (ii) minimizing the variable costs, even when using a new set of weather data that was not used during the evolutionary optimization process. The non-time-partitioned evolved controller has also been examined in more detail, showing some patterns in the feature space that may be useful as design principles for future controller designs. In addition, evolving a set of time-partitioned setpoints has produced non-dominated regions that are better than their counterparts, and using their respective hypervolumes as a performance metric shows that there is a statistically significant difference between them. Important knowledge about the optimal solutions has also been identified and explained. Although effective for comparing two relatively simple control strategies, additional work is needed to test the efficacy of using hypervolume as a performance metric with more sophisticated controllers.

6 Analyzing Genotypes of Evolved Controllers

6.1 Introduction

The goal of this chapter is to explore the behavior exhibited by the evolved versions of the control strategies described in this thesis, discussing any notable properties displayed by these control strategies, and finding key areas for improvement. A total of four strategies are examined, each of which was evolved for 100 generations to obtain a population of 80 non-dominated solutions. After examining these four, we examine key changes on the best performing controller (with respect to Pareto-optimality) when introducing a crop *value* penalty for inadequate levels of relative humidity. The chapter presents in sequence the following controllers:

Section 6.2: Evolved Vanthoor controller

Section 6.3: Evolved Vanthoor controller with setpoint partitioning based on time

Section 6.4: Evolved Vanthoor controller with partitioning based on time and fruit set occurrence

Section 6.5: Improved controller

Section 6.6: Same improved controller with crop *value* penalty for sub-optimal relative humidity

Controller implementation details are summarized in Table 6.1. Values that required some assumptions to implement are denoted with an asterisk (*). More information on how greenhouse control strategies are defined and implemented can be found in Chapters 4 and 5.

Table 6.1. General controller implementation and ODE solver details. These values are shared among all controllers described in this chapter unless otherwise specified.

Parameter Description	Parameter name/symbol	Unit	Range
Boiler heating	U_{Boil}	-	[0, 1]
CO_2 injection system	U_{ExtCO2}	-	[0, 1]
Fogging system	U_{Fog}	-	[0, 0.2]*
External shading screen	U_{ShScr}	-	[0, 1]
Semi-permanent shading screen (whitewash)	$U_{ShScrPer}$	-	[0.5, 1]**
Thermal screen	U_{ThScr}	-	[0, 1]
Roof and side ventilation system	U_{Roof}, U_{Side}, U_{Vent}	-	[0, 1]***
Controller update interval	-	Minutes	5
Greenhouse climate simulation step size (initial)	-	Seconds	10
Greenhouse crop yield simulation step size (initial)	-	Seconds	60
RK4 ODE solver absolute error	-	-	0.01
RK4 ODE solver relative error	-	%	1

* Upper bound for U_{Fog} was assumed based on prior strategies established in literature to help reduce the potential of burns on the crop leaves due to the salt content of the water supply [42]. This will be enforced unless otherwise specified.

** Although modeled internally as a control variable, it is assumed that $U_{ShScrPer}$ is always a whitewash that is applied manually based on seasonal needs and the current greenhouse design. This is consistent with Vanthoor's description and use of this variable. Since it acts as a multiplier for the greenhouse's overall light transmissivity, it cannot be zero.

*** It is assumed that both roof and side ventilation are controlled concurrently whenever ventilation is needed to remain consistent with the description and behavior of the control strategy based on Vanthoor's thesis. The combined value of these window apertures will be referred to as U_{Vent}.

The loci shown here are examined against only one objective (the crop yield value) for ease of visualization. In the figures in this chapter that plot evolved setpoints and/or variables against their corresponding crop yield values, solutions which dominate the classical Vanthoor control strategy with default setpoints are marked in green (*). The controllers examined in this chapter are presented in order of increasing performance unless otherwise specified, with each one consistently yielding similar Pareto-optimal fronts when using identical NSGA-II configuration settings. Figure 6.1 contains an example of the Pareto-optimal front that each controller type yields.

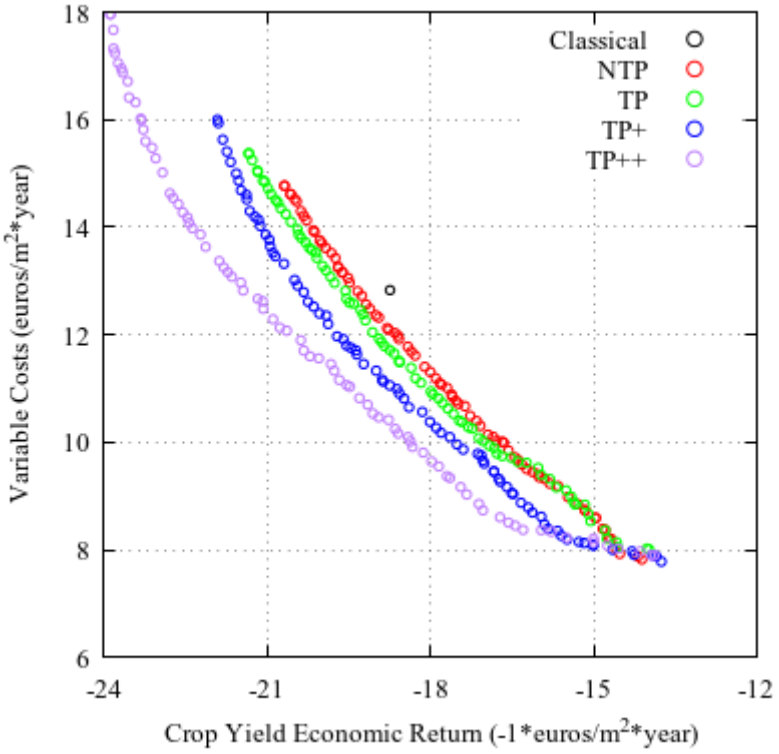

Figure 6.1. Pareto-optimal fronts for the evolved control strategies in this chapter, with a classical strategy using default setpoints for reference. Red circles represent the classical strategy with evolved setpoints (NTP). Green circles represent the classical strategy with setpoint partitioning based on time (TP). Blue circles represent a similar strategy that adds setpoint partitioning based on both time and plant development stage, but also uses sunrise and sunset calculations to transition between nighttime and daytime strategies (TP+). Purple setpoints represent a control strategy with all the previous features, additional control logic, additional nighttime setpoints, and PID control for fogging, heating, and ventilation systems (TP++).

6.2 Evolved Classical Controller (No Time Partitioning)

6.2.1 Introduction

This controller is based on a classical control strategy described by Vanthoor in his thesis [4], with the main difference being that most of the setpoints pertaining to greenhouse control are evolved. A summary of the behavior of the control strategy is shown in Figure 6.3. Since this control strategy needs to differentiate between daytime and nighttime to determine whether the thermal screen should be deployed, nighttime has been defined as the absence of global radiation (i.e., $I_{Glob} = 0$). The chromosome and its range of values is given in Table 6.2.

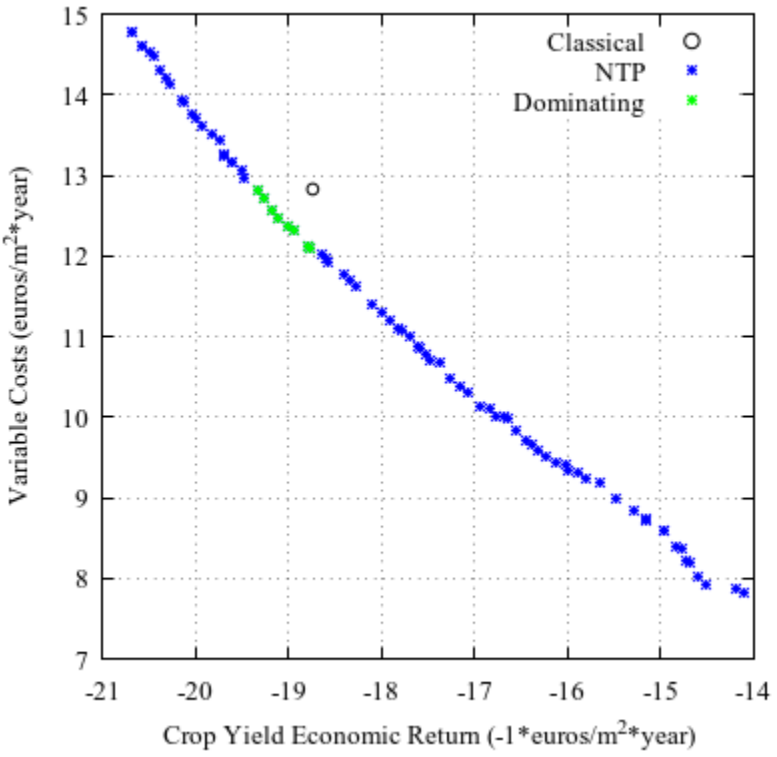

Figure 6.2. Pareto-optimal front for the control strategy discussed in this section. Solutions from this Pareto front which also dominate the classical Vanthoor strategy are marked in green.

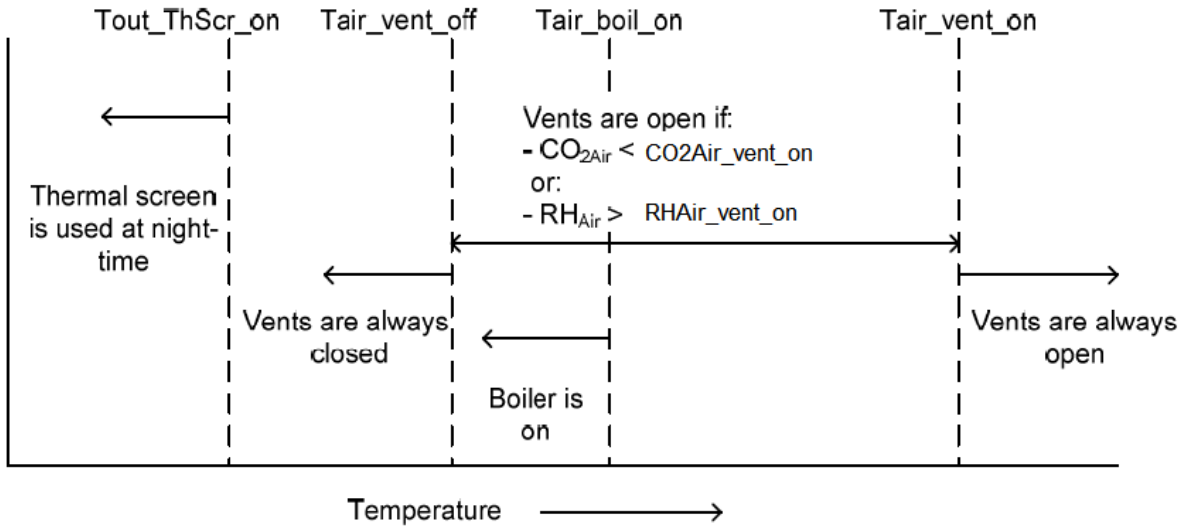

Figure 6.3. Classical control strategy example. Based on the current greenhouse air temperature, the controller will take different actions to maintain an optimal temperature range for the crop, as influenced also by CO_2 concentration and relative humidity in the greenhouse. [4]

Table 6.2. Chromosome containing the setpoints used in the evolved classical controller. The genotype consists of 9 integer values.

Parameter Description	Parameter name/symbol	Unit	Genotype Value	Range of Real Values
Temperature above which ventilation (U_{vent}) is turned on	$T_{AirVentOn}$	Degrees (Celsius)	[100, 300]	[10, 30]
Temperature below which ventilation is turned off	$T_{AirVentOff}$	Degrees (Celsius)	[100, 300]	[10, 30]
Relative humidity above which ventilation is turned on	$RH_{AirVentOn}$	%	[10, 100]	[10, 100]
CO_2 concentration below which ventilation is turned on	$CO_{2AirVentOn}$	ppm	[1000, 5000]	[100, 500]
Temperature below which the boiler (U_{Boil}) is turned on	$T_{AirBoilOn}$	Degrees (Celsius)	[100, 300]	[10, 30]
Nighttime temperature below which the thermal screen (U_{ThScr}) is deployed	$T_{OutThScrOn}$	Degrees (Celsius)	[100, 300]	[10, 30]
Upper bound for dynamic CO_2 setpoint*	$CO_{2AirExtMax}$	ppm	[2000, 10000]	[200, 1000]
Lower bound for dynamic CO_2 setpoint*	$CO_{2AirExtMin}$	ppm	[1000, 5000]	[100, 500]
Global radiation above which the dynamic CO_2 setpoint is maximized*	$I_{GlobMax}$	W/m^2	[2000, 10000]	[200, 1000]

* These variables are used for the calculation of the dynamic CO_2 setpoint, $CO_{2AirExtOn}$. See Eq. (6.1) for more details.

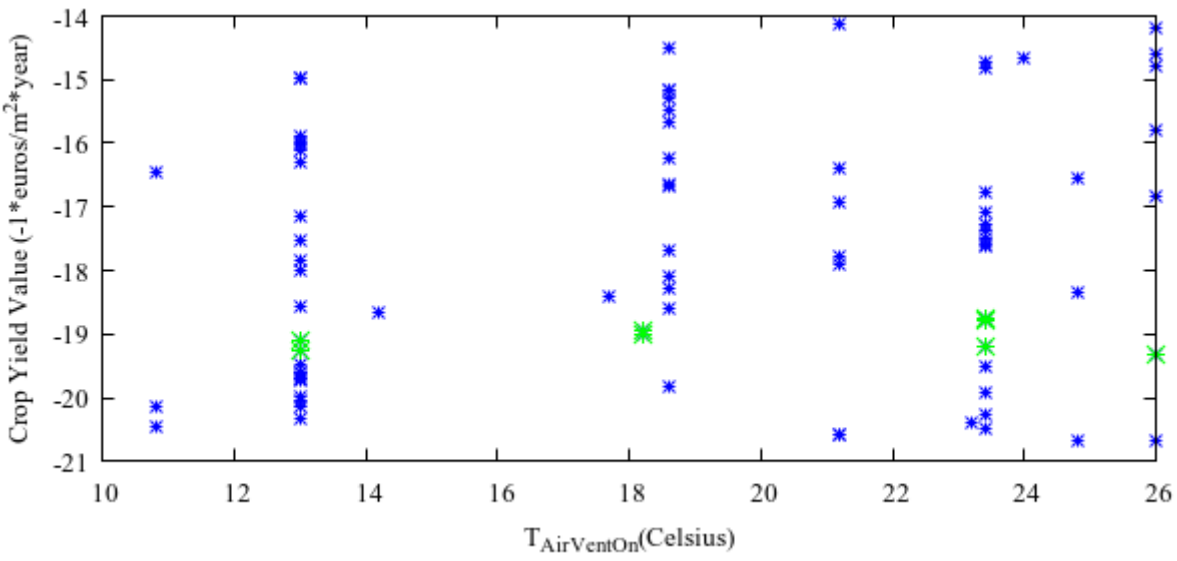

Figure 6.4. This setpoint determines the temperature above which the greenhouse controller will keep the ventilation open.

6.2.2 $T_{AirVentOn}$

Figure 6.4 shows a relatively wide range of values (between 10 – 25 degrees Celsius) that still produce non-dominated solutions. However, the temperature at which the ventilation opens unconditionally is closely tied with its counterpart $T_{AirVentOff}$—in particular, $T_{AirVentOff}$ can override $T_{AirVentOn}$ when the value is large enough, creating a strategy conditionally which prevents the greenhouse from opening based on sub-optimal levels of humidity or CO_2. This is because the classical strategy normally contains a temperature gap between $T_{AirVentOff}$ and $T_{AirVentOn}$ (see Figure 6.3), but here, these setpoints can evolve in such a way that the gap is eliminated. Without this gap, the greenhouse will remain sealed for longer periods of time, allowing for CO2 injection to occur uninhibited.

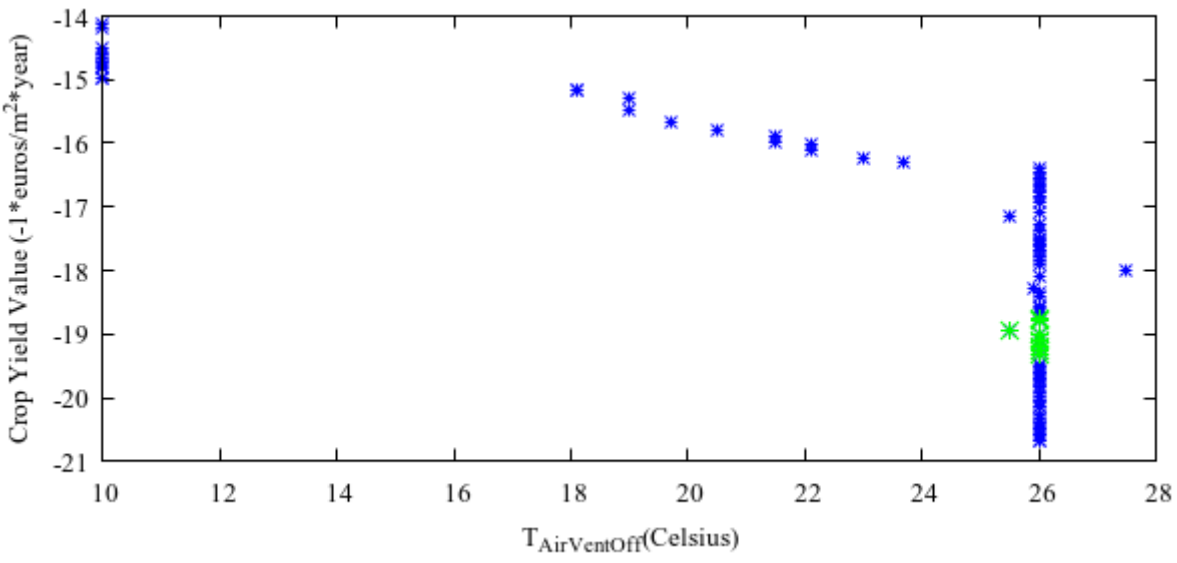

Figure 6.5. This setpoint determines the temperature below which the ventilation will always remain closed.

6.2.3 $T_{AirVentOff}$

The evolved values in Figure 6.5 clearly show a trend where increasing the temperature setpoint can produce greater crop yields at the expense of increased costs. These high-temperature setpoints cause the greenhouse to stay sealed for longer periods of time where CO_2 injection can continue uninterrupted, while relying on active cooling measures (a fogging system in this case) to maintain the tomato crop within optimal temperature ranges. Since nearly all the Pareto-optimal points are at or near 26 degrees Celsius, it is clear that the added crop yield benefit of keeping the greenhouse closed and injecting CO_2 outweighs the additional energy cost of the CO_2 and the cooling required. Moreover, all the solutions which dominate the classical Vanthoor strategy are at or near 26 degrees Celsius. This makes the process of choosing the value for $T_{AirVentOff}$ fairly straightforward, since the same value of 26 degrees Celsius would be used with the notable exception of tradeoff solutions that prioritize lower variable costs (at the expense of lower crop-yield value), but such strategies are outperformed in terms of net financial return by the classical Vanthoor strategy.

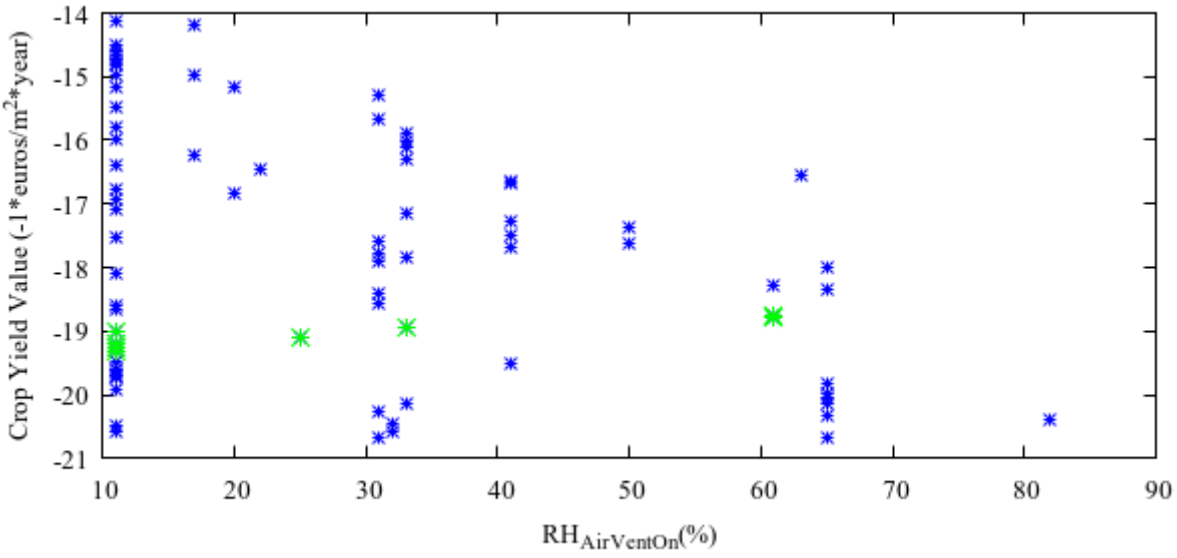

Figure 6.6. This setpoint determines the relative humidity above which ventilation is conditionally turned on.

6.2.4 $RH_{AirVentOn}$

This value is only used when the greenhouse air temperature is between $T_{AirVentOff}$ and $T_{AirVentOn}$, as shown in Figure 6.3, and only when $T_{AirVentOff}$ is also less than $T_{AirVentOn}$. We can see in Figure 6.6 that there is a wide range of values among the non-dominated solutions. The cause for this lack of pattern is that the setpoints $T_{AirVentOff}$ and $T_{AirVentOn}$ can evolve values in some controllers on the Pareto front that are very close to each other, or in which they are "inverted", ultimately causing $RH_{AirVentOn}$ to become unutilized due to the lack of the "deadband" that is normally formed between $T_{AirVentOff}$ and $T_{AirVentOn}$. Ordinarily, in real-world greenhouse practice, this setpoint would be affected by checking for sub-optimal levels of humidity, but there is clearly not enough pressure either in the crop model or in the economic model as developed by Vanthoor to maintain optimal humidity levels. Vanthoor addressed this later by proposing quality filters on the crop yield with the goal of describing the impact humidity has on the price and marketability of tomatoes [4]. The effect of such a quality filter on the controller behavior is summarized later in this chapter (see Section 6.6).

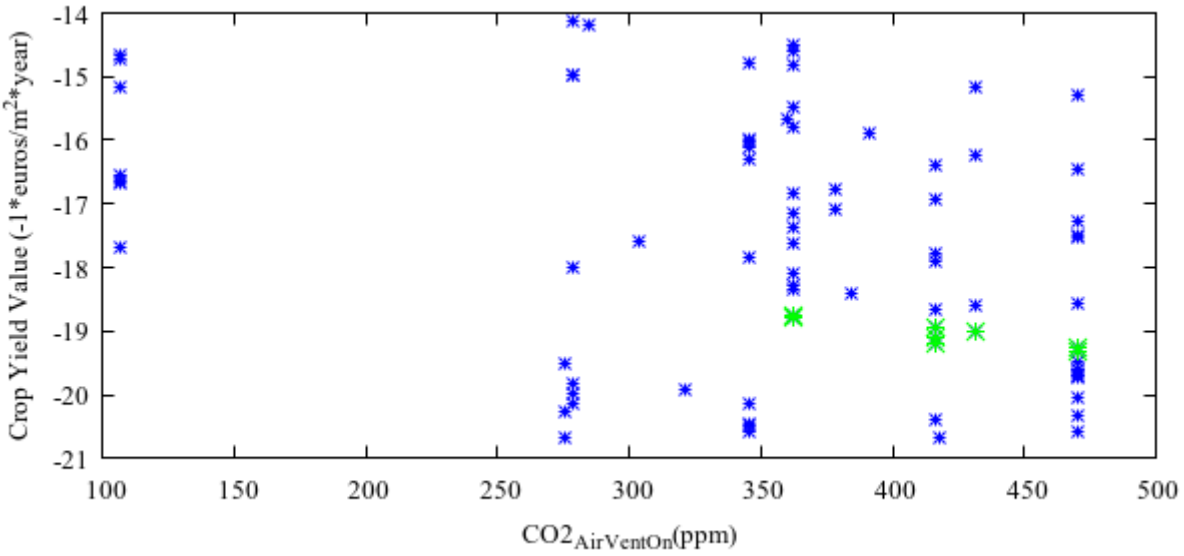

Figure 6.7. This setpoint determines the greenhouse air CO_2 concentration below which ventilation is conditionally turned on.

6.2.5 $CO_{2AirVentOn}$

Similar to Figure 6.6, $CO_{2AirVentOn}$ in Figure 6.7 contains a wide range of values among the non-dominated solutions, and this value is similarly "deprecated" among solutions that evolve values that remove the gap between $T_{AirVentOff}$ and $T_{AirVentOn}$, or invert the two. However, unlike $RH_{AirVentOn}$, the effects of CO_2 concentration on the crop are described in detail in the crop model, and this setpoint is meant to be used when the greenhouse air CO_2 concentration can be improved by ventilating the greenhouse with outside air (which would be an unusual occurrence, especially when CO_2 injection is available).

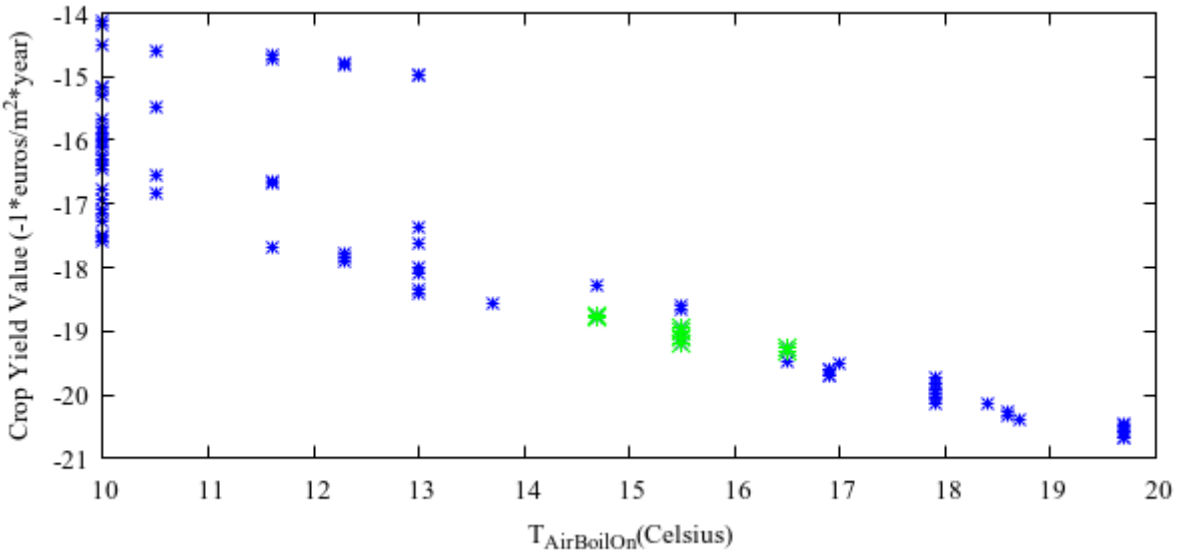

Figure 6.8. This setpoint determines the temperature below which the greenhouse controller will turn on the boiler heating.

6.2.6 $T_{AirBoilOn}$

This setpoint shows a straightforward trend (in Figure 6.8) among non-dominated solutions: a higher setpoint will increase costs while increasing the value of the crop yield. Evolved solutions do not exceed 20 degrees Celsius for the setpoint, after which those solutions are no longer non-dominated due to excessive crop growth inhibition caused by excessive heating. Solutions which dominate the classical Vanthoor strategy are at or near 15 – 17 degrees Celsius. The classical Vanthoor strategy uses 16 degrees Celsius for this setpoint, suggesting that only minor adjustments were needed to achieve better results.

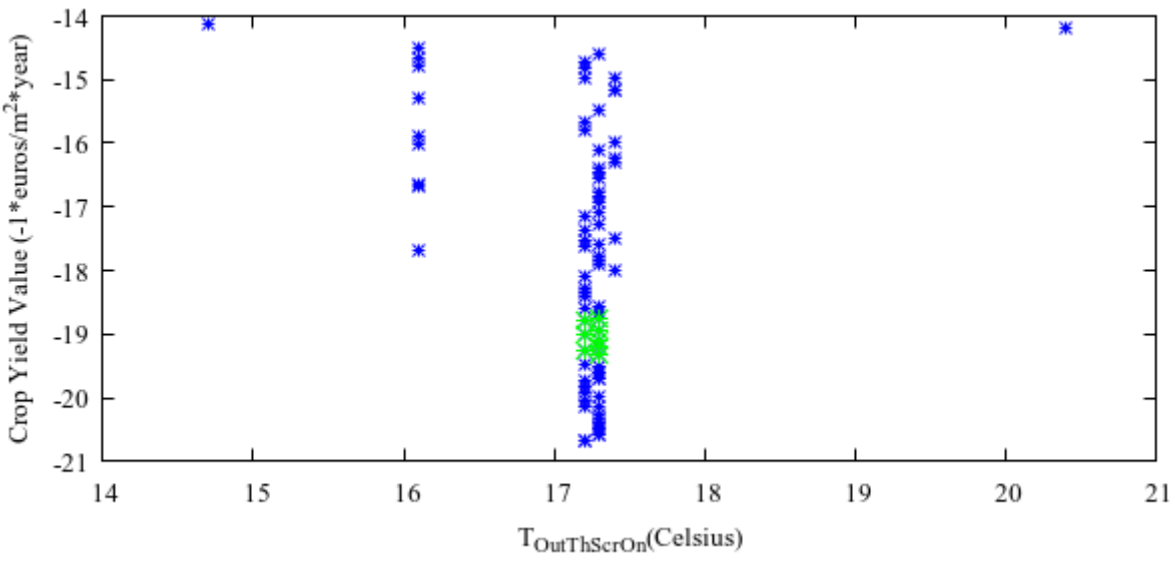

Figure 6.9. This setpoint determines the outside temperature below which the greenhouse controller will deploy the thermal screen.

6.2.7 $T_{OutThScrOn}$

As seen in Figure 6.9, most non-dominated solutions settle with this setpoint between 17 – 17.5 degrees Celsius, so values close to the value used in the classical Vanthoor strategy (18 degrees Celsius). Since the purpose of the thermal screen is to conserve heat during the nighttime, the ideal value for this setpoint must strike a balance between a) keeping the plants warm enough to stay close to the ideal instantaneous and 24-hour mean temperature ranges set by the plant growth model and b) minimizing maintenance respiration caused by said warm temperatures.

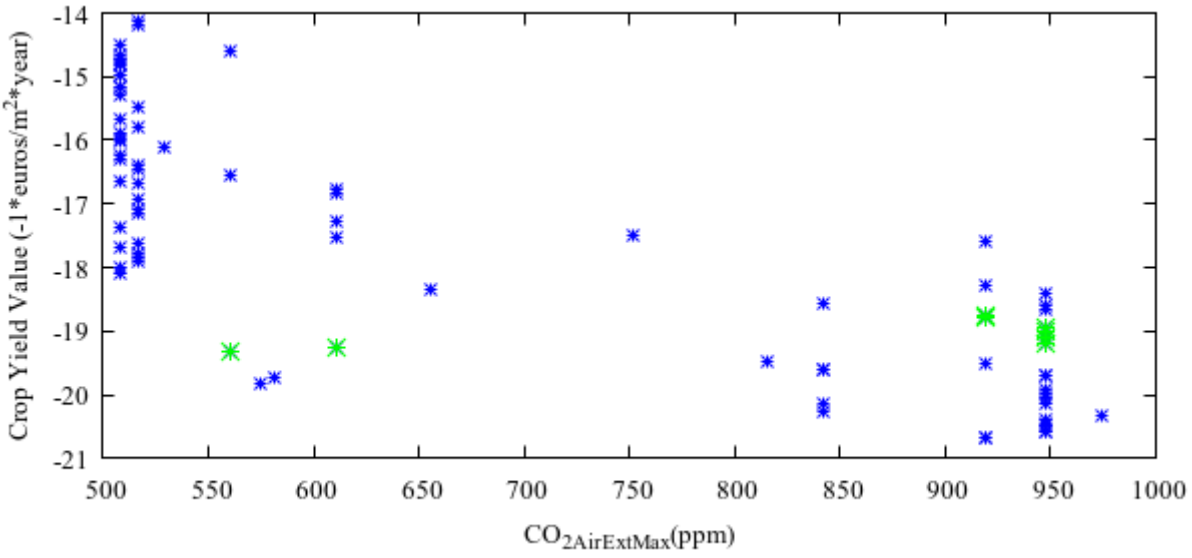

Figure 6.10. This variable determines the upper bound for the dynamic CO_2 setpoint used during CO_2 injection.

6.2.8 $CO_{2AirExtMax}$

Figure 6.10 shows a wide variety of values among the non-dominated solutions. There is some clustering near the lower and upper bounds defined for this value, which allow for low-cost and high-yield solutions, respectively. This value is part of the calculation for the variable CO_2 setpoint defined by Vanthoor [4], and is shown in Eq. (6.1) below:

$$CO_{2AirExtOn} = f(I_{Glob}) \cdot g(U_{Vent}) \cdot (CO_{2AirExtMax} - CO_{2AirExtMin}) + CO_{2AirExtMin} \quad (6.1)$$

Eq. (6.1) shows how the setpoint for opening vents to bring in atmospheric CO_2 is calculated, as a function of the incident global radiation and the current positioning of the vents. Functions *f* and *g* assume their maximum values (at 1.0) when global radiation is at the maximum value for photosynthetic yield and the U_{Vent} is fully closed. At that point, the setpoint $CO_{2AirExtOn}$ assumes the value $CO_{2AirExtMax}$, which maximally inhibits the opening of the air vents (which would move the CO_2 concentration toward atmospheric values). This makes sense because if global radiation is low, there is no need to supply more CO_2 even if it is relatively low in the greenhouse, and if the vents are mostly closed (so *g* is near 1), then supplementary CO_2 can be added to greater effect than opening the vents would produce, so the threshold for opening the vents to admit CO_2 should be raised. Thus, the setpoint for $CO_{2AirExtOn}$ increases with

higher global radiation (I_{Glob}) and lower ventilation opening (U_{Vent}). $CO_{2AirExtMax}$ defines the upper bound for the setpoint (as the difference between itself and $CO_{2AirExtMin}$), and $CO_{2AirExtMax}$ defines the lower bound. Therefore, it logically follows that increasing this value will increase the value of the crop yield at the expense of increased costs due to additional CO_2 injection, since raising it keeps the greenhouse closed more of the time, requiring CO_2 addition in order to increase crop value.

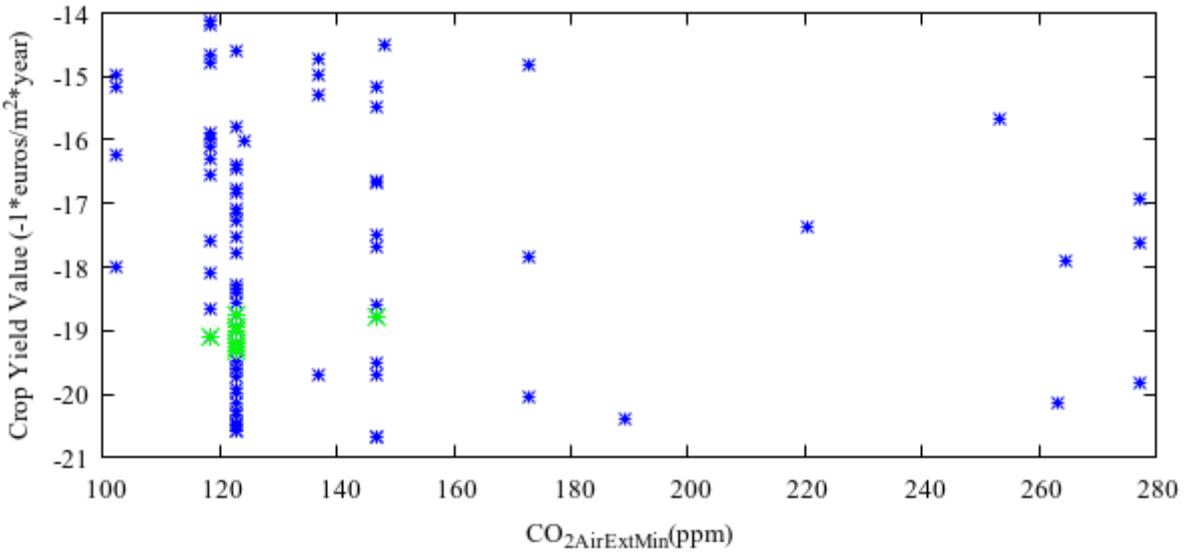

Figure 6.11. This variable determines the lower bound for the dynamic CO_2 setpoint used during CO_2 injection.

6.2.9 $CO_{2AirExtMin}$

With some exceptions, most values in Figure 6.11 form a cluster near the lower bound, keeping it consistently low, while $CO_{2AirExtMax}$ and $I_{GlobMax}$ define whether the strategy is tailored towards a low-cost or high-yield solution. Based on Eq. (6.1), this value ensures that CO_2 injection does not occur in conditions where it would be wasteful to do so. Specifically, in cases where evolved values of $CO_{2AirExtMin}$ are low enough to result in a CO_2 setpoint (i.e., $CO_{2AirExtOn}$) that is below ambient levels, it will lead to CO_2 injection being disabled.

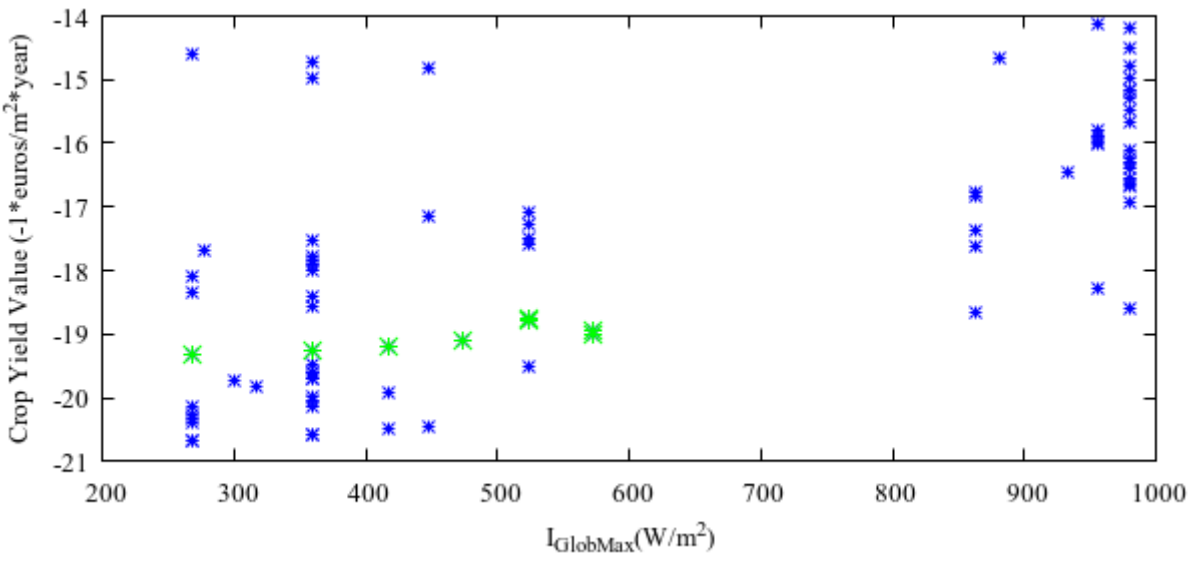

Figure 6.12. This variable determines how quickly $f(I_{Glob})$ is maximized, and subsequently contributes to how quickly the dynamic CO_2 setpoint ($CO_{2AirExtOn}$) is maximized.

6.2.10 $I_{GlobMax}$

Similar to $CO_{2AirExtMax}$, there are a wide range of solutions for $I_{GlobMax}$ in Figure 6.12 that cluster near the lower and upper bounds defined for this value, which also define whether the control strategy is tailored towards a low-cost or high-yield solution: a low-cost solution would have a higher $I_{GlobMax}$, and a high-yield solution would have a low $I_{GlobMax}$. Solutions that dominate the classical Vanthoor strategy use a value for $I_{GlobMax}$ that ranges from 250 – 600 W/m^2 (compared to the classical Vanthoor strategy which uses 500 W/m^2), suggesting that it is generally more optimal to use a lower value for $I_{GlobMax}$, causing the dynamic CO_2 setpoint to be maximized with less global radiation.

6.2.11 Discussion

Overall, the solutions that dominate the classical unevolved strategy do not form a set pattern other than being located near the "knee points" of the classical evolved strategy. This much is expected, as the fitness values for the unevolved strategy are also located near that region (see Figure 6.1). The values for $CO_{2AirVentOn}$ and $RH_{AirVentOn}$ did not form a clear pattern as they were typically not used (due to the presence of many evolved solutions where $T_{AirVentOn}$ is less than $T_{AirVentOff}$). Similarly, $T_{AirVentOn}$ contained a

wide range of values that yielded non-dominated solutions without a clear pattern due to $T_{AirVentOff}$ being greater, a situation that results in $T_{AirVentOn}$ being largely unused by the control logic. Increasing $T_{AirBoilOn}$ increased the value of the crop yield as expected, but also formed an interesting cut-off point right below 20 °C; increasing the temperature further did not provide any non-dominated solutions. Finally, the values that determine the dynamic CO_2 setpoint show that a grower who wants to calibrate the rate of CO_2 injection towards low-cost solutions should lower $CO_{2AirExtMax}$ and increase $I_{GlobMax}$, while the converse is true for high-yield solutions. With some exceptions, $CO_{2AirExtMin}$ remained consistently very low, which helps minimize costs by preventing wasteful CO_2 injection. Based on the controller logic, CO_2 injection is never actually disabled; the setpoint is simply adjusted at every time step to determine if CO_2 injection occurs. Since Eq. (6.1) is reduced to $CO_{2AirExtMin}$ under the worst conditions (i.e., no global radiation, $U_{Vent} > 0.1$), the value for $CO_{2AirExtMin}$ should ideally be low enough that it would never trigger CO_2 injection under these conditions. Pragmatically speaking, the values for $CO_{2AirExtMin}$ were all significantly below atmospheric levels to avoid wasteful CO_2 injection (atmospheric CO_2 values in Almería, Spain exceed 380ppm for the period simulated in this thesis [48]).

6.3 Evolved Classical Controller (Added Time Partitioning)

6.3.1 Introduction

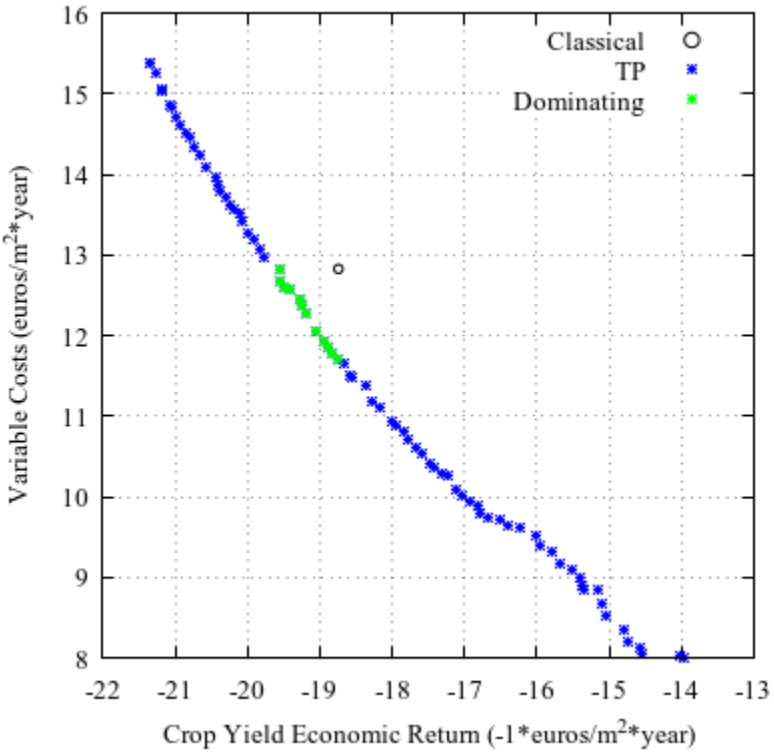

Figure 6.13. Pareto-optimal front for the control strategy discussed in this section. Solutions from this Pareto front which also dominate the classical Vanthoor strategy are marked in green.

This controller is based on a classical control strategy described by Vanthoor in his thesis [4], with the main differences being that most of the setpoints pertaining to greenhouse control are evolved. In addition, two additional copies of these setpoints are generated to be used in different time periods each day, yielding a total of three: morning (M), midday (D), and evening (E). The names of each variable or setpoint with these types of copies will have the abbreviations for these time periods appended to them (e.g. $T_{AirVentOn}$ becomes $T_{AirVentOnD}$ for the midday copy of this setpoint). A summary of the chromosome and its range of values is in Table 6.3.

With the addition of the three distinct daytime periods, there are now a total of four time periods (including nighttime). The daytime periods will begin and end at fixed points as defined in Table 6.4,

based on the number of hours that have passed by since midnight for each day. Nighttime is still defined as the absence of global radiation for purposes of this control strategy (i.e., $I_{Glob} = 0$). Since the thermal screen is the only greenhouse design element with distinct nighttime setpoints, and the greenhouse controller still needs to check whether boiler heating, fogging or ventilation is needed during nighttime, the greenhouse controller will simply choose the setpoints that are needed based on the current time (e.g., if the current time is 22:30 and the greenhouse controller is checking whether boiler heating is necessary, $T_{AirBoilOnE}$, the "evening" value will be used).

Table 6.3. Chromosome containing the setpoints used in the evolved classical controller with setpoint partitioning based on time of day. The genotype consists of 27 integer values.

Parameter Description	Parameter name/symbol	Unit	Genotype Value	Range of Real Values
Temperature above which ventilation (U_{vent}) is turned on	$T_{AirVentOnM}$, $T_{AirVentOnD}$, $T_{AirVentOnE}$	Degrees (Celsius)	[100, 300]	[10, 30]
Temperature below which ventilation is turned off	$T_{AirVentOffM}$, $T_{AirVentOffD}$, $T_{AirVentOffE}$	Degrees (Celsius)	[100, 300]	[10, 30]
Relative humidity above which ventilation is turned on	$RH_{AirVentOnM}$, $RH_{AirVentOnD}$, $RH_{AirVentOnE}$	%	[10, 100]	[10, 100]
CO_2 concentration below which ventilation is turned on	$CO_{2AirVentOnM}$, $CO_{2AirVentOnD}$, $CO_{2AirVentOnE}$	ppm	[1000, 5000]	[100, 500]
Temperature below which the boiler (U_{Boil}) is turned on	$T_{AirBoilOnM}$, $T_{AirBoilOnD}$, $T_{AirBoilOnE}$	Degrees (Celsius)	[100, 300]	[10, 30]
Nighttime temperature below which the thermal screen (U_{ThScr}) is deployed	$T_{OutThScrOnM}$, $T_{OutThScrOnD}$, $T_{OutThScrOnE}$	Degrees (Celsius)	[100, 300]	[10, 30]
Upper bound for dynamic CO_2 setpoint	$CO_{2AirExtMaxM}$, $CO_{2AirExtMaxD}$, $CO_{2AirExtMaxE}$	ppm	[2000, 10000]	[200, 1000]
Lower bound for dynamic CO_2 setpoint	$CO_{2AirExtMinM}$, $CO_{2AirExtMinD}$, $CO_{2AirExtMinE}$	ppm	[1000, 5000]	[100, 500]
Global radiation above which the dynamic CO_2 setpoint is maximized	$I_{GlobMaxM}$, $I_{GlobMaxD}$, $I_{GlobMaxE}$	W/m^2	[2000, 10000]	[200, 1000]

Table 6.4. Different times of day as defined in the greenhouse controller logic in this section. If the greenhouse controller detects nighttime due to lack of global radiation (i.e., $I_{Glob} = 0$), either morning or evening setpoints will be used (depending on the current time).

Parameter Description	Subscript	TIME
MORNING PERIOD	M	00:00 – 08:59
MIDDAY PERIOD	D	09:00 – 16:59
EVENING PERIOD	E	17:00 – 23:59

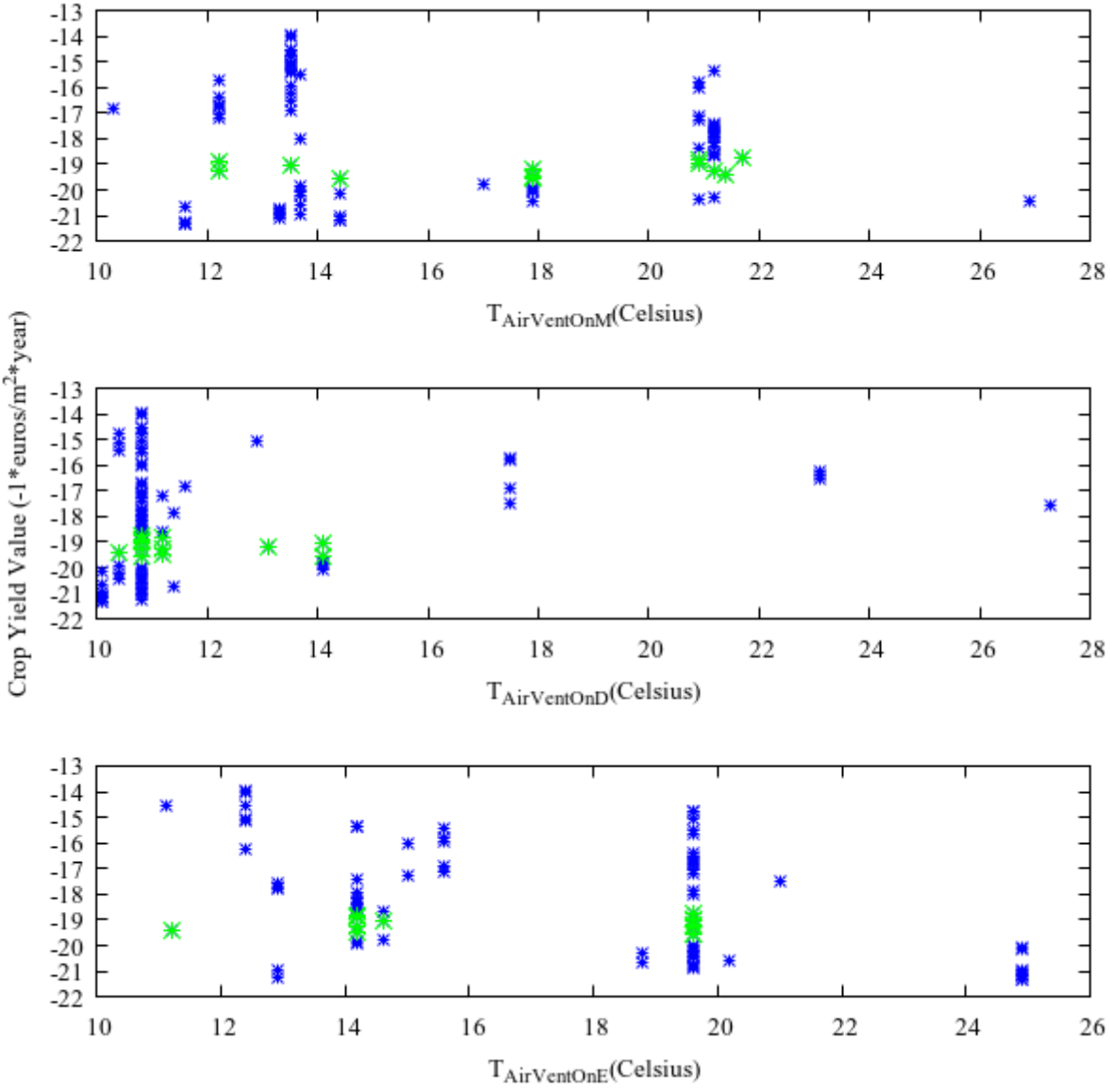

Figure 6.14. This setpoint determines the temperature above which the greenhouse controller will keep the ventilation open.

6.3.2 $T_{AirVentOn}$

Figure 6.14 contains a relatively wide range of values (between 10 – 28 degrees Celsius, depending on the time of day) that produce non-dominated solutions. Similar to the controller described in Section 6.2, the temperature at which the ventilation opens unconditionally is closely tied with its counterpart, $T_{AirVentOff}$ (due to its ability to override $T_{AirVentOn}$ in cases where it evolves to be greater). However, there is a bias towards lower temperatures during daytime which was not present without the time-partitioning feature. Many of these are overridden by $T_{AirVentOff}$, but most low-cost, low-crop-yield solutions will use a very low value for $T_{AirVentOnD}$ to ventilate the greenhouse when solar radiation is known to be at its highest (therefore contributing to higher greenhouse air temperatures which may require cooling).

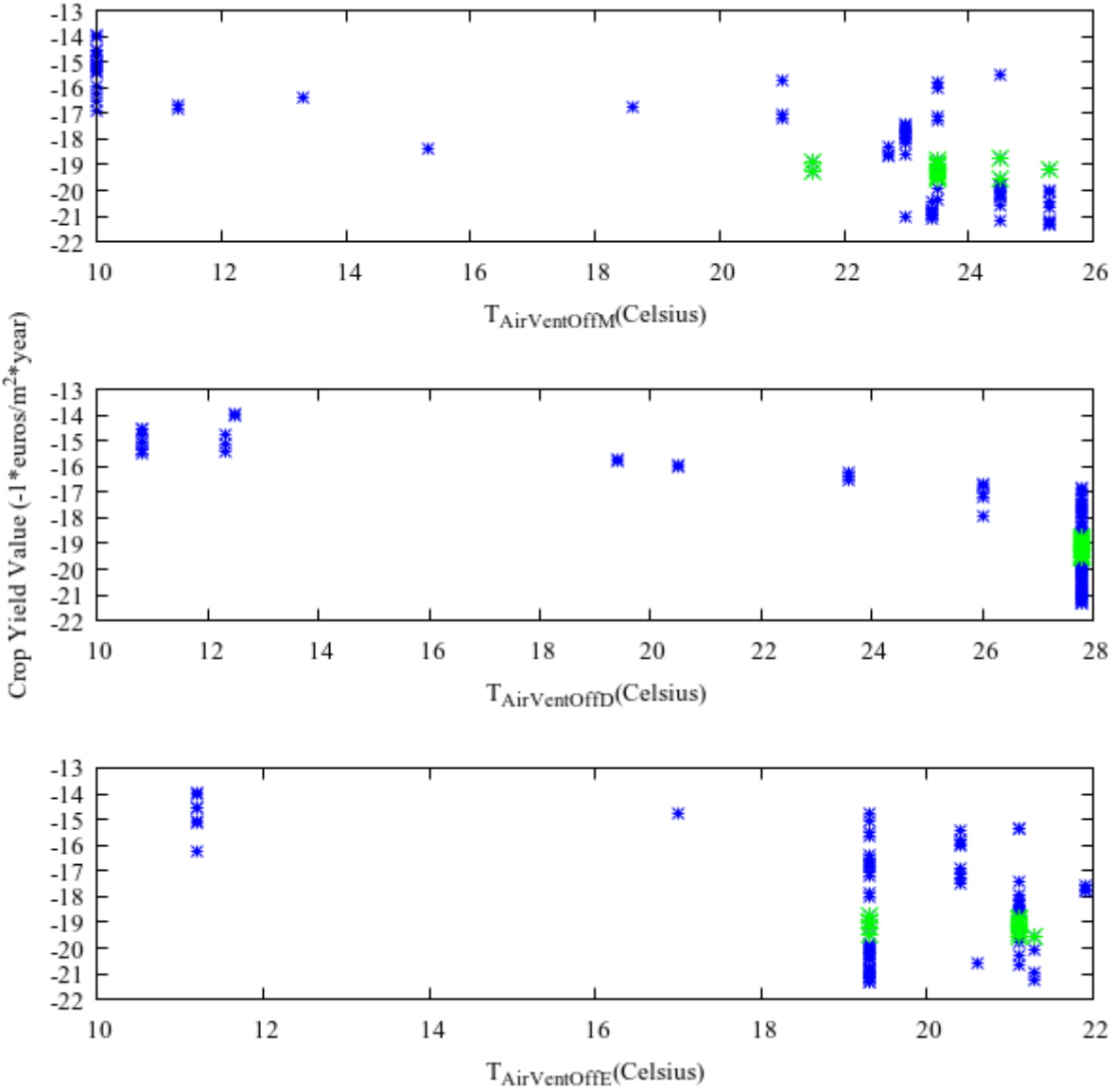

Figure 6.15. This setpoint determines the temperature below which the ventilation will always remain closed.

6.3.3 $T_{AirVentOff}$

The evolved values in Figure 6.15 clearly show a trend where increasing the temperature setpoint can produce greater crop yields at the expense of increased cooling costs. Moreover, the addition of the time-partitioning feature allowed for the evolved setpoints to better exploit the times of day where solar radiation is at its peak. Values for $T_{AirVentOff}$ corresponding to high-crop-yield solutions peak at a higher temperature during the daytime ($T_{AirVentOffD}$), while also peaking at lower temperatures during the evening

($T_{AirVentOffE}$), helping reduce plant respiration. Lastly, evolved solutions which dominate the classical Vanthoor strategy all prioritize higher temperatures.

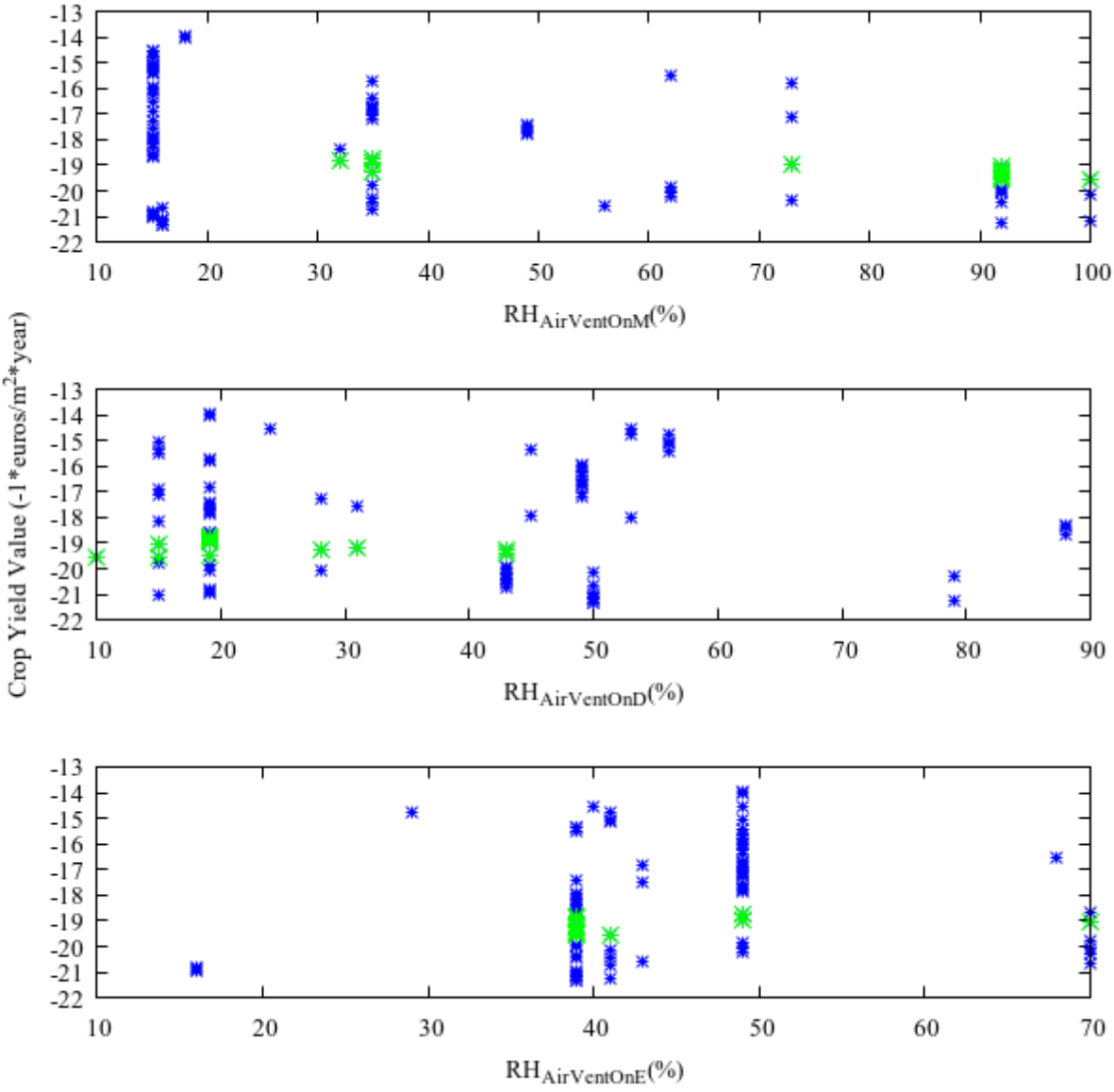

Figure 6.16. This setpoint determines the relative humidity above which ventilation is conditionally turned on.

6.3.4 $RH_{AirVentOn}$

Figure 6.16 shows that, much like with the previous controller in Section 6.2, a wide range of values work reasonably well for both low-cost and high-crop-value control strategies. The addition of the time-partitioning did not change this tendency, suggesting that Vanthoor's crop yield model does not

sufficiently penalize inadequate levels of relative humidity, since we know that, in practice, humidity control is important: if values for RH_{Air} are too low, the high vapor pressure deficit (VPD) associated with it can induce high stomatal resistance and plant water stress (PWS), while excessively high values for RH_{Air} and low VPD may reduce growth due to low transpiration (that can lead to physiological disorders), as well as disease if condensation occurs [49].

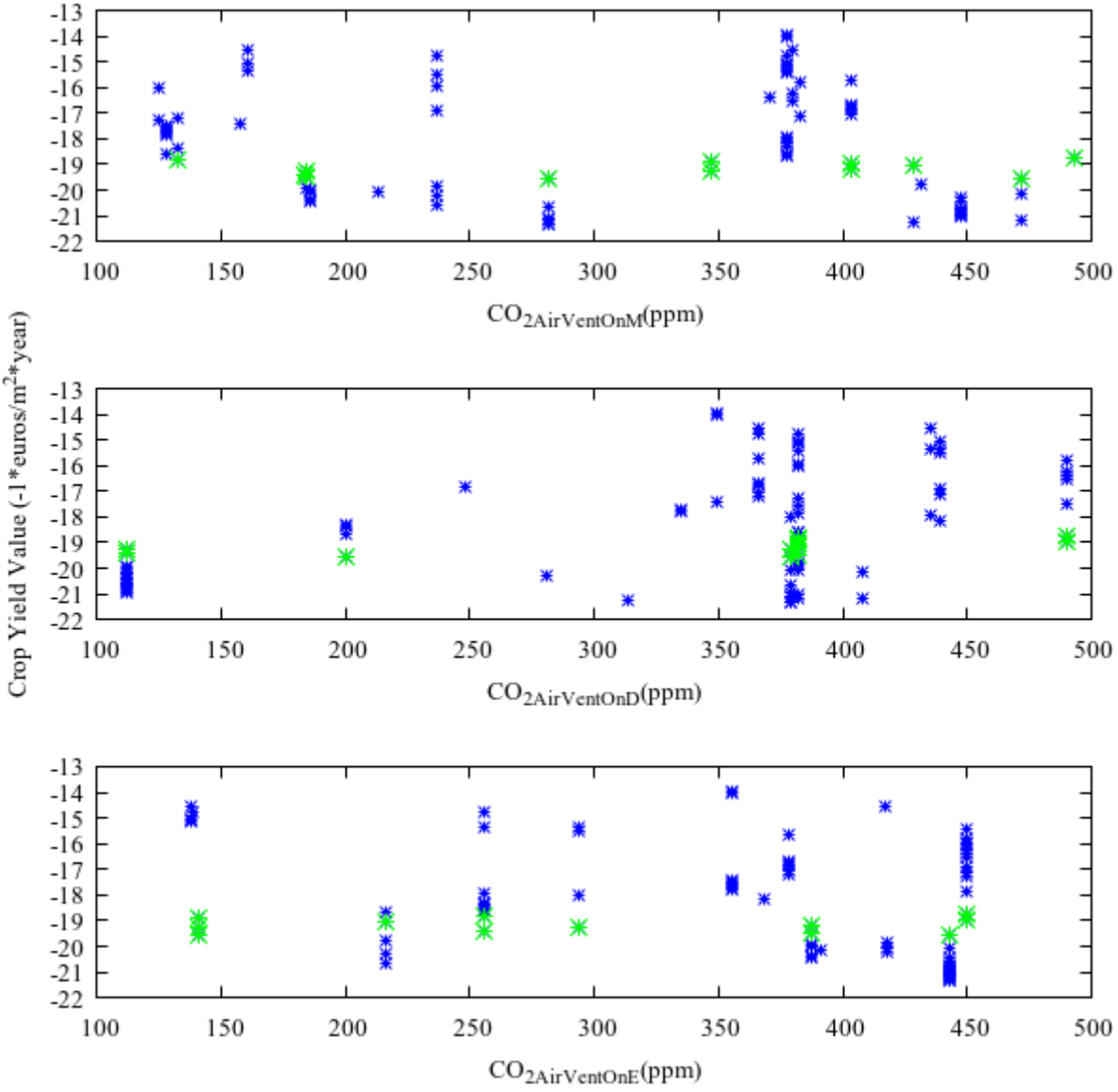

Figure 6.17. This setpoint determines the greenhouse air CO_2 concentration below which ventilation is conditionally turned on.

6.3.5 $CO_{2AirVentOn}$

Figure 6.17 shows a wide range of values that yield both low-cost and high-crop-value solutions, although this value ends up mostly unused (similar to $RH_{AirVentOn}$), due to the evolved values for $T_{AirVentOff}$ discussed in Section 6.3.3 being greater than $T_{AirVentOn}$ in most cases, resulting in evolved control strategies that disable the logic that checks for this value (see Figure 6.3).

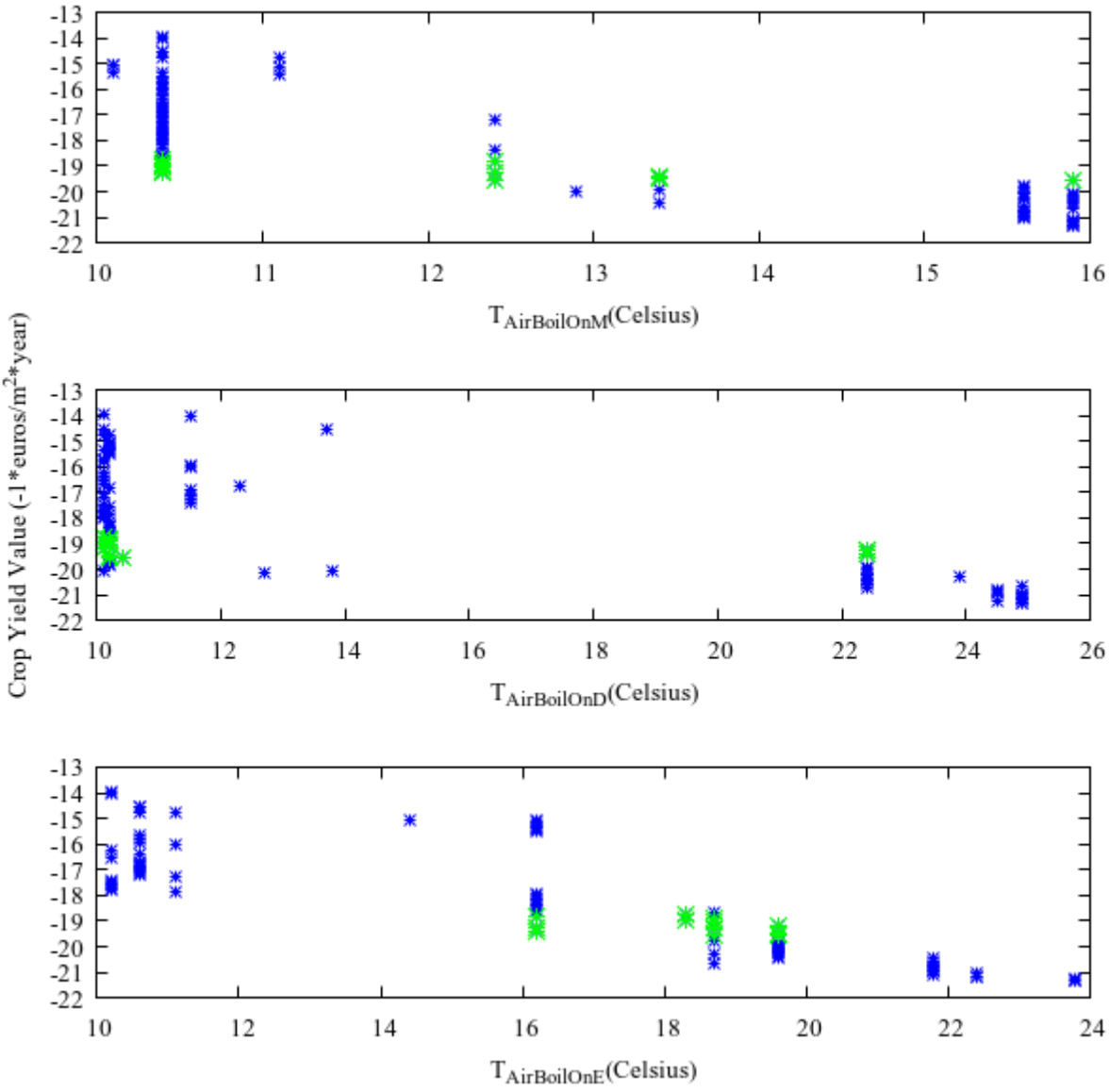

Figure 6.18. This setpoint determines the temperature below which the greenhouse controller will turn on the boiler heating.

6.3.6 $T_{AirBoilOn}$

The evolved setpoints in Figure 6.18 show a similar trend to that of $T_{AirBoilOn}$ in Section 6.2.6, although there is a clear difference in the upper bound for high-crop yield solutions depending on the time of day. Morning setpoints are significantly lower and do not exceed 16 degrees Celsius. Daytime setpoints are higher and reach almost 26 degrees Celsius. Evening setpoints are also higher, reaching almost 24 degrees Celsius. These trends show that it is advantageous to change the boiler setpoint based on different times of day (as defined in Table 6.4) if higher yields are desired. Moreover, solutions that dominate the classical Vanthoor strategy have a significantly lower value for this setpoint during the morning and daytime periods (nearing as low as 10 degrees Celsius).

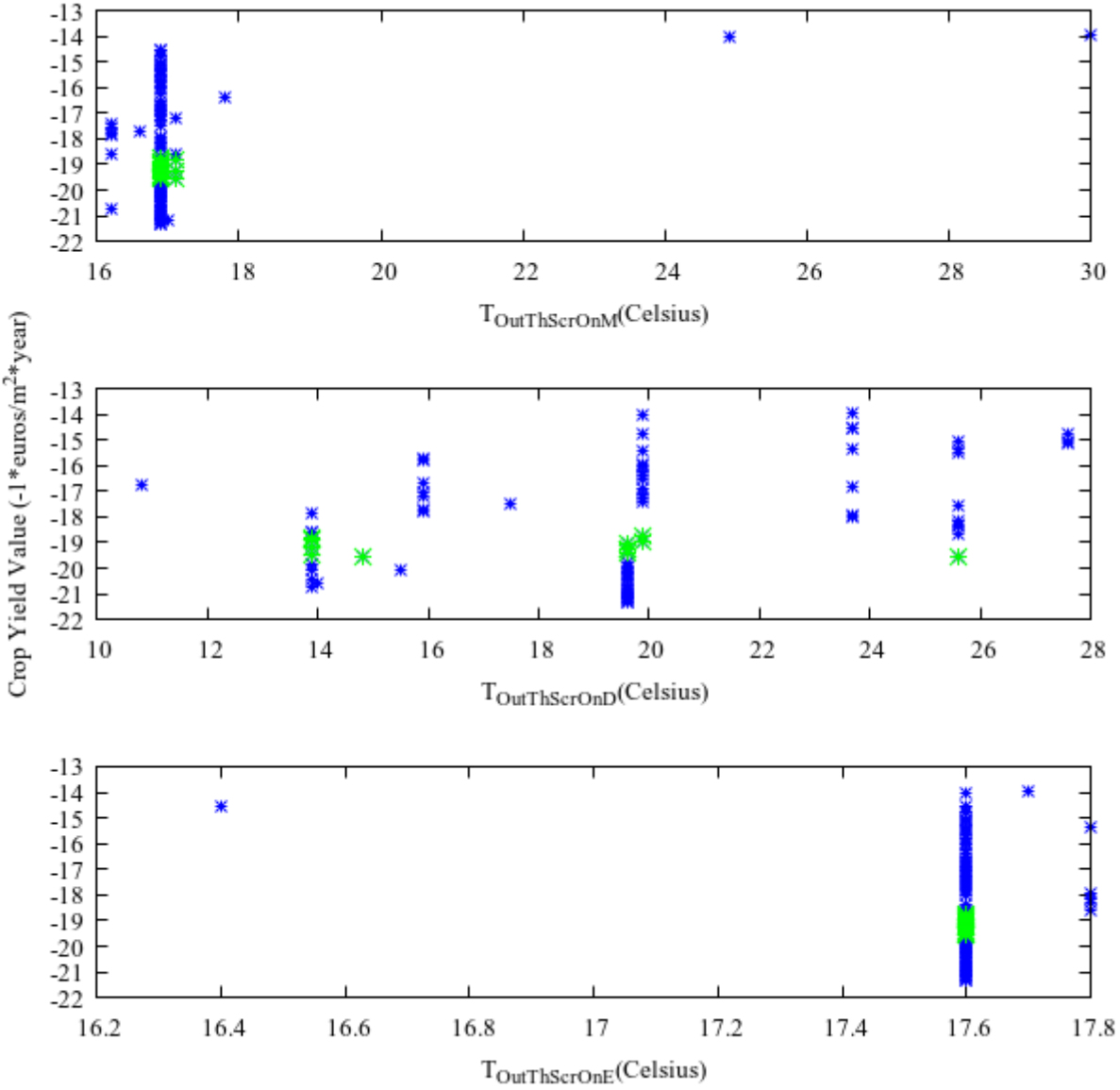

Figure 6.19. This setpoint determines the outside temperature below which the greenhouse controller will deploy the thermal screen.

6.3.7 $T_{OutThScrOn}$

For simulation purposes, nighttime is defined by the absence of solar radiation (i.e. $I_{Glob} = 0$) so it is possible, though very unlikely, for this setpoint to be used during the day. The values during the morning and evening time periods in Figure 6.19 are very similar to those discussed in Section 6.2.7. However, the values during the midday (D) period are significantly different and predominantly random due to this setpoint having no impact on greenhouse control unless it is nighttime.

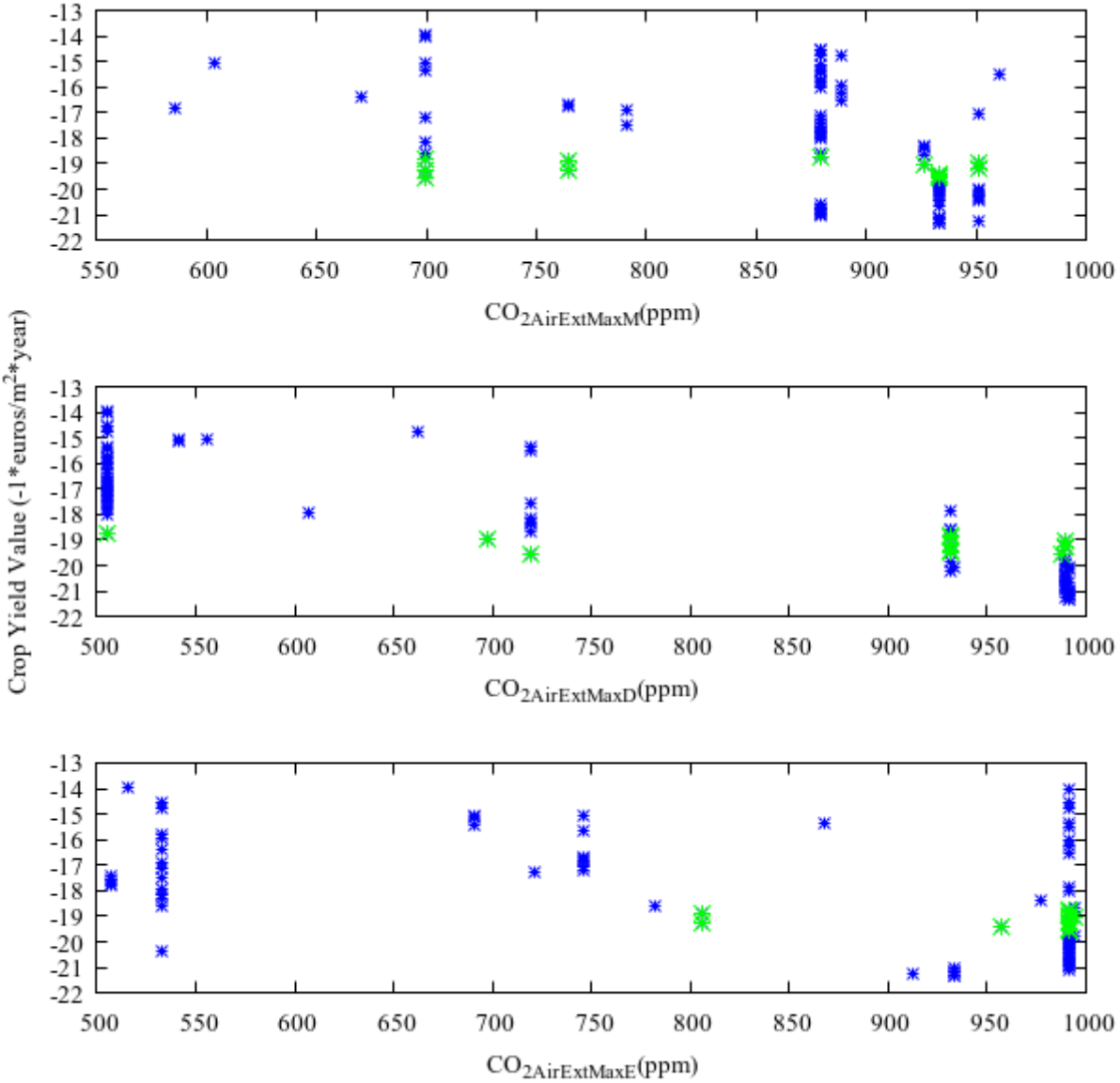

Figure 6.20. This variable determines the upper bound for the dynamic CO_2 setpoint used during CO_2 injection.

6.3.8 $CO_{2AirExtMax}$

Figure 6.20 shows the evolved values for this variable are largely similar to those discussed in Section 6.2.8. However, there is a marginal increase in the upper bound for $CO_{2AirExtMax}$ during the daytime and evening, indicating that it is advantageous to change the upper bound for the dynamic CO_2 setpoint ($CO_{2AirExtOn}$) based on the time of day.

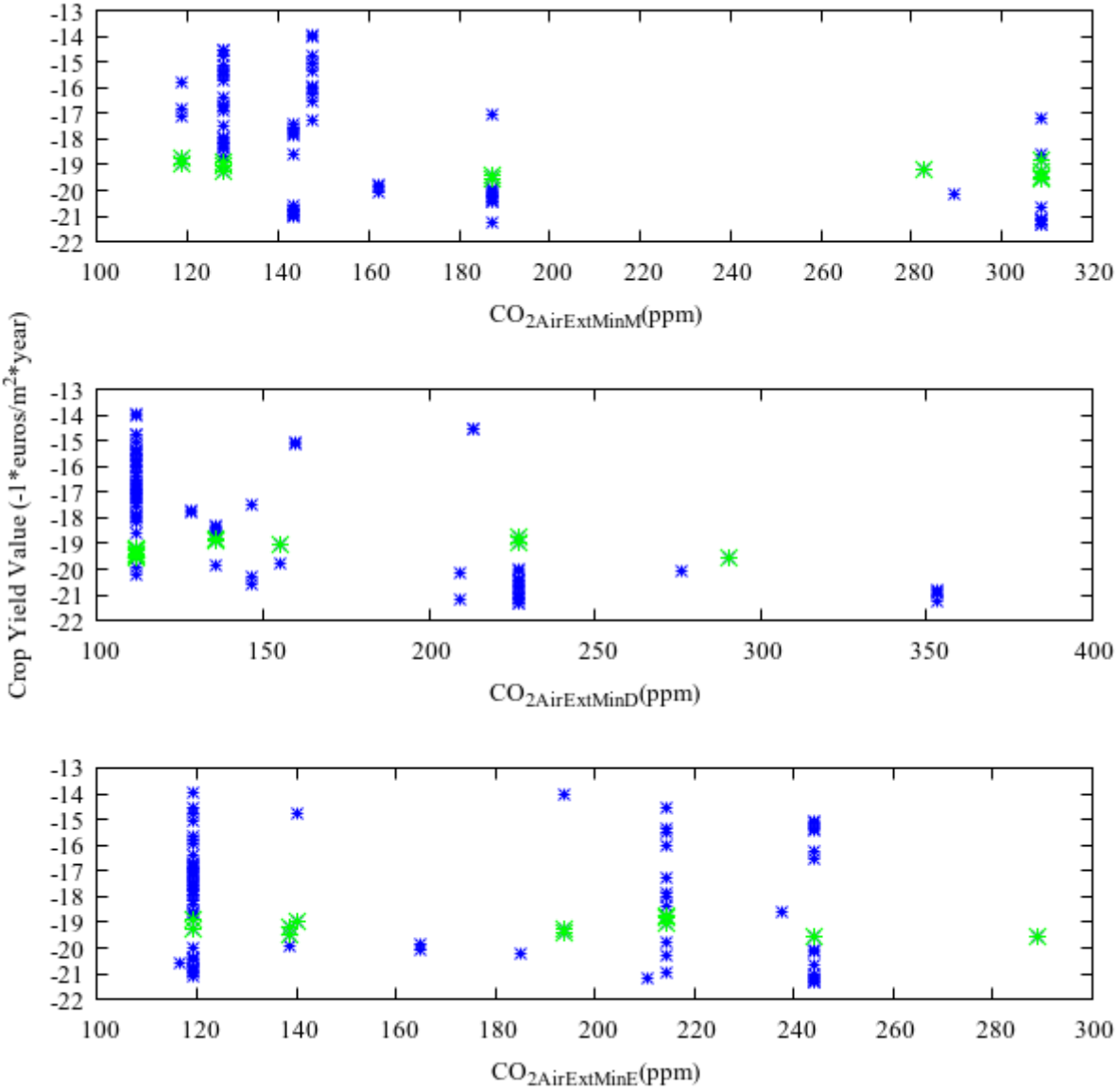

Figure 6.21. This variable determines the lower bound for the dynamic CO_2 setpoint used during CO_2 injection.

6.3.9 $CO_{2AirExtMin}$

Figure 6.21 shows the evolved values for this variable are largely similar to those discussed in Section 6.2.9. However, daytime values for $CO_{2AirExtMin}$ are marginally higher for high-crop-yield solutions, indicating that it is advantageous to change the lower bound for the dynamic CO_2 setpoint ($CO_{2AirExtOn}$) based on the time of day.

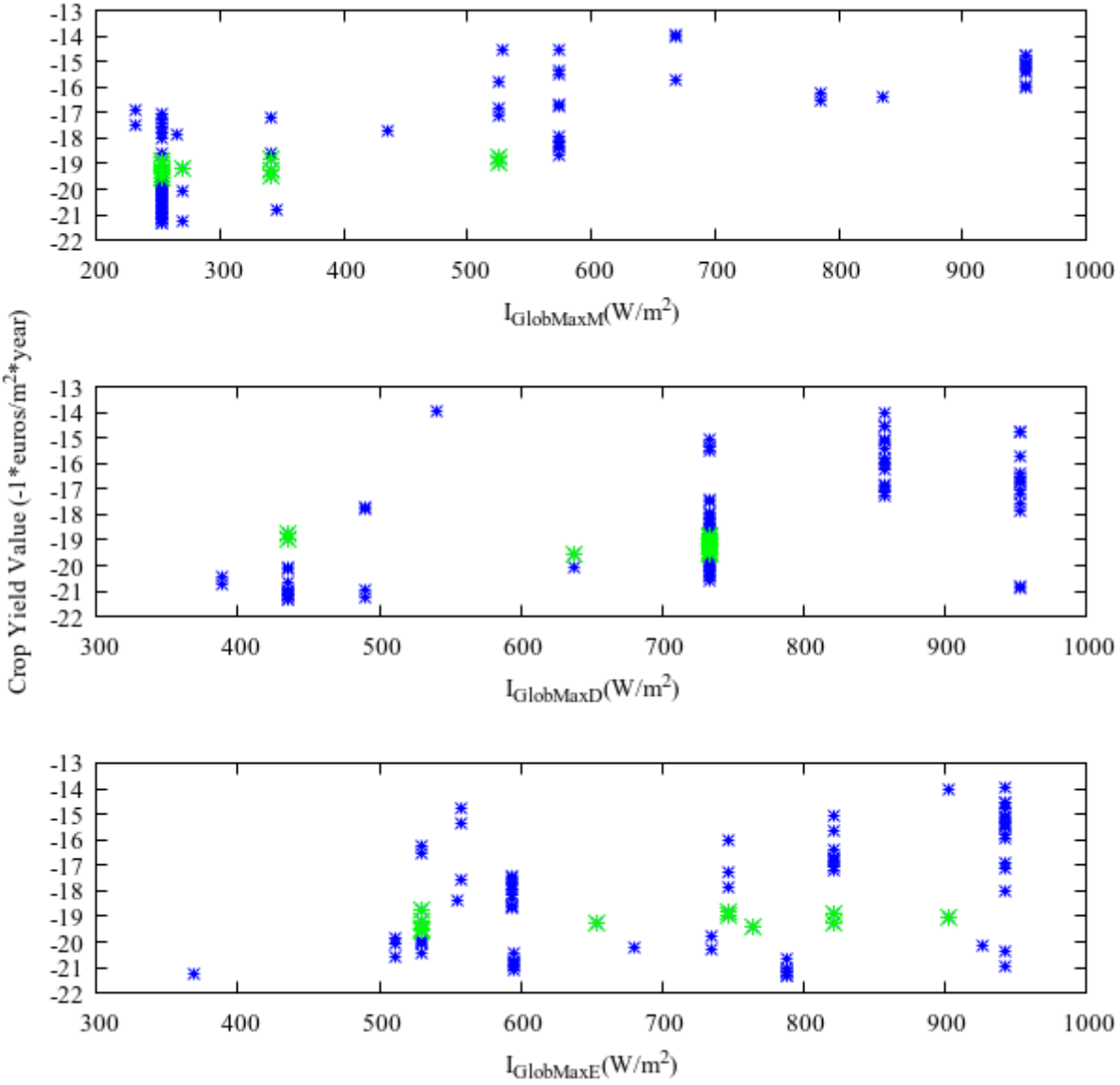

Figure 6.22. This variable determines how quickly $f(I_{Glob})$ is maximized, and subsequently contributes to how quickly the dynamic CO_2 setpoint is maximized.

6.3.10 $I_{GlobMax}$

Figure 6.22 shows the evolved values for this variable are largely similar to those discussed in Section 6.2.10, with daytime values for $I_{GlobMax}$ being overall higher for high-crop-yield solutions. Since increasing $I_{GlobMax}$ will cause the dynamic CO_2 setpoint ($CO_{2AirExtOn}$) to be maximized more slowly (see Eq. 6.1), it will reduce the benefits of CO_2 injection on crop yield. This can be counterproductive for high-crop yield solutions in some cases. However, since the overall crop-yield values are higher, and the

overall variable costs are lower (compared to the evolved classical strategy without time-partitioning), which is more indicative of a control strategy that is producing higher crop yields through other means (i.e., better control of optimal temperature ranges, longer periods of time where CO_2 injection is available due to closed ventilation, etc.), rather than a potentially sub-optimal CO_2 setpoint.

6.3.11 Discussion

There is a clear advantage to introducing the time-partitioning feature to the classical controller. The resulting Pareto-optimal front is consistently superior, particularly when taking advantage of seeding (as seen in Figure 5.3), and the loci themselves show some interesting patterns that emerged from this feature. The main benefit provided by time-partitioning is the ability for the greenhouse controller to apply various methods for saving energy without sacrificing crop yield, particularly when it comes to transitions from nighttime to daytime and vice versa. For example: the boiler setpoint, $T_{AirBoilOn}$, the temperature below which the boiler is turned on, is much higher during the daytime period when examining high-crop-yield solutions. This results in increased heating costs for that period, but it better exploits the high levels of solar radiation (I_{Glob}) that are typically present during that time. Conversely, morning and evening values are much lower, since photosynthetic activity is typically lower during these times, and maintaining optimal temperatures during that period is not as beneficial in comparison. Without time-partitioning, the greenhouse controller is forced to use a single setpoint that is adequate for all times of day, thus limiting its usefulness. Some setpoints proved to be redundant with the addition of time-partitioning (i.e., $T_{OutThScrOn}$).

One notable limitation for this controller is that the time of day is static (see definitions for morning, daytime, and evening in Table 6.4). This leads to evolved controllers that are unable to account for the changes in sunrise and sunset times throughout the year, which can limit their ability to accurately transition to daytime and nighttime strategies, respectively. Subsequent controllers in this chapter take this into account by calculating times for sunrise and sunset as transition points for the controller. Finally, while there are clear benefits to adding the time-partitioning feature, this is not just due to exploiting the

presence of climate patterns that emerge on a day-to-day basis; it is clearly advantageous to evolve as many copies of a setpoint as possible (as long as it is computationally feasible). To this end, the next section discusses a controller that also contains setpoints and variables which are evolved separately for two major stages of tomato crop development; namely, before and after fruit set has occurred.

6.4 Evolved Controller (Additional Features)

6.4.1 Introduction

This controller is similarly based on a classical control strategy described by Vanthoor in his thesis [4], with the main differences being that most of the setpoints pertaining to greenhouse control are evolved. In addition, the following features have been added:

1. Setpoint partitioning based on time of day
2. Setpoint partitioning based on fruit set occurrence
3. Nighttime period is determined by sunrise and sunset calculations
4. Adjustable time offset to determine transition point between nighttime and daytime strategies (e.g., the thermal screen, $T_{OutThScrOn}$, is only used during nighttime)

Due to the added features, the figures in this section will display up to six copies of one setpoint, depending on the time of day and whether or not fruit set has occurred. In addition, morning and evening periods will be dynamic: 1) for the morning (M), the current time for sunrise will determine the start of this period, and 2) for the evening (E), the current time for sunset will determine the end of this period. The midday (D) period remains static. Figure 6.24 shows an example of how a typical 24-hour period is partitioned using this method. If a setpoint or variable contains a copy to be used after fruit set, the corresponding abbreviation (_fr) will be appended to the end of the name, in addition to the abbreviations used to denote the time period (e.g. $T_{AirVentOn}$ becomes $T_{AirVentOnM\_fr}$ to denote the morning, post-fruit-set copy of this setpoint). The time offsets (sr_offset, and ss_offset, respectively) allow the controller to adjust the period in which a nighttime strategy is applied. A flowchart showing how these variables are

used can be seen in Figure 6.26. Lastly, a summary of the chromosome containing these changes can be seen in Table 6.5.

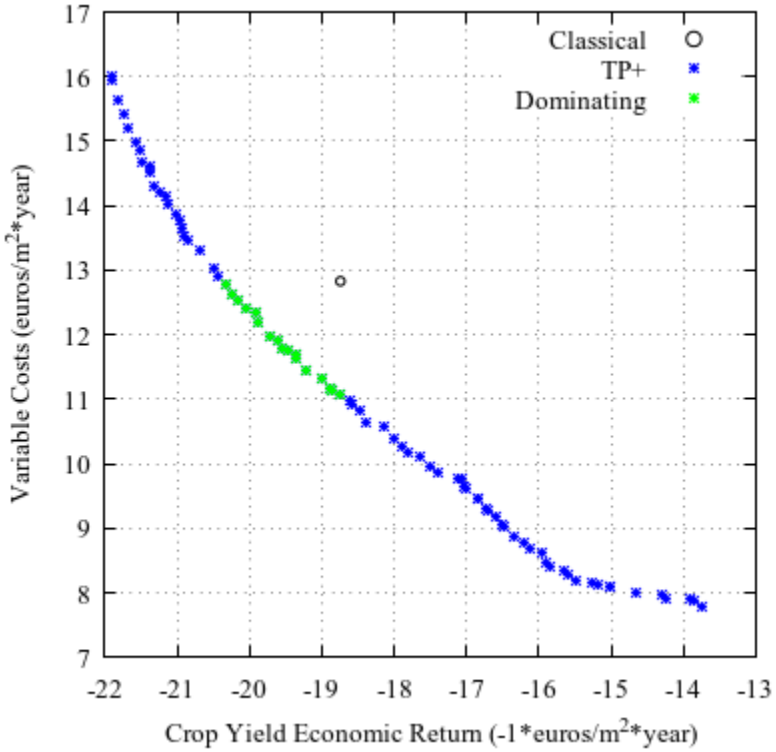

Figure 6.23. Pareto-optimal front for the control strategy discussed in this section. Solutions from this Pareto front which also dominate the classical Vanthoor strategy are marked in green.

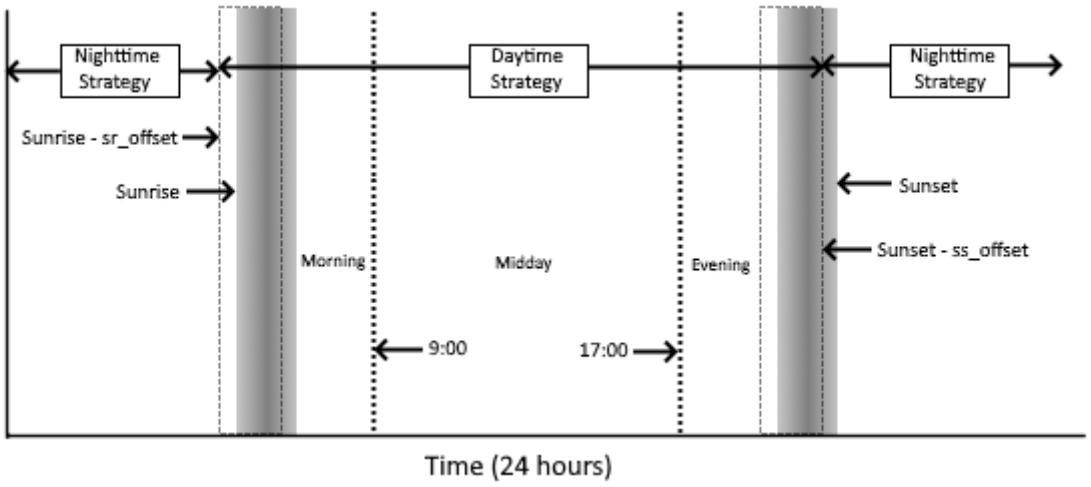

Figure 6.24. The greenhouse controller differentiates between daytime and nighttime to determine whether the thermal screen should be deployed, which is only used during nighttime. Both sr_offset and ss_offset are evolved values which will modify the overall length of both nighttime and daytime control strategies. These offsets remain fixed for each control strategy, while sunrise and sunset times (shaded region) change over the course of the year.

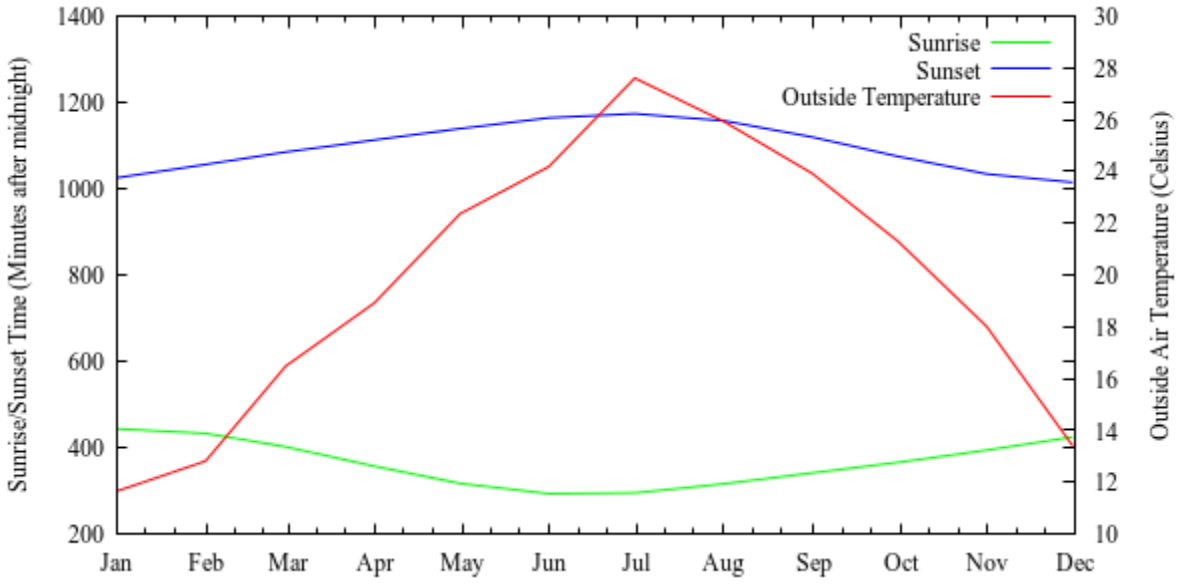

Figure 6.25. Sunrise/sunset times and average outside air temperatures calculated for the Almería, Spain location in 2006.

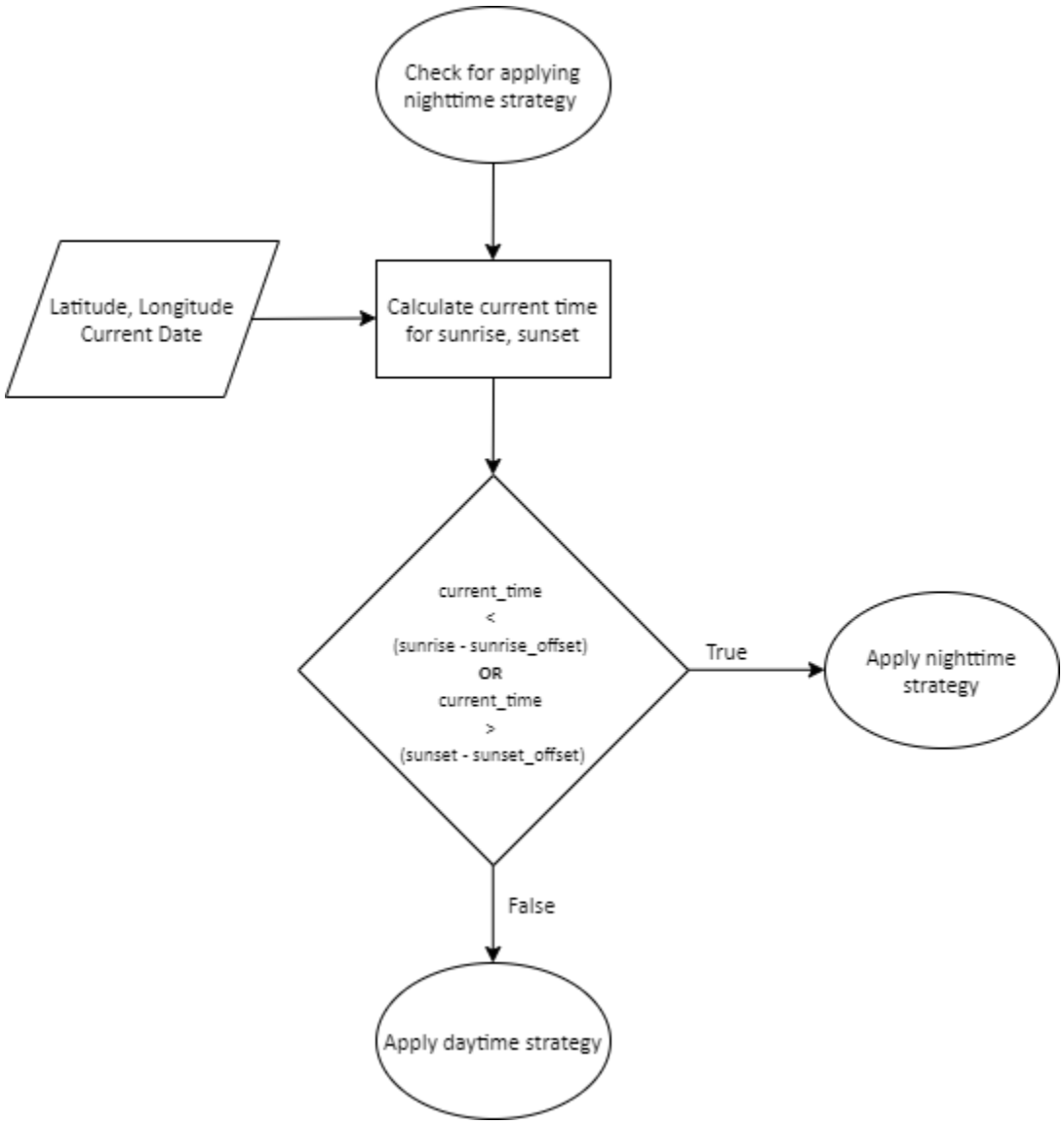

Figure 6.26. Flowchart describing the process for determining whether daytime or nighttime strategies are used.

Table 6.5. Chromosome containing the setpoints used in the evolved classical controller, with additional features. The total size of the genotype consists of 58 integer values.

Parameter Description	Parameter name/symbol	Unit	Genotype Value	Range of Real Values
Temperature above which ventilation (U_{vent}) is on	$T_{AirVentOnM}$, $T_{AirVentOnD}$, $T_{AirVentOnE}$, $T_{AirVentOnM\_fr}$, $T_{AirVentOnD\_fr}$, $T_{AirVentOnE\_fr}$	Degrees (Celsius)	[100, 300]	[10, 30]
Temperature below which ventilation is off	$T_{AirVentOffM}$, $T_{AirVentOffD}$, $T_{AirVentOffE}$, $T_{AirVentOffM\_fr}$, $T_{AirVentOffD\_fr}$, $T_{AirVentOffE\_fr}$	Degrees (Celsius)	[100, 300]	[10, 30]
Relative humidity above which ventilation is on	$RH_{AirVentOnM}$, $RH_{AirVentOnD}$, $RH_{AirVentOnE}$, $RH_{AirVentOnM\_fr}$, $RH_{AirVentOnD\_fr}$, $RH_{AirVentOnE\_fr}$	%	[10, 100]	[10, 100]
CO_2 concentration below which ventilation is on	$CO_{2AirVentOnM}$, $CO_{2AirVentOnD}$, $CO_{2AirVentOnE}$, $CO_{2AirVentOnM\_fr}$, $CO_{2AirVentOnD\_fr}$, $CO_{2AirVentOnE\_fr}$	ppm	[1000, 5000]	[100, 500]
Temperature below which the boiler (U_{Boil}) is on	$T_{AirBoilOnM}$, $T_{AirBoilOnD}$, $T_{AirBoilOnE}$, $T_{AirBoilOnM\_fr}$, $T_{AirBoilOnD\_fr}$, $T_{AirBoilOnE\_fr}$	Degrees (Celsius)	[100, 300]	[10, 30]
Nighttime temperature below which the thermal screen (U_{ThScr}) is deployed	$T_{OutThScrOnM}$, $T_{OutThScrOnD}$, $T_{OutThScrOnE}$, $T_{OutThScrOnM\_fr}$, $T_{OutThScrOnD\_fr}$, $T_{OutThScrOnE\_fr}$	Degrees (Celsius)	[100, 300]	[10, 30]
Upper bound for dynamic CO_2 setpoint	$CO_{2AirExtMaxM}$, $CO_{2AirExtMaxD}$, $CO_{2AirExtMaxE}$, $CO_{2AirExtMaxM\_fr}$, $CO_{2AirExtMaxD\_fr}$, $CO_{2AirExtMaxE\_fr}$	ppm	[2000, 10000]	[200, 1000]
Lower bound for dynamic CO_2 setpoint	$CO_{2AirExtMinM}$, $CO_{2AirExtMinD}$, $CO_{2AirExtMinE}$, $CO_{2AirExtMinM\_fr}$, $CO_{2AirExtMinD\_fr}$, $CO_{2AirExtMinE\_fr}$	ppm	[1000, 5000]	[100, 500]
Global radiation above which the dynamic CO_2 setpoint is maximized	$I_{GlobMaxM}$, $I_{GlobMaxD}$, $I_{GlobMaxE}$, $I_{GlobMaxM\_fr}$, $I_{GlobMaxD\_fr}$, $I_{GlobMaxE\_fr}$	W/m^2	[2000, 10000]	[200, 1000]
Amount to subtract from calculated sunrise time	sr_offset, sr_offset_fr	Minutes	[0, 30]	[0, 150]
Amount to subtract from calculated sunset time	ss_offset, ss_offset_fr	Minutes	[0, 30]	[0, 150]

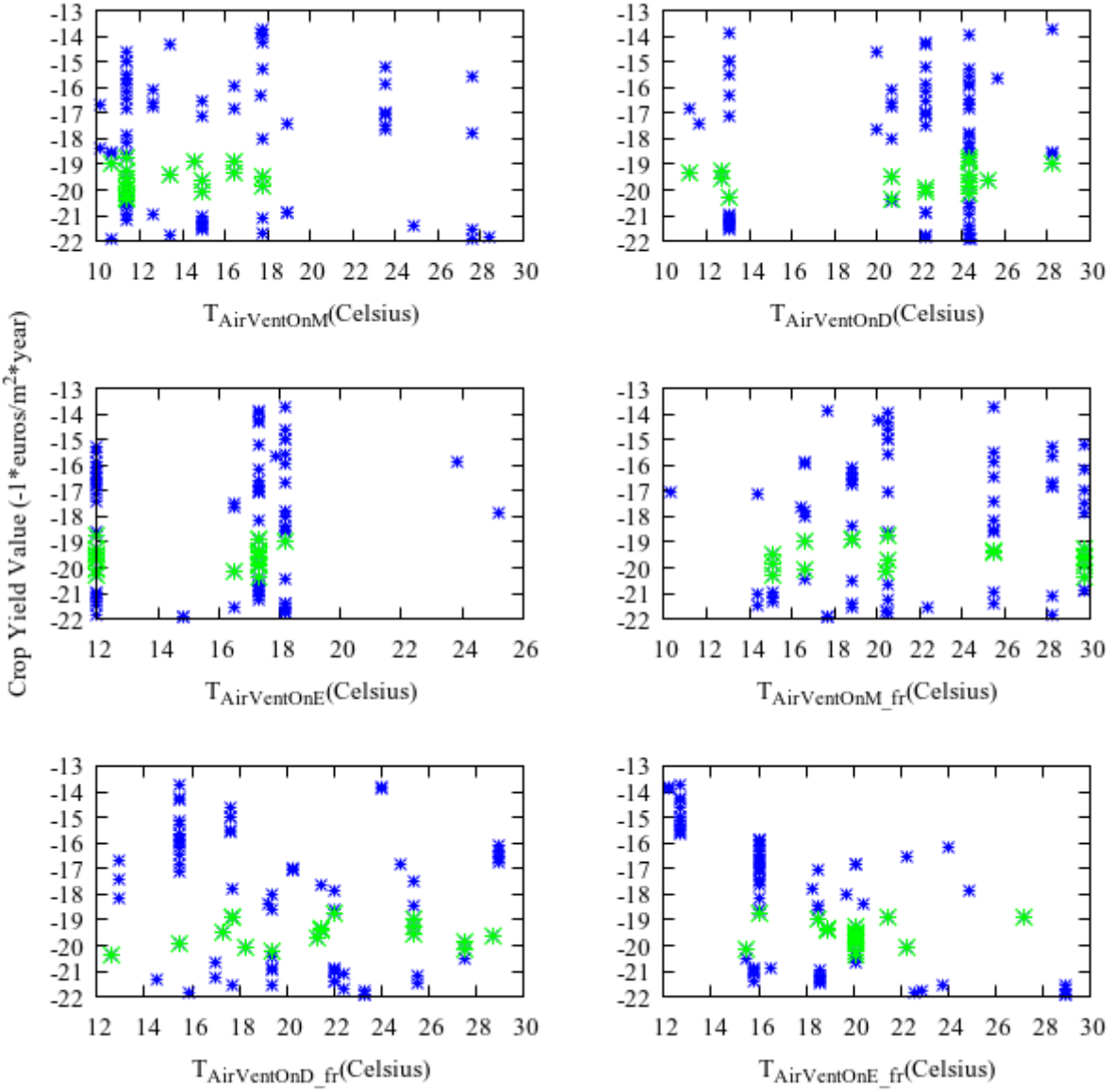

Figure 6.27. This setpoint determines the temperature above which the greenhouse controller will keep the ventilation open.

6.4.2 $T_{AirVentOn}$

Figure 6.27 shows a relatively wide range of values, depending on the time of day and whether fruit set has occurred (the first three graphs from left to right show solutions for before fruit set, while the last three graphs show solutions for after fruit set has occurred). As previously discussed, the temperature at which the ventilation opens unconditionally is closely tied with its counterpart, $T_{AirVentOff}$ (due to its ability to override $T_{AirVentOn}$ in cases where it evolves to be greater). However, the addition of distinct setpoints to

be used before and after fruit set has allowed for more values to be evolved that still retain a gap between $T_{AirVentOff}$ and $T_{AirVentOn}$. Although this allows $RH_{AirVentOn}$ and $CO_{2AirVentOn}$ to have more of an impact in greenhouse control (since they will be checked when the greenhouse air temperature falls within this gap), these results do not suggest that those values themselves are particularly important; rather, it is indicative of a strategy that "wants" to occasionally open greenhouse ventilation for purposes of temperature control.

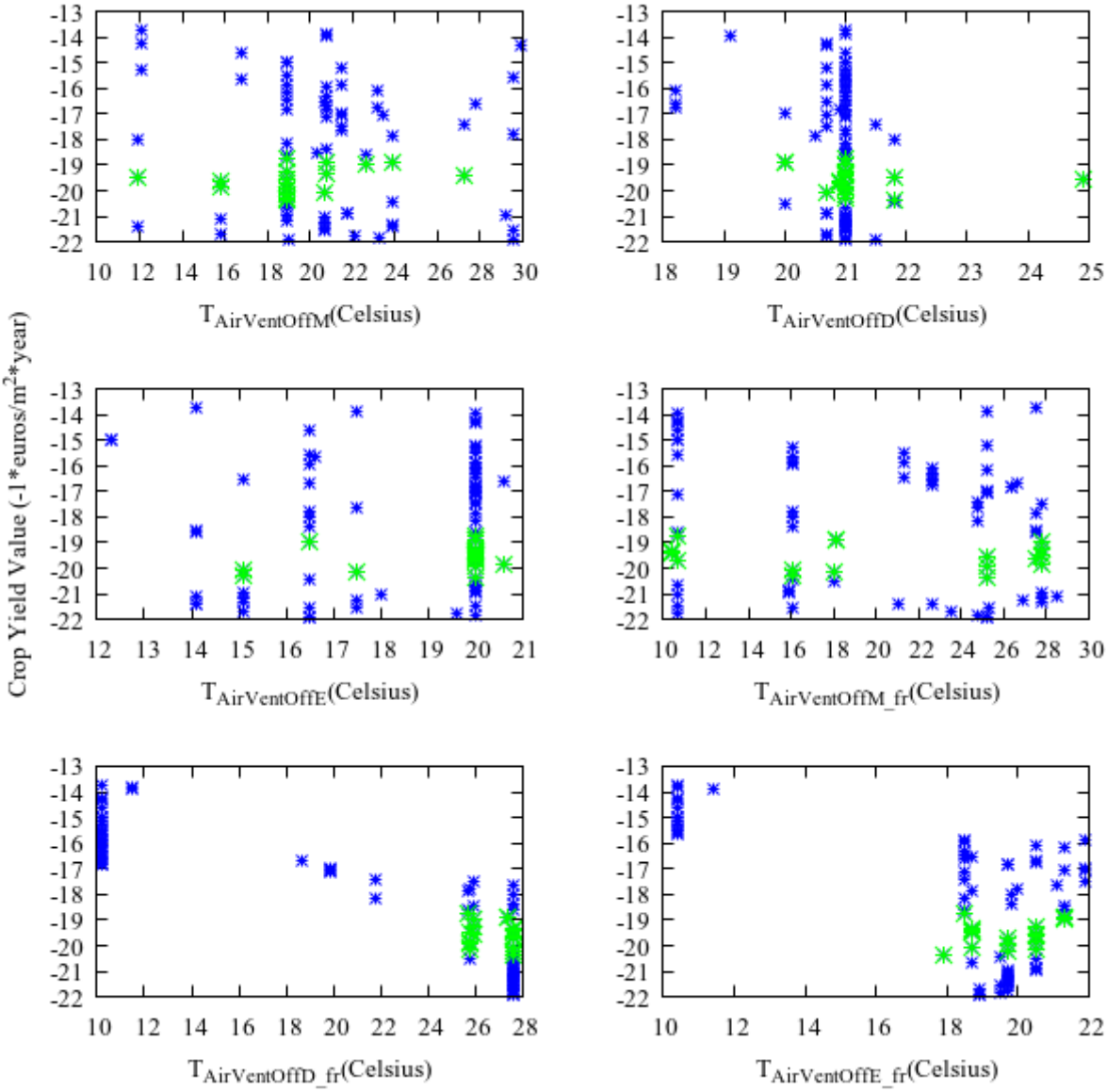

Figure 6.28. This setpoint determines the temperature below which the ventilation will always remain closed.

6.4.3 $T_{AirVentOff}$

The values in Figure 6.28 show similar trends to those discussed in Section 6.3.3, the addition of the time-partitioning feature allowed the evolved setpoints to better exploit the times of day where solar radiation is at its peak. However, the way in which this strategy does so differs significantly before and after fruit set: before, the daytime value (i.e., $T_{AirVentOffD}$), has a higher overall value while also being lower than its counterpart, $T_{AirVentOnD}$. This results in the gap present in the classical Vanthoor strategy where the greenhouse is opened conditionally (see Figure 6.3). After fruit set (i.e., $T_{AirVentOffD\_fr}$ and $T_{AirVentOffE\_fr}$), we can observe the same overall strategy discussed in Section 6.3.3, which prioritizes eliminating the gap normally present between $T_{AirVentOff}$ and $T_{AirVentOn}$ by having a value of $T_{AirVentOff\_fr}$ that is greater than $T_{AirVentOn\_fr}$. Values for $T_{AirVentOff\_fr}$ corresponding to high-crop yield solutions peak at a higher temperature during the daytime ($T_{AirVentOffD\_fr}$), while also peaking at lower temperatures during the evening ($T_{AirVentOffE\_fr}$), helping reduce plant respiration. Lastly, evolved solutions which dominate the classical Vanthoor strategy all prioritize higher temperatures, but only after fruit set has occurred.

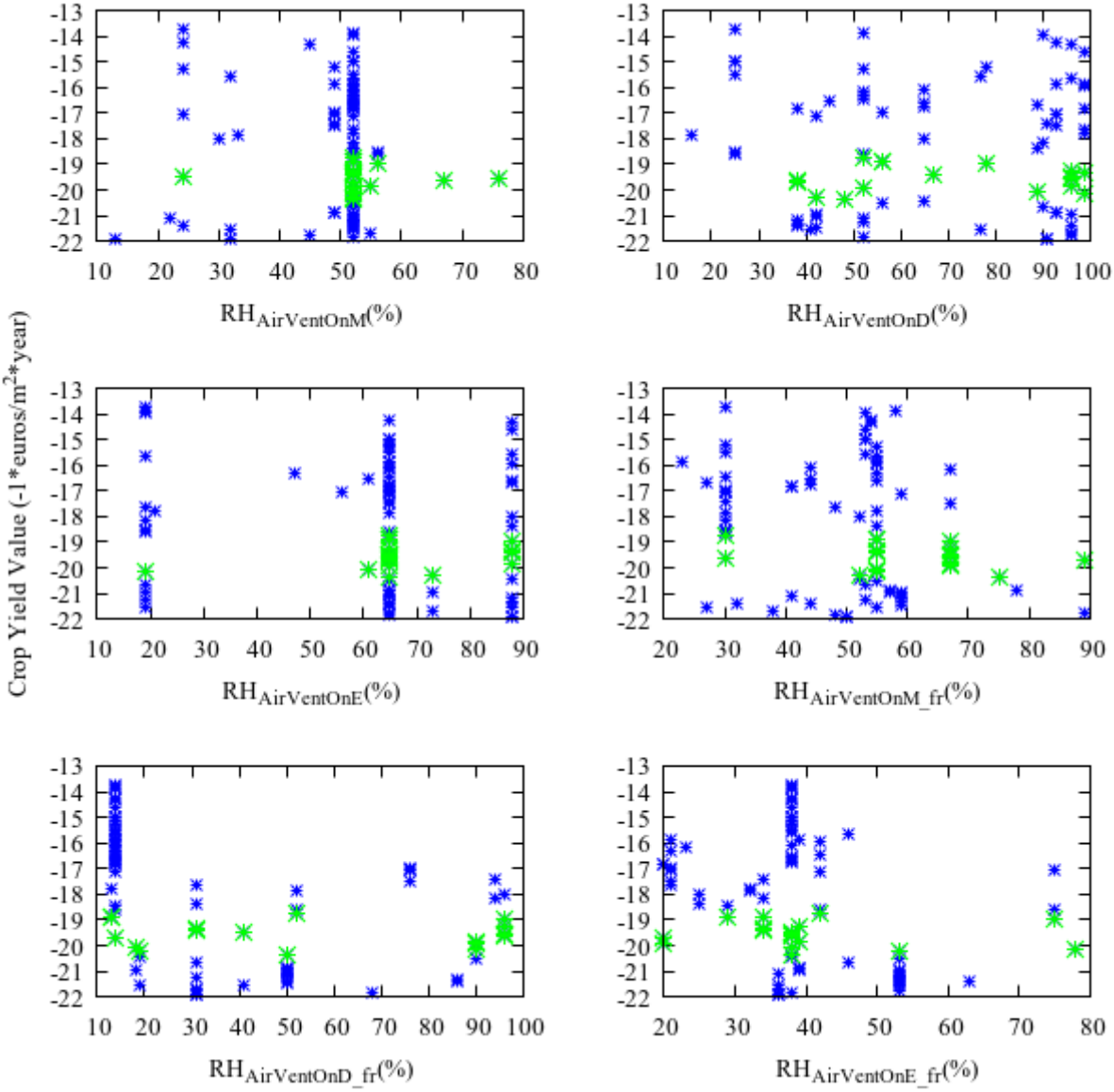

Figure 6.29. This setpoint determines the relative humidity above which ventilation is conditionally turned on.

6.4.4 $RH_{AirVentOn}$

Similar to the trends discussed in Section 6.3.4, we see in Figure 6.29 that the addition of the time-partitioning (and now distinct setpoints before and after fruit set) did not change the fact that this setpoint has little impact. This further suggests that the crop yield model does not sufficiently penalize inadequate levels of relative humidity, since we know that, in practice, humidity control is important [49].

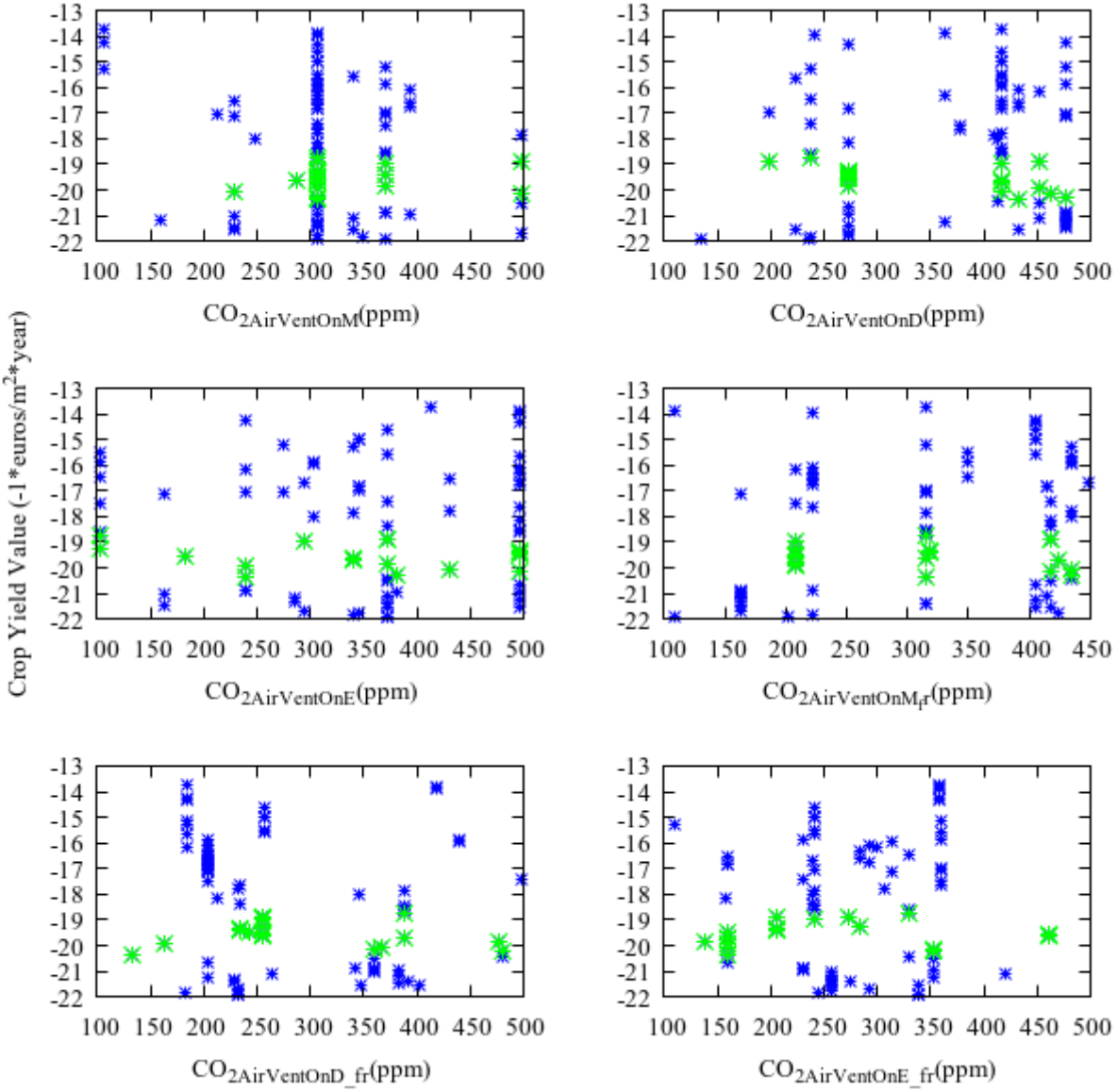

Figure 6.30. This setpoint determines the greenhouse air CO_2 concentration below which ventilation is conditionally turned on.

6.4.5 $CO_{2AirVentOn}$

Similar to the trends discussed in Section 6.3.5, the range of values among the non-dominated solutions is fairly wide despite the addition of time partitioning (and now the distinct setpoints before and after fruit set), suggesting that this setpoint still has little impact overall.

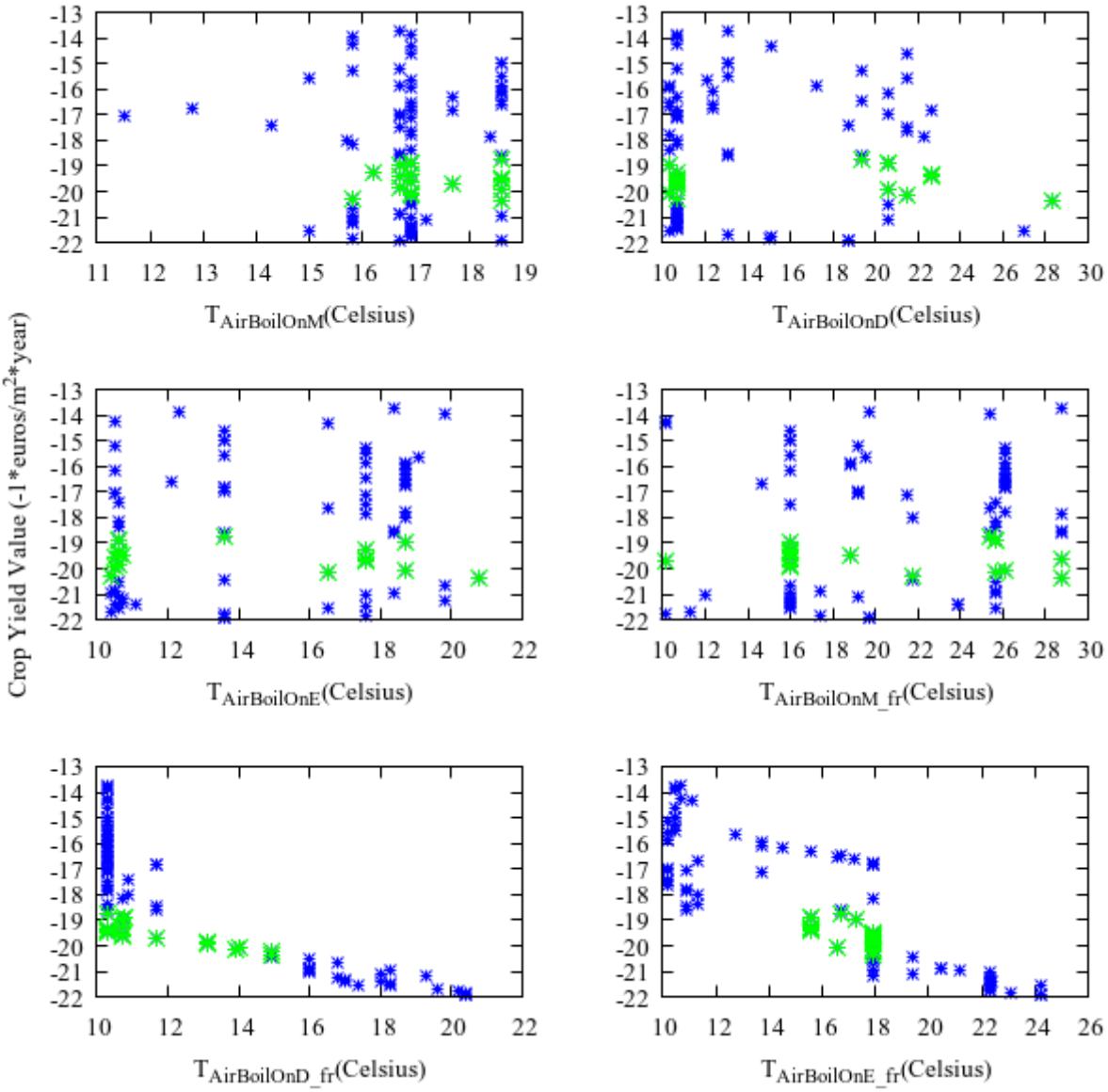

Figure 6.31. This setpoint determines the temperature below which the greenhouse controller will turn on the boiler heating.

6.4.6 $T_{AirBoilOn}$

The evolved setpoints in Figure 6.31 only show a similar trend to those discussed in Section 6.3.6 after fruit set has occurred (particularly $T_{AirBoilOnD\_fr}$ and $T_{AirBoilOnE\_fr}$). Before fruit set, there is a wide variety of values for this setpoint that yield both low-cost and high-crop-value solutions, although the morning values (i.e., $T_{AirBoilOnD}$) have a cluster of solutions that dominate the classical Vanthoor strategy at around 16 – 19 degrees Celsius. These results suggest that much of the reason for the trends discussed in Section

6.3.6 were due to major changes that only occur after fruit set; namely, the crop-yield model's requirements for optimal tomato crop growth, and the outside weather. Thus, there is significant benefit to having setpoints evolved separately for this stage of plant development.

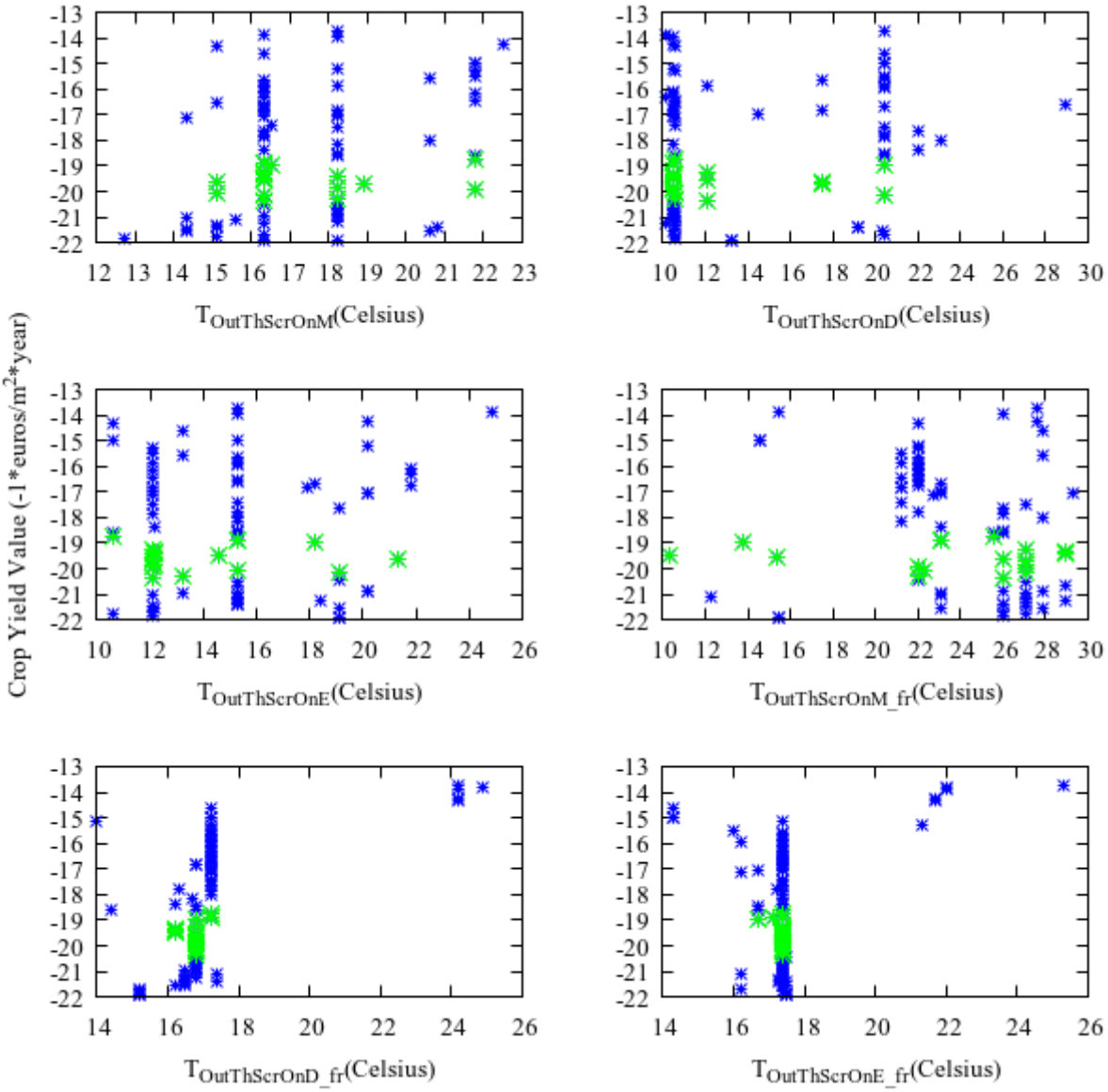

Figure 6.32. This setpoint determines the outside temperature below which the greenhouse controller will deploy the thermal screen.

6.4.7 $T_{OutThScrOn}$

Figure 6.32 shows trends that are similar to those discussed in Section 6.3.7, where the values are predominantly random when global radiation is present due to this setpoint having no impact on greenhouse control unless it is nighttime. Moreover, before fruit set occurs, we can clearly see that the evolved values for this setpoint did not converge as readily towards 18 degrees Celsius (corresponding to the classical Vanthoor strategy). However, the expected values for $T_{OutThScrOn}$ are clearly present in $T_{OutThScrOnD\_fr}$ and $T_{OutThScrOnE\_fr}$, respectively. Due to how the nighttime period is defined with this controller (i.e., beginning at sunset and ending at sunrise), the static definition for the midday time period (i.e., after 9am), and the time of year where fruit set typically occurs, $T_{OutThScrOnD\_fr}$ was pressured to evolve values that are associated with nighttime deployment of the thermal screen. In other words, the later times for sunrise typically associated with fall and winter made "proper" values for $T_{OutThScrOnD}$ more important.

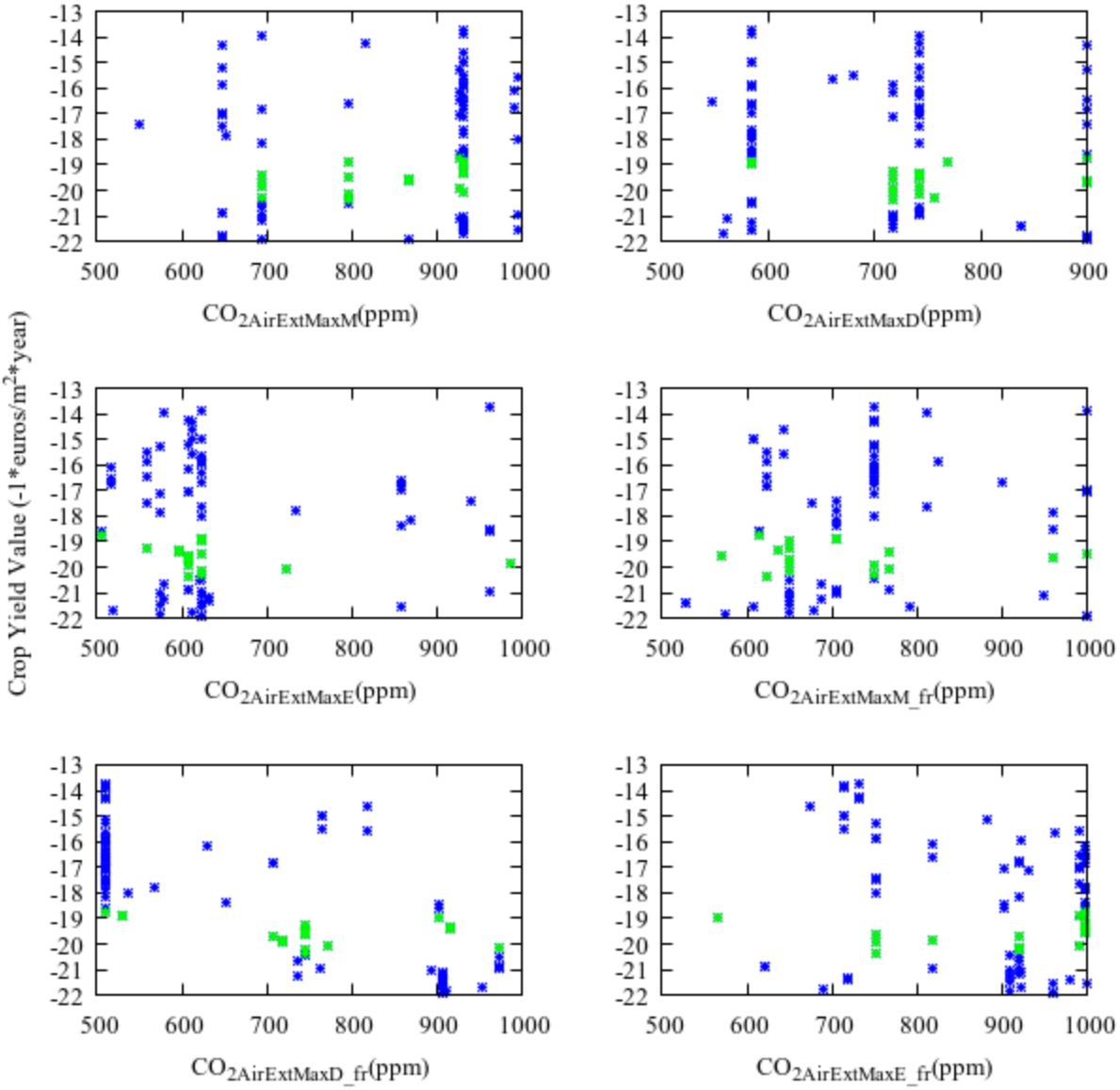

Figure 6.33. This variable determines the upper bound for the dynamic CO_2 setpoint used during CO_2 injection.

6.4.8 $CO_{2AirExtMax}$

The evolved values shown in Figure 6.33 show trends that are largely similar to those discussed in Section 6.3.8. However, before fruit set, there is a marginal *decrease* in the upper bound of the dynamic CO_2 setpoint during the daytime (i.e., decreasing $CO_{2AirExtMaxD}$ which is then used in $CO_{2AirExtOn}$), indicating that there is some benefit to changing this upper bound based on both time of day and plant development stage (in this case, to help reduce costs from CO_2 injection).

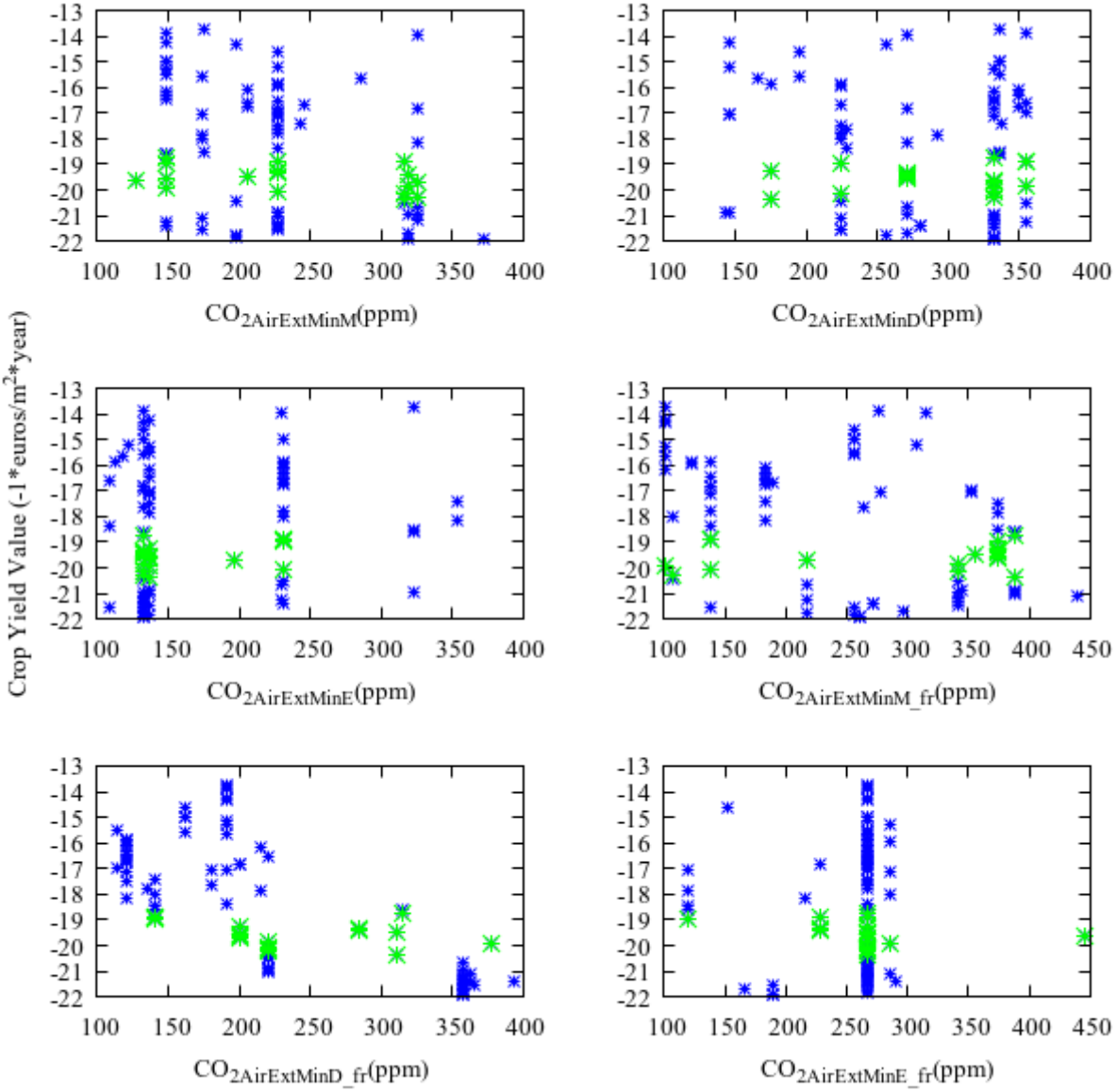

Figure 6.34. This variable determines the lower bound for the dynamic CO_2 setpoint used during CO_2 injection.

6.4.9 $CO_{2AirExtMin}$

Figure 6.34 shows trends that are largely similar to those discussed in Section 6.3.9. However, daytime values for $CO_{2AirExtMin}$ are marginally higher for high-crop-yield solutions, particularly after fruit set. Moreover, the evening setpoint after fruit set (i.e., $CO_{2AirExtMinE\_fr}$) heavily favors values near 260 ppm, which is overall higher compared to its counterpart before fruit set occurs.

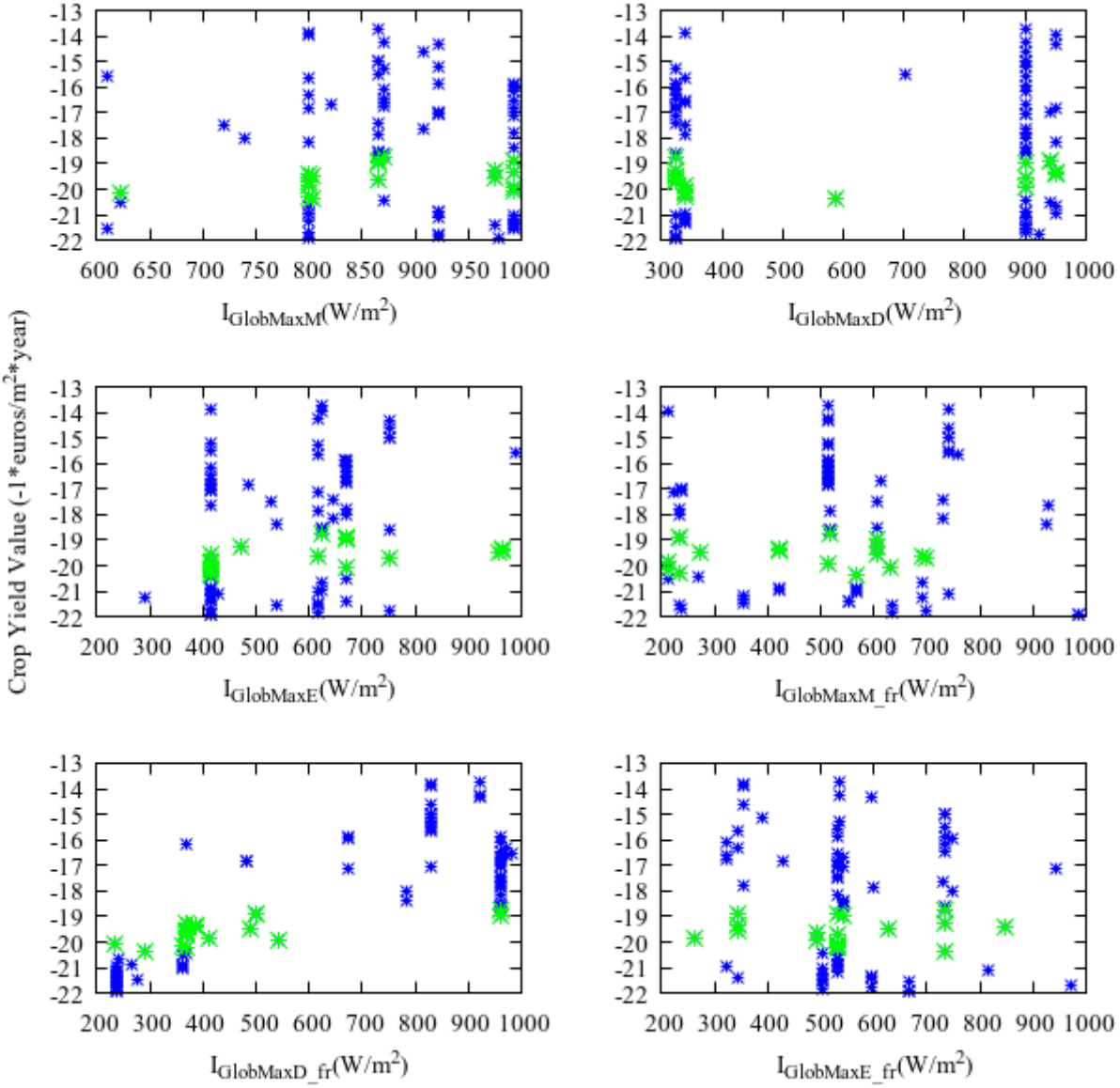

Figure 6.35. This variable determines how quickly $f(I_{Glob})$ is maximized, and subsequently contributes to how quickly the dynamic CO_2 setpoint is maximized.

6.4.10 $I_{GlobMax}$

Figure 6.35 shows trends that are largely similar to those discussed in Section 6.3.10, with some notable exceptions. In particular, the morning value before fruit set occurs (i.e., $I_{GlobMaxM}$) has a significantly higher lower bound, suggesting that it is advantageous to have a much less aggressive CO_2 injection strategy before fruit set has occurred (since increasing $I_{GlobMax}$ will cause the dynamic CO_2 setpoint to be maximized more slowly). In contrast, once fruit set has occurred, we can clearly see that a more

aggressive CO_2 injection strategy is preferred (with $I_{GlobMaxD\_fr}$ having the lowest values for high-crop-yield solutions), suggesting there is a clear benefit to a more straightforward CO_2 injection strategy that aims for a high setpoint for $CO_{2AirExtOn}$, rather than a middling value that is used more frequently by keeping the greenhouse sealed for longer periods of time.

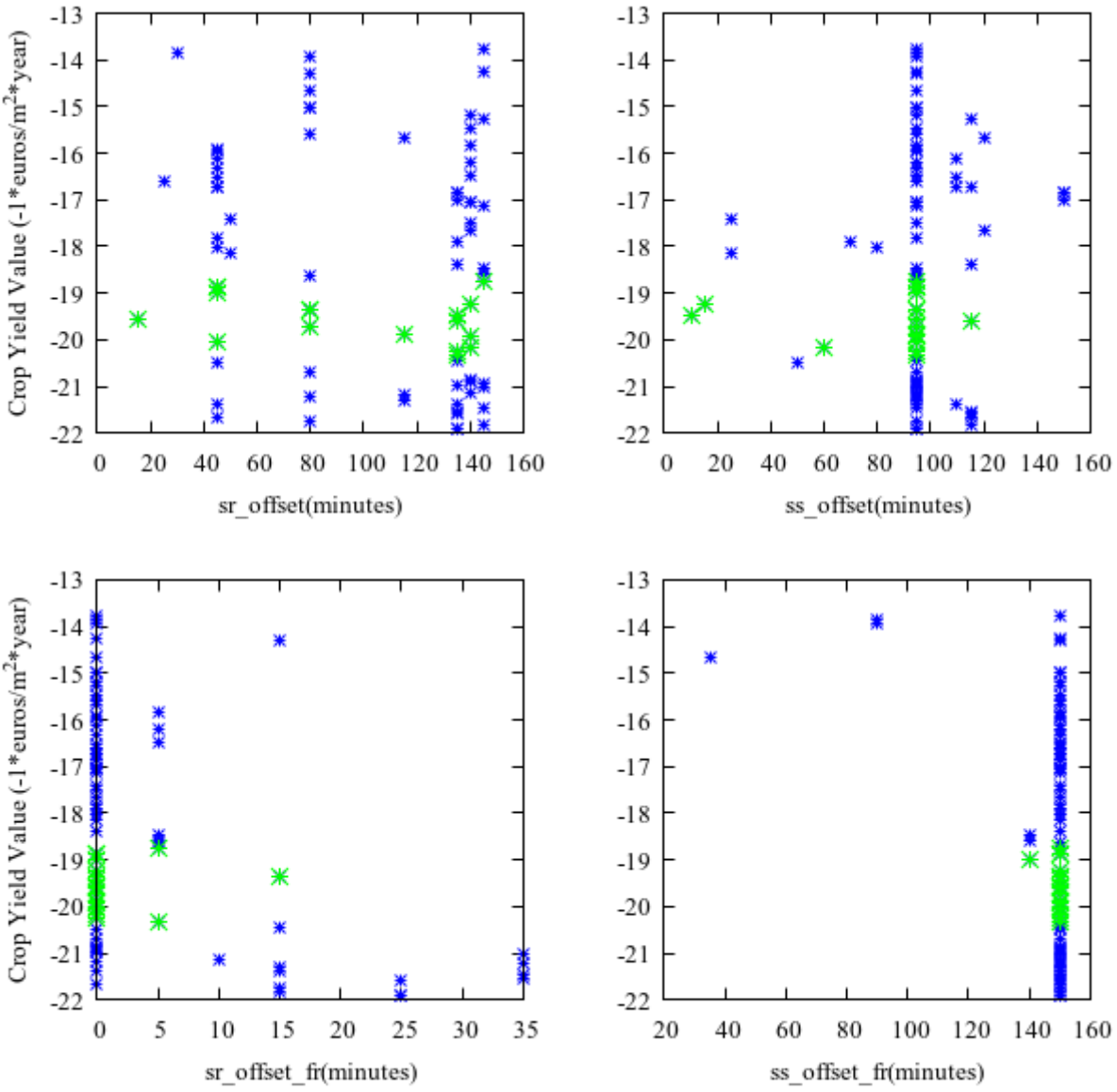

Figure 6.36. The copies of sr_offset and ss_offset are used to subtract from the current calculated time for sunrise and sunset, respectively.

6.4.11 Sunrise and Sunset Offsets (sr_offset, ss_offset)

Here in Section 6.4, we have introduced sunrise and sunset calculations to more accurately determine when the greenhouse controller should transition to daytime and nighttime strategies, respectively. In addition, we have evolved offsets to be used for both sunrise and sunset to help the controller determine how long before sunrise and sunset these transitions in control strategy should occur. That is, how long in advance of sunrise the "morning" period begins is a value evolved with the other parameters of the controller, and similarly for the sunset offset and the evening period.

Before fruit set occurs, Figure 6.36 shows there are a wide range of acceptable values for sr_offset that yield both low-cost and high-crop-value solutions. This is mainly due to a combination of the warm temperatures present at the start of the growing season (August), as well as the current plant development stage (i.e., before fruit set). Normally, one would expect this offset to prioritize either a relatively "large" or "small" value, since this would indicate that there is an advantage to prolonging or shortening the period in which a daytime strategy is applied, respectively. However, the variety of solutions indicates that there is little impact in this case. In contrast, sr_offset_fr heavily prioritizes smaller values. In typical cases, by October, fruit set has occurred (and thus harvesting begins). Around this time, sunrise begins to occur later, outside air temperatures begin to drop, and the daytime periods are shorter (see Figure 6.25). Most of the evolved values for sr_offset_fr reflect strategies that try to conserve heat as much as possible by extending the time period in which the thermal screen is used (since it is only deployed as part of the nighttime strategy). Clearly, the benefits of doing so outweigh the reduction in photosynthetic activity due to the thermal screen itself reducing the photosynthetically active radiation available to the plant during early hours, as well as the reduced amount of CO_2 injection.

Most of the evolved values for ss_offset are 95 minutes; thus, nighttime control strategies will begin 95 minutes before the current calculated time for sunset. This is the case for both low-cost and high-crop-yield value solutions. This suggests that, at least before fruit set occurs, it is not worth spending too much energy on maximizing the rate of photosynthesis of the crop as sunset is approaching, even if there is

some sunlight remaining. In the case of ss_offset_fr, most values are at 150 minutes, therefore signaling an even earlier shift to a nighttime control strategy as sunset approaches. Overall, it shows a similar trend to that of ss_offset, except the values are larger overall due to an increased need to conserve heat by using the thermal screen for longer periods of time during the fall and winter seasons, which coincide with the post-fruit-set timeframe.

6.4.12 Discussion

Clearly, the features introduced in this controller yielded some improvements over its predecessor (as seen in Figure 6.1). By introducing distinct setpoints to be used before and after fruit set, we have allowed the controller to evolve values that are better suited for the needs of the crop in a specific development stage and time of year. For example, the pre-fruit-set values used for the dynamic CO_2 setpoint (i.e., $CO_{2AirExtMax}$, $CO_{2AirExtMin}$, and $I_{GlobMax}$) produce a less aggressive CO_2 injection strategy overall compared to the previous controllers described in this chapter. In contrast, the post-fruiting values (i.e., $CO_{2AirExtMax\_fr}$, $CO_{2AirExtMin\_fr}$, and $I_{GlobMax\_fr}$), generally produce more a more aggressive CO_2 injection strategy. The pre-fruit-set values for ventilation-related setpoints (i.e., $T_{AirVentOff}$ and $T_{AirVentOn}$) do not prioritize maintaining the greenhouse sealed as much as the prior controllers; they instead allow for the greenhouse to be opened conditionally more often by having a gap between $T_{AirVentOff}$ and $T_{AirVentOn}$ (as shown in Figure 6.3). In contrast, the post-fruiting values prioritize maintaining the greenhouse sealed for longer periods of time. This is especially apparent in $T_{AirVentOffD\_fr}$, where the value of the crop yield increases with higher values on this setpoint, which is typical of control strategies that use a combination of active cooling and heating to maintain optimal temperature ranges while keeping the greenhouse sealed (even in cases where ventilation would be a viable method of cooling the greenhouse).

It was also clearly beneficial to use sunrise and sunset times to transition between nighttime and daytime control strategies (and vice-versa). This feature allows the length of the daytime strategy periods to change dynamically, thus providing finer control. In addition, both sunrise and sunset times (decremented by their respective offsets) provide a useful reference point: we know these times change daily, which

ultimately affects multiple environmental variables (e.g., the available sunlight, the length of the day, outside air temperature, etc.). However, this distinction between nighttime and daytime control could be better exploited, as the only control action that occurs during nighttime is whether the thermal screen ($T_{OutThScrOn}$) is deployed or not.

Some evolved setpoints, such as $RH_{AirVentOn}$ and $CO_{2AirVentOn}$, had little impact on the performance of the controller. In practice, we know that humidity control is important to avoid the onset of disease on the tomato crop, and that low levels of CO_2 concentration in the greenhouse air would also adversely affect the growth of the crop. Since it is unlikely that evolving these values further would yield more useful information, subsequent controllers will use default values for these setpoints that are known to be effective in practice, and in the case of the control strategy discussed in Section 6.6, we also introduce a penalty for sub-optimal levels of relative humidity in the greenhouse air.

6.5 Improved Controller without Penalty for Inadequate Relative Humidity

6.5.1 Introduction

This controller uses a combination of the features from the previous controllers, and makes additional changes based on areas where the results from the previous evolved controllers suggested there was room for improvement:

1. If $T_{AirVentOff} > T_{AirVentOn,}$ additional logic is added to the greenhouse controller to improve the handling of this special case (See Figure 6.38).
2. Ventilation, boiler, and fogging systems are all assumed to be PID controlled, and their respective gain values are all evolved.
3. $T_{AirVentOn}$, $T_{AirVentOff}$, and $T_{AirBoilOn}$ now contain additional copies to be used specifically during the nighttime period.
4. Changes in the greenhouse ventilation (U_{Vent}) caused by PID control will use the mean value of $T_{AirVentOn}$ and $T_{AirVentOff}$.

5. Setpoints and/or variables that were previously evolved, and subsequently found to have little impact on either objective were either removed or had their number of copies reduced. For example: $RH_{AirVentOn}$ and $CO_{2AirVentOn}$ have been removed entirely from the chromosome and default values found in literature are used instead, with $RH_{AirVentOn} = 0.9$ and $CO_{2AirVentOn} = 200$ ppm [4]. Setpoints like $T_{OutThScrOn}$ showed no tangible benefit from having additional copies based on the time of day, so the number of copies has been reduced to two (i.e., one copy is used before fruit set and one after fruit set).

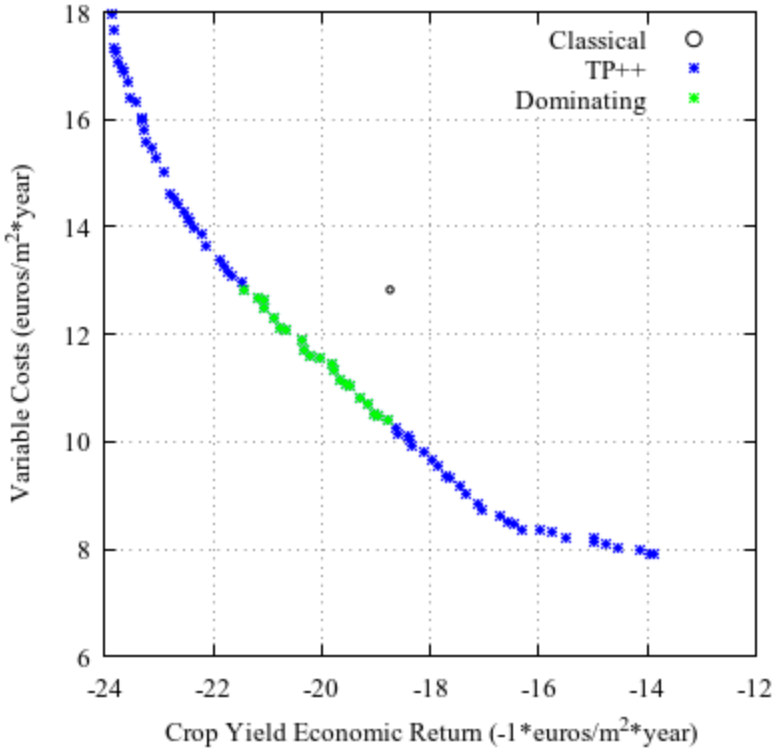

Figure 6.37. Pareto-optimal front for the control strategy discussed in this section. Solutions from this Pareto front which also dominate the classical Vanthoor strategy are marked in green.

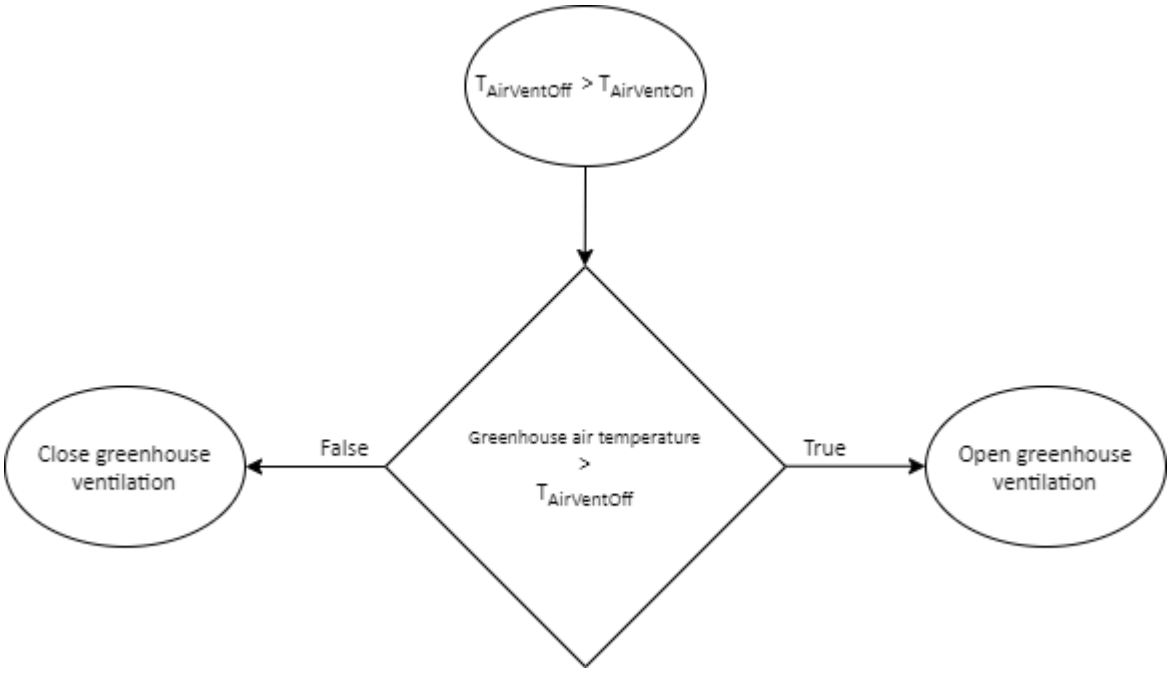

Figure 6.38. Simple flowchart describing the handling of the special case of $T_{AirVentOff} > T_{AirVentOn}$.

Table 6.6. Chromosome containing the setpoints used in this controller, with additional features. The total size of the genotype consists of 54 integer values.

Parameter Description	Parameter name/symbol	Unit	Genotype Value	Range of Real Values
Temperature above which ventilation (U_{vent}) is on	$T_{AirVentOnN}$, $T_{AirVentOnM}$, $T_{AirVentOnD}$, $T_{AirVentOnE}$, $T_{AirVentOnN\_fr}$, $T_{AirVentOnM\_fr}$, $T_{AirVentOnD\_fr}$, $T_{AirVentOnE\_fr}$	Degrees (Celsius)	[100, 300]	[10, 30]
Temperature below which ventilation is off	$T_{AirVentOffN}$, $T_{AirVentOffM}$, $T_{AirVentOffD}$, $T_{AirVentOffE}$, $T_{AirVentOffN\_fr}$, $T_{AirVentOffM\_fr}$, $T_{AirVentOffD\_fr}$, $T_{AirVentOffE\_fr}$	Degrees (Celsius)	[100, 300]	[10, 30]
Temperature below which the boiler (U_{Boil}) is on	$T_{AirBoilOnN}$, $T_{AirBoilOnM}$, $T_{AirBoilOnD}$, $T_{AirBoilOnE}$, $T_{AirBoilOnN\_fr}$, $T_{AirBoilOnM\_fr}$, $T_{AirBoilOnD\_fr}$, $T_{AirBoilOnE\_fr}$	Degrees (Celsius)	[100, 300]	[10, 30]
Nighttime temperature below which the thermal screen (U_{ThScr}) is deployed	$T_{OutThScrOn}$, $T_{OutThScrOn\_fr}$	Degrees (Celsius)	[100, 300]	[10, 30]
Proportional, integral and derivative gain values for boiler control	PID_{BoilP}, PID_{BoilI}, PID_{BoilD}, PID_{BoilP_fr}, PID_{BoilI_fr}, PID_{BoilD_fr}	(1×10^5)	[10, 100]	$[10^{-5}, 10^{-4}]$
Proportional, integral and derivative gain values for fogging system control	PID_{FogP}, PID_{FogI}, PID_{FogD}, PID_{FogP_fr}, PID_{FogI_fr}, PID_{FogD_fr}	(1×10^5)	[10, 100]	$[10^{-5}, 10^{-4}]$
Proportional, integral and derivative gain values for ventilation control	PID_{ventP}, PID_{VentI}, PID_{VentD}, PID_{VentP_fr}, PID_{VentI_fr}, PID_{BoilD_fr}	(1×10^5)	[10, 100]	$[10^{-5}, 10^{-4}]$
Upper bound for dynamic CO_2 setpoint	$CO_{2AirExtMax}$, $CO_{2AirExtMax\_fr}$	ppm	[2000, 10000]	[200, 1000]
Lower bound for dynamic CO_2 setpoint	$CO_{2AirExtMin}$, $CO_{2AirExtMin\_fr}$	ppm	[1000, 5000]	[100, 500]
Amount to subtract from calculated sunrise time	sr_offset, sr_offset_fr	Minutes	[0, 30]	[0, 150]
Amount to subtract from calculated sunset time	ss_offset, ss_offset_fr	Minutes	[0, 30]	[0, 150]
Global radiation above which the dynamic CO_2 setpoint is maximized	$I_{GlobMax}$, $I_{GlobMax\_fr}$	W/m^2	[2000, 10000]	[200, 1000]

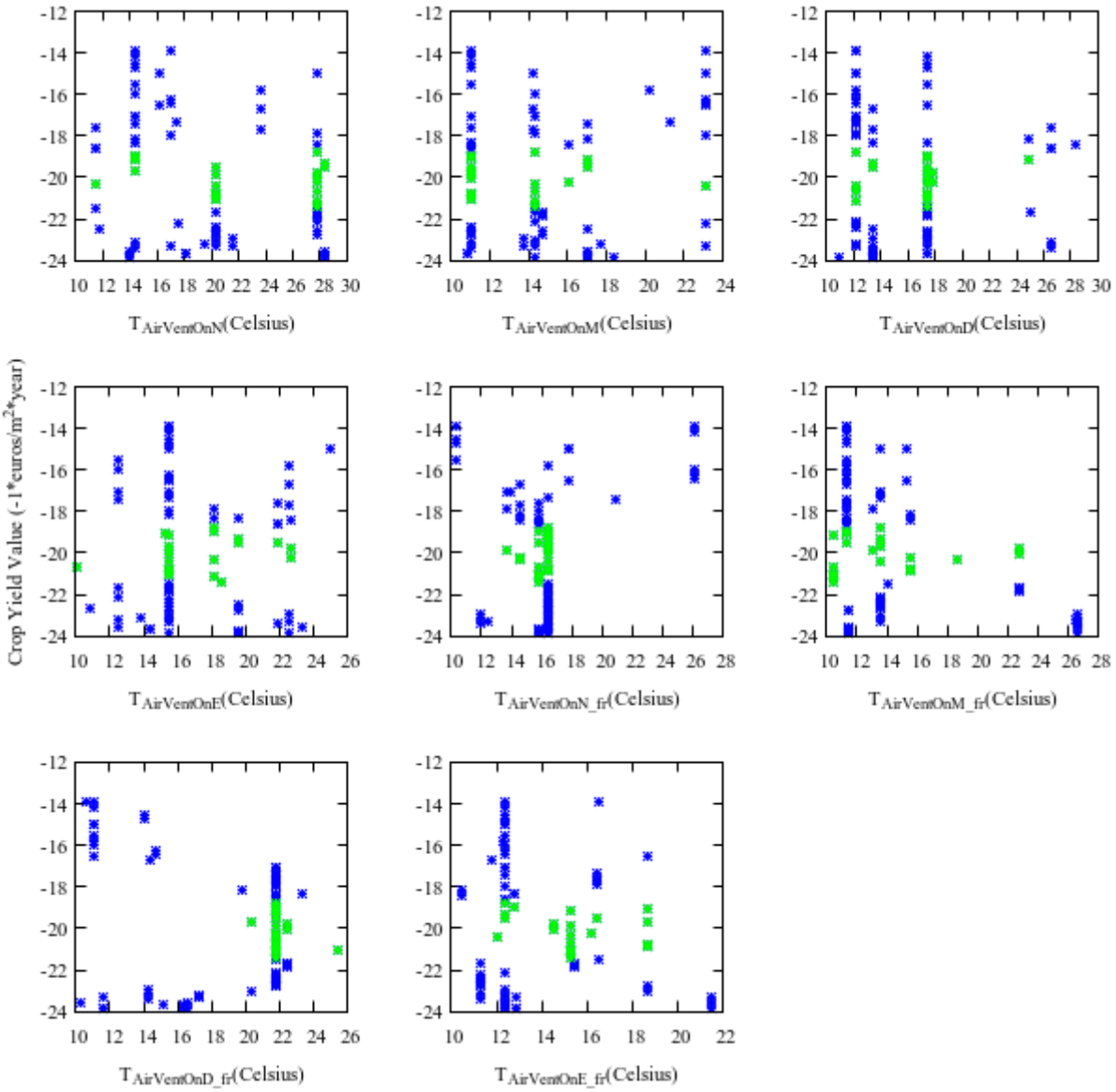

Figure 6.39. This setpoint determines the temperature above which the greenhouse controller will keep the ventilation open.

6.5.2 $T_{AirVentOn}$

Figure 6.39 shows that, compared to the previous controllers covered in this chapter, there are two additional copies of this setpoint to account for the nighttime period: $T_{AirVentOnN}$ and $T_{AirVentOnN\_fr}$. While $T_{AirVentOnN}$ clearly has a wide range of acceptable values that produce both low-cost and high-crop-value solutions, $T_{AirVentOnN\_fr}$ prioritizes values at or near 16 degrees Celsius. This value is close to temperatures below which a greenhouse would be heated up in practice, so immediately ventilating a greenhouse above

such a temperature would not be ideal. However, the corresponding values of $T_{AirVentOffN\_fr}$ in the next section are slightly greater and thus override $T_{AirVentOnN\_fr}$. However, even in cases where a copy of $T_{AirVentOn}$ is overridden by $T_{AirVentOff}$, it still meaningfully contributes to Pareto-optimal solutions because of its use when calculating the reference temperature for the PID-controller-operated ventilation.

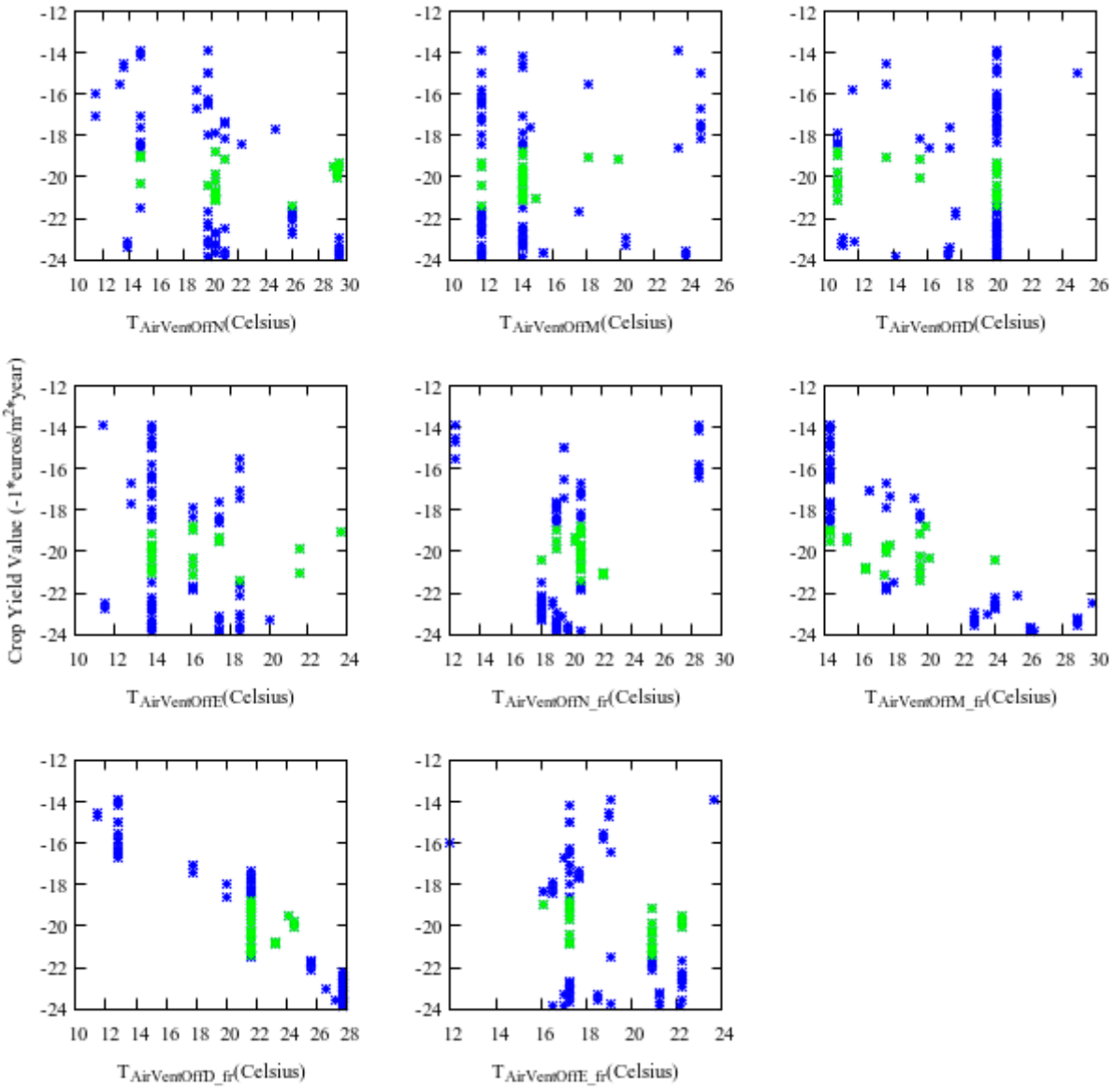

Figure 6.40. This setpoint determines the temperature below which the ventilation will always remain closed.

6.5.3 $T_{AirVentOff}$

Similarly, Figure 6.40 shows there are two new copies of this setpoint: $T_{AirVentOffN}$ and $T_{AirVentOffN\_fr}$. Of these two, $T_{AirVentOffN\_fr}$ (i.e., the nighttime, post-fruiting setpoint for $T_{AirVentOff}$) is noteworthy due to all the solutions being at or slightly above 18 degrees Celsius. Almost all these values are higher than $T_{AirVentOnN\_fr}$ in the previous section, creating a control strategy where the greenhouse remains unconditionally sealed until the air temperature exceeds the current value of $T_{AirVentOffN\_fr}$. In addition, values for $T_{OutThScrOn\_fr}$ (covered below in Section 6.5.5) are mostly centered around 17.5 degrees Celsius, which overall shows an emphasis on maintaining nighttime greenhouse temperatures at around this range. Finally, $T_{AirVentOffM\_fr}$ and $T_{AirVentOffD\_fr}$ both show a clear trend in which increasing the value of these setpoints leads to increased crop yield value. This is consistent with control strategies that prioritize keeping the greenhouse sealed at the expense of increased variable costs (from additional cooling, heating, and CO_2 injection).

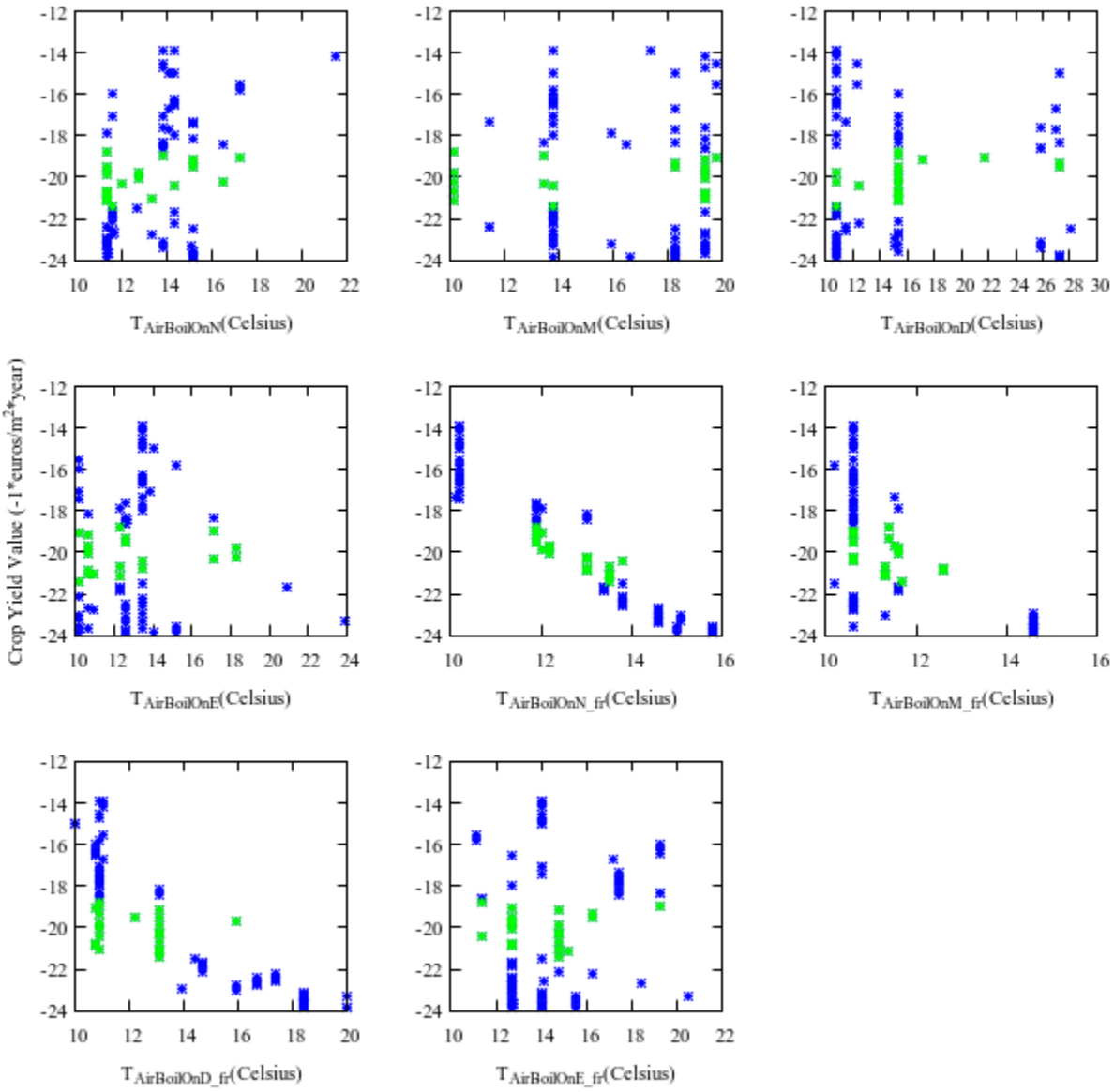

Figure 6.41. This setpoint determines the temperature below which the greenhouse controller will turn on the boiler heating.

6.5.4 $T_{AirBoilOn}$

Figure 6.41 shows that the values for this setpoint are largely random before fruit set, although the nighttime copy, $T_{AirBoilOnN}$, has a relatively narrow range of values (mostly between 10 – 18 degrees Celsius). Naturally, lower temperatures are preferred during nighttime to reduce plant respiration (as long as these temperatures are not low enough to damage the crop). After fruit set, $T_{AirBoilOnN\_fr}$, $T_{AirBoilOnM\_fr}$, and $T_{AirBoilOnD\_fr}$ all show a clear trend in which higher values for this setpoint lead to higher crop yield

values (at the expense of higher variable costs). In the case of $T_{AirBoilOnN\_fr}$, any boiler heating that occurs because of this setpoint will be during the nighttime control strategy period, and thus very little to no photosynthesis occurs during this time. Therefore, this setpoint contributes to the value of the crop yield more indirectly: that is, it is reducing crop growth inhibition due to sub-optimal temperatures, rather than helping to maximize the rate of photosynthesis during the daytime.

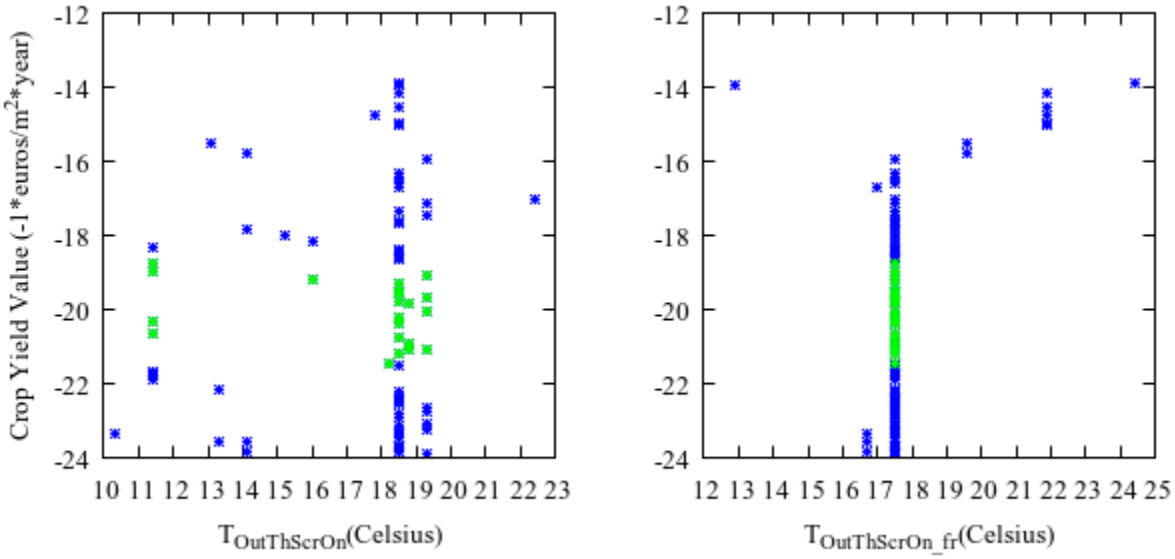

Figure 6.42. This setpoint determines the outside temperature below which the greenhouse controller will deploy the thermal screen.

6.5.5 $T_{OutThScrOn}$

Figure 6.42 shows that evolved values for $T_{OutThScrOn}$ and $T_{OutThScrOn\_fr}$ are largely consistent with those from previous controllers discussed in this chapter, with most values being near 18 degrees Celsius.

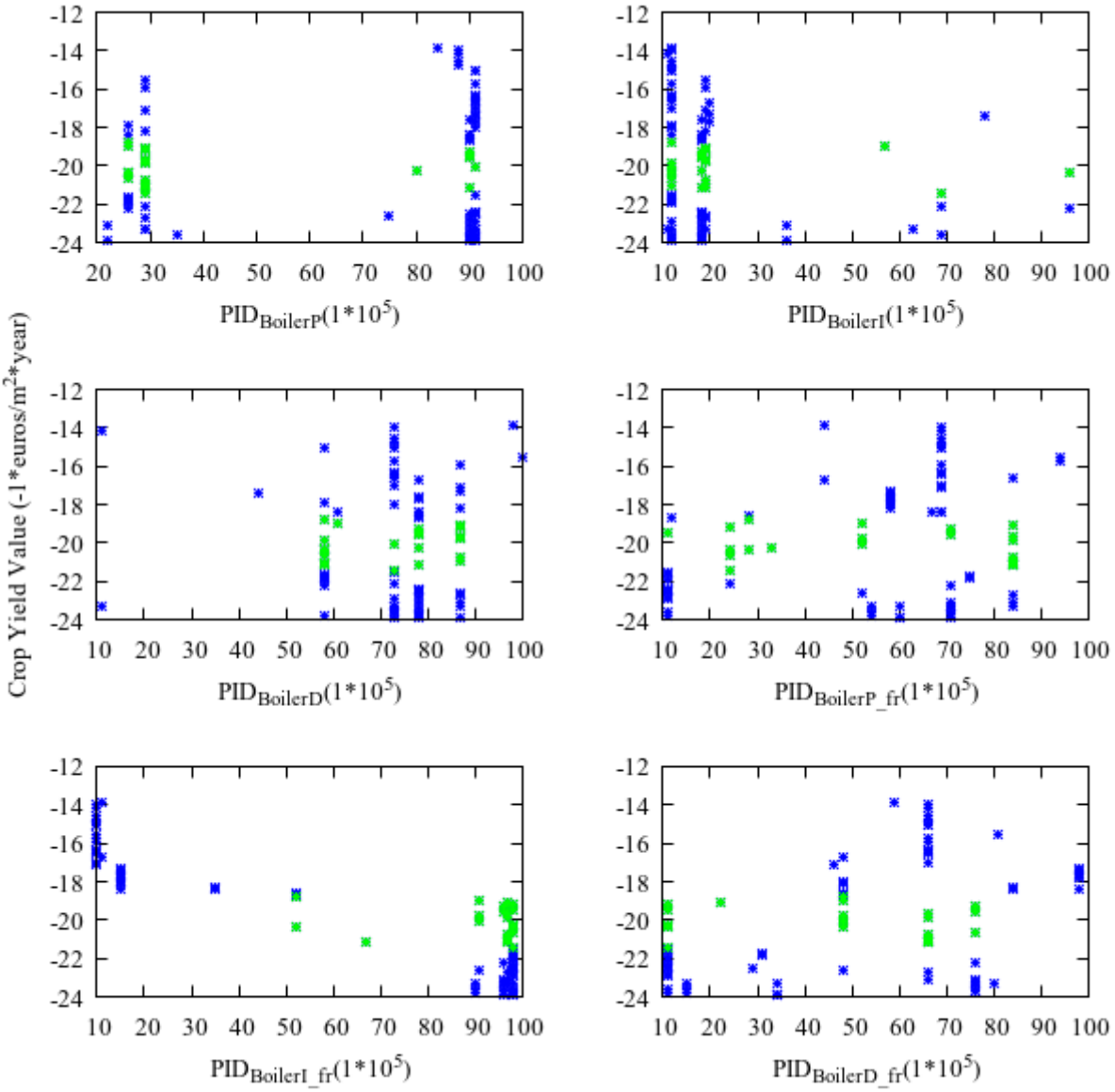

Figure 6.43. PID gain parameters for boiler heating control.

6.5.6 PID_{Boiler}

Figure 6.43 shows that before fruit set, the gain parameters for boiler heating have a wide range of values that yield both low-cost and high-crop-value solutions. Notably, the integral gain before fruit set ($PID_{BoilerI}$) remained consistently low, with most control strategies relying on the proportional gain ($PID_{BoilerP}$) to provide an initial value that sufficiently heats the greenhouse air. In contrast, the integral gain after fruit set ($PID_{BoilerI\_fr}$) follows a clear trend where higher integral gain results in higher crop yield

value. In other words, a high integral gain causes the boiler heating value, U_{Boil}, to reach its maximum very quickly. Naturally, this will maximize the output of the boiler heating at the expense of increased variable costs.

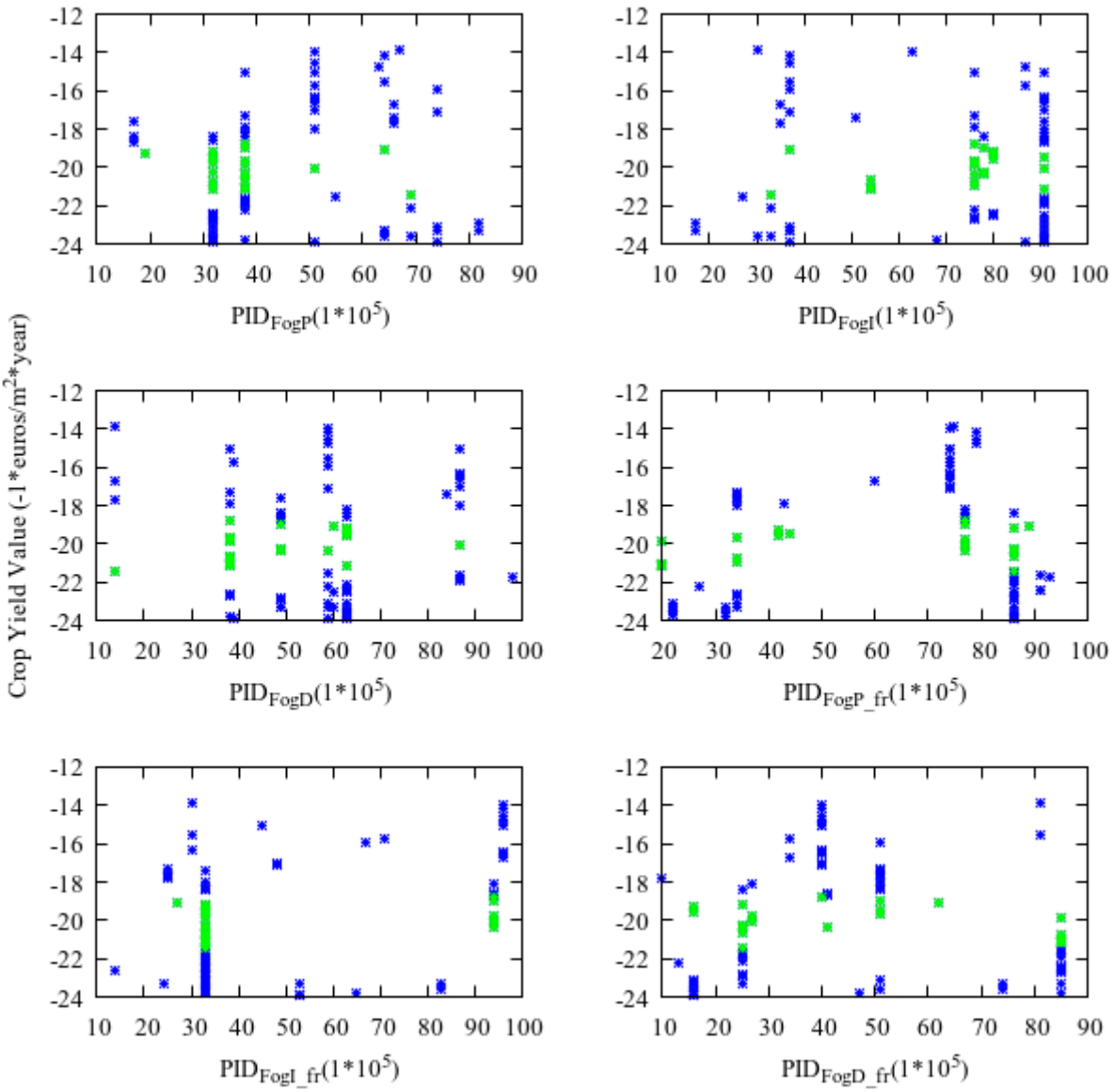

Figure 6.44. PID gain parameters for fogging system control.

6.5.7 PID_{Fog}

Similarly, Figure 6.44 shows that there are a wide range of values for the fogging system's gain parameters which yield both low-cost and high-crop-value solutions. Unlike the boiler and ventilation

systems, the restrictions placed on the output of the fogging system force it to operate for limited time periods. This translates to many combinations of PID gain parameters being sufficient to meet or exceed that limit. If we could operate the fogging system uninterrupted for longer periods of time, the evolved gain parameters might show clear patterns. Despite the small effect of these fogging system PID parameters, it is well known that excessively high levels of humidity can lead to disease in the crop [49], and salt content in the fogging system's water reservoir can cause burns on the leaves of the crop [42]. However, since these adverse effects are not implemented in the combined microclimate-crop-yield model, it is preferable to maintain best practices that aim to avoid these problems altogether.

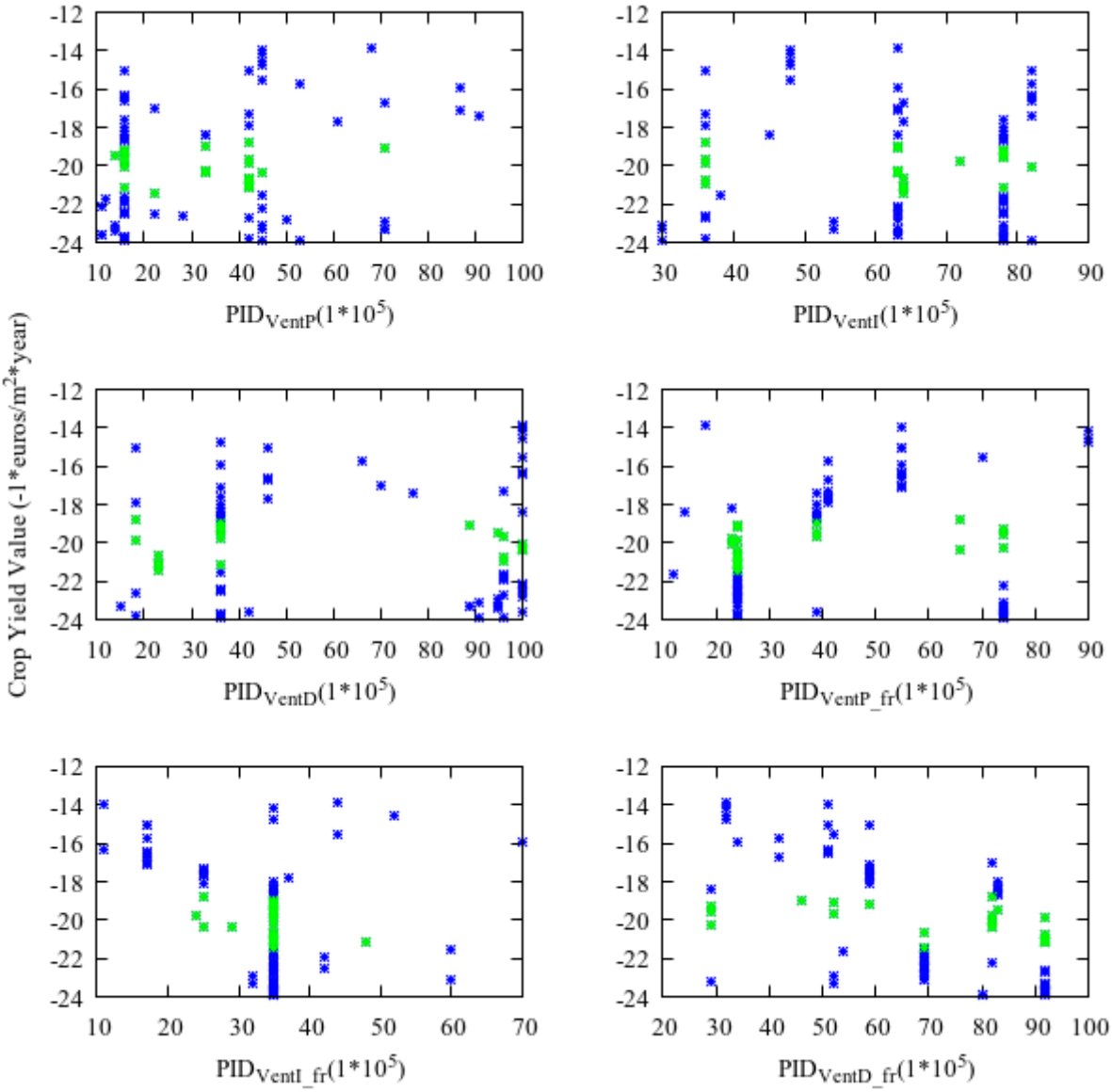

Figure 6.45. PID gain parameters for greenhouse ventilation control.

6.5.8 PID_{Vent}

Once again, Figure 6.45 shows that there are a wide range of values for the ventilation system's gain parameters which yield both low-cost and high-crop-value solutions. However, most values for PID_{VentI_fr} are on the lower end (with 10 being the lowest possible value), suggesting that at least after fruit set occurs there is some benefit to lowering the integral gain, thus somewhat slowing down the rate at which the greenhouse ventilation fully opens. Since most of the post-fruit-set period takes place during the

winter and spring seasons (with accompanying colder outside air temperatures), it stands to reason that there is an advantage to controlling greenhouse ventilation openings more carefully.

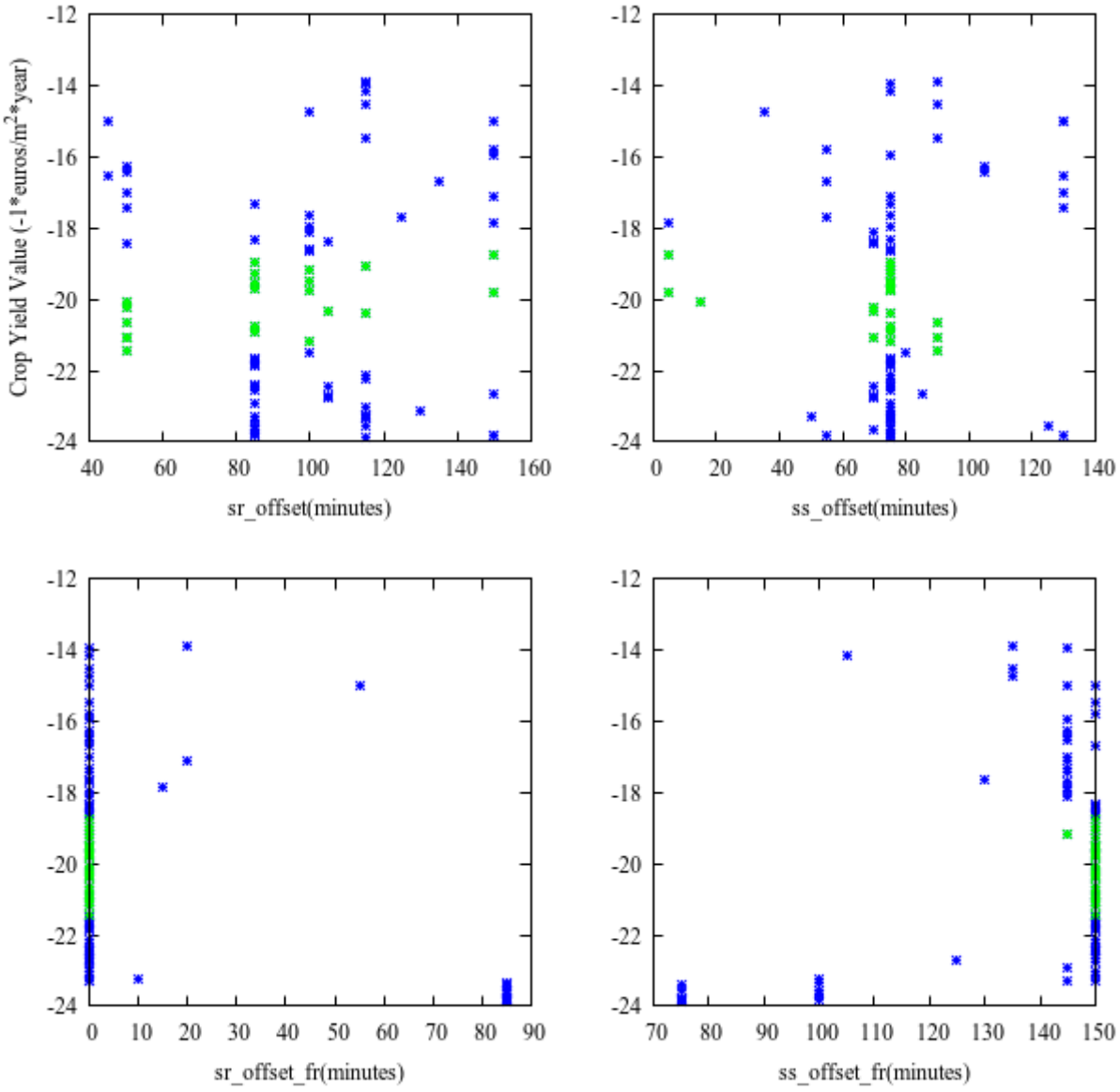

Figure 6.46. The copies of sr_offset and ss_offset are used to subtract from the current calculated time for sunrise and sunset, respectively.

6.5.9 Sunrise and Sunset Offsets (sr_offset, ss_offset)

Figure 6.46 shows values that follow largely similar trends to those discussed in Section 6.4.11. The offset applied to the current sunrise time (sr_offset) is largely random, while its post-fruit-set counterpart (sr_offset_fr) is heavily biased towards 0.The offset applied to the current sunset time (ss_offset) has

many values at or near 75 minutes, while its post-fruit-set counterpart has most of its values at or near 150 minutes. Despite there being three additional setpoints with distinct nighttime values compared to previous controllers (i.e., $T_{AirVentOnN}$, $T_{AirVentOffN}$, $T_{AirBoilOnN}$), the trends shown by these offsets still reflect an overall strategy that aims to conserve heat as much as possible by extending the time period in which the thermal screen is used (since it is only used during nighttime).

Unlike the previous controller in Section 6.4.11, sr_offset_fr and ss_offset_fr show clusters of extreme values at 85 minutes and 75 minutes, respectively. Both offsets would serve to extend the total duration of the daytime control strategy period relative to the other non-dominated solutions. Naturally, extending the time period in which a daytime strategy is applied will result in increased variable costs (particularly when prioritizing crop yield value), since more active cooling and/or heating measures, as well as CO_2 injection, are expected to take place to maximize the rate of photosynthesis of the crop.

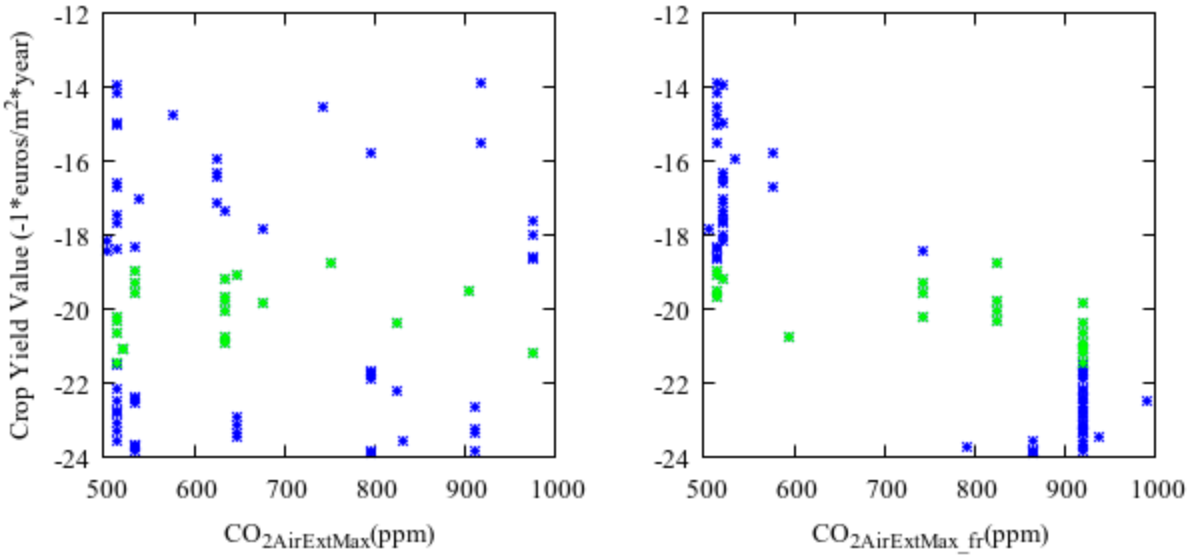

Figure 6.47. This variable determines the upper bound for the dynamic CO_2 setpoint used during CO_2 injection.

6.5.10 $CO_{2AirExtMax}$

Figure 6.47 shows that, while $CO_{2AirExtMax}$ has a wide range of values with no clear pattern, $CO_{2AirExtMax\_fr}$ clearly shows a pattern of increasing crop yield value as it also increases. This shows that the dynamic CO_2 setpoint, $CO_{2AirExtOn}$, is being reached many times during the post-fruit-set period and that its upper

bound, $CO_{2AirExtMax\_fr}$, has a significant impact on the crop yield value. Since most of the post-fruit-set period takes place during the fall and winter seasons, the accompanying lower temperatures (as well as proper evolved values for setpoints pertaining to temperature control) allow the greenhouse to remain sealed, allowing for CO_2 injection to occur uninhibited.

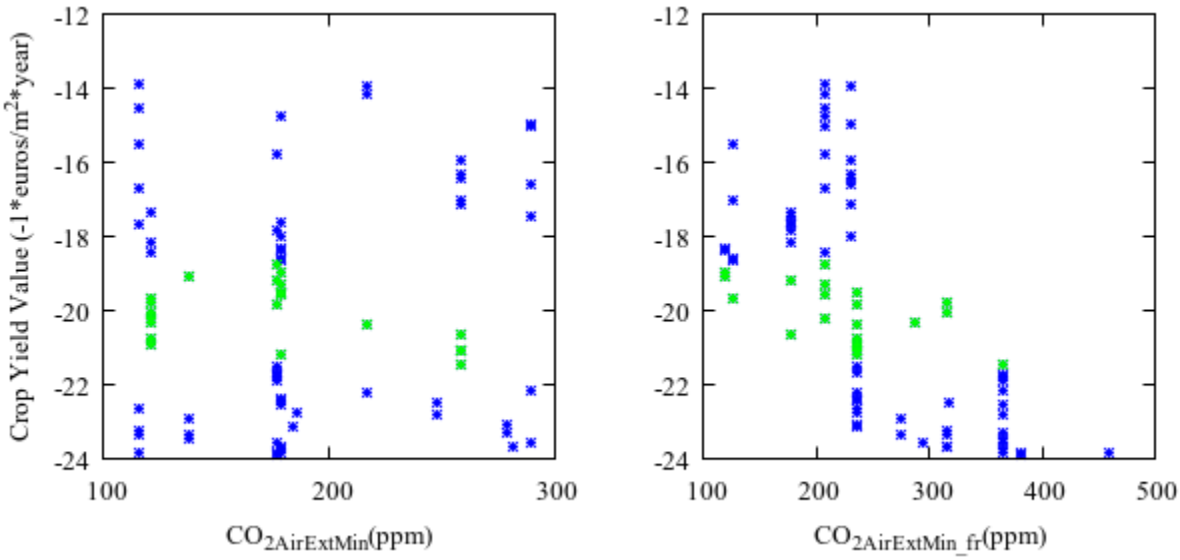

Figure 6.48. This variable determines the lower bound for the dynamic CO_2 setpoint used during CO_2 injection.

6.5.11 $CO_{2AirExtMin}$

Similar to $CO_{2AirExtMax}$ in Section 6.5.10, $CO_{2AirExtMin}$ in Figure 6.48 shows a wide range of values with no clear pattern before fruit set. After fruit set occurs, the crop yield generally increases with increasing $CO_{2AirExtMin\_fr}$.

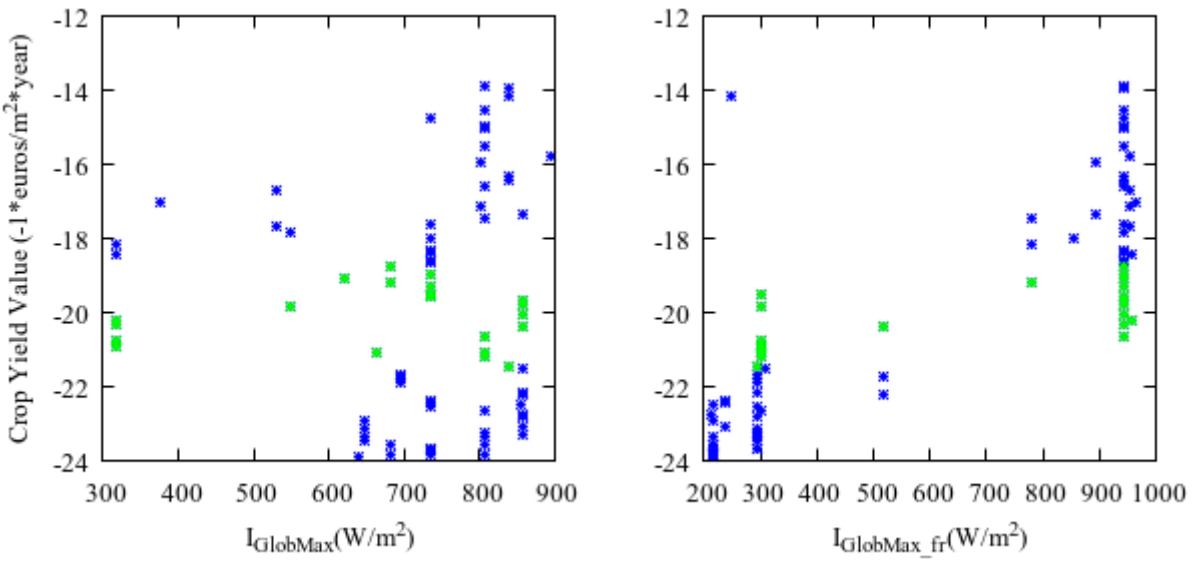

Figure 6.49. This variable determines how quickly $f(I_{Glob})$ is maximized, and subsequently contributes to how quickly the dynamic CO_2 setpoint is maximized.

6.5.12 $I_{GlobMax}$

Figure 6.49 shows that $I_{GlobMax}$ contains a relatively wide range of values that yield both low-cost and high-crop-value solutions, although most are within the 600 – 900 W/m^2 range. Even though a higher value for $I_{GlobMax}$ will cause $f(I_{Glob})$ to be maximized more slowly (thus causing the dynamic CO_2 setpoint to be maximized more slowly), one would normally expect a relatively high value of I_{GobMax} to translate to lower crop yield value and/or lower variable costs due to the reduction in CO_2 injection. However, CO_2 injection does not have enough of an impact on the crop yield value before fruit set occurs, which results in the wide range of values of $I_{GlobMax}$ that yield solutions with both low and high crop yield values.

After fruit set occurs, most solutions of $I_{GlobMax\_fr}$ follow a trend where a decrease in this variable tends to increase the crop yield value. This is consistent with the other evolved variables used to calculate the dynamic CO_2 setpoint in this section ($CO_{2AirExtMax}$ and $CO_{2AirExtMin}$), in that changing these variables to increase the dynamic CO_2 setpoint will tend to increase the value of the crop yield at the expense of increased variable costs.

6.5.13 Discussion

One of the main disadvantages of the previous controllers was the lack of distinct setpoints for a nighttime strategy, resulting in situations where morning (M) and evening (E) copies of a setpoint needed to contain values that were appropriate for both the time period it was defined for, as well as for a portion of what would be considered nighttime for purposes of deploying the thermal screen. This is due to how the morning and evening periods are defined (see Table 6.4) and the controller still requiring setpoints to be defined for typical greenhouse control purposes during nighttime (e.g., using boiler heating to heat up the greenhouse). Thus, introducing distinct nighttime copies for each setpoint where this occurred "freed up" these setpoints to be used strictly for the time period for which they were defined, leading to overall better results.

The most notable effect of introducing distinct nighttime setpoints (where applicable) could be observed after fruit set, where $T_{AirVentOnN\_fr}$, $T_{AirVentOffN\_fr}$, $T_{AirBoilOnN\_fr}$ and $T_{OutThScrOn\_fr}$ formed many sets of values centered around maintaining temperatures near the $T_{OutThScrOn\_fr}$ setpoint. In most cases, for a given value of $T_{OutThScrOn\_fr}$, there is an accompanying pair of values of $T_{AirVentOnN\_fr}$ and $T_{AirVentOffN\_fr}$ that are slightly greater, as well as a value of $T_{AirBoilOnN\_fr}$ that is lower. This is consistent with the nighttime temperatures that the classical Vanthoor strategy aims to maintain, as well as the setpoint values used to achieve these results.

The addition of PID control to greenhouse ventilation had some benefits. In particular the post-fruit-set integral gain (PID_{VentI_fr}) is overall lower compared to its pre-fruit-set counterpart (PID_{VentI}), indicating that there is some benefit to slowing down the rate at which the ventilation fully opens after fruit set occurs. While it was not detrimental, a PID-controlled fogging system did not seem to provide a tangible benefit, mainly due to the restrictions present to prevent the overuse that is known to cause adverse effects in practice. In the case of boiler heating, it was always PID controlled (with gain parameters pre-determined to approximate the fuel consumption of the classical Vanthoor strategy), thus the main change was in allowing its gain parameters to be evolved. The pre-fruit-set integral gain ($PID_{BoilerI}$) prioritized

lower values overall, thus slowing down the rate at which the boiler heating is maximized for most solutions. In contrast, the post-fruit-set integral gain ($PID_{BoilerI\_fr}$) followed a trend where higher values for this gain result in increased crop yield value (at the expense of increased variable costs due to the more aggressive heating that results).

One of the disadvantages observed in previous sections was the lack of penalties on either crop growth or crop yield value due to inadequate levels of relative humidity. This is most apparent in the evolved values for the $T_{AirVentOn}$ and $T_{AirVentOff}$ setpoints. In the classical Vanthoor strategy, most of the humidity control occurs when greenhouse air temperatures are between $T_{AirVentOn}$ and $T_{AirVentOff}$, ventilating the greenhouse when the greenhouse air is above a relative humidity threshold. However, when these values are evolved, the gap that allows for this check to occur is typically eliminated. The next section will cover the same control strategy discussed in this section except that, importantly, a crop value penalty for sub-optimal levels of relative humidity is added.

6.6 Same Improved Controller with Penalty for Inadequate Relative Humidity

6.6.1 Introduction

This control strategy is identical to the one described in Section 6.5, but a penalty has been introduced for sub-optimal levels of relative humidity in the greenhouse air. This aims to reflect the real-world valuation of tomato crops, in which tomato growth and development, fungal contamination, and other problems are associated with sub-optimal relative humidity. The penalty consists of two trapezoid functions [4]. The first function determines the fraction of first-class tomatoes based on the 24-hour mean value of the vapor pressure deficit (VPD_{24}) between the canopy and the greenhouse air. The second function determines the fraction of marketable tomatoes based on the 48-hour mean value of the relative humidity (RH_{48}) of the greenhouse air. This only impacts the resulting crop yield *value*, and therefore has no effect on the microclimate-crop yield model. However, this still induces significant changes in evolved control strategies: if a hypothetical greenhouse controller were to fail to maintain an acceptable range for either VPD_{24} or RH_{48}, the entire crop could end up having no monetary value. It is expected that 1) using the

same evolved solutions as the previous section will yield sub-optimal results, and 2) evolving setpoints once more under a modified economic model should mitigate the effects of the penalty introduced in this section. Therefore, the main goal of this section is to observe and discuss notable changes in the overall behavior of the evolved controller, rather than examining the change in magnitude for each objective. Figure 6.50 contains the Pareto-optimal front that results from adding this penalty, with the classical Vanthoor strategy also being subject to said penalty.

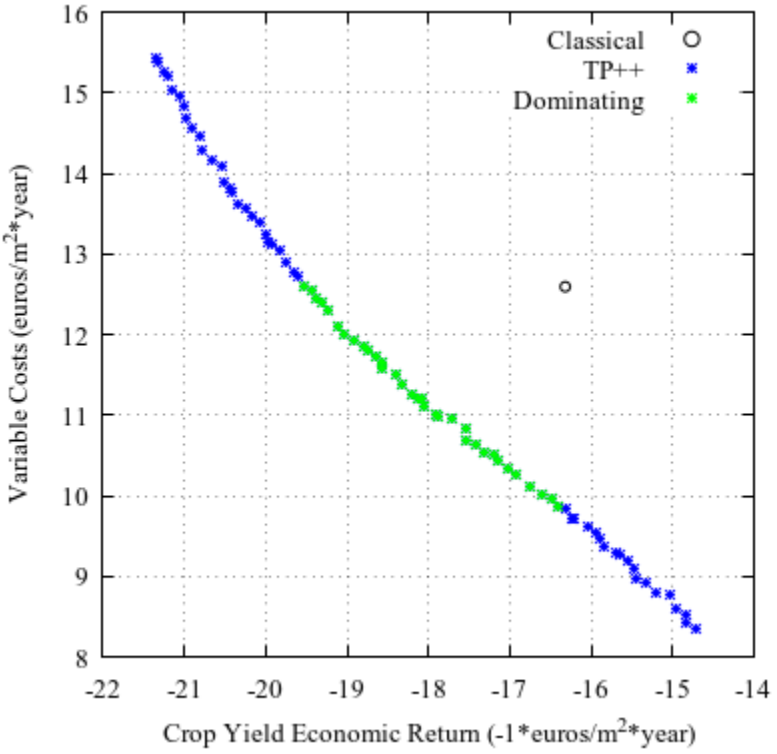

Figure 6.50. Pareto-optimal front for the control strategy discussed in this section. Solutions from this Pareto front which also dominate the classical Vanthoor strategy are marked in green.

6.6.2 $T_{AirVentOn}$ and $T_{AirVentOff}$

The addition of a crop value penalty changed the range of values considerably for both $T_{AirVentOn}$ and $T_{AirVentOff}$. In this section, these setpoints will be plotted together to show the overall change in these pairs of values before and after introducing the crop value penalty. Due to the large number of control strategies contained in each Pareto-optimal front, we will only examine solutions which dominate the classical Vanthoor strategy (see Figure 6.50). In addition, since the behavior of the controller changes

significantly depending on which of these two values are greater (i.e., whether $T_{AirVentOn} > T_{AirVentOff}$ or $T_{AirVentOff} > T_{AirVentOn}$), they will be marked accordingly in Figure 6.51, Figure 6.52, Figure 6.53, and Figure 6.54.

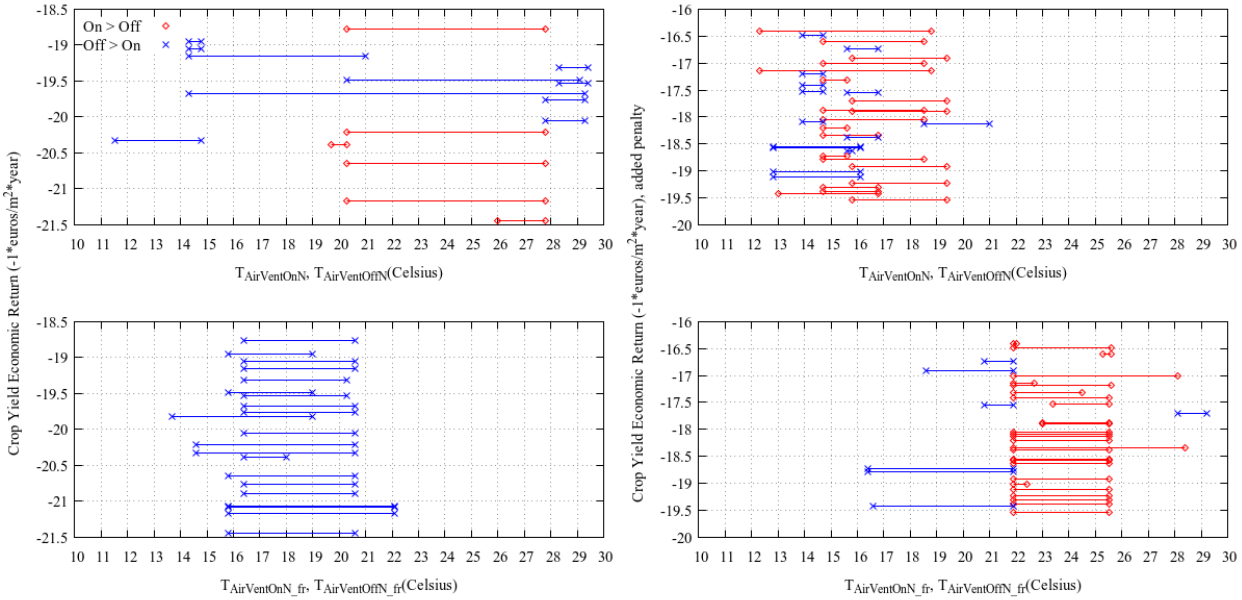

Figure 6.51. Evolved nighttime setpoints for $T_{AirVentOn}$ and $T_{AirVentOff}$. The effects of adding a crop value penalty on the resulting evolved setpoints are examined (right) and compared with the same setpoints without the crop value penalty (left). Red values are cases when $T_{AirVentOn}$ is greater than $T_{AirVentOff}$.

6.6.2.1 Nighttime Setpoints

Figure 6.51 shows that, with the addition of a crop value penalty, the average temperature of the nighttime setpoints ($T_{AirVentOn}$ and $T_{AirVentOff}$) lowered significantly. In addition, there are significantly more instances in which $T_{AirVentOn}$ is greater than $T_{AirVentOff}$ (red pairs of values on the upper right). Many of these pairs of values have relatively large temperature gaps between them which allow the control strategy to open ventilation conditionally for purposes of humidity control. Based on the classical Vanthoor strategy, a temperature gap of 3 degrees Celsius is typical ($T_{AirVentOn} = 23$, $T_{AirVentOff} = 20$), and many of these evolved pairs form similarly sized gaps, with some exceptions.

After fruit set occurs, the addition of a crop value penalty causes the average temperature of the nighttime setpoints ($T_{AirVentOn\_fr}$ and $T_{AirVentOff\_Fr}$) to increase significantly. Moreover, most solutions develop

instances in which $T_{AirVentOn}$ is greater than $T_{AirVentOff}$ (as seen in Figure 6.51, red pairs of values on the lower right).

Overall, the addition of a crop value penalty produced nighttime setpoints which emphasize ventilating the greenhouse for purposes of reducing the relative humidity of the greenhouse air. $T_{AirVentOn}$ and $T_{AirVentOff}$ had lower average temperatures which resulted in a control strategy that would ventilate the greenhouse quite often, especially during August where the outside air temperature is much warmer (see Figure 6.25). After fruit set, $T_{AirVentOnN\_fr}$ and $T_{AirVentOffN\_fr}$ both emphasize ventilation for purposes of relative humidity control, although the average temperatures are higher. By the time this stage of plant development is reached (typically around October), average outside air temperatures will have dropped significantly, and thus ventilating the greenhouse will rapidly cool the greenhouse air to sub-optimal temperature ranges for plant growth.

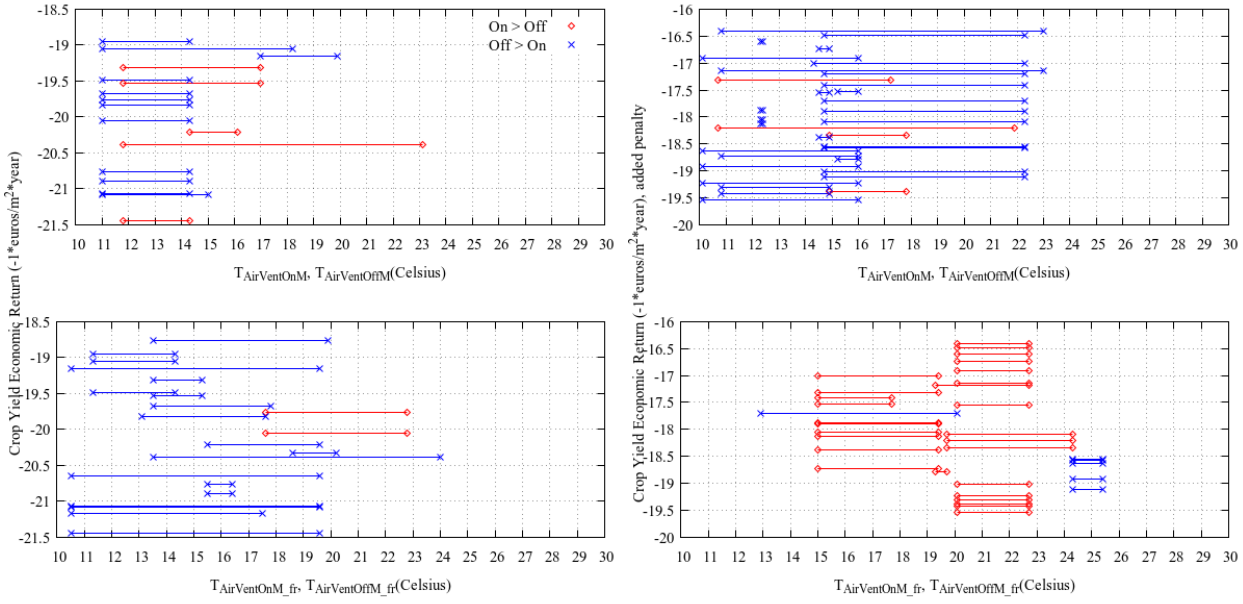

Figure 6.52. Evolved morning setpoints for $T_{AirVentOn}$ and $T_{AirVentOff}$. The effects of adding a crop value penalty on the resulting evolved setpoints are examined (right) and compared with the same setpoints without the crop value penalty (left). Red values are cases when $T_{AirVentOn}$ is greater than $T_{AirVentOff}$.

6.6.2.2 Morning Setpoints

Figure 6.52 shows that, before fruit set, the addition of a crop value penalty increased the both the average temperature and the occurrence of setpoints in which $T_{AirVentOffM}$ is greater than $T_{AirVentOnM}$, thus resulting in most control strategies not ventilating the greenhouse for purposes of humidity control. There clearly is not enough of an incentive to decrease relative humidity during this time period, and the benefits of maintaining the greenhouse closed to take advantage of CO_2 injection in the presence of global radiation outweigh the crop value penalties from sub-optimal levels of relative humidity. This can be further exacerbated when outside air temperatures are low enough during this period that using the fogging system is mostly unnecessary for cooling down the greenhouse.

After fruit set, the addition of a crop value penalty increased the average temperature, with most control strategies containing values in which $T_{AirVentOnM\_fr}$ is greater than $T_{AirVentOffM\_fr}$. This results in most of the control strategies ventilating the greenhouse often for purposes of humidity control. In addition, the values for many pairs of $T_{AirVentOnM\_fr}$ and $T_{AirVentoffM\_fr}$ mirror those of the classical Vanthoor strategy (i.e., $T_{AirVentOn} = 23$ and $T_{AirVentOff} = 20$), indicating that, at least for this time period, these values are effective for both high-crop-value and low-cost solutions.

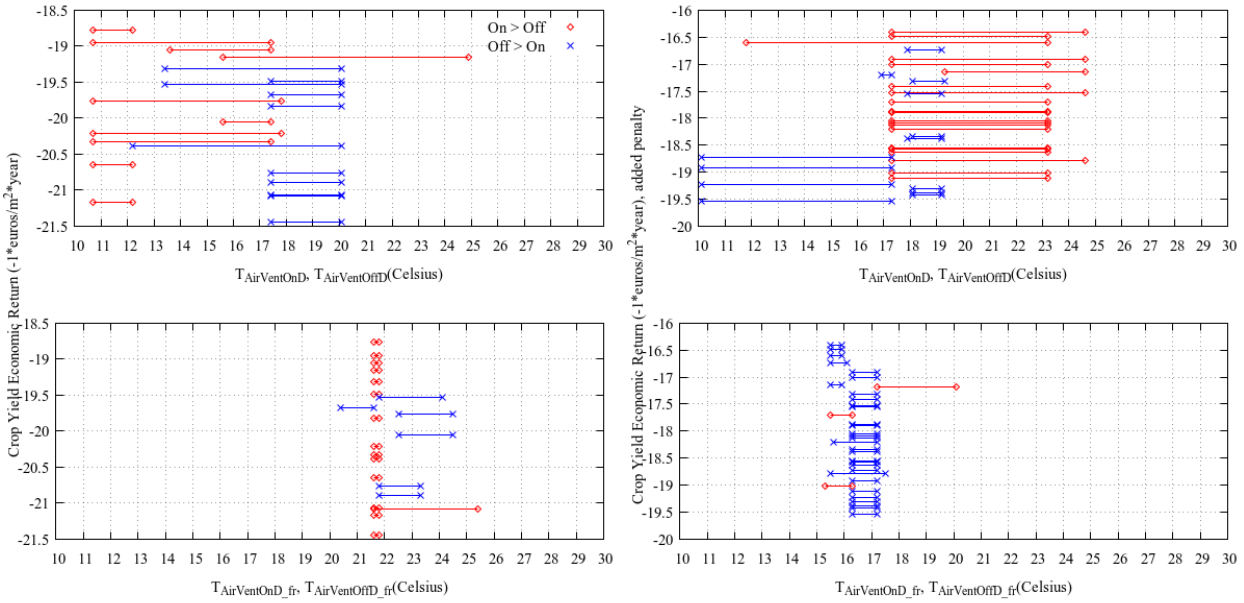

Figure 6.53. Evolved midday setpoints for $T_{AirVentOn}$ and $T_{AirVentOff}$. The effects of adding a crop value penalty on the resulting evolved setpoints are examined (right) and compared with the same setpoints without the crop value penalty (left). Red values are cases when $T_{AirVentOn}$ is greater than $T_{AirVentOff}$.

6.6.2.3 Midday Setpoints

Figure 6.53 shows that, before fruit set, the addition of a crop value penalty increased the average temperatures for both $T_{AirVentOnD}$ and $T_{AirVentOffD}$, with most pairs of values allowing ventilation of the greenhouse for humidity control. Pairs of values which did not allow this kind of humidity control had lower temperature setpoints overall, suggesting that in the absence of the ability to open the greenhouse ventilation *conditionally* based on humidity levels, a lower temperature setpoint for opening the greenhouse ventilation *unconditionally* can work as an alternative.

After fruit set, the addition of a crop value penalty decreased the average temperatures for both $T_{AirVentOnD\_fr}$ and $T_{AirVentOffD\_fr}$. Most of these pairs of values do not allow ventilating the greenhouse for humidity control, instead opting for opening (and closing) greenhouse ventilation *unconditionally* at a relatively low setpoint of around 17 degrees Celsius. Despite the cooler outside temperatures present after fruit set occurs, this results in some ventilation during the midday period (particularly when global radiation is at its peak), while keeping the greenhouse sealed and its air temperature as close to 17 degrees Celsius as possible otherwise. At a setpoint of around 17 degrees Celsius, this is slightly below the

optimal 24-hour mean canopy temperature range for the crop, which is 18 – 22 degrees Celsius [4]. However, due to the higher average temperature setpoints during the nighttime, morning, and evening periods (coming up in Section 6.6.2.4), the 24-hour mean canopy temperature remains at or above 18 degrees Celsius, helping prevent tomato crop growth inhibition.

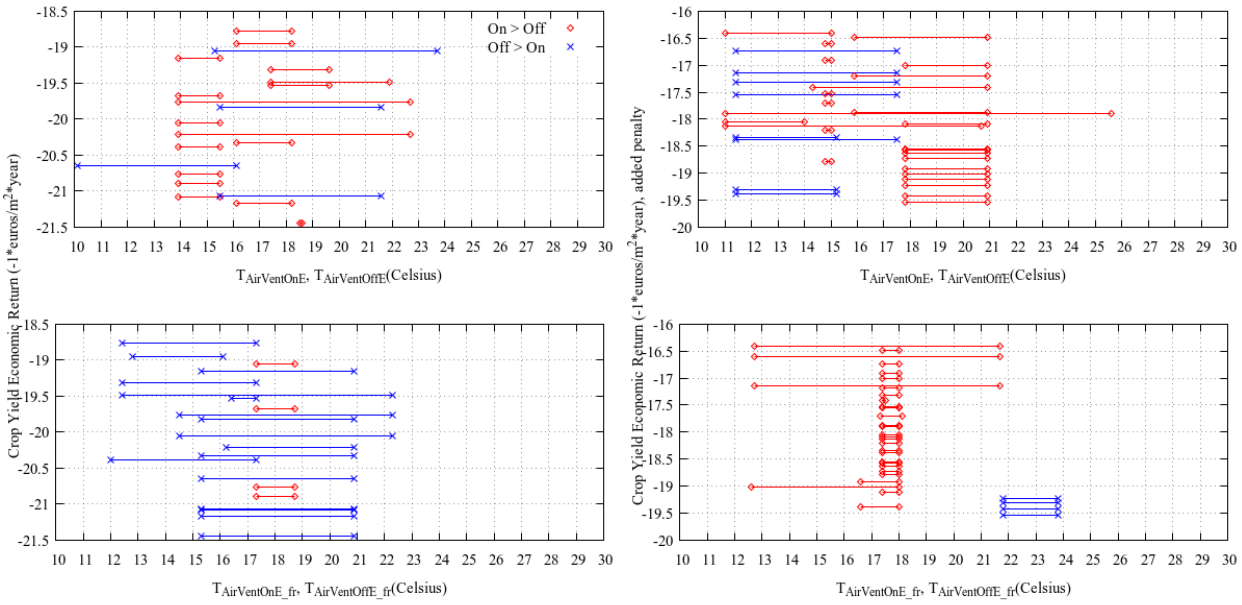

Figure 6.54. Evolved evening setpoints for $T_{AirVentOn}$ and $T_{AirVentOff}$. The effects of adding a crop value penalty on the resulting evolved setpoints are examined (right) and compared with the same setpoints without the crop value penalty (left). Red values are cases when $T_{AirVentOn}$ is greater than $T_{AirVentOff}$.

6.6.2.4 Evening Setpoints

Figure 6.54 shows that, before fruit set, the addition of a crop value penalty significantly increased the instances in which these setpoints allowed ventilation of the greenhouse for purposes of humidity control. Most of these setpoints allow the controller to open the greenhouse ventilation unconditionally at a lower temperature compared to its midday counterpart (i.e., $T_{AirVentOnD}$ and $T_{AirVentOffD}$) which suggests that, in most cases, it is beneficial to open the greenhouse ventilation more frequently once the levels of photosynthetically active radiation and outside air temperatures begin to drop (since the costs associated with CO_2 injection and managing higher canopy temperatures for maximizing photosynthesis become an unacceptable tradeoff).

After fruit set, the addition of a crop value penalty also significantly increased the instances in which greenhouse ventilation occurs for purposes of humidity control. However, most of these setpoints form a narrow temperature range that allows for this to occur, around 17 – 18 degrees Celsius. In contrast, the values for its midday counterpart (i.e., $T_{AirVentOnD\_fr}$ and $T_{AirVentOffD\_fr}$) only allow for the greenhouse ventilation to *unconditionally* open and close when above and below 17 degrees Celsius, respectively, in most cases. This suggests that, once the evening period begins during the post-fruit-set period, it is beneficial to start reducing the frequency with which a control strategy opens the greenhouse ventilation, albeit by a very slight amount. Based on the post-fruit-set nighttime setpoints displayed in Figure 6.51 we can see that this culminates in an evening-to-nighttime transition during which these nighttime temperature setpoints (i.e., $T_{AirVentOnN\_fr}$ and $T_{AirVentOffN\_fr}$) increase significantly to conserve heat by reducing overall ventilation, while still maintaining a temperature range in which ventilation can still occur for purposes of humidity control.

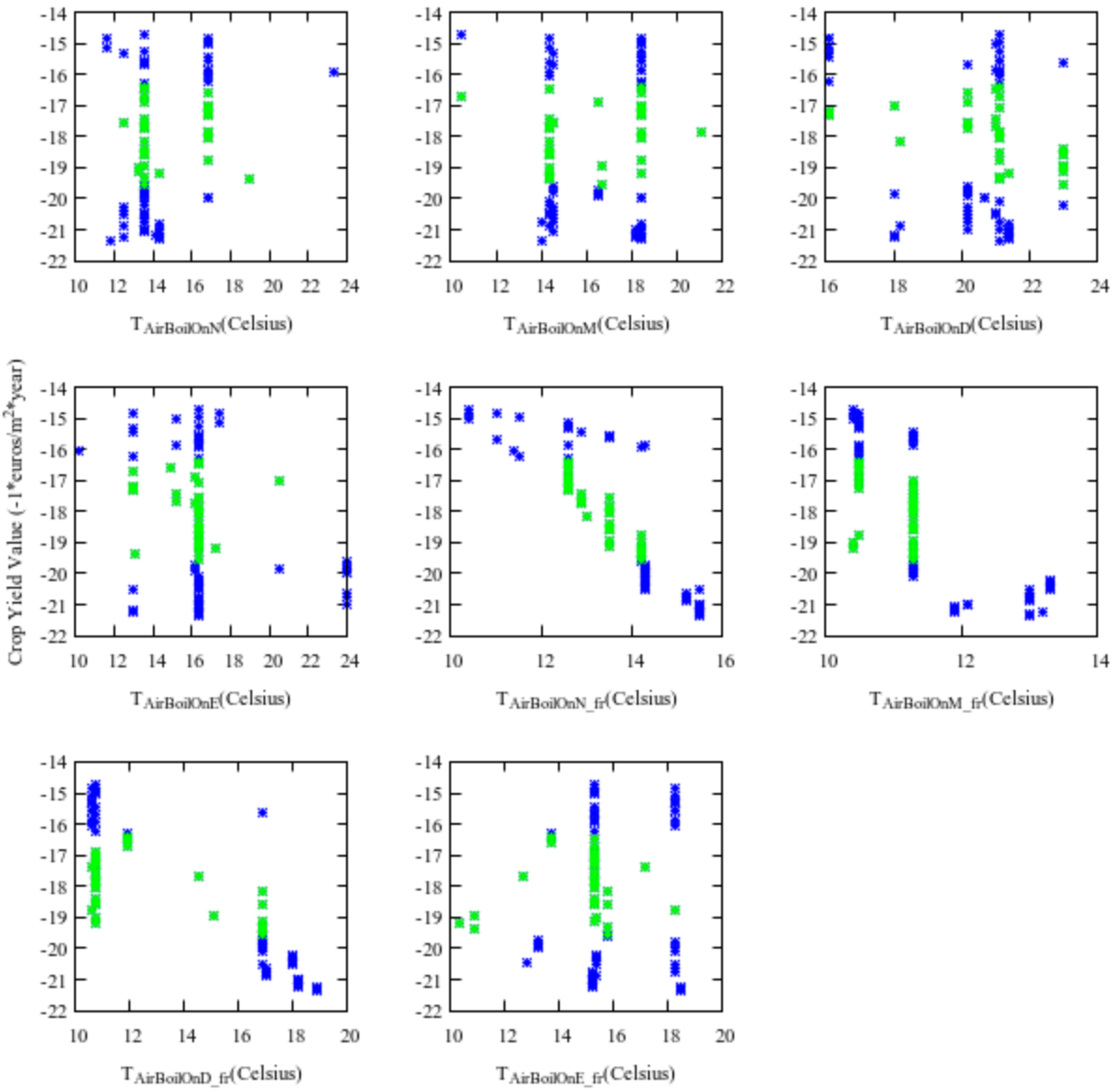

Figure 6.55. This setpoint determines the temperature below which the greenhouse controller will turn on the boiler heating.

6.6.3 $T_{AirBoilOn}$

Figure 6.55 shows that, before fruit set, the evolved values for this setpoint did not change considerably with the addition of a crop value penalty, with a wide range of values producing both high-crop-value and low-cost solutions. Most notably, the midday setpoint (i.e., $T_{AirBoilOnD}$), has a narrower range of around 16 – 24 degrees Celsius compared to these same setpoints evolved without the crop value penalty (around 10 – 28 degrees Celsius). Due to the high average outside air temperatures present before fruit set (see Figure

6.25), even a relatively high setpoint for the boiler was not correlated with increased crop yield value and/or variable costs.

After fruit set, the evolved values for this setpoint show largely similar trends to those discussed in Section 6.5.4: that is, increasing the nighttime, morning, and midday setpoints also tends to increase the value of the crop yield (at the expense of increased variable costs), suggesting that introducing the crop value penalty did not significantly alter the role of this setpoint overall.

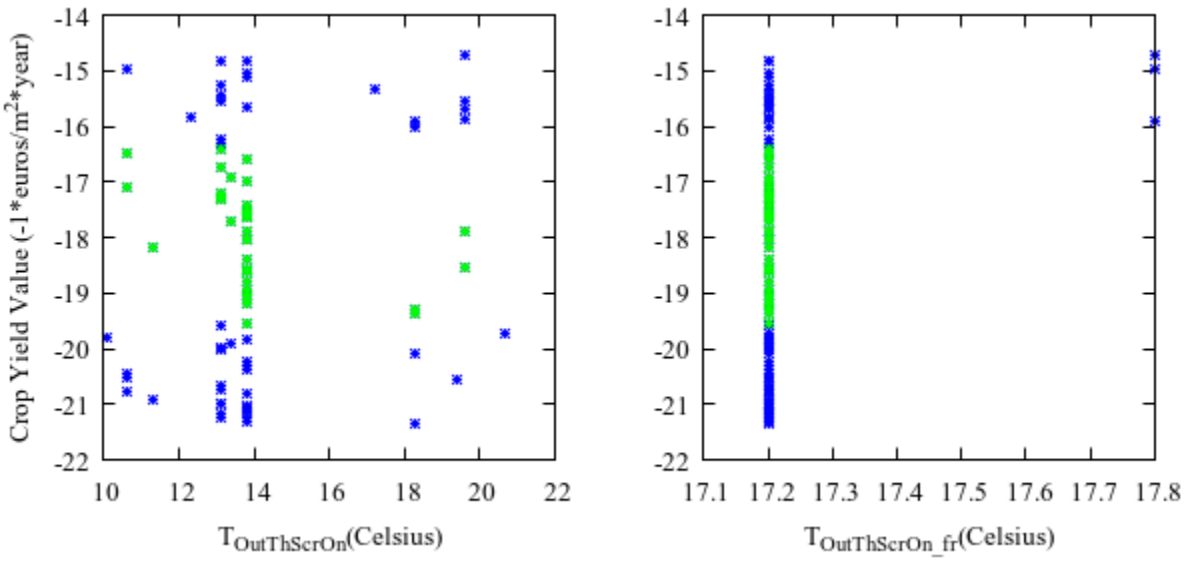

Figure 6.56. This setpoint determines the outside temperature below which the greenhouse controller will deploy the thermal screen.

6.6.4 $T_{OutThScrOn}$

Figure 6.56 shows that the evolved values for $T_{OutThScrOn}$ and $T_{OutThScrOn\_fr}$ are largely consistent with those from previous controllers discussed in this chapter, although $T_{OutThScrOn}$ contains values which are lower on average compared to those discussed in Section 6.5.5.

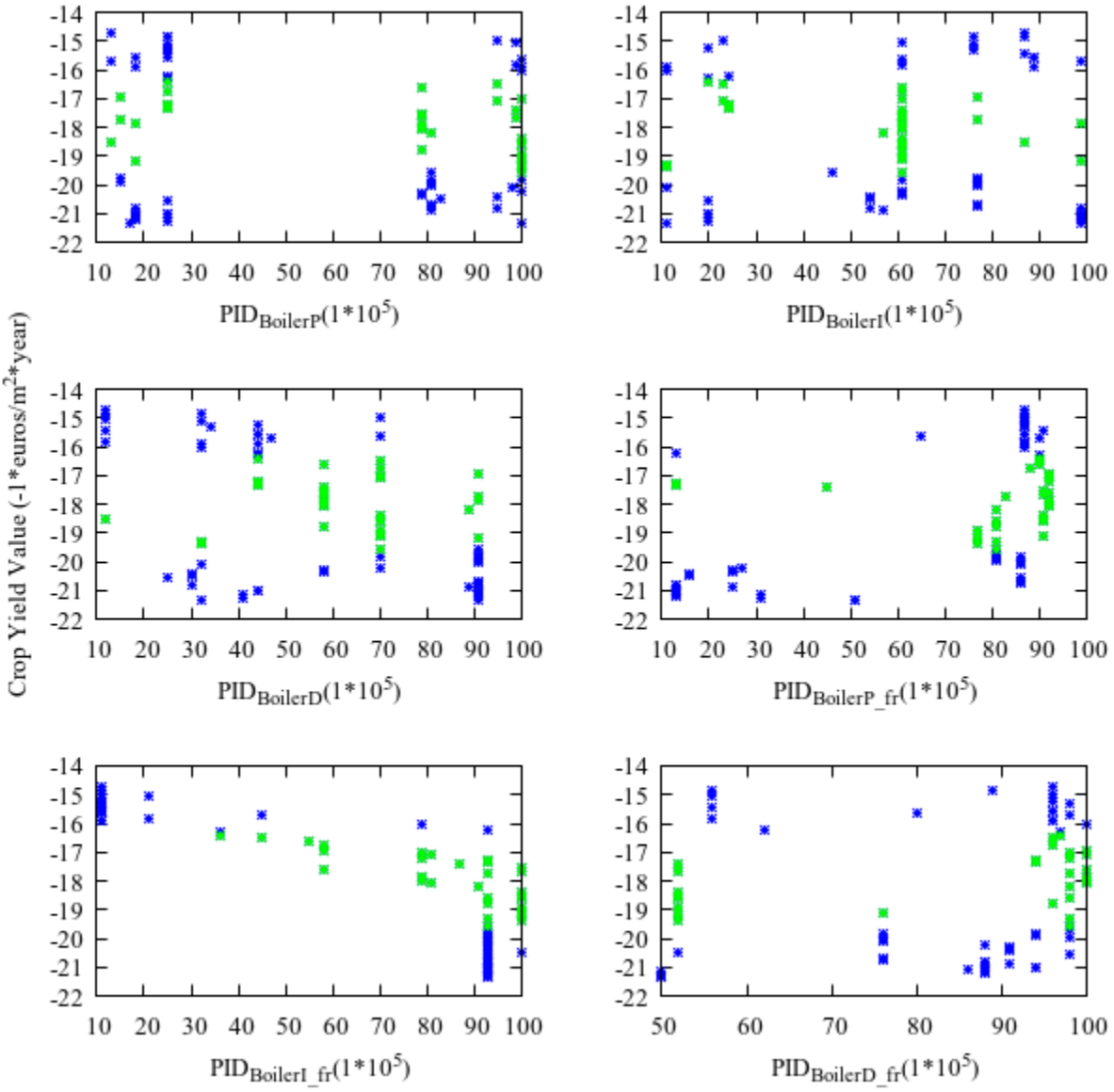

Figure 6.57. PID gain parameters for boiler heating control.

6.6.5 PID_{Boiler}

Figure 6.57 shows that, before fruit set, the gain parameters for boiler heating show largely similar trends, except for the integral gain (i.e., $PID_{BoilerI}$) which contains much larger values on average compared to its counterpart in Section 6.5.6. While the introduction of a crop value penalty did not affect the overall "intent" behind the evolved gain parameters, this difference in the integral gain values suggest that a wider range of values for the integral gain were acceptable when in conjunction with the evolved values

for $T_{AirVentOn}$ and $T_{AirVentOff}$ discussed earlier in Section 6.6.2 (since changes in the setpoints for greenhouse ventilation will also affect the frequency and output necessary for the boiler heating to maintain optimal temperature ranges for the tomato crop).

After fruit set, most control strategies favor a stronger proportional response compared to its counterpart without the crop value penalty (see Section 6.5.6). This is especially true for solutions which dominate the classical Vanthoor strategy, with very few control strategies using a value of $PID_{BoilerP\_fr}$ that is below 50. The integral gain (i.e., $PID_{BoilerI\_fr}$) follows a largely similar trend even with the introduction of a crop value penalty, indicating that increasing the rate at which the output of the boiler is maximized also increases the value of the crop yield (at the expense of increased variable costs).

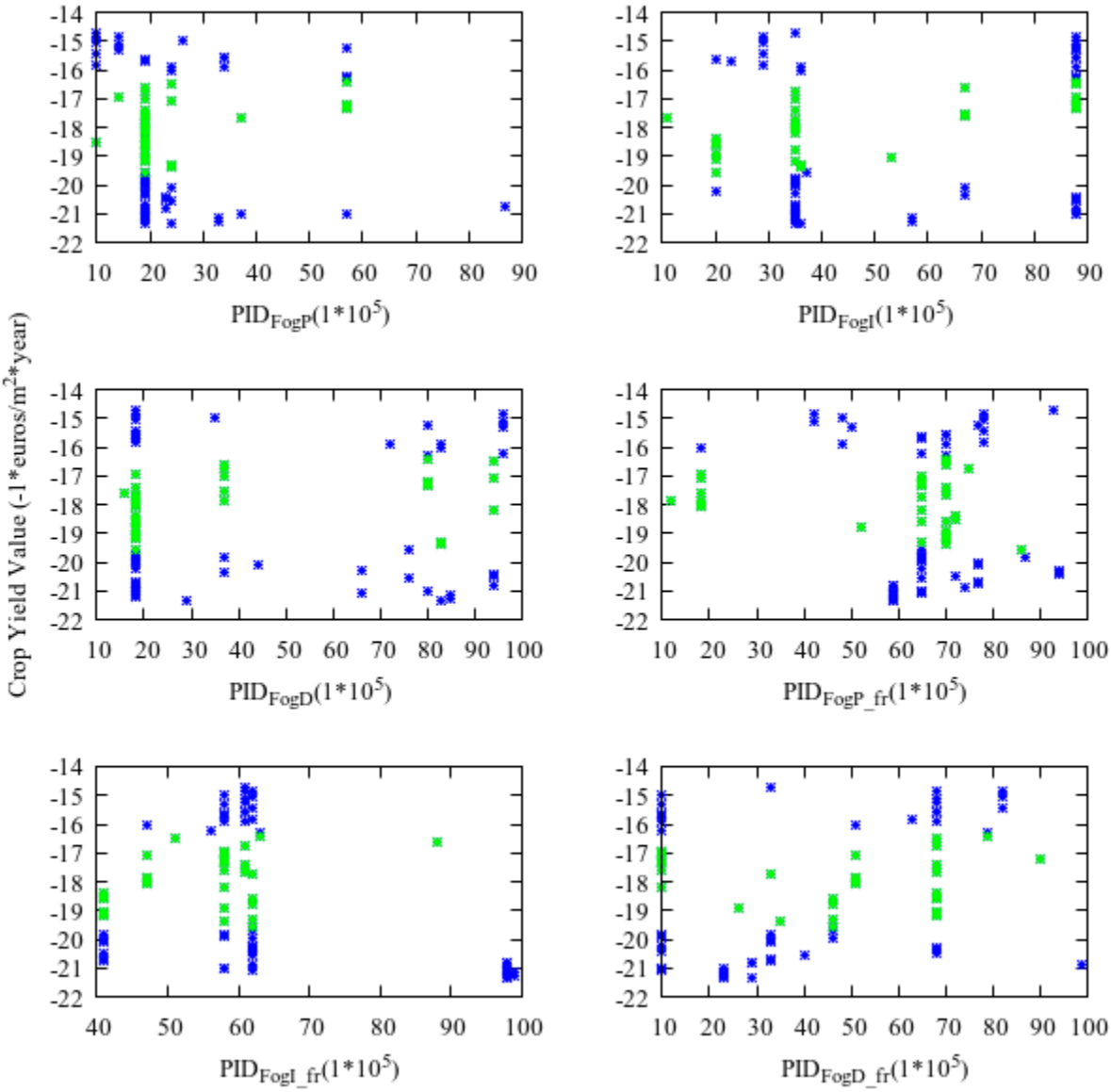

Figure 6.58. PID gain parameters for fogging system control.

6.6.6 PID_{Fog}

Figure 6.58 shows that, before fruit set, the gain parameters for the fogging system show largely similar trends to their counterparts without the crop value penalty in Section 6.5.7, with the exception of the proportional gain (i.e., PID_{FogP}). Most of these proportional gain values became significantly lower with the introduction of a crop value penalty, indicating that in many cases, a slower initial response from the fogging system was needed as a result.

After fruit set, both proportional and integral gain (i.e., PID_{FogP_fr} and PID_{FogI_fr}) increased overall with the introduction of a crop value penalty; therefore, a control strategy in which the fogging system maximizes its output very quickly is preferred.

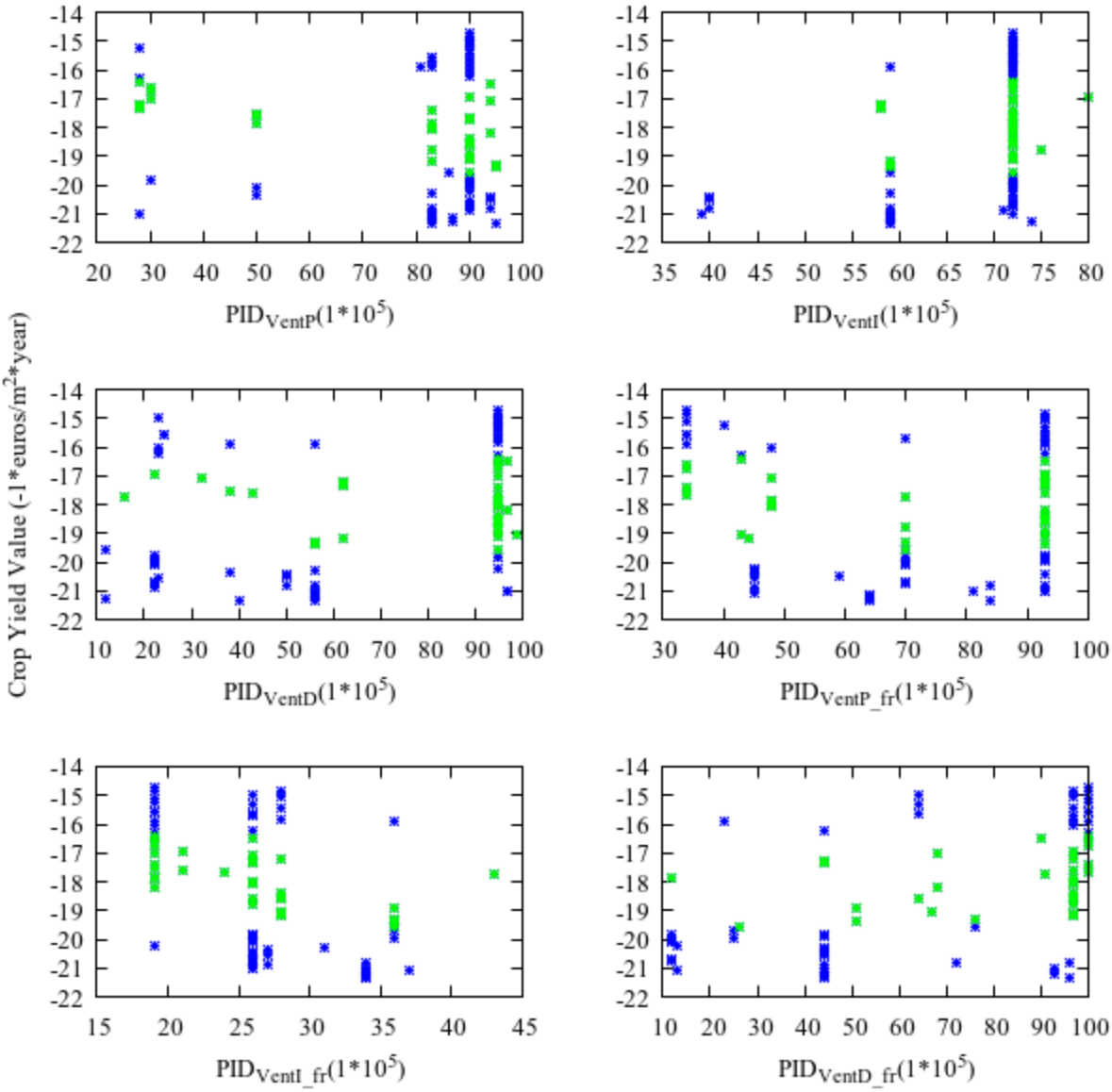

Figure 6.59. PID gain parameters for greenhouse ventilation control.

6.6.7 PID_{Vent}

Figure 6.59 shows that, before fruit set, the introduction of a crop value penalty significantly increased both proportional and integral gain parameters (i.e., PID_{VentP} and PID_{VentI}) on average. This results in

control strategies which maximize the greenhouse ventilation openings almost immediately, and that such behavior is preferred now indicates that the crop value penalty introduced a need for much more frequent ventilation for purposes of humidity control.

After fruit set, the gain values show largely similar trends, with the integral gain (i.e., PID_{VentI_fr}) showing a more narrow range of values (around 15 – 45) compared to its counterpart without the crop value penalty in Section 6.5.8 (around 10 – 70). Similarly, it shows that most control strategies favor a slower rate at which ventilation openings are maximized.

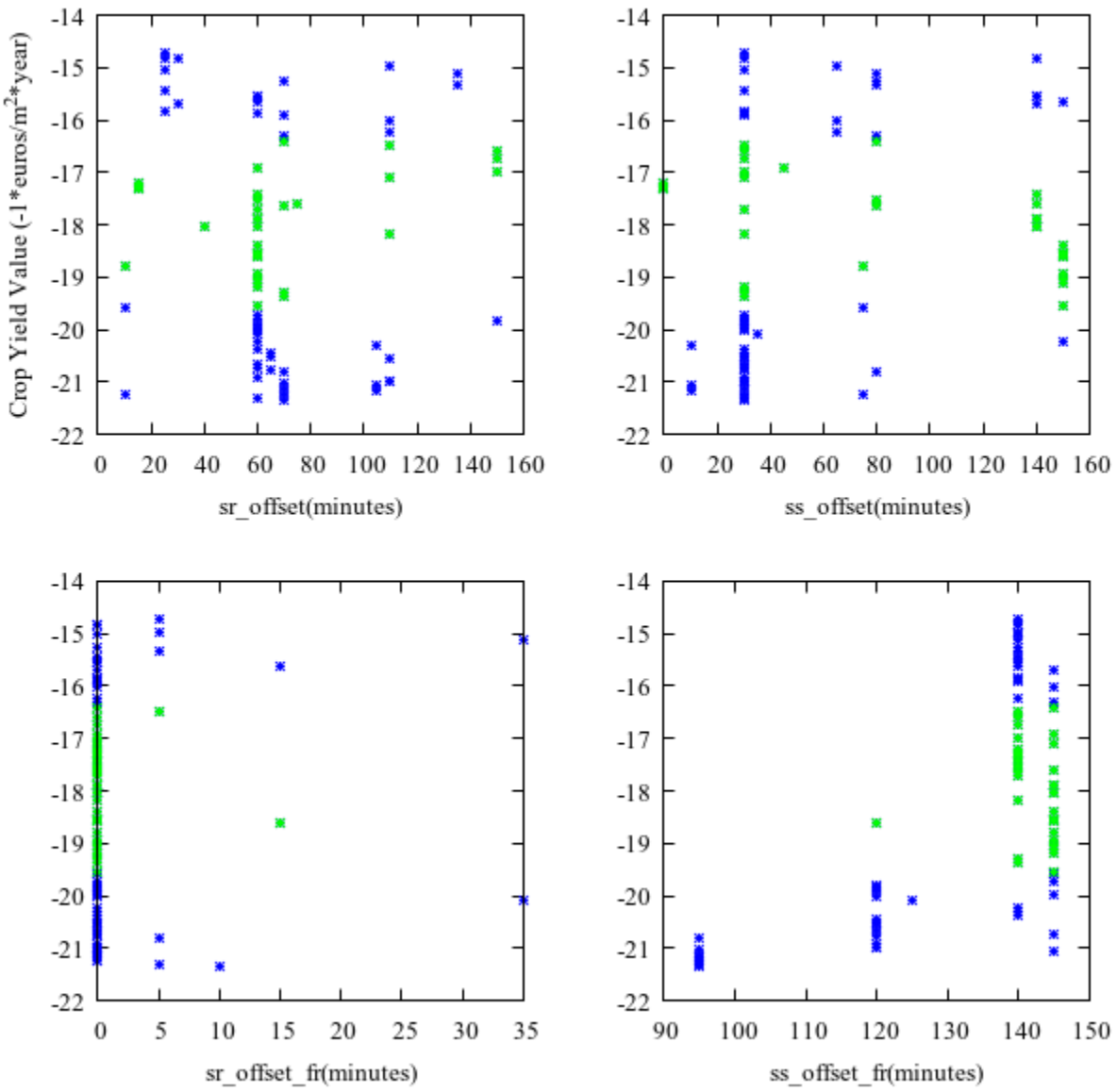

Figure 6.60. The copies of sr_offset and ss_offset are used to subtract from the current calculated time for sunrise and sunset, respectively.

6.6.8 Sunrise and Sunset Offsets (sr_offset, ss_offset)

Figure 6.60 shows that, before fruit set, most of the evolved values for sr_offset and ss_offset contain similar trends to those discussed in Section 6.5.9, where there are a wide range of values which produce both high-crop-yield and low-cost solutions. However, some of these values do not "settle" in the same regions (e.g., ss_offset with the crop value penalty has a large number of values near 30 minutes, while ss_offset without said penalty does not), suggesting that the crop value penalty's effect on the overall

control strategy (i.e., setpoints for $T_{AirVentOn}$ and $T_{AirVentOff}$ that prioritize humidity control) required these offsets to change to some extent to maximize their efficacy.

After fruit set, the evolved values for sr_offset_fr and ss_offset_fr show trends that are nearly identical to those discussed in Section 6.5.9 even with the introduction of a crop value penalty, suggesting that the overall strategy of reducing the time in which morning and evening setpoints are used remains efficient for this stage of plant development. Moreover, reducing the value of ss_offset_fr to as low 95 minutes can result in a marginal increase in crop yield (at the expense of increased variable costs).

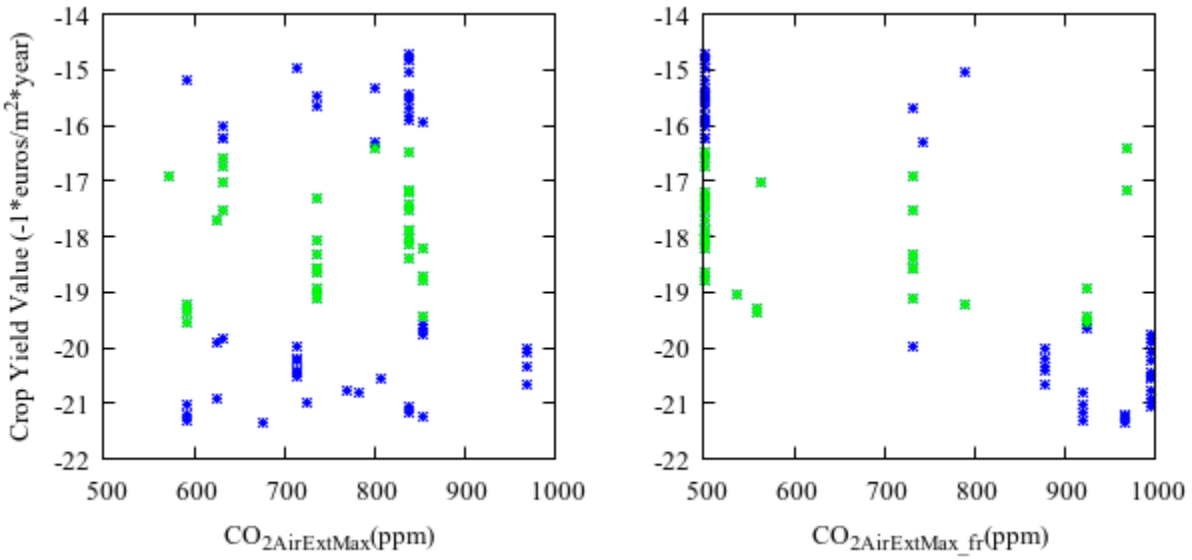

Figure 6.61. This variable determines the upper bound for the dynamic CO_2 setpoint used during CO_2 injection.

6.6.9 $CO_{2AirExtMax}$

Figure 6.61 shows that, before fruit set, the evolved values for $CO_{2AirExtMax}$ did not change significantly with the addition of the crop value penalty and shows a wide range of values that produce both high-crop-value and low-cost solutions. This trend is expected, as most of the strategies discussed in earlier sections did not typically meet the upper bound for the CO_2 setpoint due to the frequency in which ventilation is needed during this warmer period. The introduction of a crop value penalty only reinforces this trend due to the additional ventilation that occurs for purposes of humidity control.

After fruit set, the evolved values for $CO_{2AirExtMax\_fr}$ show a similar trend to the one described in Section 6.5.10, where an increase in this value also tends to increase the value of the crop yield. However, this trend is much less pronounced, and suggests that the increase in ventilation that occurred thanks to the crop value penalty limits the ability of the greenhouse controller to find the right conditions to enable CO_2 injection, as well as reaching the upper bound of the CO_2 setpoint defined by $CO_{2AirExtMax\_fr}$ when CO_2 injection does occur.

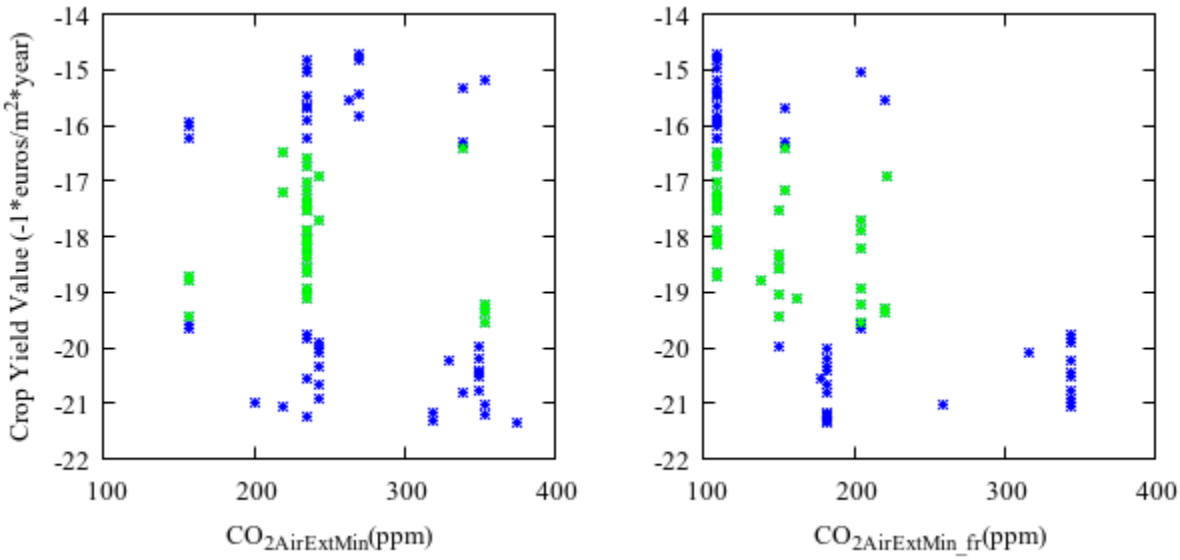

Figure 6.62. This variable determines the lower bound for the dynamic CO_2 setpoint used during CO_2 injection.

6.6.10 $CO_{2AirExtMin}$

Figure 6.62 shows that the evolved values for this variable are consistent with those of previous controllers discussed in this chapter. After fruit set occurs, $CO_{2AirExtMin\_fr}$ shows a significantly less pronounced trend of increasing as the value of the crop yield also increases, similar to $CO_{2AirExtMax\_fr}$ as described in Section 6.6.9.

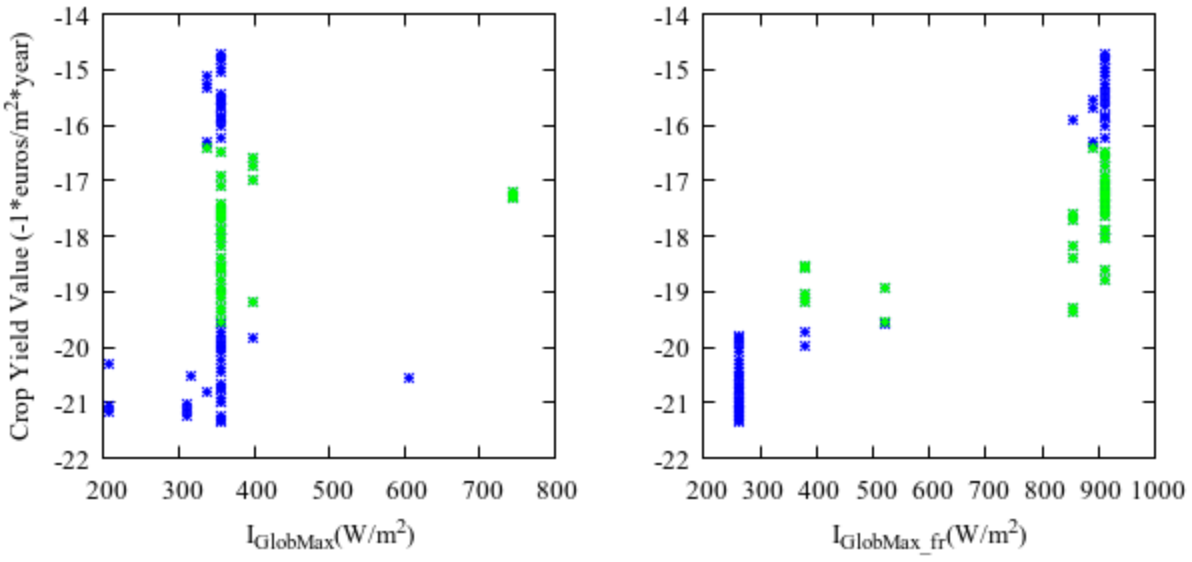

Figure 6.63. This variable determines how quickly $f(I_{Glob})$ is maximized, and subsequently contributes to how quickly the dynamic CO_2 setpoint is maximized.

6.6.11 $I_{GlobMax}$

Figure 6.63 shows that, before fruit set, the addition of a crop value penalty significantly reduced the evolved values for $I_{GlobMax}$, with most of them being at or near 350 W/m^2. This indicates that, in the presence of increased ventilation requirements for humidity control (and subsequently, a reduction in the frequency in which CO_2 injection is possible), maximizing the dynamic CO_2 setpoint (i.e., $CO_{2AirExtOn}$) at lower levels of global radiation is preferable.

After fruit set, the evolved values for $I_{GlobMax\_fr}$ reflect nearly identical trends to those described in Section 6.5.12, where a decrease in this variable tends to increase the crop yield value (at the expense of increased variable costs).

6.6.12 Discussion

Overall, a crop value penalty resulted in some major differences in the genotypes of the evolved control strategies, especially after fruit set occurs. Most of these differences translated into control strategies that prioritize opening the greenhouse ventilation conditionally based on supra-optimal levels of relative humidity. Some time periods did not evolve setpoints that provide as much humidity control as one would

normally expect (e.g., $T_{AirVentOnD\_fr}$ and $T_{AirVentOffD\_fr}$), and instead rely on the other time periods to perform more aggressive humidity control to compensate. This provides an opportunity for the greenhouse to remain sealed more often during the midday period, thus providing more chances for CO_2 injection to occur uninhibited in times where global radiation is expected to be at its peak. Other genotype values evolved to accommodate the overall increase in ventilation required for producing Pareto-optimal solutions (e.g., $I_{GlobMax}$ evolved values that are overall lower).

Based on the crop value penalty that was introduced, there were distinct changes that were observed in the control strategies discussed in Section 6.6. Relative humidity management became a lot more important, although the results show that evolved control strategies did not always need to check for sub-optimal levels of relative humidity to do so: it is also possible to simply choose temperature setpoints that are low enough that the greenhouse ventilation will open unconditionally. In addition, given the current model for crop value penalty, there were control strategies that simply allow some of the midday periods to have sub-optimal levels of relative humidity in exchange for a higher rate of photosynthesis (by keeping the greenhouse sealed and injecting CO_2), and only doing tighter relative humidity control during the nighttime, morning or evening periods.

6.7 Conclusions

The goal of this chapter was fulfilled, which is to explore the behavior exhibited by the evolved control strategies described in this thesis, as well as to obtain useful information from the evolved genotypes. The control strategies described in this section are initially based on the classical Vanthoor strategy described in his thesis [4], with each iteration adding complexity to the controller logic itself. This iterative process was valuable in determining the effects and overall efficacy of certain features (e.g., time-based partitioning).

Using the classical Vanthoor strategy as reference, evolving the setpoints instead of using the default values yielded some improvements. This much is expected, as this classical Vanthoor strategy is not presented as an optimal strategy; rather, it is a control strategy that would be typical of the locale that was

chosen (Almería, Spain) that worked sufficiently well for their study involving the optimization of greenhouse design elements, rather than greenhouse operating parameters. Without making any changes to the controller logic itself, this essentially serves as a method to recalibrate setpoints based on historical weather data. While this clearly has its benefits, it is also extremely computationally intensive, as it requires around 24 hours to optimize these setpoints for 100 generations using the currently available resources, which allows us to run 40 instances of the microclimate-crop-yield model in parallel. This makes it impractical to use in an online setting (i.e., for optimizing setpoints in an already deployed greenhouse). Therefore, this is better suited for greenhouse control optimization to aid the grower in early stages of planning before committing to making significant financial investments.

Allowing for setpoints to change based on the time of day was clearly beneficial. Although ideal conditions for the tomato crop are a well-studied subject, obtaining a greenhouse control strategy that can efficiently reach and maintain these conditions is still extremely difficult, and is further exacerbated by the unpredictability of the weather. By dividing the setpoints into several distinct copies based on the time of day, we allow these setpoints to evolve into values which are better suited for these time periods. Despite the unpredictability of the weather, we can still surmise that there are several major time periods in which we can expect a shift in control strategy: nighttime, morning, midday, and evening. The results in Figure 6.1 show that adding this time-partitioning feature yields superior Pareto-optimal solutions overall compared to control strategies without that feature.

Allowing distinct setpoints based on two main stages of plant development (i.e., before and after fruit set) provided significant benefits. Before fruit set, some of the main requirements of the tomato crop include maintaining an acceptable level for the 24-hour mean canopy temperature and reaching the temperature sum threshold for fruit set to occur. After fruit set, the greenhouse controller must maintain acceptable levels for both instantaneous and 24-hour mean canopy temperatures, as well as increasing the canopy temperature sum up to a maximum amount (after which the rate of fruit growth will be maximized). Failure to meet these canopy temperature requirements will result in complete crop growth inhibition in

extreme cases (by halting all carbohydrate generation from photosynthesis). Although these requirements are similar before and after fruit set, the addition of sub-optimal instantaneous canopy temperatures as a source of crop growth inhibition after fruit set (as well as seasonal weather differences) still create distinct enough conditions that evolving separate values for this stage of plant development was justifiable.

Introducing sunrise and sunset calculations, as well as offsets for each of these calculations, was also beneficial. The less complex controllers discussed in this chapter used fixed transition points between nighttime and daytime (and vice versa) and could not account for basic weather patterns that could normally be exploited. Ideally, these offsets should have the ability to be dynamic as well (based on current environmental conditions or other properties of the greenhouse controller), but these offsets were still beneficial in their current state due to allowing for control strategies to adjust the overall duration of nighttime and daytime control strategies.

Prior to adding to the controllers the capability to evolve boiler PID gain values, the boiler would operate under fixed, predetermined gain values in order to approximate the fuel consumption of the classical Vanthoor strategy. When allowed to evolve, many control strategies had gain values which provided a noticeable improvement in the boiler's ability to maintain optimal temperature ranges for the crop, thus improving the value of the crop yield. This naturally comes with a respective increase in variable costs (associated with fuel consumption) but creating distinct copies of these values based on whether fruit set has occurred or not helped to minimize the impact of this variable cost increase.

By introducing PID-controlled behavior to both ventilation and fogging systems, we observed significant differences in the overall behavior compared to their original operating modes (i.e., fully on or fully off). In addition, having distinct copies of these values based on whether fruit set has occurred or not allowed for the behavior of these systems to be "customized" to better suit the current season and plant development stage. However, since the benefits were not as substantial when compared to evolving the boiler control's PID gain values, future studies including both fixed and variable costs associated with adding this PID-controlled functionality may affect its economic viability.

It was clearly beneficial to adjust the transition points of nighttime control strategies to daytime strategies (and vice versa) based on sunrise and sunset times. Further improvements could likely be achieved by allowing the other transition points (i.e., morning to midday, and midday to evening) to be dynamic as well. Lastly, much like the dynamic CO_2 setpoint ($CO_{2AirExtOn}$) described in Eq. (6.1), other setpoints may be improved by allowing them to change dynamically based on current environmental conditions. The overall behavior displayed by the evolved control strategies in this chapter can be a useful starting point to determine their development, although caution is still needed to make sure any novel control strategies do not violate known best practices for humidity control during all stages of plant growth.

7 Metrics for Decision Making

7.1 Introduction

The goal of this chapter is to briefly summarize various performance metrics for narrowing down the number of control strategies that may suit the needs of a grower. Due to the multi-objective optimization approach used in this thesis, the number of solutions available can be unwieldy and challenging to interpret, so various methods are proposed for narrowing the choices down among a set of Pareto-optimal solutions. In addition, we briefly discuss a method for comparing the performance of newly developed control strategies against other ones by calculating their hypervolumes.

For purposes of this chapter, the crop value penalty described in Section 6.6 is not included in the economic model output, since it does not affect the methodology behind the performance metrics described in the following sections. The sections are presented as follows:

Section 7.2: Net Financial Result (NFR)

Section 7.3: Normalized Hypervolume Between Controllers

Section 7.4: Robustness Against Unknown Weather Data

Section 7.5: Robustness Against Genotype Perturbations

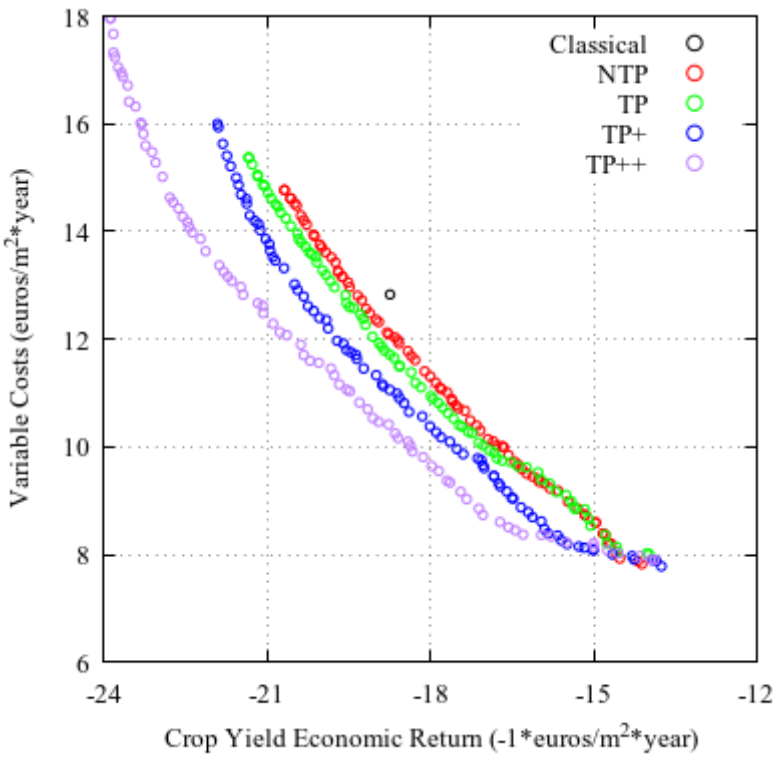

Figure 7.1. Example Pareto fronts of all the control strategies described in this thesis, compared with the classical Vanthoor strategy. All control strategies were evolved for 100 generations.

7.2 Net Financial Result (NFR)

The most straightforward method to filter out results from a Pareto front for this problem is to use a scalarization that aggregates the results of the two objectives into a single number, net financial result (NFR). Defined in Eq. (5.1), this consists of the sum of the fixed costs and the two objectives used for multi-objective optimization throughout this thesis (i.e., the variable costs and crop yield value/crop yield economic return).

Table 7.1. Economic model output for the four main greenhouse controller types described in this thesis.

Control Strategy Type	Mean NFR (euros/m^2×year)	Median NFR	Standard Deviation	Highest NFR	Lowest NFR
NTP	-1.351	-1.125	0.235	-1.059	-1.948
TP	-1.183	-1.162	0.324	-0.786	-1.891
TP+	-0.584	-0.424	0.5	-0.089	-1.947
TP++	0.055	0.407	0.747	0.783	-1.853

Based on Table 7.1, it is clear that the last control strategy (TP++) is preferable: most of the available solutions will be profitable, and solutions with the same NFR as less complex controllers will provide better tradeoffs between the two main objectives; that is, for a given NFR, the more complex controller can provide higher crop value yield or lower variable costs, as seen in Figure 7.1.

There are some clear drawbacks to this method. Since the two objectives are "flattened" into a single objective, useful information can be lost in the process. Broadly speaking, it can be beneficial to consider whether the resulting NFR is due to control strategies producing an exceptionally high crop yield value at the expense of increased variable costs (or, conversely, exceptionally low variable costs while sacrificing some crop yield value). This economic model also does not consider constraints a grower might encounter in practice. For example, minimum (or maximum) crop yield requirements for meeting current demands are not considered, and it is assumed that any quantity/quality of crop yield is acceptable (unless the crop value penalty in Section 6.6 is used, in which case a percentage of the crop yield will be rendered unmarketable if relative humidity control is inadequate). All other factors that contribute to variable costs, such as fossil fuel, CO_2, water, and labor are also not limited. It would be possible to break these factors apart and make this a many-objective optimization problem; it would also be possible to do a sensitivity analysis of how these factors influence the crop yield value/variable cost tradeoffs. However, both are beyond the scope of the current work.

Despite these drawbacks, a grower could circumvent them with sufficient knowledge of the available resources to invest in a greenhouse. This way, constraints can be defined for all components that make up the variable costs and/or crop yield value can be included in the economic model. Since much of the information necessary to apply these constraints will be highly dependent on the location, greenhouse design, as well as myriad other factors, a more generic approach was presented here instead.

7.3 Normalized Hypervolume Between Controller Types

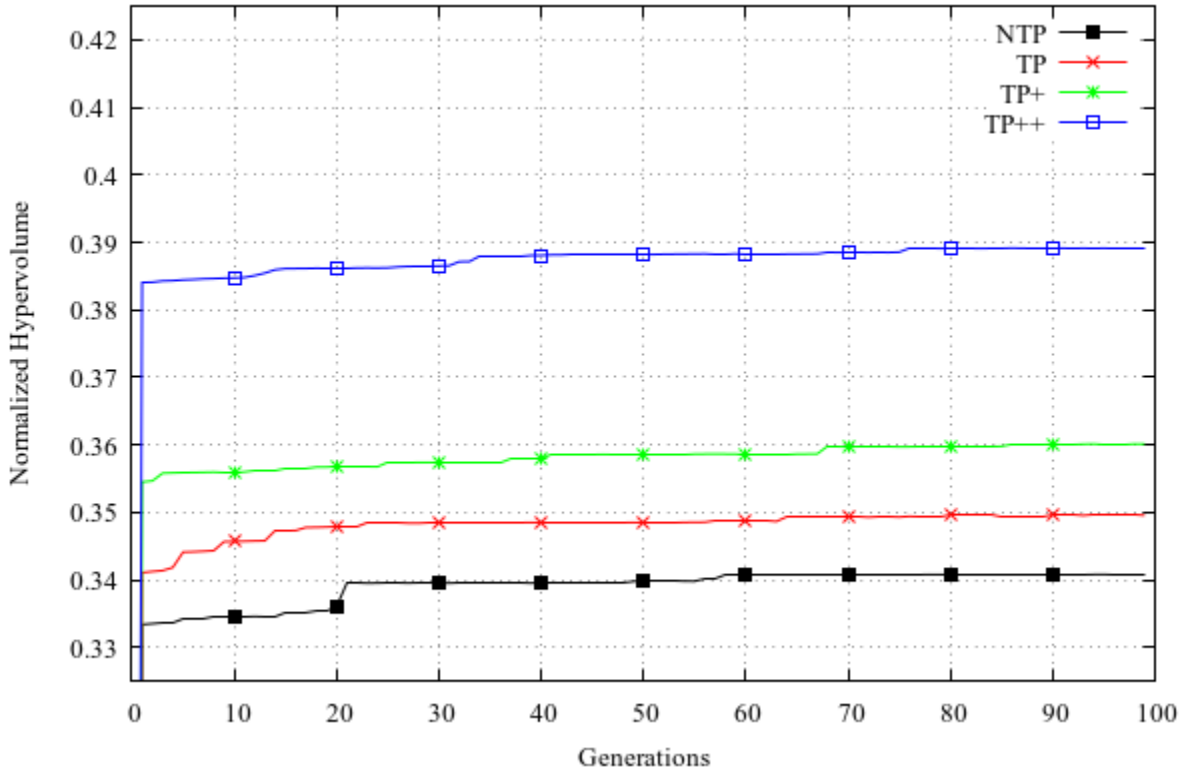

Figure 7.2. Example of normalized hypervolumes for each evolved controller described in this thesis, calculated every generation.

Given a theoretical ideal point and anti-ideal (or nadir) point, we can calculate the hypervolume for a given Pareto front: for two objectives, it is the area of the two-dimensional polygon created between a Pareto front and the nadir point. This provides a method to summarize the overall efficacy of a population of evolved control strategies. However, this can have similar drawbacks to relying on NFR like in Section 7.2, and unlike NFR, it does not provide a value that can easily tell a decision maker whether a particular control strategy is viable or not. That said, this can still be a valuable tool for comparing different types of greenhouse controllers, particularly to determine whether or not a feature introduced in a novel controller is currently outperforming (or can eventually outperform) older and/or simpler controllers. It is one means of quantifying the differences between two Pareto fronts—i.e., comparing their hypervolumes.

Figure 7.2 shows one instance in which each controller type in this thesis is evolved for 100 generations. The hypervolume is computed after each generation of evolution and appears as the vertical axis. Clearly, TP++ shows the best performance overall by this metric, and the rate at which the hypervolume increases for each controller slows down considerably long before 100 generations are reached. Sometimes, evolved controllers whose logic is less complex and which are known to be outperformed can still appear to be superior initially (as seen in earlier chapters in Figure 5.8) due to all populations of control strategies being initialized with random values. This underscores the importance of allowing each controller to evolve for many generations, as well as having a large enough sample size to observe a statistically significant difference in hypervolume. In Section 5.4, a Mann-Whitney's U test showed that a sample size of 5 with 100 generations each was sufficient to show a statistically significant difference in hypervolume between the NTP and TP controller types.

If a novel controller is unable to produce hypervolumes that are on-par with or superior to other controllers within 100 generations, it may indicate that it is currently unviable. This is especially true if computational resources are limited, and significantly increasing the number of generations in which a controller is evolved is prohibitively expensive. As an alternative to changing a seemingly unviable controller, other NSGA-II configuration parameters, as well as other MOEAs, may be explored to obtain better results with a similar investment in computational time.

7.4 Robustness Against Unknown Weather Data

Table 7.2. Example of economic model output (euros×m^{-2}×$year^{-1}$), comparing the classical Vanthoor strategy with the same strategy with evolved setpoints. Weather data for the 2009 – 2010 season was only used to evaluate control strategies after the optimization step was completed. The fogging system is assumed to have no restrictions in this example to illustrate how some weather seasons can be economically unviable (due to negative NFR), but still have an overall positive result if multiple weather seasons are considered.

	Original			**Low Cost**			**High Value**		
Period	**Crop Value**	**Var. Costs**	**NFR**	**Crop Value**	**Var. Costs**	**NFR**	**Crop Value**	**Var. Costs**	**NFR**
2006-2007	19.03	10.98	0.19	17.29	8.65	0.79	19.39	10.88	0.66
2007-2008	20.69	11.41	1.44	18.72	9.11	1.76	21.10	11.42	1.83
2008-2009	17.95	10.97	-0.88	16.20	8.62	-0.27	18.29	10.93	-0.49
2009-2010	18.90	10.96	0.09	17.23	8.76	0.62	19.29	10.95	0.49
Total			**0.85**			**2.91**			**2.49**

One approach to narrow down potential solutions is to simply test evolved control strategies against unknown weather data. By using multiple seasons of weather data, we evolved control strategies that adapt to more general weather patterns associated with the locale. To test the efficacy of these evolved controllers, a new weather season was used to measure their fitness. This approach was covered earlier in Chapter 5, and an example of the outputs of said approach is in Table 7.2. Naturally, control strategies that provide the highest NFR against unknown weather data would be preferred in these cases and are considered "robust" to unknown weather in this respect.

One drawback is that simulating additional weather seasons adds considerable computational cost. While it is not as costly to add multiple unknown weather seasons as a post-optimization step, each additional weather season added *during* the optimization process as part of the fitness calculation can be prohibitively expensive. Moreover, it is possible that too many seasons of weather data will cause an "overfitting" effect and end up underperforming when tested against unknown weather data. This creates a challenging problem in and of itself, since the "ideal" number of weather seasons that should be used for evolving control strategies will depend on many factors, including but not limited to: the available

computational resources, the weather patterns in a locale, and the availability of historical weather data. Such a study is beyond the scope of this thesis, and it was assumed that three weather seasons was sufficient for evolving control strategies (with one additional, unknown weather season as a post-optimization step to help filter results).

7.5 Robustness Against Genotype Perturbations

The goal in this section is to present a method to examine the robustness of a control strategy against perturbations of its genotype. This may be used for obtaining solutions that are also "robust" in practice, but modeling such perturbations (e.g., inaccurate readings in temperature sensors) would require extensive knowledge specific to a greenhouse implementation, such as the tolerance values pertaining to the greenhouse sensors, how they are deployed inside such a greenhouse, weather conditions, and myriad other factors. In this case, we used a simple model to generate these perturbations to show how this metric can be used to filter out undesirable control strategies from a Pareto front, as the effect of systematic biases in sensors can mimic the effect of a non-optimal setting of an evolved setpoint.

One of the earliest examples bringing attention to the issue of robustness in MOEAs was described by Deb et al. [46], noting that in practice a decision maker may not always be interested in a global optimal solution; rather, solutions that are *robust* to small perturbations in its genotype may be preferred. Based on this study, we propose using the following variation:

1. All the values in a genotype have perturbations applied to them for every sample.
2. For each original solution in the Pareto front, every locus *L* at index *i* of its genotype will have perturbations applied to it, assuming a normal distribution with a mean $\mu = L_i$, and variance $\sigma^2 = 0.1 \times L_i$.
    - 100 samples are generated for each original solution, and their fitness functions are calculated.
3. Each original solution is assigned a value based on the area of the convex hull created by the outer points among all the samples.

- Original solutions with smaller convex hull area are considered more robust.

Based on this method, the output provides a single value that can be easily sorted to quantify the sensitivity of each solution. While this procedure has similar drawbacks to that of NFR in Section 7.2, it provides additional information that NFR does not provide, and the convex hulls themselves can be easily visualized to better interpret these results (see Figure 7.3).

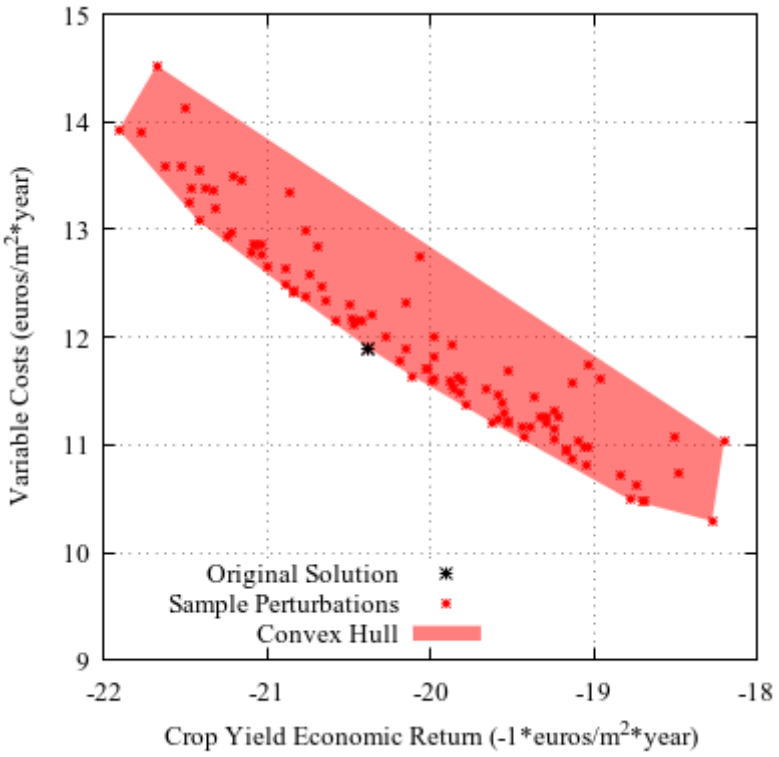

Figure 7.3. Example output of the proposed metric. A solution from the original Pareto front (black) is sampled 100 times with random perturbations, and their fitness function is calculated for each new sample (red). The outer points of these new solutions are used to obtain the convex hull (red shaded region).

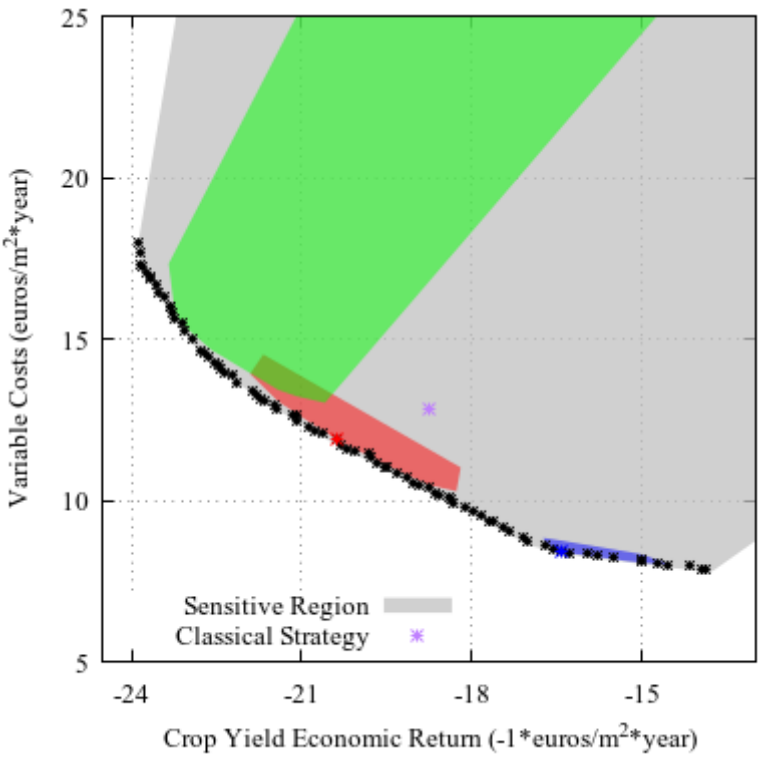

Figure 7.4. Example Pareto front showing the effects of adding perturbations to each solution. The grey region shows the union of all the polygons generated by the perturbed samples of the Pareto front. The least sensitive solutions tend to be low-variable-cost solutions (blue region), while high-crop-value solutions can be extremely sensitive (green region).

Table 7.3. Partial list of evolved solutions sorted by increasing convex hull area.

Convex Hull Area	**Crop Yield Value (euros×m^{-2}×year^{-1})**	**Variable Costs (euros×m^{-2}×year^{-1})**	**Original NFR (euros×m^{-2}×year^{-1})**	**Mean NFR (euros×m^{-2}×year^{-1})**
0.589	16.441	8.449	0.141	-0.153
0.826	14.747	8.078	-1.181	-1.181
0.908	17.034	8.733	0.451	0.199
0.986	15.493	8.225	-0.582	-0.814
1.226	17.109	8.853	0.406	0.092
1.439	16.563	8.506	0.206	-0.064
1.473	17.334	9.029	0.454	0.067
1.971	18.133	9.807	0.476	0.133
2.051	17.442	9.166	0.426	0.057
2.064	17.695	9.369	0.476	0.181

Based on Table 7.3, we can see that a small convex hull area associated with a solution does not guarantee that the mean and/or original NFR will be positive. However, it is still a useful tool to filter out

undesirable results, as an excessively high convex hull area will lead to unviable NFR values that are, on average, far inferior to the classical Vanthoor strategy (e.g., the green shaded region in Figure 7.4 is partially dominated by the classical strategy). In addition, based on the results we can see a tendency for high-crop-value solutions to be highly sensitive to genotype perturbations. If robust solutions are desired that are viable with respect to having a positive NFR, solutions near the low-variable-cost region of the Pareto front are superior. Solutions that provide good values on both objectives are slightly more sensitive (e.g., the red shaded region in Figure 7.4), but can still provide positive mean NFR values despite the perturbations. In addition, these types of solutions dominate the classical Vanthoor strategy, with their perturbed versions becoming non-dominated only in their worst cases, and, of course, that is when comparing them to an unperturbed classical Vanthoor strategy.

8 Summary and Conclusions

In this chapter we will briefly summarize the results in this thesis, discuss some of the challenges encountered during research, as well as possible directions this research could continue to further improve existing methods for optimizing greenhouse control.

Based on the results and discussion from the previous chapters, the goal of this thesis was fulfilled. We used an existing microclimate-crop-yield model [4], which was originally developed with greenhouse design optimization in mind. We then modified this methodology for optimizing and developing control strategies instead, using MOEAs as the primary tool for doing so. Using a classical control strategy as a basis, we developed three new versions, each of which improved upon the previous controller by providing better tradeoffs between the two main objectives: maximizing crop yield value and minimizing variable costs. In addition, we were able to observe some interesting properties in these evolved controllers which provided valuable information on how to iteratively improve control strategies, as well as identified potential limitations of the microclimate-crop-yield model.

One of the biggest challenges was overcoming the large amount of computational resources required to apply MOEAs for this type of optimization problem. Early attempts at addressing this issue included modifying the differential equations that describe the microclimate-crop-yield model (see Chapter 3) in order to reduce the stiffness of these equations (and thus improve the overall speed of the ODE solver by allowing larger simulation step sizes that are still within acceptable margins of error). This approach showed some promise, but it ultimately proved to have considerable challenges for validation of results, including providing insufficient crop yields to match those reported in existing literature.

As an alternate solution to the previous problem, implementing a subset of the microclimate-crop-yield model described by Vanthoor (as described in Chapter 4) was sufficient to achieve the main goal of this thesis. This model was originally developed to be modular in nature, considering the possibility of many different greenhouse design configurations, which made this approach possible. This subset of the microclimate-crop-yield model describes a relatively complex greenhouse design while still having

acceptable simulation times, which allowed us to adequately explore and optimize challenging greenhouse control problems. However, there is clear room for improvement in this regard, as there are many greenhouse design elements that were not considered, including but not limited to: retractable shading screens, supplemental lighting, passive greenhouse heating, mechanical/pad and fan cooling, direct air heating, etc. Such greenhouse design elements should ideally be considered in future studies for greenhouse control optimization as this would improve the practicality of our optimization method, but doing so requires examining existing models that incorporate these greenhouse design elements, and potentially modifying these models to improve simulation speeds to the extent that optimization with MOEAs can still remain feasible. Moreover, these model modifications would require independently validating the results obtained in a real greenhouse to verify their efficacy and/or make corrections to the model, as needed, which is beyond the scope of what we could attempt here.

Despite introducing various distinct controller types in this thesis (in Chapters 5 and 6), each with increasing complexity, we did not reach a point where the computational resources were the primary bottleneck when developing and evolving more complex control strategies. This is mostly due to the focus of this thesis being on iteratively improving existing controller types (as seen in Chapter 6): using the classical greenhouse control strategy as a starting point, we gradually increased its complexity, observed the overall behavior these new control strategies produced, and subsequently used those results to find useful properties to improve further (or features that were detrimental and therefore removed). While it would be trivial to present a control strategy whose genotype takes considerably longer to evolve, meaningfully interpreting the results of such a controller would take considerable time without additional techniques to aid in this process. Ideally, this should be streamlined by at least partially automating the process with which key properties, rules, and/or design principles can be extracted from the Pareto fronts generated by each new controller type that is introduced. Multi-objective optimization problems are uniquely suited for this kind of discovery process (coined as “innovization”), and multiple attempts have been made in the past to present viable approaches for automated innovization [50, 51].

The results in Section 6.6 show that while the current microclimate-crop-yield model is adequate for simulating tomato crop growth in a greenhouse setting, inadequate humidity control is not sufficiently penalized in cases where a model-based optimization approach is used to improve control strategies (e.g., this dissertation). The trapezoid functions that make up the crop value penalty primarily affect the post-fruit-set stage of plant growth, since these penalties are only applied *after* harvest begins. This penalty still has an effect on the overall behavior of the control strategy *before* fruit set, due to maintaining a 24-hour mean value of the vapor pressure deficit (VPD_{24}) between the canopy and the greenhouse air, as well as a 48-hour mean value of the relative humidity (RH_{48}) of the greenhouse air. However, this would have a marginal effect overall before fruit set, since the pre-fruit-set control strategy only needs to yield an acceptable range of both VPD_{24} and RH_{48} shortly before fruit set begins. Values like RH_{48} were proposed to model the effect of the onset of the fungus *Botrytis cinerea* on the crop, but this type of fungal infection is not limited to affecting the yield of marketable tomatoes, and can infect all the plant tissue [52]. Ideally, the microclimate-crop yield model should penalize sub-optimal levels of relative humidity at all stages of plant growth to better reflect the real-world effects of fungal infections and other diseases on the tomato crop.

It was assumed that no additional costs would be incurred from the implementation of these control strategies (other than the costs of any resources they utilize), and that the features described in each controller in this section would already be available to use. Although an effort was made to avoid major greenhouse design changes, both fixed and variable costs associated with the development of additional controller logic and upgrades to greenhouse design elements should be included (when applicable). Depending on their real-world cost, these may affect the viability of more complex control strategies.

Both objectives, the variable costs and crop yield value, may also be divided into individual components that can be treated as their own separate objectives (thus turning this into a many-objective optimization problem, as opposed to two-objective). Assuming that the appropriate computational resources are

available, doing so can provide more insight on the tradeoffs that occur for the "subobjectives" that comprise the variable costs and crop yield value, which may be of interest to a decision maker in practice.

Finally, the metrics for decision making presented in Chapter 7 allow a user to significantly narrow down solutions that may be of interest. When using both net financial result (NFR) and the convex hull area (as seen in Section 7.5) as performance metrics, we are able to narrow down potential solutions quickly while visualizing the overall robustness (with respect to genotype perturbations) when picking a specific solution. The method proposed for measuring robustness against genotype perturbations assumes that these perturbations can be modeled using a simple normal distribution, and as such does not reflect the inconsistencies that one would encounter in practice. However, such a method could still be applied if there is sufficient knowledge of a greenhouse implementation to model these perturbations, providing a valuable tool for assessing the overall "risk" associated with an evolved control strategy.

LITERATURE CITED

LITERATURE CITED

[1] G. van Straten, G. van Willigenburg, E. van Henten, and R. van Ooteghem, *Optimal Control of Greenhouse Cultivation*. Boca Raton, Florida, USA: CRC Press, 2010, p. 326.

[2] K. Fernandez-Stark, P. Bamber, G. Gereffi, G. Ahmed, S. J. Heil, and C. Root, "The fruit and vegetables global value chain: Economic upgrading and workforce development," *Center on Globalization, Governance & Competitiveness (CGGC), Duke University, North Carolina, USA,* 2011.

[3] K. J. Boote and J. M. S. Scholberg, "Developing, parameterizing, and testing of dynamic crop growth models for horticultural crops," in *International Symposium on Models for Plant Growth, Environmental Control and Farm Management in Protected Cultivation*, Wageningen, The Netherlands, L. F. M. Marcelis, G. v. Straten, C. Stanghellini, and E. Heuvelink, Eds., 2006, Wageningen, The Netherlands, in HortiModel 2006, pp. 23-34, doi: http://doi.org/10.17660/ActaHortic.2006.718.1.

[4] B. H. E. Vanthoor, "A Model-Based Greenhouse Design Method," Wageningen University, Wageningen, The Netherlands, 2011. [Online]. Available: https://www.cabdirect.org/cabdirect/abstract/20113204235

[5] W. L. Price, "A Controlled Random Search Procedure for Global Optimisation," *The Computer Journal,* vol. 20, no. 4, pp. 367-370, 1977.

[6] K. Deb, A. Pratap, S. Agarwal, and T. Meyarivan, "A Fast and Elitist Multiobjective Genetic Algorithm: NSGA-II," *IEEE Transactions on Evolutionary Computation,* vol. 6, no. 2, pp. 182-197, 2002, Art no. Pii s 1089-778x(02)04101-2, doi: 10.1109/4235.996017.

[7] C. A. C. Coello, G. B. Lamont, and D. A. Van Veldhuizen, *Evolutionary Algorithms for Solving Multi-objective Problems* (Genetic and Evolutionary Computation). Springer US, 2007, p. 800.

[8] V. P. Sethi and S. K. Sharma, "Survey of Cooling Technologies for Worldwide Agricultural Greenhouse Applications," *Solar Energy,* vol. 81, no. 12, pp. 1447-1459, 2007.

[9] C. A. Medina-Ruíz, I. A. Mercado-Luna, G. M. Soto-Zarazúa, I. Torres-Pacheco, and E. Rico-García, "Mathematical Modeling on Tomato Plants: A Review," *African Journal of Agricultural Research,* vol. 6, no. 33, pp. 6745-6749, 2011.

[10] N. Sigrimis and N. Rerras, "A Linear Model for Greenhouse Control," *Transactions of the ASAE,* vol. 39, no. 1, pp. 253-261, 1996, doi: https://doi.org/10.13031/2013.27505.

[11] H. J. Tantau, "Optimal Control for Plant Production in Greenhouses," *IFAC Proceedings Volumes,* vol. 24, no. 11, pp. 1-6, 1991, doi: https://doi.org/10.1016/B978-0-08-041273-3.50005-7.

[12] E. J. van Henten and J. Bontsema, "Optimal Control of Greenhouse Climate," *IFAC Proceedings Volumes,* vol. 24, no. 11, pp. 27-32, 1991, doi: https://doi.org/10.1016/B978-0-08-041273-3.50010-0.

[13] K. G. Arvanitis, P. N. Paraskevopoulos, and A. A. Vernardos, "Multirate Adaptive Temperature Control of Greenhouses," *Computers and Electronics in Agriculture,* vol. 26, no. 3, pp. 303-320, 2000, doi: https://doi.org/10.1016/S0168-1699(00)00082-X.

[14] I. Seginer and R. W. McClendon, "Methods for Optimal Control of the Greenhouse Environment," (in English), *Transactions of the ASAE (USA),* vol. 35, no. 4, pp. 1299-1307, 1992.

[15] Y. Su and L. Xu, "A Greenhouse Climate Model for Control Design," in *2015 IEEE 15th International Conference on Environment and Electrical Engineering (EEEIC)*, Rome, Italy, 2015, Rome, Italy, pp. 47-53, doi: 10.1109/EEEIC.2015.7165318.

[16] A. Hasni, R. Taibi, B. Draoui, and T. Boulard, "Optimization of Greenhouse Climate Model Parameters Using Particle Swarm Optimization and Genetic Algorithms," *Energy Procedia,* vol. 6, pp. 371-380, 2011, doi: https://doi.org/10.1016/j.egypro.2011.05.043.

[17] Q. Zou, J. Ji, S. Zhang, M. Shi, and Y. Luo, "Model Predictive Control Based on Particle Swarm Optimization of Greenhouse Climate for Saving Energy Consumption," in *2010 World Automation Congress*, Kobe, Japan, 2010: IEEE, pp. 123-128.

[18] A. Ramírez-Arias, F. Rodríguez, J. L. Guzmán, and M. Berenguel, "Multiobjective Hierarchical Control Architecture for Greenhouse Crop Growth," *Automatica,* vol. 48, no. 3, pp. 490-498, 2012.

[19] L. Xu, Y. Su, and Y. Liang, "Requirement and Current Situation of Control-Oriented Microclimate Environmental Model in Greenhouse System," *Transactions of the Chinese Society of Agricultural Engineering,* vol. 29, no. 19, pp. 1-15, 2013.

[20] H. Hu, L. Xu, R. Wei, and B. Zhu, "Multi-Objective Control Optimization for Greenhouse Environment Using Evolutionary Algorithms," *Sensors,* vol. 11, no. 6, 2011, doi: 10.3390/s110605792.

[21] M. Mahdavian, S. Sudeng, and N. Wattanapongsakorn, "Multi-Objective Optimization and Decision Making for Greenhouse Climate Control System Considering User Preference and Data Clustering," *Cluster Computing,* vol. 20, no. 1, pp. 835-853, 2017.

[22] Y. Su, L. Xu, and E. D. Goodman, "Nearly Dynamic Programming NN-Approximation–Based Optimal Control for Greenhouse Climate: A Simulation Study," *Optimal Control Applications and Methods,* vol. 39, no. 2, pp. 638-662, 2018, doi: 10.1002/oca.2370.

[23] L. Xu and Q. Hu, "A Multi-Objective Compatible Control (MOCC) Algorithm for the Greenhouse Energy-Saving Control," presented at the 2007 ASAE Annual Meeting, St. Joseph, MI, 2007. [Online]. Available: http://elibrary.asabe.org/abstract.asp?aid=22944&t=5.

[24] J. H. Holland, *Adaptation in Natural and Artificial Systems: An Introductory Analysis with Applications to Biology, Control and Artificial Intelligence*. Cambridge, MA, USA: MIT press, 1992.

[25] D. E. Goldberg, *Genetic Algorithms in Search, Optimization and Machine Learning*, 1st ed. USA: Addison-Wesley Longman Publishing Co., Inc., 1989.

[26] A. E. Eiben and J. E. Smith, "Introduction to Evolutionary Computing," *Assembly Automation,* vol. 24, no. 3, pp. 324-324, 2004, doi: 10.1108/aa.2004.24.3.324.1.

[27] J. W. Jones, E. Dayan, L. H. Allen, H. Van Keulen, and H. Challa, "A Dynamic Tomato Growth and Yield Model (TOMGRO)," *Transactions of the ASAE,* vol. 34, no. 2, pp. 663-0672, 1991.

[28] W. Lentz, "Model Applications in Horticulture: a Review," *Scientia Horticulturae,* vol. 74, no. 1-2, pp. 151-174, 1998.

[29] S. N. Lisson, N. G. Inman-Bamber, M. J. Robertson, and B. A. Keating, "The Historical and Future Contribution of Crop Physiology and Modelling Research to Sugarcane Production Systems," *Field Crops Research,* vol. 92, no. 2-3, pp. 321-335, 2005.

[30] F. Tap, "Economics-Based Optimal Control of Greenhouse Tomato Crop Production," Wageningen University, Wageningen, The Netherlands, 2000.

[31] C. Zhu *et al.*, "Robust Multi-Objective Evolutionary Optimization to Allow Greenhouse Production/Energy Use Tradeoffs," in *International Symposium on New Technologies for Environment Control, Energy-Saving and Crop Production in Greenhouse and Plant Factory*, Jeju Island, South Korea, 2014: International Society for Horticultural Science (ISHS), Leuven, Belgium, in Greensys 2013, 1037 ed., pp. 525-532, doi: https://doi.org/10.17660/ActaHortic.2014.1037.65.

[32] J. J. Magán, J. C. López, A. Escudero, and J. Pérez-Parra, "Comparación de Dos Estructuras de Invernadero (Cristal vs. Plástico) Equipadas con Sistemas de Control Activo del Clima," *Actas de Horticultura,* vol. 48, pp. 880-883, 2007.

[33] NMIC. *Dedicated Meteorological Dataset for the Analysis of Building Thermal Environment*, China Construction Industry Press, Beijing, China.

[34] S. Arlot and A. Celisse, "A Survey of Cross-Validation Procedures for Model Selection," *Statistics Surveys,* vol. 4, pp. 40-79, 2010.

[35] K. Deb and H. Gupta, "Introducing Robustness in Multi-Objective Optimization," *Evolutionary Computation Journal,* vol. 14, no. 4, pp. 463-494, 2006, doi: 10.1162/evco.2006.14.4.463.

[36] J. R. Llera, E. D. Goodman, E. S. Runkle, and L. Xu, "Improving Greenhouse Environmental Control Using Crop-Model-Driven Multi-Objective Optimization," in *Proceedings of the Genetic and Evolutionary Computation Conference Companion*, Kyoto, Japan, 2018 2018: Association for Computing Machinery, in GECCO '18, pp. 292-293, doi: 10.1145/3205651.3205724. [Online]. Available: https://doi.org/10.1145/3205651.3205724

[37] C. Gagné and M. Parizeau, "Open BEAGLE: A New Versatile C++ Framework for Evolutionary Computation," in *Late-Breaking Papers of the 2002 Genetic and Evolutionary Computation Conference*, New York, USA, 2002: Citeseer, in GECCO 2002, pp. 161-168.

[38] L. Dagum and R. Menon, "OpenMP: an Industry Standard API for Shared-Memory Programming," *IEEE Computational Science and Engineering,* vol. 5, no. 1, pp. 46-55, 1998.

[39] M. Galassi *et al.*, *GNU Scientific Library*, 1.15 ed.: Network Theory Limited, 2011, p. 521.

[40] MeteoBlue. "Weather History Download Almería." https://www.meteoblue.com/en/weather/archive/export/almer%c3%ada_spain_2521886 (accessed 2018).

[41] P. Tans. co2_mm_mlo.txt [Online] Available: ftp://ftp.cmdl.noaa.gov/ccg/co2/trends/co2_mm_mlo.txt

[42] J. J. Magán, A. B. López, J. J. Pérez-Parra, and J. C. López, "Invernaderos con Cubierta de Plástico y Cristal en el Sureste Español," in "Cuadernos de investigación," Fundación Cajamar, Almería, Spain, 2008, vol. 54.

[43] J. R. Llera, K. Deb, E. Runkle, L. H. Xu, and E. Goodman, "Evolving and Comparing Greenhouse Control Strategies using Model-Based Multi-Objective Optimization," *2018 IEEE Symposium Series on Computational Intelligence (IEEE SSCI),* pp. 1929-1936, 2018.

[44] E. Zitzler, D. Brockhoff, and L. Thiele, "The Hypervolume Indicator Revisited: On the Design of Pareto-Compliant Indicators Via Weighted Integration," in *Evolutionary Multi-Criterion Optimization*, Berlin, Heidelberg, S. Obayashi, K. Deb, C. Poloni, T. Hiroyasu, and T. Murata, Eds., 2007: Springer Berlin Heidelberg, pp. 862-876.

[45] H. B. Mann and D. R. Whitney, "On a Test of Whether one of Two Random Variables is Stochastically Larger than the Other," *The Annals of Mathematical Statistics,* vol. 18, no. 1, pp. 50-60, 1947.

[46] K. Deb and A. Srinivasan, "Innovization: Innovating Design Principles through Optimization," in *Proceedings of the 8th Annual Conference on Genetic and Evolutionary Computation*, Seattle, Washington, USA, 2006: Association for Computing Machinery, in GECCO '06, pp. 1629-1636, doi: 10.1145/1143997.1144266. [Online]. Available: https://doi.org/10.1145/1143997.1144266

[47] L. Xu, H. Hu, and B. Zhu, "Energy-Saving Control of Greenhouse Climate Based on MOCC Strategy," in *Proceedings of the first ACM/SIGEVO Summit on Genetic and Evolutionary Computation*, 2009, pp. 645-650.

[48] "National Oceanic and Atmospheric Administration (NOAA)." ftp://ftp.cmdl.noaa.gov/ccg/co2/trends/co2_mm_mlo.txt (accessed 2018).

[49] O. Körner and H. Challa, "Process-Based Humidity Control Regime for Greenhouse Crops," *Computers and Electronics in Agriculture,* vol. 39, no. 3, pp. 173-192, 2003, doi: https://doi.org/10.1016/S0168-1699(03)00079-6.

[50] S. Bandaru and K. Deb, "Automated Innovization for Simultaneous Discovery of Multiple Rules in Bi-Objective Problems," in *Evolutionary Multi-Criterion Optimization*, Berlin, Heidelberg, R. H. C. Takahashi, K. Deb, E. F. Wanner, and S. Greco, Eds., 2011: Springer Berlin Heidelberg, pp. 1-15, doi: https://doi.org/10.1007/978-3-642-19893-9_1.

[51] A. Gaur and K. Deb, "Adaptive Use of Innovization Principles for a Faster Convergence of Evolutionary Multi-Objective Optimization Algorithms," in *Proceedings of the 2016 on Genetic and Evolutionary Computation Conference Companion*, Denver, Colorado, USA, 2016: Association for Computing Machinery, in GECCO '16 Companion, pp. 75-76, doi: *10.1145/2908961.2909019* [Online]. Available: https://doi.org/10.1145/2908961.2909019

[52] O. Körner and N. Holst, "Model Based Humidity Control of Botrytis in Greenhouse Cultivation," 2005: International Society for Horticultural Science (ISHS), Leuven, Belgium, 691 ed., pp. 141-148, doi: 10.17660/ActaHortic.2005.691.15. [Online]. Available: https://doi.org/10.17660/ActaHortic.2005.691.15